ISSN 0973-8916

Current Trends in Biotechnology and Pharmacy

Volume 7 Issue 4 October 2013

www.abap.co.in

Current Trends in Biotechnology and Pharmacy
ISSN 0973-8916 (Print), 2230-7303 (Online)

www.abap.co.in

ISSN 0973-8916

Current Trends in Biotechnology and Pharmacy

(An International Scientific Journal)

Volume 7 Issue 4 October 2013

www.abap.co.in

Indexed in Chemical Abstracts, EMBASE, ProQuest, Academic SearchTM, DOAJ, CAB Abstracts, Index Copernicus, Ulrich's Periodicals Directory, Open J-Gate Pharmoinfonet.in Indianjournals.com and Indian Science Abstracts.

Current Trends in Biotechnology and Pharmacy
Vol. 7 (4) October - 2013, ISSN 0973-8916 (Print), 2230-7303 (Online)

Association of Biotechnology and Pharmacy

(Regn. No. 28 OF 2007)

The *Association of Biotechnology and Pharmacy (ABAP)* was established for promoting the science of Biotechnology and Pharmacy. The objective of the Association is to advance and disseminate the knowledge and information in the areas of Biotechnology and Pharmacy by organising annual scientific meetings, seminars and symposia.

Members

The persons involved in research, teaching and work can become members of Association by paying membership fees to Association.

The members of the Association are allowed to write the title ***MABAP*** (Member of the Association of Biotechnology and Pharmacy) with their names.

Fellows

Every year, the Association will award Fellowships to the limited number of members of the Association with a distinguished academic and scientific career to be as Fellows of the Association during annual convention. The fellows can write the title ***FABAP*** (Fellow of the Association of Biotechnology and Pharmacy) with their names.

Membership details

(Membership and Journal)		India	SAARC	Others
Individuals	– 1 year	Rs. 600	Rs. 1000	$100
	LifeMember	Rs. 4000	Rs. 6000	$500
Institutions	– 1 year	Rs. 1500	Rs. 2000	$200
(Journal only)	Life member	Rs.10000	Rs.12000	$1200

Individuals can pay in two instalments, however the membership certificate will be issued on payment of full amount. All the members and Fellows will receive a copy of the journal free

Association of Biotechnology and Pharmacy
(Regn. No. 28 OF 2007)
#5-69-64; 6/19, Brodipet
Guntur – 522 002, Andhra Pradesh, India

Current Trends in Biotechnology and Pharmacy
Vol. 7 (4) October - 2013, ISSN 0973-8916 (Print), 2230-7303 (Online)

Current Trends in Biotechnology and Pharmacy

ISSN 0973-8916

Volume 7 (4) **CONTENTS** **October - 2013**

Research Papers

Reviews

Current Trends in Biotechnology and Pharmacy
Vol. 7 (4) October - 2013, ISSN 0973-8916 (Print), 2230-7303 (Online)

Information to Authors

The *Current Trends in Biotechnology and Pharmacy* is an official international journal of *Association of Biotechnology and Pharmacy*. It is a peer reviewed quarterly journal dedicated to publish high quality original research articles in biotechnology and pharmacy. The journal will accept contributions from all areas of biotechnology and pharmacy including plant, animal, industrial, microbial, medical, pharmaceutical and analytical biotechnologies, immunology, proteomics, genomics, metabolomics, bioinformatics and different areas in pharmacy such as, pharmaceutics, pharmacology, pharmaceutical chemistry, pharma analysis and pharmacognosy. In addition to the original research papers, review articles in the above mentioned fields will also be considered.

Call for papers

The Association is inviting original research or review papers and short comunications in any of the above mentioned research areas for publication in Current Trends in Biotechnology and Pharmacy. The manuscripts should be concise, typed in double space in a general format containing a title page with a short running title and the names and addresses of the authors for correspondence followed by Abstract (350 words), 3 – 5 key words, Introduction, Materials and Methods, Results and Discussion, Conclusion, References, followed by the tables, figures and graphs on separate sheets. For quoting references in the text one has to follow the numbering of references in parentheses and full references with appropriate numbers at the end of the text in the same order. References have to be cited in the format below.

Mahavadi, S., Rao, R.S.S.K. and Murthy, K.S. (2007). Cross-regulation of VAPC2 receptor internalization by m2 receptors via c-Src-mediated phosphorylation of GRK2. Regulatory Peptides, 139: 109-114.

Lehninger, A.L., Nelson, D.L. and Cox, M.M. (2004). Lehninger Principles of Biochemistry, (4th edition), W.H. Freeman & Co., New York, USA, pp. 73-111.

Authors have to submit the figures, graphs and tables of the related research paper/article in Adobe Photoshop of the latest version for good illumination and allignment.

Authors can submit their papers and articles either to the editor or any of the editorial board members for onward transmission to the editorial office. Members of the editorial board are authorized to accept papers and can recommend for publication after the peer reviewing process. The email address of editorial board members are available in website www.abap.in. For submission of the articles directly, the authors are advised to submit by email to krssrao@abap.co.in or krssrao@yahoo.com.

Authors are solely responsible for the data, presentation and conclusions made in their articles/research papers. It is the responsibility of the advertisers for the statements made in the advertisements.

Current Trends in Biotechnology and Pharmacy
Vol. 7 (4) 825-836 October 2013, ISSN 0973-8916 (Print), 2230-7303 (Online)

Fast Microwave-based DNA Extraction from Vegetative Mycelium and Fruiting Body Tissues of Agaricomycetes for PCR Amplification

Bastian Dörnte and Ursula Kües*
Büsgen-Institute, Division of Molecular Wood Biotechnology and Technical Mycology, University of Goettingen, Büsgenweg 2, 37077 Goettingen, Germany
*For correspondence – ukuees@gwdg.de

Abstract

In this study, we tested a microwave-based DNA extraction method for subsequent DNA amplifications by PCR on vegetative mycelia and mushrooms of different Agaricomycetes. The extraction method requires tiny amounts of fungal material, is rapid and achieved within minutes, why it is superior to classical extraction methods which are work-intensive and require larger amounts of starting material, hours of time for performance and in addition specific expensive and hazardous chemicals for cell lysis and DNA purification. The microwave method with highest reliability is suitable for vegetative mycelium harvested from fresh and also from aged fungal cultures. It is especially attractive for slow-growing species of which larger amounts of mycelium are difficult to obtain from. The method is further applicable with success rates between 76.9% and 90.9% to fleshy mushrooms over a wide range of families of Agaricomycetes, both in fresh as well as in dried form, and also to firm young and older fruiting bodies of more robust leathery, corky and woody textures. Also non-cultivable species can thus be accessed for DNA analyses. Finally, we show that also fungal infested plant material such as millet, straw, wood and bark can be used. However, here the success depends on freshness of the material and on presence of sufficient surface mycelium.

Keywords: Agaricomycetes, mushrooms, mycelium, microwaving, DNA extraction, PCR amplification

Introduction

Classically, fungal DNA isolation involves cultivation of individual clones, harvesting the mycelium and isolating the DNA from usually frozen or freeze-dried samples (1-6). Depending on the growth capacity of a species the whole process can take up several weeks, provided that a fungus can be cultured. Due to the rigid character of fungal cell walls, the applied isolation protocol requires an effective method to break the cells and thereby release the DNA. Conventional DNA isolation protocols include an initial mechanical grinding and a successive treatment with chemicals to disrupt the fungal cell walls and membranes. The released DNA is subsequently purified from cell wall debris, proteins and other molecules, mostly applying a mixture of phenol-chloroform followed by centrifugation and ethanol precipitation of the DNA from the watery supernatant. The obtained genomic DNA is used for a broad spectrum of molecular biological applications such as DNA library construction, sequence analyses, subcloning of (PCR-amplified) DNA fragments, Southern blot analyses, screening of genetic transformants, fungal species and strain identification (barcoding), fungal population analyses, and more. However, conventional isolation protocols apply some hazardous chemicals like liquid nitrogen, CTAB (cetyltrimethylammonium bromide), SDS (sodium dodecyl sulfate), phenol:chloroform and β-mercaptoethanol. Furthermore, common methods require sufficient amounts of starting

material, are time consuming due to extensive handling and purification steps, involve costs for chemicals and are an extra investment when applied in form of commercial kits.

Not all applications require high quality, not much sheared DNA. In recent years, alternative short-protocols were developed for isolation of DNA from fungi for applications in connection with PCR (7-15). Some of these alternatives use microwave irradiation for breaking up the fungal cell walls and membranes to release the DNA from the cells without former mechanical grinding (11-15) and in some instances this is also done without any specific lysis buffer (12-15). To our knowledge, there are currently only two reports on higher basidiomycetes (Agaricomycetes) using such technique (14,15). Nakazawa *et al.* (14) applied microwaving for quick screening of collections of transformants of the fungus *Coprinopsis cinerea* whereas Izumitsu *et al.* (15) presented a protocol for rapid DNA isolation from young mycelium grown on artificial medium and from fresh fleshy mushrooms of a range of Agaricomycetes. Here, we test these methods on fungal cultures and diverse biological materials taken from nature.

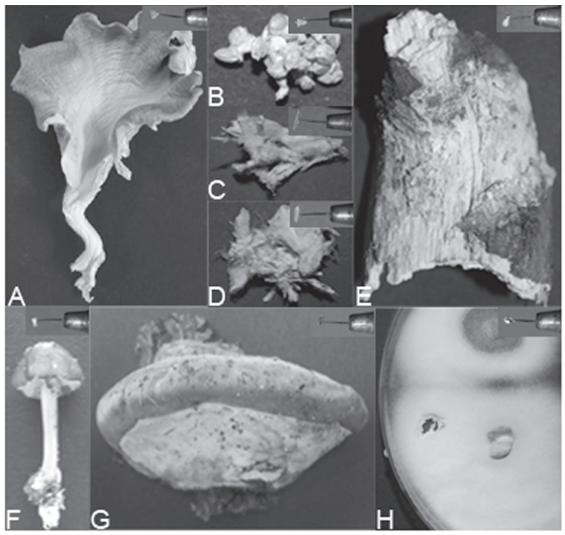

Fig. 1. Exemplary fungal materials used in this study. **A.** Dried cultivated mushroom of *Pleurotus sajor-caju*. **B.** Millet infested with *Pleurotus djamor*. **C.** Wheat straw and **D.** poplar wood chips infested with mycelium of *Coprinellus micaceus*. **E.** White-rotting lilac branch infested with *Daedaleopsis* sp.2. **F.** Fleshy *Entoloma* sp. mushroom and **G.** firm *Fomes fomentarius* fruiting body collected from the wild. **H.** Fresh mycelium of *Coprinopsis cinerea* FA2222 grown on a YMG/T agar plate. Insets in subfigures indicate amounts of material collected for microwaving.

Material and Methods

***Fungal materials*:** *C. cinerea* strain FA2222 (16) was cultivated at 37°C on solid YMG/T medium (17), *Heterobasidion irregulare* strain TC-32-1 (18) at 25°C on 2% malt extract agar (1% agar) and some unknown slow-growing basidiomycetes (kindly supplied by Prof. F. Schauer, Greifswald, Germany) at 25°C on either solid YMG/T, rich YMPS (3 g/l yeast extract, 3 g/l malt extract, 5 g/l peptone, 10 g/l sucrose, solidified by 20 g/l agar) and *Ustilago* complete medium (19). Fresh and air-dried fruiting bodies of *Pleurotus* species (*calyptratus*, *cystidiosus*, *djamor*, and *sajor-caju*) and *P. cystidiosus* and *P. djamor* mycelium grown on millet (Fig. 1A,B) were kindly supplied by A.A. Shnyreva, straw and birch and poplar wood chips infested with mycelium of *Coprinellus* species (*micaceus*, *radians* and *xanthrothrix*) by J. Barb (Fig. 1C,D). Miscellaneous fleshy and firm mushrooms grown on wood or in meadows (Fig. 1E-G) were collected from the grounds of the Goettingen University North Campus and from forests of the surroundings of Goettingen, Germany. Genera and, where possible, also species names were determined using the guide books of Breitenbach and Kränzlin (20). Purified genomic DNA of *C. cinerea* strain AmutBmut (16) was kindly supplied by Dr. B. Pickel.

***Microwaving and PCR*:** Fungal mycelium, tissue sections from basidiocarps (where possible separated in cap and stipe), and infested millet, straw and wood (Fig. 1) were directly used for DNA extraction in sterile dd$H_2$0 or TE-buffer (10 mM Tris, 1 mM EDTA; pH 8.0). A pinhead sample of mycelium from fungal cultures (ca 2 x 2 mm^2, corresponding to about 2 mg) was scraped from the surface of plates thereby taking care to avoid

the agar (Fig. 1H). Similar small samples from basidiocarps (about 5 mg; Fig. 1A,F,G) and from infested plant materials (Fig. 1B-E) were obtained by cutting with a flamed razorblade or by picking with a sterile needle. Individual samples were transferred into 1.5 ml sterile micro-centrifuge tubes (E-tubes; Sarstedt AG & Co., Nümbrecht, Germany) and 100 µl sterile ddH_2O or TE buffer were added. In standard reactions, the closed tubes were microwaved for 1 min at 600 W in a household microwave oven (MS 197 H 700W, LG Electronics Deutschland GmbH, Ratingen, Germany), shortly vortexed, stored for 30 sec at room temperature (RT) and microwaved again for 1 min at 600 W. Afterwards, tubes were transferred for about 10 min to -20°C and then centrifuged at 9.300 x *g* for 5 min at RT. Typically, 1 µl of resulting supernatants was directly used in PCR in a reaction mixture of 25 µl containing PCR buffer (final concentration: 10 mM Tris pH 8.8, 50 mM KCl, 0.1% Triton X-100), 1.5 mM $MgCl_2$, 0.2 mM dNTPs (Fermentas GmbH, St. Leon-Rot, Germany), 0.4 µM of each primer, and 1 U of *Taq* DNA polymerase. The fungal universal primers ITS1 (5'-TCCGTAGGTG AACCTGCGG-3') and ITS4 (5' -TCCTCCGCTTA TTGATATGC-3') were used for amplification of the ITS1-5.8S-ITS2 ribosomal DNA regions (21,22). Control reactions contained no DNA (negative controls) or 1.25 ng of purified genomic DNA of *C. cinerea* AmutBmut. PCR conditions were 2-min initial denaturation at 94°C, followed by 35 cycles of 30 s at 94°C, 30 s at annealing temperature of 55°C, and 30 s for primer extension at 72°C, and a final extension step at 72°C for 10 min. 5 µl per reaction were analyzed by electrophoresis on 1% agarose gels in TAE buffer (23). Gels were photographed with a Gel Doc 2000 Imaging and Documentation System and band intensities were estimated with Quantity One 4.2 software (Bio-Rad GmbH, Munich, Germany). Resulting DNA amounts were multiplied by 5 to calculate the total DNA amounts in the respective 25 µl PCR samples.

***Sample boiling and PCR*:** Mycelial and fruiting body samples of similar size than in the microwaving approach were transferred into 1.5 ml E-tubes with 100 µl sterile ddH_20. E-tubes were transferred for 1 min into boiling water, then 30 s stored at RT, a second time transferred for 1 min into boiling water and finally for 10 min into -20°C. After centrifugation at 9.300 x *g* for 5 min at RT, 1 µl of respective supernatants was applied in PCR reactions as described above.

Results and Discussion

Microwaving fungal mycelium from laboratory cultures on agar-medium in Petri dishes: Initially, we used fresh mycelium of fully grown *C. cinerea* FA2222 cultures on YMG/T plates to test the two protocols described in literature for microwaving basidiomycete samples (14,15). Main differences were the type of liquid and its volume (30 µl ddH_20 versus 100 µl TE, pH 8), the time (10 min versus 2x 1 min) and the applied power (500 W versus 600 W) of microwaving. First trials following the protocol of Nakazawa *et al.* (14) lead to explosive opening of the E-tube lids with loss of liquid and also melting of the E-tubes already after about 2 to 5 min of microwaving (Fig. 2). Such effects were not encountered with the 2x 1 min short time microwave exposure. Thus, we continued with the protocol of Izumitsu *et al.* (15). Alterations were done to change from TE buffer to ddH_20

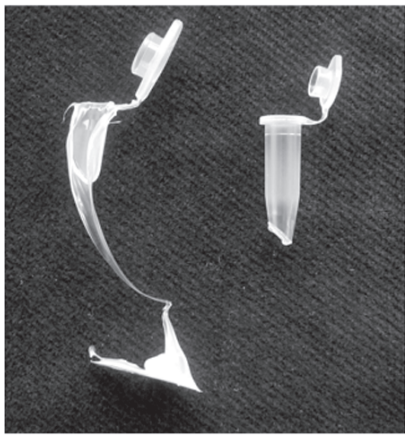

Fig. 2. 1.5 ml and 0.5 ml E-tubes after microwave treatment for 5 min at 500 W. Lids were opened, liquids were lost and tubes were molten.

with no negative consequences for subsequent PCR amplifications with primers ITS1 and ITS4 (not shown). Visible PCR bands in agarose-gels were obtained from up to 100fold dilutions of DNA-H_20 samples from fresh *C. cinerea* mycelium (Fig. 3A). Considering 60-90 copies of the rRNA gene clusters per *C. cinerea* genome (24) and a genome size of 36.2 Mb (25) and a DNA amount of 145 pg after 35 cycles of PCR amplification of the 599 bp-long ITS region from a 10fold dilution of the original sample (the dilution that still gave a reasonably visible band in a not fully saturated PCR reaction, compare Fig. 3A), about 47-70 fg genomic DNA (i.e. about 1.2 to 1.8 copies of the complete *C. cinerea* genome) should be present in 1 µl of the undiluted solution after microwaving of mycelium. In the PCRs with 1 µl of the 1:10 dilution of DNA (i.e. about 4.7-7.0 fg DNA), we expect thus originally about 7.7 - 10.6 copies of the ITS region which proofed to be sufficient for amplification of the fragment with primers ITS1 and ITS4. Similar amounts of genomic DNA have already been shown in previous studies with other lower eukaryotes to be sufficient for amplification of ITS regions by PCR (26,27). Furthermore, we even amplified a fine band in PCRs of 1 µl of the 1:100 DNA dilution (Fig. 3A) that by the above calculation originally should only have had 1.1 copies of the ITS region. Theoretically, this should result in 35 cycles in 2.5 ng DNA in total. However, the DNA amount of the fine band in Fig. 3A is possibly twice as that (5 ng) which suggests that our calculation is probably a 10fold underestimation in actual original DNA concentration.

The standard method was further used to extract and compare DNA from fresh and from 4-month old, cold-stored mycelium of *C. cinerea* from fully-grown Petri dishes, from fresh small 2-day old *C. cinerea* colonies (ca. 1 cm in Ø), from 4-month old, cold-stored mycelium from fully grown plates of *H. irregulare* and from 1 to 4 cm sized colonies of very slow growing unknown basidiomycetes that were cultivated on different media (see Material and methods) for 2 weeks to 2 months at 25°C. In total, 24 different mycelial samples of *C. cinerea*, 2 samples of *H. irregulare* and 6 samples from three unknown species were analysed. In all instances (100% of reactions), the respective ITS regions of the fungi were successfully amplified with primers ITS1 and ITS4 after microwaving, indicating that neither the age of the mycelium nor the size of colonies or the media used for cultivation of the fungi hindered DNA isolation and subsequent PCRs (Fig. 3B). Furthermore, PCR amplifications to saturation of reaction with other primers of single copy genes on fragments sized up to 3.5 kb were also possible without difficulty with 0.5 to 1 µl solution of the undiluted samples (experiments not further shown). Also these results suggest that the DNA concentration in the microwaved samples is likely somewhat higher than the amounts calculated above.

Izumitsu *et al.* (15) in their studies used always fresh mycelium (4 to 6 days old). These authors applied the technique to mycelium of the Agaricales *Agaricus bisporus*, *Lentinula edodes*, *Flammulina velutipes*, *Pleurotus eryngii*, *Pleurotus pulmonarius*, *Hypsizygus marmoreus*, *Grifola frondosa*, and *Mycena chlorophos*. Our analysis expands the range of species to which the technique was successfully applied to. Important new findings from our study are that quite old mycelium and also very small cultures can be used for microwave-preparation of DNA. The latter is especially beneficial for species determination of fungi that are difficult to grow and of which therefore only relative old mycelium in minute amounts can be available.

Microwaving mycelium from infested plant substrates: Basidiomycetes often infest dead or living recalcitrant plant materials and it is not easy to obtain fungal DNA in quantity and of quality from such substrates. Co-extracted ingredients from the complex organic substrates such as organic acids or phenolic compounds can have an inhibiting effect on the PCR reaction (28-31). Therefore, small samples of infested millet, straw, wood and bark samples (Fig. 1B-E) were directly used in DNA extraction by microwaving as

Vol. 7 (4) 825-836 October 2013, ISSN 0973-8916 (Print), 2230-7303 (Online)

examples of fungal infected plant materials. ITS regions were successfully amplified by PCR from all microwaved samples of the two tested *Pleurotus* species (Fig. 3C) cultivated for 3 months at RT on millet (each species was tested 2x) and of the three different *Coprinellus* species (Fig. 3D, *C. micaceus* is exemplarily shown) kept for 4 months under laboratory conditions in jars on moisturized straw, on birch and on poplar wood chips (each two samples per substrate were tested for *C. micaceus* and each one sample per substrate for *C. radians* and *C. xanthrothrix*).

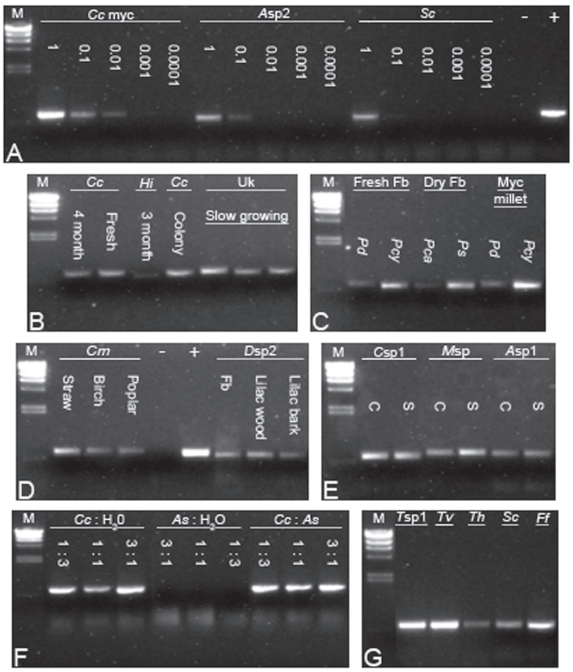

Fig. 3. Analysis of PCR amplifications of fungal ITS regions with primers ITS1 and ITS4 on 1% agarose gels, using per reaction 1 µl of solution after microwaving fungal materials by the standard method if not otherwise stated. **A.** Serial dilution of DNA solution (1 to 10^{-4} µl) from fresh *Coprinopsis cinerea* FA2222 mycelium (*Cc* myc), a fresh fleshy *Agrocybe* sp.2 fruiting body (*A*sp2) and a firm *Schizophyllum commune* fruiting body (*Sc*). **B.** Samples from a 4-month old *C. cinerea* culture, fresh mycelium from the outer region of a fully grown 9 cm Petri dish culture of *C. cinerea*, a 4-month old *Heterobasidion irregulare* (*Hi*) culture, an 1 cm sized 2-day-old *C. cinerea* colony, and three different unknown slow-growing basidiomycetes (Uk). **C.** Samples from fresh fruiting bodies (Fb) and mycelium (Myc) on millet of *Pleurotus djamor* (*Pd*) and *Pleurotus cystidiosus* (*Pcy*) and dried fruiting bodies of *Pleurotus calyptratus* (*Pca*) and *Pleurotus sajor-caju* (*Ps*). **D.** Samples from straw and birch and poplar wood chips infested with *Coprinellus micaceus* (*Cm*) and a sample of a firm *Daedaleopsis* sp.2 (*D*sp2) fruiting body compared with samples of lilac wood and bark infested by the same fungus. **E.** Samples from exemplary fleshy mushrooms: *Conocybe* sp.1 (*C*sp1), *Mycena* sp. (*M*sp) and *Agrocybe* sp.1 (*A*sp1). **F.** PCR reactions of 1 µl from 1:3, 1:1 and 3:1 ddH_2O diluted samples of pure genomic DNA of *C. cinerea* (*Cc*) AmutBmut (which corresponds to 0.3 , 0.6 and 0.9 ng, respectively) and of mere solution (0.75, 0.5 and 0.25 µl, respectively) of microwaved *Amanita strobiliformis* cap tissue (*As*) in comparison with 1:3, 1:1 and 3:1 mixtures of both. **G.** Samples of exemplary tough mushrooms: *Trametes* sp.1 (*T*sp1), *Trametes versicolor* (*Tv*), *Trametes hirsuta* (*Th*), *S. commune* (*Sc*) and *Fomes fomentarius* (*Ff*). Lanes marked M = 200 ng Lambda DNA/*Hin*dIII marker, + = positive PCR control performed with 1.25 ng purified genomic AmutBmut DNA, - = negative control. Positive and negative controls were done in all series of PCR amplifications although the controls are shown here only in some cases.

Microwave based DNA extraction

The samples from the laboratory were from pure cultures of single organisms and characterized by presence of surface mycelium, factors which both could ease the release of enough fungal DNA into solution. Therefore, we also tried unsterile bark and white-rotted wood from infested dying branches of *Ribes sanguineum* (red-flowering currant) and *Syringae tigerstedtii* (lilac) bushes (each two samples per type of substrate and plant species). Only one bark and one wood sample of the lilac functioned subsequently in PCR (Fig. 3D). Samples of decaying deadwood of beech were also unsuccessfully applied in microwaving and PCR. In total, only 1/6 wood samples and 1/4 bark samples from wild collections resulted in PCR bands. Positive samples had strong fresh mycelium on the surface. Samples with some dried mycelium on the surface and samples with no surface mycelium were ineffective. The results indicate that the microwave technique has only limited application for wood samples. However, this differs not from other techniques applied in fungal DNA isolation from wooden substrate for PCR amplifications (30,31).

Microwaving tissues from fleshy fruiting bodies: DNA was extracted by the standard microwaving method from cap samples of fresh *P. cystidiosus and P. djamor* fruiting bodies cultivated in the lab and from cap and stipe samples from fresh fleshy fruiting bodies from seven different species (*Amanita strobiliformis*, *Agrocybe* sp.1, *Agrocybe* sp.2, *Conocybe* sp.1, *Conocybe* sp.2, *Entoloma* sp., *Mycena* sp., *Psathyrella* sp.) taken from nature. From all species except *A. strobiliformis* (Fig. 3F), it was possible with primers ITS1 and ITS4 to amplify in PCR the respective ITS-regions after microwaving (see examples in Fig. 3A,E). Izumitsu *et al.* (15) reported in their studies that success with wild mushrooms was greater with stipe than with gill tissue [95.3% (41/43 tested cases) versus 73.5% (25/34 of tested cases) positive reactions]. Instead of gills, we used always inner pileus tissue from the caps but success rates were similar to those obtained by Izumitsu *et al.* (15) with gills. Apart from *A. strobiliformis*, 76.9% (10/13) of all cap samples and 90.9% (10/11) of all stipe samples from wild mushrooms gave positive results in PCR. Furthermore, ITS bands were obtained in PCR from all *Pleurotus* cap samples (2 per species) (Fig. 3C). In conclusion from this series of experiments, we can confirm the earlier observation of Izumitsu *et al.* (15) that the microwave technique can easily be applied to most fresh fleshy mushrooms. Izumitsu *et al.* (15) successfully isolated DNA from fleshy mushrooms of cultivated species (*A. bisporus*, *L. edodes*, *F. velutipes*, *P. eryngii*, *G. frondosa*, *H. marmoreus*) and of species collected from the wild [*Agrocybe chaxingu*, 9 different *Amanita* species (*flavipes*, *farinosa*, *fritillaria*, *fuliginea*, *oberwinklerana*, *imazekii*, *sychnopyramis* f. *subannulata*, *vaginata*, sp.), *Boletus rubropunctus*, *Cantharellus cibarius*, *Hymenopellis raphanipes*, 2 different *Inocybe* species (*sphaerospora*, sp.), 4 different *Russula* species (*crustosa*, *mariae*, *subnigricans*, cf. *subnigricans*), *Tricholoma bakamatsutake*]. Together with our study, this gives in total 35 different species from 18 different genera and 17 different families of which DNA of sufficient amount and quality for PCR amplifications of ITS regions was obtained from microwaving fresh fruiting body tissues.

Following the standard protocol, we unsuccessfully tested in total 3 cap samples and 2 stipe samples from fresh mushrooms of *A. strobiliformis* collected at two different occasions from underneath a birch tree. Also PCR with 10 fold sample dilutions did not lead to amplification of the ITS region and neither PCRs with 5 µl and with 10 µl of undiluted solution per sample. The ITS4 primer (combined with a primer ITS1F) has previously been shown to work on isolated DNA of this species (32) and the ITS1 primer in combination with ITS4 on several closely related *Amanita* species (33) and both primers work perfectly with multiple species over the broad range of Agaricomycetes and also other fungi (21,22,31-34, this study). It is therefore not likely

that the failure in PCR with *A. strobiliformis* samples based simply on unsuitability of the two primers. As another possibility, some type of metabolic product(s) of the fungus could hinder the PCR reactions. Therefore, a set of PCR reactions was done in which aliquots from microwaved *A. strobiliformis* cap tissues (0.75 to 0.25 µl) and purified genomic *C. cinerea* AmutBmut DNA (0.3 ng to 0.9 ng) were mixed, parallel to PCRs with only respective aliquots of *A. strobiliformis* material and PCRs with respective amounts of pure *C. cinerea* DNA. All PCR reactions with *C. cinerea* DNA gave strong bands of identical size (corresponding to the *C. cinerea* ITS region) in agarose gels unlike the PCRs with only aliquots from microwaving *A. strobiliformis* tissues (Fig. 3F), implying that the cause of failure in PCR is not an inhibitor within the samples. As another reason, it might just be that microwaving did not freely release the *A. strobiliformis* DNA from the hyphal cells into solution or that released DNA was quickly degraded (see discussion below).

Fleshy mushrooms tend to have only a very short life time due to fast onset of decay, even when stored at colder temperature. Not surprisingly therefore, we were not anymore able to obtain DNA functional in PCR from disintegrating mushrooms such as *Conocybe* sp. when stored for one week in the fridge (not further shown). However, experiments with pileus tissues from air-dried mushrooms from *P. sajor-caju* and *P. calyptratus* (stored for 4 weeks at RT) showed that it is also possible to employ freshly harvested and directly dried mushrooms for later use in DNA preparations for PCR (Fig. 3C).

Microwaving tissues from fruiting bodies of tough structure: New in this study, DNA was extracted by the microwave-based method also from cap tissues of collections of firm durable bracket fungi that are characterized by a tougher and fairly dry consistency. With increasing degree of toughness, we divided mushrooms collected in nature from wood logs and infested branches into fruiting bodies with leathery structure (*Daedaleopsis* sp.1, *Schizophyllum commune*, *Trametes versicolor*, *Trametes* sp.1), corky texture (*Trametes hirsuta*, *Trametes* sp.2) and woody appearance (*Daedaleopsis* sp.2 grown on the *S. tigerstedtii* branch analysed above, *Ganoderma* sp., *Fomes fomentarius*). Microwaving for DNA isolation was done when the fruiting bodies were freshly collected as well as after storage for two and a half months at 5°C, resulting in 2 to 4 reactions per species. PCR reactions were successful for 23 of the 25 samples analysed in total (92%) and from every species at least one of two samples were positive regardless of their degree of rigidity (see positive results of five exemplary species in Fig. 3G). Notably, the size of the amplified ITS fragment of the *Daedaleopsis* sp.2 fruiting body was identical to those obtained from the bark and the branch of *S. tigerstedtii* on which the fruiting body grew on (Fig. 3D).

Taken the same parameters as used above for the calculation of the *C. cinerea* DNA concentrations, DNA amounts obtained from bracket fungi were comparable to amounts from fleshy mushrooms (ca. 8 fg/µl) but about 10fold lower than DNA amounts obtained from fresh mycelia (Fig. 3A). The experiments also revealed that tough, fairly dry bracket fungi can be accessible for DNA extraction by microwaving even after longer storage. However, we also tested tissues of two different decomposing *Trametes* fruiting bodies of rubbery-crumby consistency (collected from rotting wood) but the decay of the specimens was apparently too advanced to still result in quality DNA isolation.

Further analysis of the method: Microwaving can affect the biological material in two ways, by its electromagnetic field ("non-thermal-effect") and by the heat it produces (35-41). Heat can also be applied to cells just by boiling. Accordingly, some rapid DNA extraction procedures for PCR applications appoint (repetitive) quick heating (e.g. to 95-100°C between 1 and 30 min) and rapid cooling (8,9). Here, we also tested the effect of boiling on DNA-release from *C. cinerea* mycelium and from a

selection of mushrooms of different textures. In subsequent PCRs, no major difference was observed between DNA obtained from a material by the microwaving procedure and by the boiling procedure described in detail in the methods section (Fig. 4). In conclusion, heat must be a main factor for the release of DNA from the cells and both methods might be used.

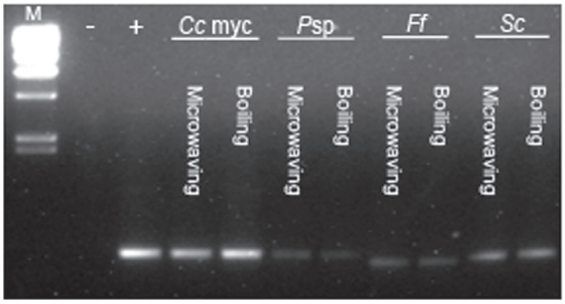

Fig. 4. Comparison of PCR amplifications of fungal ITS regions with primers ITS1 and ITS4 on 1% agarose gels, using per reaction 1 µl of solution after microwaving and after boiling of samples from fresh *Coprinopsis cinerea* mycelium (*Cc* myc), a fresh fleshy *Psathyrella* sp. mushroom (*P*sp), and firm fruiting bodies of *Fomes fomentarius* (*Ff*) and *Schizophyllum commune* (*Sc*). Lanes marked M = 200 ng Lambda DNA/*Hin*dIII marker, + = positive PCR control performed with 1.25 ng purified genomic AmutBmut DNA, - = negative control.

Comparing the two principles, the general handling of microwaving is easier and much faster since no bath of boiling water has to be prepared and there is no danger of burning oneself with the hot water when moving samples in or out. Importantly, Stroop and Schaefer (35) pointed out that microwaves are less aggressive in breaking down DNA and preserve the DNA chain lengths better than heat treatment at the boiling point of water. In cells, electromagnetic fields produced by microwaves are understood in non-thermal manner to affect the cell membrane integrity and to cause pore formation. This eventually leads to cellular leakage of proteins, electrolytes and DNA (36-39). Microwaves in dose-dependent manner also cause opening of DNA double-strands below their melting temperature (40) and may result in single- and double-strand breaks such as under influence of certain metal ions (41). We tested different irradiation schemes on fresh *C. cinerea* mycelium and on tissue samples of fresh fleshy, corky and woody mushrooms. Time of irradiation mattered for good yields in PCR amplification in case of the mushrooms but less in case of the generally more effective vegetative mycelium (Fig. 5). Shorter 1-min irradiation was better for mushroom tissues than in total 2-min irradiation, regardless of whether done as in the standard protocol in two 1-min steps or whether done consecutively. Since there was a decrease up to failure in DNA amplification by PCR upon longer microwaving (Fig. 5), it must be assumed that (parts of) released DNA will be degraded through microwaving in the liquid. Izumitsu *et al.* (15) stated that the 10-min -20°C freezing step in the protocol was optional. In our reactions, application of a freezing step appeared sometimes sub-optimal compared to non-freezing (Fig. 5). Since the quality assay in our study for DNA release is a PCR reaction that does not depend on double-stranded DNA, it is not as likely that due to quick freezing a problem was generated by lack of reformation of DNA double-strands. More likely appears that slower cooling down to RT will allow longer permeability of the membranes made porous by the rotational energy transferred onto dipole molecules within the membranes through the microwaves (38) and, in consequence, more leakage of DNA from the cells. Such longer DNA release may then compensate former decline by microwave-induced DNA degradation. If such different effects function at the same time, the results will be more visible in samples from mushrooms releasing less easily higher amounts of DNA than in samples from vegetative mycelium being more effective in the DNA release. In conclusion, while the standard protocol of microwaving as given in the methods might be applied for vegetative mycelium as it is, for mushroom samples a single 1-min treatment with cooling down to RT appears to be the better choice for future studies.

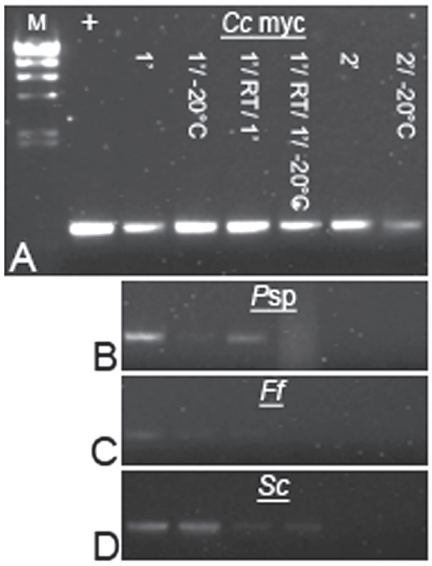

Fig. 5. Comparison of PCR amplifications of fungal ITS regions with primers ITS1 and ITS4 on 1% agarose gels, using per reaction 1 µl of solution after microwaving under different irradiation schemes, with and without subsequent 10-min freezing at -20°C. **A.** Samples from fresh *Coprinopsis cinerea* mycelium (*Cc* myc), **B.** a fresh fleshy *Psathyrella* sp. mushroom (*P*sp), and firm fruiting bodies of **C.** *Fomes fomentarius* (*Ff*) and **D.** *Schizophyllum commune* (*Sc*), loaded in the same order of irradiation schemes. Applied irradiation schemes: 1 min irradiation (1'); 1 min irradiation with subsequent 10-min freezing at -20°C (1'/ -20°C); 1 min irradiation followed by 30 sec at RT and another 1 min irradiation (1'/ RT/ 1'); 1 min irradiation followed by 30 sec at RT, 1 min irradiation and subsequent 10-min freezing at -20°C (1'/ RT/ 1'/ -20°C); 2 min of continued irradiation without (2') and with freezing (2'/-20°C). Lanes marked M = 200 ng Lambda DNA/*Hin*dIII marker, + = positive PCR control performed with 1.25 ng purified genomic AmutBmut DNA. Negative control not shown.

Conclusions

In this study, we successfully tested the rapid and cheap microwaving-protocol recently published by Izumitsu *et al.* (15) for DNA extraction from vegetative mycelium and fleshy mushrooms of Agaricomycetes for subsequent applications in PCR amplifications. As Izumitsu *et al.* (15), we observed highest success rates with this method. 100% of all mycelial samples and 76.9 to 90.9% of samples from fresh fleshy mushrooms gave positive results in subsequent PCR amplifications. In addition to verifying the observations of the former publication, we show here that the technique can also be applied to very old mycelium of well growing species, to poorly growing mycelium, and to mycelium growing on diverse plant materials. Low success rates in subsequent PCR amplifications were only encountered with infested wood and bark collected from nature but such material presents a general resisting problem in fungal DNA isolation (30,31). In this study, the method was furthermore effectively applied to dried mushrooms and to fruiting bodies of tough and dryer structures. In total, 92% of samples of firm bracket fungi performed positively in PCR amplifications.

In summary, the standard protocol is suitable for extraction of fungal DNA for PCR amplifications of non-cultivable species, slow and poorly growing species, old cultures, and of fresh and dried fleshy and tough fruiting bodies. However, the results show that shorter times of microwaving (1x1 min) should be applied for mushrooms and that the 10-min freezing at -20°C is better omitted in favour of slowly cooling down to RT. Overall, the method of DNA extraction by microwaving is rapid and easily performed within minutes, and needs only tiny amounts of fungal material and no expensive and hazardous chemicals. Negative effects by release of inhibitors of PCR amplifications were not observed. Furthermore, the ease of handling with minimal labour and time input enables simultaneous treatment of large numbers of samples.

Acknowledgements

We are indebted to Prof. F. Schauer for sending us slow growing unknown fungal strains and to colleagues and students from our group who supplied material for this study (Dr. B. Pickel, A.A. Shnyreva, J. Barb) and observations on first experimental trials of the methods (Y. Yu) and who helped to cultivate fungi (M.-C. Hsieh, M.

Zomorrodi) and in collecting mushrooms (K.K.R. Lakkireddy, A.-K. Straten).

References

1. Raeder, U. and Broda, P. (1985). Rapid preparation of DNA from filamentous fungi. Letters in Applied Microbiology, 1: 17-20.
2. Zolan, M.E. and Pukkila, P.J. (1986). Inheritance of DNA methylation in *Coprinus cinereus*. Molecular and Cellular Biology, 6: 195-200.
3. Mutasa, E.S., Tymon, A.M., Göttgens, B., Mellon, F.M., Little, P.F.R. and Casselton, L.A. (1990). Molecular organization of an *A* mating type factor of the basidiomycete fungus *Coprinus cinereus*. Current Genetics, 18: 223-229.
4. Möller, E.M., Bahnweg, G., Sandermann, H. and Geiger, H.H. (1992). A simple and efficient protocol for isolation of high molecular weight DNA from filamentous fungi, fruit bodies, and infected plant tissues. Nucleic Acids Research, 20: 6115-6116.
5. Van Burik, J.-A.H., Schreckhise, R.W., White, T.C., Bowden, R.A. and Myerson, D. (1998). Comparison of six extraction techniques for isolation of DNA from filamentous fungi. Medical Mycology, 36: 299-303.
6. Osmundson, T.W., Eyre, C.A., Hayden, K.M., Dhillon, J. and Garbelotto, M.M. (2013). Back to basics: an evaluation of NaOH and alternative rapid DNA extraction protocols for DNA barcoding, genotyping, and disease diagnostics from fungal and oomycete samples. Molecular Ecology Resources, 13: 66-74.
7. Cenis, J.L. (1992). Rapid extraction of fungal DNA for PCR amplification. Nucleic Acids Research, 20: 2380.
8. Manian, S., Sreenivasaprasad, S. and Mills, P.R. (2001). DNA extraction method for PCR in mycorrhizal fungi. Letters in Applied Microbiology, 33: 307-310.
9. Griffin, D.W., Kellogg, C.A., Peak, K.K. and Shinn, E.A. (2002). A rapid and efficient assay for extracting DNA from fungi. Letters in Applied Microbiology, 34: 210-214.
10. Zhang, Y.J., Zhang, S., Liu, X.Z., Wen, H.A. and Wang, M. (2010). A simple method of genomic DNA extraction suitable for analysis of bulk fungal strains. Letters in Applied Microbiology, 51: 114-118.
11. Goodwin, D.C. and Lee, S.B. (1993). Microwave miniprep of total genomic DNA from fungi, plants, protists and animals for PCR. BioTechniques, 15: 438, 441-442, 444.
12. Tendulkar, S.R., Gupta, A. and Chatto, B.B. (2003). A simple protocol for isolation of fungal DNA. Biotechnology Letters, 25: 1941-1944.
13. Suzuki, S., Taketani, H., Kusumoto, K.-I. and Kashiwagi, Y. (2006). High-throughput genotyping of filamentous fungus *Aspergillus oryzae* based on colony direct polymerase chain reaction. Journal of Bioscience and Bioengineering, 102: 572-574.
14. Nakazawa, T., Ando, Y., Kitaaki, K., Nakahori, K. and Kamada, T. (2011). Efficient gene targeting in Δ*Cc.ku70* or Δ*Cc.lig4* mutants of the agaricomycete *Coprinopsis cinerea*. Fungal Genetics and Biology, 48: 939-946.
15. Izumitsu, K., Hatoh, K., Sumita, T., Kitade, Y., Morita, A., Gafur, A., Ohta, A., Kawai, M., Yamanaka, T., Neda, H., Ota, Y. and Tanaka, C. (2012). Rapid and simple preparation of mushroom DNA directly from colonies and fruiting bodies for PCR. Mycoscience, 53: 396-401.
16. Kertesz-Chaloupková, K., Walser, P.J., Granado, J.D., Aebi, M. and Kües, U. (1998). Blue light overrides repression of asexual sporulation by mating type genes in the

basidiomycete *Coprinus cinereus*. Fungal Genetics and Biology, 23: 95-109.

17. Granado, J.D., Kertesz-Chaloupková, K., Aebi, M. and Kües, U. (1997). Restriction enzyme-mediated DNA integration in *Coprinus cinereus*. Molecular and General Genetics, 256: 28-36.

18. Olson, Å., Aerts, A., Asiegbu, F., Belbahri, L., Bouzid, O., Broberg, A., Canbäck, B., Coutinho, P.M., Cullen, D., Dalman, K., Deflorio, G., Diepen, L.T.A., Dunand, C., Duplessis, S., Durling, M., Gonthier, P., Grimwood, J., Fossdal, C.G., Hansson, D., Henrissat, B., Hietala, A., Himmelstrand, K., Hoffmeister, D., Högberg, N., James, T.Y., Karlsson, M., Kohler, A., Kües, U., Lee, Y.H., Lin, Y.C., Lind, M., Lindquist, E., Lombard, V., Lucas, S., Lundén, K., Morin, E., Murat, C., Park, J., Raffaello, T., Rouzé, P., Salamov, A., Schmutz, J., Solheim, H., Ståhlberg, J., Vélëz, H., Vries, R.P., Wiebenga, A., Woodward, S., Yakovlev, I., Garbelotto, M., Martin, F., Grigoriev, I.V. and Stenlid, J. (2012). Insight into trade-off between wood decay and parasitism from the genome of a fungal forest pathogen. New Phytologist, 194: 1001–1013.

19. Walser, J.P., Hollenstein, M., Klaus, M.J. and Kües, U. (2001). Genetic analysis of basidiomycete fungi. In: Talbot, N.J. (Ed.), Molecular and cellular biology of filamentous fungi – A pratical approach. Oxford University Press, Oxford, UK, pp. 59-90.

20. Breitenbach, J. and Kränzlin, F. (1984). Fungi of Switzerland, Vol. 2-4. Mykologia, Lucerne, Switzerland.

21. White, T.J., Bruns, T., Lee, S. and Taylor, J.W. (1990). Amplification and direct sequencing of fungal ribosomal RNA genes for phylogenetics. In: Innis, M.A., Gelfand, D.H., Sninsky, J.J. and White, T.J. (Eds.), PCR Protocols: A Guide to Methods and Applications. Academic Press, New York, USA, pp. 315-322.

22. Gardes, M. and Burns, D. (1993). ITS primers with enhanced specificity for basidiomycetes – application to the identification of mycorrhizae and rusts. Molecular Ecology, 2: 113-118.

23. Sambrook, R. and Russell, D.W. (2001). Molecular cloning – A laboratory manual (3rd ed.), Vol. 3. Cold Spring Harbor Laboratory Press, Cold Spring Harbor, New York, USA.

24. Cassidy, J.R., Moore, D., Lu, B.C. and Pukkila, P.J. (1984). Unusual organization and lack of recombination in the ribosomal RNA genes of *Coprinus cinereus*. Current Genetics, 8: 607-613.

25. Stajich, J.E., Wilke, S.K., Ahrén, D., Au, C.H., Birren, B.W., Borodovsky, M., Burns, C., Canbäck, B., Casselton, L.A., Cheng, C.K., Deng, J., Dietrich, F.S., Fargo, D.C., Farmann, M.L., Gathman, A.C., Goldberg, J., Guigó, R., Hoegger, P.J., Hooker, J.B., Huggins, A., James, T.Y., Kamada, T., Kilaru, S., Kodira, C., Kües, U., Kupfer, D., Kwang, H.S., Lomsadze, A., Lin, W., Lilly, W.W., Ma, L.J., Mackey, A.J., Manning, G., Martin, F., Muraguchi, H., Natvig, D.O., Palmerini, H., Ramesh, M.A., Rehmeyer, C.J., Roe, B.A., Shenoy, N., Stankea, M., Ter-Hovhannisyan, V., Tunlid, A., Velagapudi, R., Visione, T.J., Zeng, Q., Zolan, M.E. and Pukkila, P.J. (2010). Insights into evolution of multicellular fungi from the assembled chromosomes of the mushroom *Coprinopsis cinerea* (*Coprinus cinereus*). PNAS, 107: 11889-11894.

26. Chandelier, A., Ivors, K., Garbelotto, M., Zini, J., Laurent, F. and Cavelier, M. (2006). Validation of a real-time PCR method for the detection of *Phytophthora ramorum*. Bulletin OEPP, 36: 409-414.

27. Lorch, J.M., Gargas, A., Uphoff Meteyer, C., Berlowski-Zier, B.M., Green, D.E., Shearn-Bochsler, V., Thomas, N.J. and Blehert, D.S. (2010). Rapid polymerase chain reaction diagnosis of white-nose syndrome in bats.

Journal of Veterinary Diagnostics Investigation, 22: 224-230.

28. Wilson, I.G. (1997). Inhibition and facilitation of nucleic acid amplification. Applied and Environmental Microbiology, 63: 3741-3751.
29. Rachmayanti, Y., Leinemann, L., Gailing, O. and Finkeldey, R. (2006). Extraction, amplification and characterization of wood DNA from Dipterocarpaceae. Plant Molecular Biology Reporter, 24: 45-55.
30. Hoegger, P.J. and Kües, U. (2007). Molecular detection of fungi in wood. In: Kües, U. (Ed.), Wood production, wood technology, and biotechnological impacts. Goettingen University Press, Goettingen, Germany, pp. 159-177.
31. Jasalavich, C.A., Ostrofsky, A. and Jellison, J. (2000). Detection and identification of decay fungi in spruce wood by restriction fragment length polymorphism analysis of amplified genes encoding rRNA. Applied and Environmental Microbiology, 66: 4725-4734.
32. González, V., Arenal, F., Platas, G., Esteve-Raventós, F. and Peláez, F. (2002). Molecular typing of Spanish species of *Amanita* by restriction analysis of the ITS region of the DNA. Mycological Research, 106: 903-910.
33. Kårén, O., Högberg, N., Dahlberg, A., Jonsson, L. and Nylund, J.-E. (1997). Inter- and intraspecific variation in the ITS region of rDNA of ectomycorrhizal fungi in Fennoscandia as detected by endonuclease analysis. New Phytologist, 136: 313-325.
34. Naumann, A., Navarro-González, M., Sánchez-Hernández, O., Hoegger P.J. and Kües, U. (2007). Correct identification of wood-inhabiting fungi by ITS analysis. Current Trends in Biotechnology and Pharmacy, 1: 41-61.
35. Stroop, W.G. and Schaefer, D.G. (1989). Comparative effect of microwaves and boiling on the denaturation of DNA. Analytical Biochemistry, 182: 222-225.
36. Ponne, C.T. and Bartels, P.V. (1995). Interaction of electromagnetic energy with biological material-relation to food processing. Radiation Physics and Chemistry, 45: 591-607.
37. Shamis, Y., Croft, R., Taube, A., Crawford, R.J. and Ivanova, E.P. (2012). Review of the specific effects of microwave radiation on bacterial cells. Applied and Environmental Microbiology, 96: 319-325.
38. Campanha, N.H., Pavarina, A.C., Brunetti, I.L., Vergani, C. E., Machado, A. L. and Spolidorio, D.M.P. (2007). *Candida albicans* inactivation and cell membrane integrity damage by microwave irradiation. Mycoses, 50: 140-147.
39. Campanha, N.H., Jorge, J.H., Giampaolo, E.T., Martins de Oliveira, C.S.B., Nor di Dovigo, L., G. Maia, D.G. and Pavarina, A.C. (2013). Cell membrane integrity of *Candida albicans* after different protocols of microwave irradiation. American Journal of Infectious Diseases and Microbiology, 1: 38-45.
40. Edwards, W.F., Young, D.D. and Deiters, A. (2009). The effect of microwave irradiation on DNA hybridization. Organic & Biomolecular Chemistry, 7: 2506-2508.
41. Sagripanti, J.L., Swicord, M.L. and Davis, C.C. (1987). Microwave effects on plasmid DNA. Radiation Research, 110: 219-231.

Current Trends in Biotechnology and Pharmacy
Vol. 7 (4) 837-846 October 2013, ISSN 0973-8916 (Print), 2230-7303 (Online)

Maximum Phenylalanine Ammonium Lyase (PAL) Enzyme activity at Mid Stage of Growth Imparts Highest Hypoglycemic Property to Fenugreek

Imtiyaz Murtaza[1]*, Omi Laila[1,3], M .Z .Abdin[3]*, Kousar Parveen[2], Tariq Raja[1], Sheikh Abid Ali[1] and Girish Sharma[4],

. [1]Biochemistry and Molecular Biotechnology Laboratory, Division of Post-Harvest Technology, SKUAST-K, Shalimar campus-191121, Jammu and Kashmir, India..
[2]Division of Vegetable Sciences, SKUAST-K, Shalimar campus-191121, Jammu and Kashmir, India.
[3]Centre for transgenic plant development, Department of Biotechnology, Jamia Hamdard, Hamdard Nagar, New Delhi-110062, India
[4]Dept. of Biotechnology, Amity University, Noida, UP-201303, India
*For Correspondence - imz_murtaza@hotmail.com; mzabdin@rediffmail.com

Abstract

PAL catalyzes the first step in the biosynthesis of phenylpropanoids, which are further modified into a wide variety of phenolic compounds. In the current study, we estimated the change in PAL enzyme activity and total phenol content in six cultivars of fenugreek (ML1-ML6) seeds and vegetative green leafy parts of their respective plants taken at early, mid and late stages of growth. The results obtained were correlated with their respective hypoglycemic activities. Our study demonstrated that, at the mid stage of growth all the cultivars showed maximum PAL activity with simultaneous increase in phenol production and hypoglycemic activities. The results of this study taken together suggest that all the fenugreek cultivars possess good hypoglycemic activity that is directly related to increase in total phenol content and PAL activity. Among six selected cultivars, ML-2 cultivar in addition to possess maximum hypoglycemic activity in terms of inhibiting α-amylase (72.53 %) and α-glucosidase (52 %) activities also showed maximum PAL enzyme activity (0.01008 μM cinnamic acid/mg protein / min) as well as total phenol production (560 mg/ 100g fresh weight) at mid stage of growth. A highly significant correlation was found between PAL activity and total phenols (r=0.759) which were significantly correlated with α-amylase inhibitory activity (r=0.439, r='0.690 respectively) as well as with α glucosidase inhibitory activity (r=0.507, r=0.552 respectively). It was observed that extracts from such cultivars especially that of ML2 cultivar taken at mid stage of growth when incorporated into diet could act as a potential chemopreventive functional food for better management of hyperglycemia.

Keywords: Fenugreek, Phenylalanine Ammonium Lyase, Phenols, α-amylase, α-glucosidase**,** hypoglycemic activity.

Introduction

Diabetes is a major health problem predisposing to markedly increased complications. The frequency of this disorder is on the rise globally, and is likely to hit 300 million by 2025, with India projected to have the largest number of diabetic cases (1). The modern medicines available for management of diabetes exert serious side effects such as hepatotoxicity, abdominal pain, flatulence, diarrhea, and acute hypoglycemia including drug resistance (2). For this reason, a less expensive phytomedicine capable of treating the disease at early stages will be of great help to the diabetic patients, especially due to the extended belief that natural

treatments with fewer side effects cause less harm to the organism (3). Therefore, apart from currently available therapeutic options, many herbal medicines have been designed for treatment of diabetes. However, the World Health Organization expert committee on diabetes has recommended that such methods of treatment should be further investigated in order to make them realistic possibilities for proper management of diabetes (4).

In plants, the phenolic metabolism is governed by an important key enzyme of phenylpropnoid metabolic pathway called Phenylalanine Ammonium Lyase (PAL). It catalysis the deamination, of L-Phenylalanine to produce the trans–cinnamic acid that is primary intermediary in the biosynthesis of phenolics (5). Recent studies have shown that PAL activity is directly correlated with the production of phenolic compounds and its high activity has been reported to be associated with the accumulation of anthocyanins and other phenolic compounds in fruit tissues of several species (6). Thus, catalytic step by PAL enzyme in plants is considered to be the first commited step for the biosynthesis of the phenylpropanoid skelton that can be used for the synthesis of phenolics, flavonoids, phenylpropane and lignins (7) and such secondary metabolites especially phenolic constituents have been reported to be involved in retardation of α amylase as well as in α glucosidase enzyme activities (8). These two enzymes are involved in starch breakdown and intestinal glucose absorption respectively. Unfortunately, plants with such compounds have not yet gained much importance due to the lack of sustained scientific evidence, even knowing that currently available inhibitors in clinical use have their limitations, are non-specific, produce serious side effects and even elevate diabetic complications. Fenugreek (*Trigonella foenum graecum*) plant indigenous to the Mediterrian region, Ukraine, India and China has received a great deal of attention in medical research for its antidiabetic activity against both type I and type II diabetes (2). In addition to alkaloids and steroids, the antidiabetic activity of fenugreek has mainly been attributed to its phenolic compounds which are also involved in plant defense against various toxic insults including oxidative stress, abiotic and biotic stresses (9).

Therefore, in the current study an attempt has been made to contribute to this field of research by investigating extracts from six cultivars of fenugreek seeds as well as their respective green leafy parts at different stages of growth for their respective PAL activities as well as total phenolic compounds. Simultaneously, α-amylase and α-glycosidase inhibiting activities of each extract was determined and correlated with PLA and total phenols for development of functional food against diabetes.

Materials and Methods

Chemicals: All the chemicals and reagents used in this current study were of analytical reagent grade. α-glucosidase and 4-nitrophenyl α-D-glucopyranoside were obtained from Sigma Aldrich (India) while cinnamic acid, catechol, phenylalanine and dinitrosalicylic acid (DNSA) from SRL Pvt. Ltd. (Mumbai, India). Starch, sodium carbonate ethanol, sodium phosphate monobasic (Na_2HPO_4), sodium phosphate (NaH_2PO_4) dibasic, sodium potassium tartrate, and sodium hydroxide (NaOH), were purchased from Qualigens, (Mumbai, India). Porcine pancreatic α-amylase and sodium chloride (NaCl) were obtained from Hi Media Laboratories (Mumbai, India).

Plant Material. : For the current investigation, 100% pure and promising seeds belonging to six different cultivars of fenugreek were collected from the local market as well as from the Division of Vegetable Sciences, Sher-e-Kashmir University of Agricultural Sciences and Technology, Shalimar, Kashmir, India. The seeds collected from SKUAST-K were ML1 (Methi Shalimar), ML2 (6AGR), ML3 (Shalimar improved), ML4 (SAW) and ML5 (Methi local). Whereas ML6 (Kasuri methi) was collected from local market. All the seeds were identified by

Vol. 7 (4) 837-846 October 2013, ISSN 0973-8916 (Print), 2230-7303 (Online)

subject expert from the Division of Vegetable Sciences, SKUAST-K, Shalimar. These selected seeds were grown under controlled atmospheric conditions for further studies and the vegetative green leafy samples from each cultivar collected at an early (40 days after sowing), mid (62 days after sowing) and late stage (105 days after sowing) of growth. The collected samples were subjected for further analysis and the measurements were conducted in triplicates for each sample.

PAL extraction and assay: Approximately, 500 mg of seed as well as leafy samples collected randomly from five plants each was homogenized in 15 ml of 5 Mm Tris-HCl buffer (pH 8.5) containing 1.4 mM β- mercaptoethanol and the resulting slurry was filtered through two layers of cheese cloth. The filtrate was centrifuged at 12000 g for 15 minutes at 4°C and stored on ice. The resulting supernatant was directly used in the estimation of total protein as well as for PAL enzyme assay as crude extract. The protein content was measured by Bradford method (10). The PAL activity in these extracts was measured by the method developed by Khan *et al* (11). 0.1 ml of enzyme extract was combined with 1 ml of 50 mM Tris HCl , 0.5 ml of 20 mM L-phenylalanine and 0.4 ml of double distilled water and the resulting reaction mixture was incubated for 60 minutes at 30°C. The reaction was stopped by the addition of 250 µl of 2 N HCl and the cinnamic acid formed in reaction mixture was extracted in 2 ml of toluene. In one ml of separated toluene layer, a pinch of anhydrous sodium sulphate was added and absorbance was measured at 290 nm. The standard curve was established using cinnamic acid as standard. The specific activity of the enzyme was expressed as µ moles of cinnamic acid produced /min/mg protein.

Total Phenol assay: Total phenolic content in fenugreek samples was determined according to method reported by Malick *et al* (12). Approximately, 500mg of each sample was homogenized in ten time volume of 80% ethanol and centrifuged at 11900 g. Supernatant was collected and the residue was again re-extracted with five times the volume of 80% ethanol. The pooled supernatants were evaporated to dryness and finally reconstituted with a known volume of double distilled water. To determine phenol content, 500µl of the reconstituted extract was combined with 2.5ml of double distilled water and 0.5ml of Folin cioucalteau reagent. After 3 minutes of incubation period, 20% sodium carbonate was added to each sample, vortexed and boiled in a water bath for exactly one min. The absorbance was measured at 650nm against reagent blank. A standard curve was established using catechol as standard. Absorbance values were converted to milligram of phenolics per 100g of fresh tissue. For each cultivar three replicates were analyzed

α-Amylase Inhibition Assay*:* The α-amylase inhibition activity of fenugreek extracts was measured by following the method reported by Catherine Nkirote *et al* (13). 100 µL of 1% starch solution in 0.02 M sodium phosphate buffer (pH 6.9) was added to mixture of 100 µL of ethanolic extract and 100 µL of 0.02 M sodium phosphate buffer (pH 6.9) containing α-amylase solution (1 unit liberates 1.9 µL of maltose from starch in 1 min at pH 6.9 and temperature 25°C), and was incubated at 25°C for 30 minutes. After the incubation, the reaction was stopped with 1 mL of DNSA reagent. The test tubes were then incubated in a boiling water bath for 5 min and cooled to room temperature. The reaction mixture was then diluted to 10-fold with distilled water and the absorbance was measured at 540 nm. The readings were compared with the control, which contained buffer instead of sample extract. Based on the absorbance value, the percent inhibition activity was calculated for all the samples (8).

Absorbance was calculated by using following formula:

The % α-amylase inhibitory activity = $(Ac^{+}) - (Ac) - (As-Ab) / (Ac^{+}) - (Ac^{-}) \times 100$

"Ac^{+}" and "Ac^{-}" are defined as the absorbance of 100% enzyme activity (reaction mixture with

enzyme but without test sample extract), and 0% enzyme activity (reaction mixture without enzyme as well as test sample) respectively. Where "As" represent "AC^{+}" including sample extract and "Ab" represent "Ac^{-}" excluding sample extract) respectively.

α-Glucosidase Inhibition Assay: The α-glucosidase inhibition activity was determined according to the method described by Worthington (14). A total of 100 μL of ethanolic extract and 200 μL of 0.1 M phosphate buffer (pH 6.9) containing α-glucosidase solution (1 unit/mL) were taken in tubes and incubated at 25°C for 5 min. After the pre-incubation, 100 μL of 5 mM *p*-nitrophenyl-α-D-glucopyranoside solution in 0.1 M phosphate buffer (pH 6.9) was added to each tube and the reaction mixture was incubated at 25°C for 5 minutes After the incubation period, the reaction was stopped by addition of 0 .1M Na_2CO_3 and the aliquots were diluted to 10-fold with distilled water, and the absorbance readings recorded at 405 nm and compared to a control that had 100 μL of buffer solution in place of the extract. The results were calculated and expressed as percentage of α-glucosidase inhibition.

Absorbance was calculated by using following formula (8):

The % α-glucosidase inhibitory activity = (Ac+) - (Ac-) - (As-Ab) / (Ac+) - (Ac-) × 100

Ac+, and Ac- are defined as the absorbance of 100% enzyme activity (reaction mixture with enzyme but without test sample extract), and 0% enzyme activity (reaction mixture without enzyme as well as test sample) respectively. Whereas "As" represent "AC^{+}" including sample extract and Ab represent "Ac^{-}" excluding sample extract respectively.

Statistical Analysis **:** Statistical analysis of data was performed by using one way analysis of variance (ANOVA) and correlation tests. The data was analyzed by using comprehensive statistical package SPSS (Version 20) for windows.

Results and Discussion

Plants synthesize a vast range of secondary metabolites including phenolic and flavonoid antioxidants that are currently being aggressively exploited to develop preventive and treatment measures for common oxidative stress linked degenerative diseases such as diabetes, cardiovascular disease, certain cancers and even aging (15). Among plants, fenugreek has been viewed as miraculous herb due to its unprecedented health promoting activities. In the current study, six different cultivars of fenugreek possessing varied phenotypic and genotypic characteristics were analyzed for their phenol production and their correlation to PAL enzyme activity. As during growth, there exists change in different type of secondary metabolites including total phenols, therefore in order to determine which stage of growth had the highest level of phenolics and PAL activity, six cultivars of fenugreek (ML1-ML6) were analyzed and compared with each other. A high variation in terms of phenolic content (95-560 mg / 100g fw) was observed in the selected fenugreek seed cultivars as well as their respective green leafy parts collected at different stages of growth (Fig. 1B-4B). Such significant differences among the different cultivars have been reported to be likely due to genotopic and environmental differences (namely, climate, location, temperature, fertility, diseases and pest exposure) within species, choice of parts tested, time of taking samples and determination methods (16). Further, a steady increase in phenols was observed while moving from seed stage to mid stage of growth. However, towards late stage of growth there was a gradual decrease in total phenol content attributed to decreased metabolic activities during this phase. In production of phenolic compounds, Phenyl-alanine Ammonium Lyase (PAL) enzyme plays a very crucial role. It catalyses the first step in the biosynthesis of phenylpropanoids, that are further modified into a wide variety of phenolic secondary metabolites. Therefore, for various scientific interventions including metabolic engineering and hyperexpression of phenols and their derivatives,

Vol. 7 (4) 837-846 October 2013, ISSN 0973-8916 (Print), 2230-7303 (Online)

this enzyme has recently gained much interest. In the current study, we also evaluated the changes in PAL enzyme activity in all the six cultivars of fenugreek (ML1-ML6 series) at different stages of growth. PAL activity was found to follow the same trend as found in case of phenols and was found to lie in between 0.00017-0.01008 μM cinnamic acid/min/mg protein (Fig. 1A-4A). There was gradual increase in PAL activity from seed stage till mid stage that was followed by slight decrease while moving towards late stage of growth. Among all the six selected cultivars, ML2 possessed the highest PAL activity (0.01008 μM cinnamic acid/min/mg protein) whereas ML4 the lowest i.e 0.00290 μM cinnamic acid/min/mg protein at mid stage of growth.

Overall, in this study it was found that at mid stage of growth phase all the cultivars possessed maximum PAL activity as well as maximum phenol production (Fig. 1-4). These results corroborated well with the previous reports indicating that PAL enzyme plays a key role in synthesis of phenolics in plant system (5). Thus, among these selected cultivars, ML-2 showed the maximum PAL enzyme activity as well as total phenol content (560mg/ 100g fw) at mid stage of growth (Fig. 3A). Phenolic compounds are currently been viewed as strong antioxidants therefore, current study clearly suggests that at mid stage of growth, ML2 cultivar of fenugreek can act as a potent antioxidant rich food.

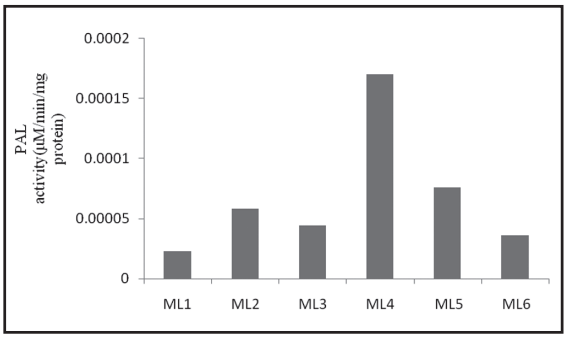

A Fenugreek Cultivars

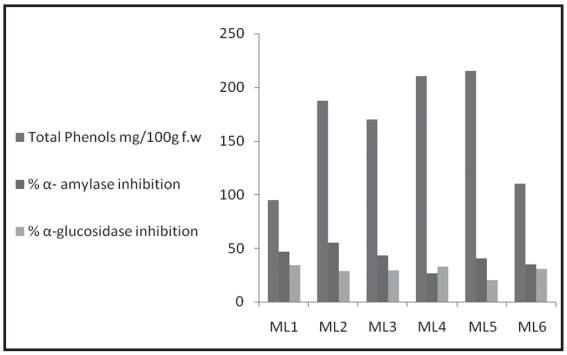

B Fenugreek Cultivars

Fig. 1. (A) PAL activity of different cultivars of fenugreek seeds. (B) Total phenol content, α amylase inhibition and α glucosidase inhibition shown by different cultivars of fenugreek seed extracts.

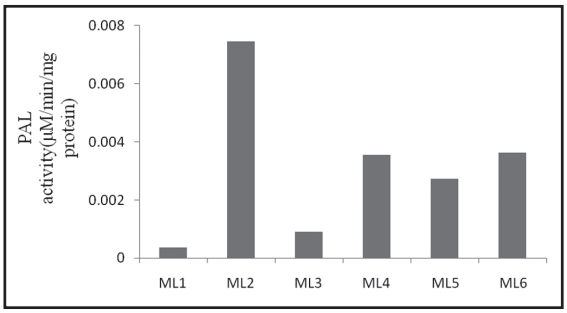

A Fenugreek Cultivars

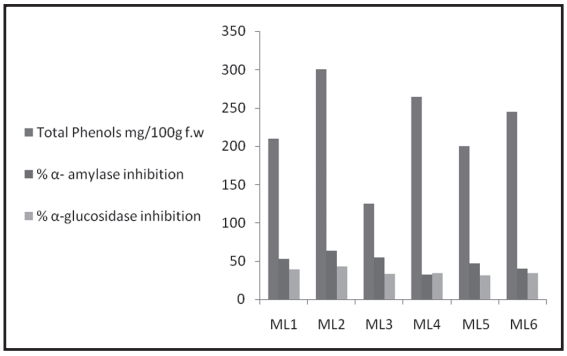

B Fenugreek Cultivars

Fig. 2. (A) PAL activity of different cultivars of fenugreek at early stage of growth. (B) Total phenol content, α amylase inhibition and α glucosidase inhibition shown by different cultivars of fenugreek extracts at early stage of growth.

PAL enzyme activity

In previous studies, it has been reported that production of PAL can get increased due to number of reasons including sprouting, physical wounding as well as by modern biotechnological interventions resulting in many fold increase in total phenol content or their precursors (17). Since, in our investigation, all the cultivars were grown under same environmental conditions as well as by all means followed same procedural evaluations. Therefore, the variation observed in PAL activity and total phenol content among different cultivars can be mostly attributed to genetic differences and not to environmental influences. It has been reported that high concentration of phenolics can cause astringent undesirable effects and thus make that food unacceptable for consumption (18). Therefore, our current study moves in different direction and in addition to evaluate PAL and Phenol content the potential functionality of these samples in terms of hypoglycemic property of phenol was evaluated.

The study was carried out by targeting two Key enzymes viz pancreatic alpha-amylase and intestinal alpha-glucosidase, involved in the enzymatic breakdown of starch and absorption of complex carbohydrates respectively. The inhibition of their activities has been viewed as potential avenues for modulation of type 2 diabetes-associated post-prandial hyperglycemia (19).

As per previous reports, it has been shown that individual phenolic compounds present in plants possess hypoglycemic activity and can thus act as therapeutic agents. Recently, it has been cited that the presence of certain bioactive compounds of phenolic nature like quercetin, pose to be α-amylase and α-glucosidase inhibitors, and thus play an important role in treatment of managing hyperglycemia and related complications with minimum side effects as compared to currently available therapeutic regimes (8, 20-23). However, instead of using such compounds individually, it is suggested that they perform much better in combination due to synergestic effects and varied bioavalibilities. In our study, ethanolic extracts of fenugreek demonstrated very effective α-amylase inhibitory activity that varied in between 26.72% to 72.53% at different stages of growth (Fig. 1- 4). As the main issue to attempt to manage diabetes at first step in hyperglycemic patients is to target this potent enzyme found in saliva as well as pancreatic juice (20). Therefore, our study demonstrates very encouraging results by inhibiting α-amylase activity especially by fenugreek extracts prepared from leaves collected at mid stage of growth and thus indicate to play a great role in controlling fluctuating blood glucose levels. As discussed above, the inhibitory activities of this enzyme are often linked to certain phenolic compounds present in plant foods. Therefore, the inhibition of this enzyme could vary by being high or low depending on the presence of phenolic phytochemicals present in specific food that modulate its activity (24,25). Extracts from ML2 cultivar possessing maximum phenol content and high PAL activity at mid stage of growth demonstrates highest inhibition activity (72.5 %) against this potent chemotherapeutic target enzyme (Fig. 3B) followed by other cultivers. These food based phenolic compounds have been reported to bind to the reactive sites of enzymes and alter their catalytic activity (2). Therefore, the maximum inhibition of α-amylase by extracts possessing high phenolic content may also occur through the direct blockage of the active centre at several subsites of the enzyme (26).

In diabetes, in addition to target α amylase it is a well-established fact that therapeutic approach to decrease postprandial hyperglycemia in this disease is by slowing the absorption of glucose, by inhibition of α-glucosidase enzyme in digestive system (27). Thus, it is important that dietary α-glucosidase inhibitors are present in sufficient quantity, to prevent the absorption of glucose in small intestine (28). In the current study, ethanolic extracts of fenugreek under *in vitro* conditions also demonstrated α-glucosidase inhibitory activity that varied between 20.08% to 52 %% (Fig. 3B). Interestingly, among

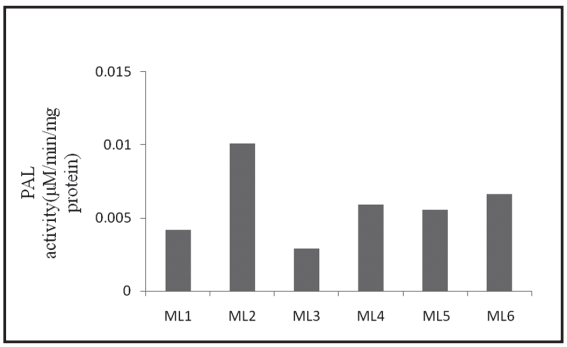

A Fenugreek Cultivars

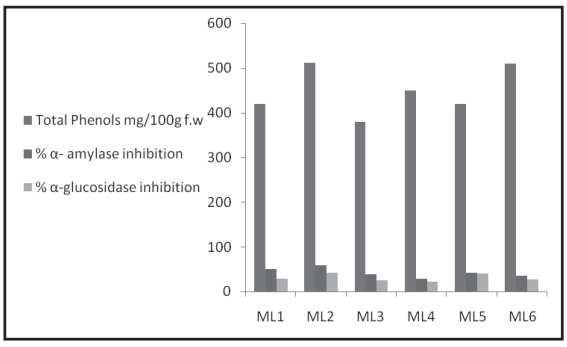

A Fenugreek Cultivars

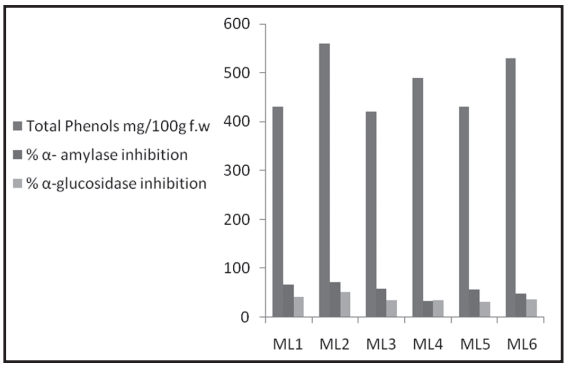

B Fenugreek Cultivars

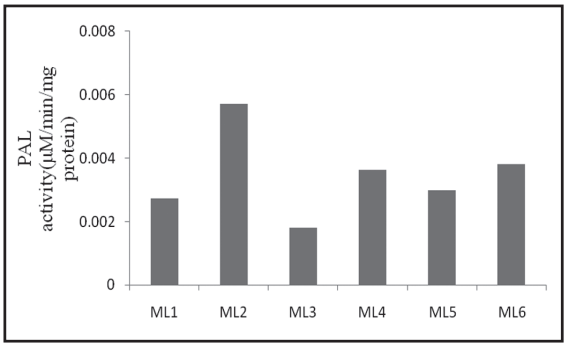

B Fenugreek Cultivars

Fig. 3. (A) PAL activity of different cultivars of fenugreek at mid stage of growth. (B) Total phenol content, α–amylase inhibition and α–glucosidase inhibition shown by different cultivars of fenugreek extracts at mid stage of growth.

Fig. 4. (A) PAL activity of different cultivars of fenugreek at late stage of growth. (B) Total phenol content, α–amylase inhibition and α–glucosidase inhibition shown by different cultivars of fenugreek extracts at late stage of growth.

Table 1. Correlation matrix of variables

Variables	PAL	Total Phenols	α-amylase inhibition	α-glucosidase inhibition
PAL activity	1			
Total Phenols	0.759**	1		
α-amylase inhibition	0.439*	0.690*	1	
α-glucosidase inhibition	0.507*	0.552*	0.656*	1

** Highly significant
* Significant

PAL enzyme activity

the six different cultivars, ML2 possessing highest α-amylase activity also showed the maximum inhibitory α-glucosidase inhibitory activity (52 %) among the selected cultivars at mid stage of growth. Thus, extract from ML2 can act as a potent health food to regulate carbohydrate metabolism and manage hyperglycemia. Interestingly, a direct correlation between increase in phenolic content and inhibition of α-amylase and α-glucosidase was observed. It has been reported that such type of food grade materials offer cost effective and locally based strategies to control postprandial hyperglycemia with minimum side effects (23).

The statistical analysis data (Table 1) indicates that there exists highly significant correlation between increase in PAL activity and total phenols (r=0.759) that were in turn significantly related to α-amylase inhibitory activity (r=0.439, r='0.690 respectively) as well as with α -glucosidase inhibitory activity (r=0.507, r=0.552 respectively). Overall mean along with standard deviation for PAL activity, total phenols, α amylase inhibitory activity and α -glucosidase inhibitory activity was recorded as 0.00312 ± 0.00272, 328.2 ± 147.07, 47.03 ± 12.301 and 33.73 ± 7.75 respectively. Using ANOVA it was found that ML2 cultivar with respect to phenols, α -amylase inhibitory activity and α -glucosidase inhibitory activity shows highest and significant results of 382.25, 62.50 and 40.006 respectively and among stages, mid stage shows significant results for the above variables with 476.67, 56.313 and 39.625 respectively. Through this study, we were able to provide the strong rationale for determining the best cultivar and best stage of growth in fenugreek to be used as potential therapeutic chemopreventive food against diabetes. Further such type of study paves way to identify promising genotypes for breeding and industrial use.

Conclusion

In this study, we observed that hypoglycemic activity varies in fenugreek at each stage of growth that is directly related to corresponding change in phenol production as well as in PAL activity. Therefore, through this novel approach, we identified in this important crop that stage of growth which possesses maximum PAL activity as well as total phenol content and that in turn lowers the glycemic index and controls the post-prandial hyperglycemia by targeting α -amylase and α-glucosidase enzymes involved in carbohydrate metabolism. Thus, it is suggested that extracts of such fenugreek cultivars, especially from ML2 cultivar taken at mid stage of growth when incorporated into diet could act as a potential chemopreventive food for better management of hyperglycemia related to diabetes. However, despite such encouraging results, it is suggested that more research in this direction is required for developing such food based effective and valuable functional food and herbal formulations for anti-diabetic therapy.

Acknowledgement:

Authors are highly thankful to Director Research, SKUAST-K, Shalimar Campus, Kashmir and Dr. N. Ahmad, Director CITH, Kashmir for their encouragement and to UGC, New Delhi for its Financial Assistance (F.No.37-525/2009-SR).

References

1. Sudha S. Deo, Avinash Zantye, Rajashree Mokal., Shilpa Mithbawkar and Sujata Raneet. (2006). To identify the risk factors for high prevalence of diabetes and impaired glucose tolerance in Indian population. Int J Diab Dev Ctries. 26(1): 19-23.

2. Sougata Ghosh, Mehul Ahire, Sumersing Patil, Amit Jabgunde, Meenakshi Bhat and Dusane. (2012). Antidiabetic Activity of Gnidia glauca and Dioscorea bulbifera: Potent Amylase and Glucosidase Inhibitors. Evi-Bas Compl and Alt Med. 12: 1-10.

3. Hiba A. Bawadi, Sofyan N. Maghaydah, Rabab F. Tayyem and Reema F. Tayyem (2009). The postprandial Hypoglycemic Activity of Fenugreek Seed and Seeds

Extract in Type 2 Diabetics: A Pilot Study. Pharma Magz. 5(18):134-138.

4. WHO (2007.) Monographs on selected medicinal plants (Volume 3). WHO press, Geneva, Switzerland
5. Wout Boerjan, John Ralph and Marie Baucher. (2003). Lignin Biosynthesis. Ann Rev Pl Biol 54: 519-546.
6. Reinaldo Campos-Vargasa, Hiroyuki Nonogakia, Trevor Suslowa and Mikal E. Saltveit (2005) Heat shock treatments delay the increase in wound-induced phenylalanine ammonia-lyase activity by altering its expression, not its induction in Romaine lettuce (Lactuca sativa) tissue Physiologia Plantarum 123: 82–91.
7. Guiwen W. Cheng and Patrick J. Breen (1991). Activity of Phenyl analine ammonia –lyase (PAL) and concentrations of anthocyanins and phenolics in developing strawberry fruits. J Amer Soci Hort Scl 116(5): 865-869
8. Dinesh Kumar, B, Mitra, A. and Manjunatha, M. (2010). A comprative study of alpha amylase inhibitory activities of common antidiabetic plants at Kharagpur block I. Int J Green Pharm 4:115-121
9. Pathirage K. Perera and Yunman Li (2012). Functional herbal food ingredients used in type 2 diabetes mellitus. Pharm Rev. 6(11): 37-45.
10. Bradford, M. M. (1976). A rapid and sensitive method for the quantification of microgram quantities of protein utilizing the principle of protein-dye binding. Annu. Biochem. 72:248–254.
11. Khan, N. U. and Vaidyanathan, C. S. (1986). A new simple spectrophotometric assay of phenylalanine ammonium lyase. Curr Sci. 55(8):391-393.
12. Malick, C. P and Singh, M. B. (1980) Plant Enzymology and Histoenzymology. Kalyani publications, New Delhi.
13. Catherine, N. K, Jasper, K. I., Michael, O., Clare, M. and Han, K. B. (2011) Antioxidant and Antidiabetic Properties of Condensed Tannins in Acetonic Extract of Selected Raw and Processed Indigenous Food Ingredients from Kenya. J Food Sci. 76, (4):525-530.
14. Worthington, V. (1993). Worthington Enzyme Manual: Biochemical Corp. Freehold, New Jersey.
15. Ali, G. and Neda, G. (2011). Flavonoids and phenolic acids: Role and biochemical activity in plants and human. J Med Pl Res. 5(31): 6697-6703.
16. Aneta Wojdy, o., Jan Oszmian´Ski and Renata Czemerys (2007). Antioxidant activity and phenolic compounds in 32 selected herbs. Food Chem. 105: 940–949.
17. Edward, C. Lulai., Jeffrey, C. Suttle and Shana, M. P. (2008). Regulatory involvement of abscisic acid in potato tuber wound-healing. J Expet Bot. 9 (6): 1175–1186.
18. Hann, P., Keith, K. B and Ann, C. N. (1998). The Influence of Acid on Astringency of Alum and Phenolic Compounds. Chem. Sens. 23: 371-378.
19. McCue, P., Kwon, Y. I. and Shetty, K. (2005). Anti-amylase, anti-glucosidase and anti-angiotensin I-converting enzyme potential of selected foods. J Food Biochem. 29: 278-294.
20. Etxeberria, U., de la Garza, A.L., Campión, J., Martínez, J.A. and Milagro, F.I. (2012) Antidiabetic effects of natural plant extracts via inhibition of carbohydrate hydrolysis enzymes with emphasis on pancreatic alpha amylase. Expert Opin Ther Targets. 16(3):269-97.
21. Li,Y.Q., Zhou, F.C., Gao, F., Bian, J.S. and Shan, F. (2009) Comparative evaluation of quercetin, isoquercetin and rutin as inhibitors of alpha-glucosidase. J Agric Food Chem. 57(24):11463-8

22. Shetty, K., Adyanthaya, I., Kwon, Y. I., Apostolidis, E., Min, B. J. and Dawson, P. (2008). Postharvest enhancement of phenolic phytochemicals in apples for preservation and health benefits: Postharvest Biology and Technology of Fruits, Vegetables and Flowers (Paliyath G, Murr D, Handa AK, Lurie S {3eds}). Wiley-Blackwell Publishing, Ames, Iowa, USA.

23. Pinto, M. D. S. and Shetty, K. (2010). Health Benefits of Berries for Potential Management of Hyperglycemia and Hypertension. In: Flavor and Health Benefits of Small Fruits, ACS Publications, Washington, DC, USA.

24. Kwon, Y. I., Vattem, D. V. and Shetty, K. (2006). Evaluation of clonal herbs of Lamiaceae species for management of diabetes and hypertension. Asia Pac J Clin Nutr. 15: 107–118.

25. Pinto, M. D., Ranilla, L. G., Apotolidis, E., Lajolo, F. M., Genovese, M. I. and Shetty, K. (2009). Evaluation of antihyperglycemia and antihypertension potential of native Peruvian fruits using *in vitro* models. J Med Food. 12: 278-291.

26. P, P. McCue and Shetty, K. (2004). Inhibitory effects of rosmarinic acid extracts on porcine pancreatic amylase *in vitro*. Asia Pac J of Clin. Nutr. 13 (1): 10 –106.

27. Ramachandran, Vadivelan.,, Sanagai, Palaniswami, Dhanabal., Ashish, Wadhawani and Kannan, Elango. (2012) α-Glucosidase and α -amylase inhibitory activities of Raphanus Sativus Linn. Int J Pharm.Sc. and Res. 3(9):3186-3188.

28. Ranilla, L. G., Kwon, Y. I., Apostolidis, E and Shetty, K. (2010). Phenolic compounds, antioxidant activity and *in vitro* inhibitory potential against key enzymes relevant for hyperglycemia and hypertension of commonly used medicinal plants, herbs and spices in Latin America. Biores. Technol. 101: 4676-4689.

Current Trends in Biotechnology and Pharmacy
Vol. 7 (3) 847-853 October 2013, ISSN 0973-8916 (Print), 2230-7303 (Online)

Structure-based Computational analysis of Protein Binding sites for Function and Druggability in Macrophage Infectivity Potentiator (MIP) Protein of *Legionella pneumophila*

C. Kumaraswamy Naidu and Y. Suneetha*
Department of Zoology, Sri Venkateswara University, Tirupati – 517502, India.
*For Correspondence - ysuneethareddy4@gmail.com

Abstract

Legionaries Disease is one of the top 10 bacterial infections in the world occurring to humans. The bacterial infection of Legionaries Disease, survive in wet environments. The infection will cause symptoms similar to the flu, but if not taken care of early, can cause renal disease. The macrophage infectivity potentiator (MIP) protein is a major virulence factor of *Legionella pneumophila*, the causative agent of Legionnaires' disease. MIP belongs to the FK506-binding proteins (FKBP) and is necessary for optimal intracellular survival and lung tissue dissemination of *L. pneumophila*. In the present study, we used Virtual screening approach to successfully find an inhibitor against *L. pneumophila* MIP. Results showed that (4-{(2R)-2-[(1S,3S,5S)-3,5-dimethyl-2-oxocyclohexyl]-2-hydroxyethyl}-2,6-dioxopiperidin-1-yl)acetate can act as a novel inhibitor against *L. pneumophila* MIP.

Keywords: Legionaries Disease; *Legionella pneumophila*; Macrophage infectivity potentiator protein; Molecular docking.

Introduction

Legionnaires' disease is a severe and sometimes a fatal form of infection caused by *Legionella* species. Since 32 years it was recognized that Legionnaires' disease was caused by *Legionella pneumophila* (1). Epidemiology of Legionnaires' disease shows an average of 356 cases between 1980 and 1998 in the United States (2). In Europe, a total of 5,907 cases were reported by 33 countries in 2007 and 5,960 cases were reported by 34 countries in 2008 (3). During August and September 2010, an outbreak comprising 22 cases of Legionnaires' disease were identified in Wales (4). In May 2010, a cluster of three cases of Legionnaires' disease were identified in France (5). In 2001, 400 cases were reported in Spain (6). This disease is classically described as a severe pneumonia accompanied by systemic symptoms such as fever, diarrhoea, myalgia, impaired renal and liver functions, and delirium. The disease mainly affects people over 50 years of age, generally men more than women and the fatality rate can vary from 1% to 17% of cases in the general population and may be higher in the risk groups (7). Among the *Legionella* species, *Legionella pneumophila* is the aetiological agent of approximately 90% of all Legionnaires' disease cases (8). *Legionella pneumophila*, is a Gram-negative bacteria that evolved infecting unicellular protozoa in freshwater reservoirs (9). *L. pneumophila* possesses many of the traditional bacterial determinants like lipopolysaccharide (LPS), flagella, pili, a type II secretion system (T2SS), and outer membrane proteins that are important for pathogenicity in other bacteria (10).

The ability *L. pneumophila* to cause Legionnaires' disease predominantly depends on the components and characteristics of its cell

envelope. The macrophage infectivity potentiator (mip), is a membrane-associated homodimeric protein that is mainly found on the bacterial surface of *L. pneumophila* is required for the transmigration of *L. pneumophila* across an *in vitro* model of the lung epithelial barrier and efficient replication within host cells. The C-terminal domain of Mip displays peptidyl–prolyl *cis/trans* isomerase (PPIase) activity and is related to the human FK506-binding protein and binds to collagen of types I, II, III, IV, V, and VI (11). The *mip* product is a 24-kDa protein, sharing an amino acid sequence similarity with the mainly eukaryotic family of FK506 binding proteins. The crystal structure of Mip revealed that the fold of the catalytic domain resembles the family of human protein FK506 binding proteins (10). The exact function of Mip in virulence have not been identified yet.

In general, the interaction of a protein with other molecules like ligands, nucleic acids or other proteins are critical to its biochemical function and these interactions occur at defined locations, called the protein binding sites (12). Thus, the identification and characterization of these protein binding sites and their interacting ligands is crucial to understand molecular interactions and recognition. Comparison of binding pockets of multiple proteins can infer the function of the orphan protein thereby inferring the new ligands they may be capable to bind at the binding pocket of the orphan protein. In the present study, we used the same approach to predict and analyze the inihibitors that are capable to show the binding affinity for the Mip of *L. pneumophila.*

Materials and Methods

***Protein Structure retrieval*:** The solution structure of the fkbp-domain of *L. pneumophila* macrophage infectivity potentiator protein (mip) in complex with rapamycin protein (mip) (PDB ID: 2VCD) (Ceymann et al., 2008) was retrieved from the protein data bank (PDB).

***Prediction of structural homologs for L. pneumophila mip*:** Structure homologs for *L. pneumophila* mip was predicted using 3D-BLAST (http://3d-blast.life.nctu.edu.tw/), a very fast and accurate method for discovering the homologous proteins and evolutionary classifications of a newly determined protein structure. It searches for the longest common substructures, called SAHSPs (structural alphabet high-scoring segment pairs), existing between the query structure and every structure in the structural database and ranks the search homology structures based on both SAHSP and *E*-value calculating from the substitution scoring matrix of structural alphabets (13) (14).

Molecular docking: Molecular docking was performed using the Autodock 4.2 and PyRx program (15) was employed to generate the docking input files. Empirical free energy function and Lamarckian genetic algorithm (LGA) were used for docking with the following settings: a maximum number of 2,500,000 energy evaluations, an initial population of 150 randomly placed individuals, a maximum number of 27,000 generations, a mutation rate of 0.02, a crossover rate of 0.8 and an elitism value (number of top individuals to survive to next generatione) of 1. For the local search, the so-called Solis and Wets algorithm was applied with a maximum of 300 iterations per search. Default values were used for all the other parameters not mentioned.

Results and Discussion

3D-BLAST search of *L. pneumophila* mip resulted in 100 PDB structures with identity greater than or equal to 40 %. Among them top ten structures with identity percentage greater than 44% were selected. The respective structures along with their identity percentages were shown in the Table 1 given below. *L. pneumophila* mip 3D structure (PDB ID: 2VCD) is found contain Rapamycin (RAP) as a ligand. The chemical structure of RAP was shown in the figure 1given below. The respective bonding interactions of RAP with *L. pneumophila* mip was shown in the figure 2 given below. PDB structures that are found to be identical to *L. pneumophila* mip resulted by 3D-BLAST search were subjected to multiple sequence alignment using

CLUSTALX2 (16). Multiple sequence alignment showed that residues are conserved in the region where RAP is bound in *L. pneumophila* mip (figure 3). Structures which showed identity to *L. pneumophila* mip showed several in bound ligands as shown in the table 1. Among, these ligands we eliminated Seleno Methionine (MSE) and Cesium (Cs) for our consideration. Remaining ligands were docked into *L. pneumophila* mip protein constructing as grid box with the following dimensions; X-dimension: 60, Y-dimension: 56, Z-dimension: 52, Spacing:

Table 1. Protein structures that are identical to *L. pneumophila* mip three dimensional structure

PDB ID	Protein Name	E-Value	Percentage identity	Ligands
1JVW Chain A	*Trypanosoma cruzi* macrophage infectivity potentiator (tcmip)	2e-50	54.3	-
1Q6I Chain B	Crystal structure of a truncated form of fkpa from *Escherichia coli*, in complex with immuno suppressant fk506	1e-47	53.5	FK5, MSE
1Q6H Chain A	Crystal structure of a truncated form of fkpa from *Escherichia coli*	1e-44	49.6	MSE
1Q6U Chain A	Crystal structure of fkpa from *Escherichia coli*	8e-68	44.7	Cs
2KO7 Chain A	Solution structure of peptidyl-prolyl cis-trans isomerase from *Burkholderia pseudomallei* complexed with Cycloheximide-N-ethylethanoate	7e-37	49.1	JZF
1D7I Chain A	FKBP complexed with methyl methylsulfinyl methyl sulfide (DSS)	2e-36	55.3	DSS

Table 2. Molecular docking interactions of the ligands

PDB ID	Ligand Name	AutoDock Binding Energy ÄGb (kcal/mol)	Inhibition co-efficient	Interacting / Close contact Residues	Hydrogen bonding residues
2VCD	RAP	-7.23	5.02	TYR55,PHE65,ASP66,ALA75, THR76, PHE77,GLN81,VAL82, ILE83,TYR109,VAL114,GLY115, PHE126	TYR55
2VCD	FK5	-7.72	2.20	TYR55,THR76,PHE77,GLN78, GLN81,VAL82,TRP86,ILE83, TYR109	GLN78,ILE83
2VCD	JZF	-7.28	4.62	TYR55,GLY57,ASP66,PHE77, GLN81,VAL82, ILE83, PRO84, TRP86,TYR109,PHE126	TYR55
2VCD	DSS	-3.27	4.00	PHE77, VAL82,ILE83, TRP86	ILE83

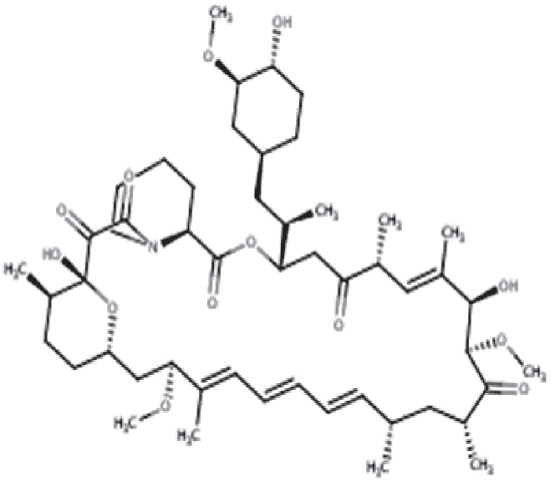

Fig. 1. Chemical structure of Rapamycin (RAP)

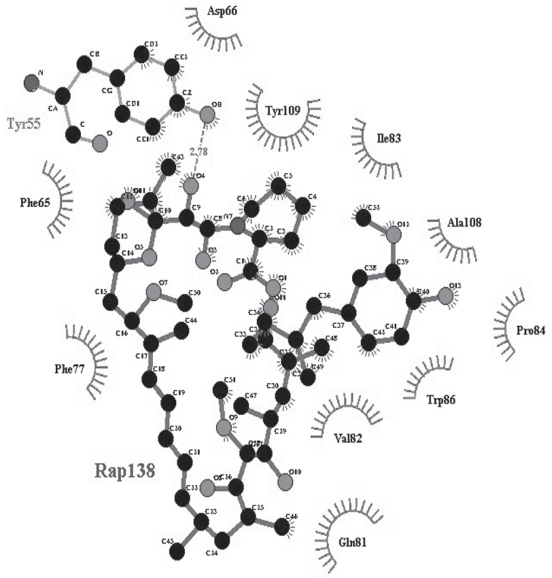

Fig. 2. Interactions of RAP with *L. pneumophila* mip.

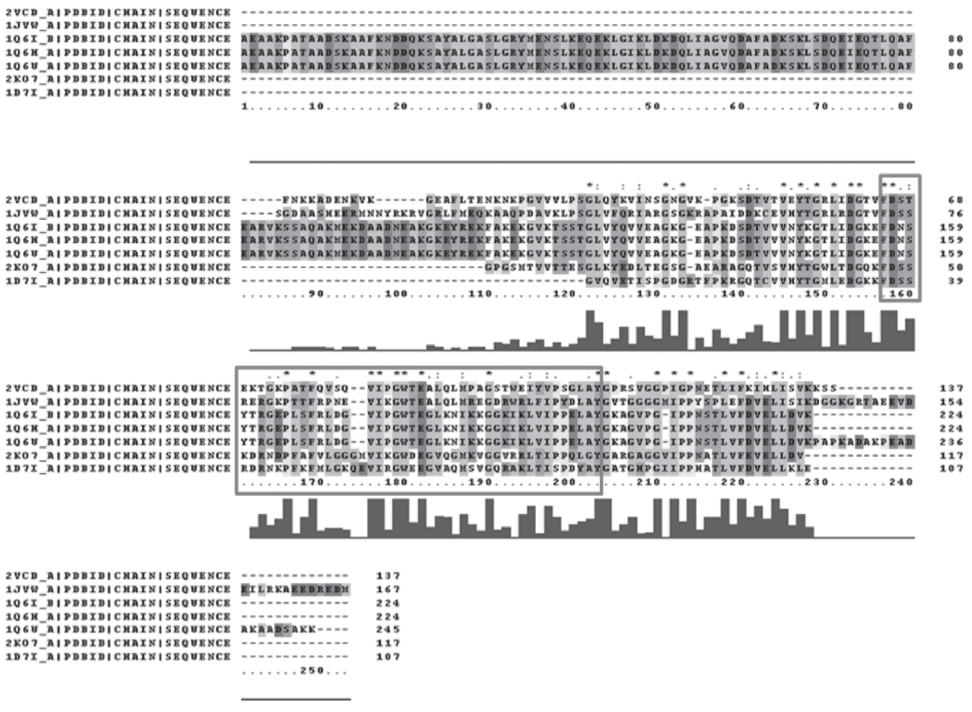

Fig. 3. Multiple sequence alignment of proteins identical to *L. pneumophila* mip

0.375, X center: 102.882, Y center: 4.667, Z center: -7.296. Before docking the ligands to *L. pneumophila* mip structure, the docking protocol was validated by docking the RAP into the binding pocket to obtain the docked pose. The RMSD (Root Mean Square Deviation) of all atoms between these two conformations is 0.44 A° indicating that the parameters for docking simulation are good in reproducing the structure.

The orientation of docking pose of RAP showed that the binding site was occupied by the residues TYR55, PHE65, ASP66, ALA75, THR76, PHE77, GLN81, VAL82, ILE83, TYR109, VAL114, GLY115, PHE126, LEU 327, PHE 328, LEU 324, LEU 405, VAL 491 with an Binding energy of -7.23 kcal/mol , Inhibition Constant kI of 5.02μM (micromolar), Intermolecular Energy of -9.91 kcal/mol, Internal Energy of -1.73 kcal/mol and Torsional Energy 2.68 kcal/mol. Molecular

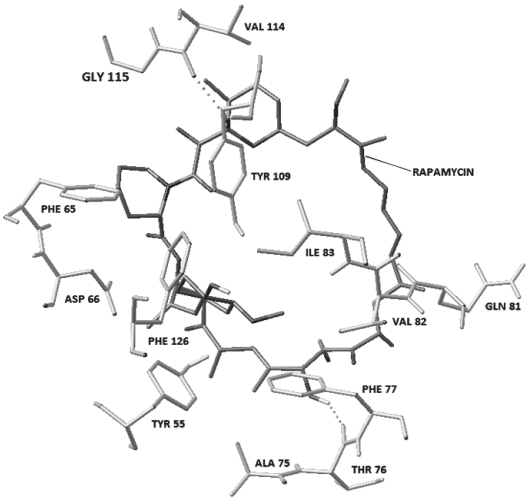

Fig. 4. Molecular docking Interaction of RAP with *L. pneumophila* mip.

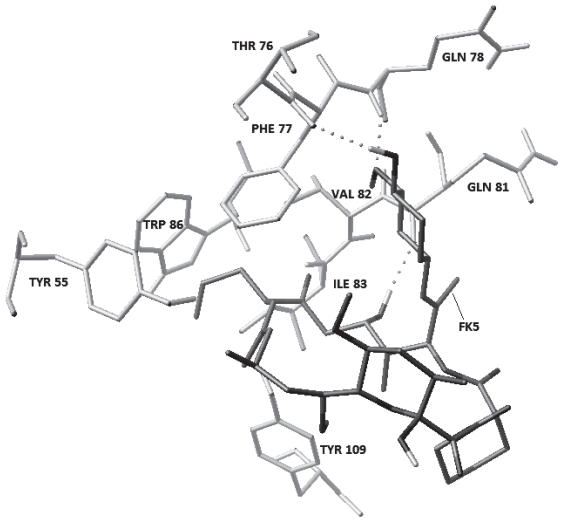

Fig. 5. Molecular docking Interaction of FK5 with *L. pneumophila* mip

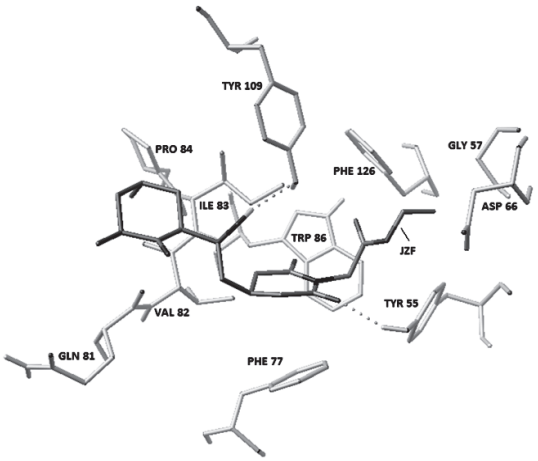

Fig. 6. Molecular docking Interaction of JZF with *L. pneumophila* mip.

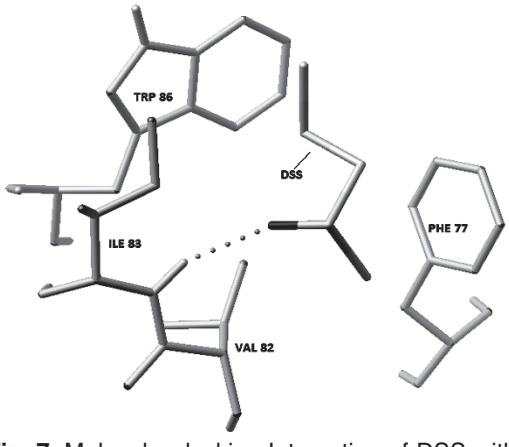

Fig. 7. Molecular docking Interaction of DSS with *L. pneumophila* mip.

docking interaction of RAP with *L. pneumophila* mip was shown in the figure 4 given below. Molecular docking of other ligand 8-deethyl-8-[but-3-enyl]-ascomycin (FK5) showed an Binding energy of -7.72 kcal/mol, Inhibition Constant kI of 2.2μM (micromolar), Intermolecular Energy of -10.7 kcal/mol, Internal Energy of -3.19 kcal/mol and Torsional Energy 2.98 kcal/mol with two hydrogen bonding interactions at the residues GLN78 and ILE83 as shown in the figure 5. Molecular docking of ethyl (4-((2R)-2-[(1S,3S,5S)-3,5-dimethyl-2-oxocyclohexyl]-2-hydroxyethyl)-2,6-dioxopiperidin-1-yl)acetate (JZF) on the other hand showed an Binding energy of -7.28 kcal/mol, Inhibition Constant kI of 4.62μM (micromolar), Intermolecular Energy of -9.66 kcal/mol, Internal Energy of -0.82 kcal/mol and Torsional Energy 2.39 kcal/mol with one hydrogen bonding interaction at the residue TYR55 as shown in the figure 6 whereas methyl methylsulfinylmethyl sulfide (DSS) showed an Binding energy of -3.27 kcal/mol, Inhibition Constant kI of 4.0μM (micromolar), Intermolecular Energy of -3.87 kcal/mol, Internal Energy of -0.05 kcal/mol and Torsional Energy 0.68 kcal/mol with one hydrogen bonding interaction at the residue ILE83 as shown in the figure 7. The respective interacting or close contact residues for all the ligands were shown in the Table 2 given below. These results showed that apart from Rapamycin, ligand JZF can also act as a novel inhibitor against *L. pneumophila* mip.

Conclusion

Virtual screening methods are extensively used to reduced cost and time of drug discovery. The present approach utilized in this study is successful in finding an inhibitor against *L. pneumophila* mip. In particular, the present study showed that residue ILE 83 is interacting with both FK5 and DSS using Hydrogen bonds. Results from the present study also suggest that JZF can act as a novel inhibitor against *L. pneumophila* mip. Further, work can be extended to study the receptor-ligand interactions experimentally.

References

1. Hilbi, H., Jarraud, S., Hartland, E. and Buchrieser, C. (2010). Update on Legionnaires' disease: pathogenesis, epidemiology, detection and control. Mol Microbiol, 76(1): 1-11.
2. Fields, B. S., Benson, R. F. and Besser, R. E. (2002). Legionella and Legionnaires' disease: 25 years of investigation. Clin Microbiol Rev, 15(3): 506-526.
3. Ceymann, A., Horstmann, M., Ehses, P., Schweimer, K., Paschke, A. K. and Steinert, M. (2008). Solution structure of the Legionella pneumophila Mip-rapamycin complex. BMC Struct Biol, 8: 17.
4. Keramarou, M. and Evans, M. R. (2010). A community outbreak of Legionnaires' disease in South Wales, August-September 2010. Euro Surveill, 15(42).
5. Campese, C., Roche, D., Clement, C., Fierobe, F., Jarraud, S. and de Waelle, P. (2010). Cluster of Legionnaires' disease associated with a public whirlpool spa, France, April-May 2010. Euro Surveill, 15(26).
6. Joseph, C. A. and Ricketts, K. D. (2010). Legionnaires disease in Europe 2007-2008. Euro Surveill, 15(8): 19493.
7. Bull, M., Hall, I. M., Leach, S. and Robesyn, E. (2012). The application of geographic information systems and spatial data during Legionnaires disease outbreak responses. Euro Surveill, 17(49).
8. Beaute, J., Zucs, P. and de Jong, B. (2013). Legionnaires disease in Europe, 2009-2010. Euro Surveill, 18(10).
9. Massis, L. M. and Zamboni, D. S. (2011). Innate immunity to legionella pneumophila. Front Microbiol, 2, 109.
10. Newton, H. J., Ang, D. K., van Driel, I. R. and Hartland, E. L. (2010). Molecular pathogenesis of infections caused by

Legionella pneumophila. Clin Microbiol Rev, 23(2): 274-298.

11. Shevchuk, O., Jager, J. and Steinert, M. (2011). Virulence properties of the legionella pneumophila cell envelope. Front Microbiol, 2: 74.
12. Nisius, B., Sha, F. and Gohlke, H. (2012). Structure-based computational analysis of protein binding sites for function and druggability prediction. J Biotechnol, 159(3): 123-134.
13. Tung, C. H., Huang, J. W. and Yang, J. M. (2007). Kappa-alpha plot derived structural alphabet and BLOSUM-like substitution matrix for rapid search of protein structure database. Genome Biol, 8(3): R31.
14. Yang, J. M. and Tung, C. H. (2006). Protein structure database search and evolutionary classification. Nucleic Acids Res, 34(13): 3646-3659.
15. Dallakyan, S. (2008-2010). PyRx-Python Prescription v.0.8. *The Scripps Research Institute*. Joseph, C. (2013). Investigation of outbreaks: epidemiology. Methods Mol Biol, 954: 73-86.
16. Larkin, M. A., Blackshields, G., Brown, N. P., Chenna, R., McGettigan, P. A. and McWilliam, H. (2007). Clustal W and Clustal X version 2.0. Bioinformatics, 23(21): 2947-2948.

Current Trends in Biotechnology and Pharmacy
Vol. 7 (4) 854-861 October 2013, ISSN 0973-8916 (Print), 2230-7303 (Online)

Curcumin Potentiates Antitumor effect of Gemcitabine in Human Breast Cancer *in vitro*

Mamatha Serasanambati, Shanmuga Reddy Chilakapati, Pavan Kumar Manikonda and Jagadeeswara Reddy Kanala *
Sugen Life Sciences Pvt. Ltd, 4/86, S. V. Nagar, Perumalla Palli, Tirupati – 517 505, A.P, India
*For Correspondence - kjreddy32@gmail.com

Abstract

Breast cancer is the most commonly diagnosed disease among women. In recent years, chemotherapeutic drugs such as gemcitabine, erlotinib, etc. have been developed for the treatment of breast cancer. Breast cancers relapse due to the generation of chemoresistance that makes therapeutic drugs ineffective. Hence, agents that can reduce the chemoresistance to the therapeutic drugs are being developed for better advancement of in cancer therapy. The present study evaluates the efficiency of curcumin, in suppression of gemcitabine induced NF-kB activity and in the enhancement of anti-tumor effect of gemcitabine on MCF-7 and MDA MB-231breast cancer cells. 10 or 20 µM of curcumin and 10 or 100 µM of gemcitabine, alone or in combination, were used. Cell proliferation by MTT assay, apoptotic effects by Live/Dead assay, nuclear factor-kB (NF-kB) activation or suppression by EMSA were determined. The results indicated a decrease in cell proliferation of up to 61% ($p \leq 0.01$) and 45% ($p \leq 0.01$) at 20 µM curcumin and 100 µM of gemcitabine in MCF-7 and MDA MB-231, respectively. Whereas 20 µM curcumin potentiated the apoptotic effects of gemcitabine (100µM) predominantly in MCF-7 by 61% and in MDA MB-231 by 46% which was determined by using Live/Dead assay. However, curcumin (20 µM) significantly ($p \leq 0.05$) suppressed NF-kB activation by 80% which was induced by gemcitabine (100µM) in both cell lines. The data obtained from the present investigation shows the dose dependent changes in MCF-7 and MDA MB-231. The combined results revealed the beneficial role of curcumin in potentiating the anti-tumor effects of gemcitabine through NF-kB suppression and apoptotic effects.

Keywords: Apoptosis, Curcumin, Gemcitabine, NF-kB

Introduction

Nowadays, breast cancer is a major risk factor among women worldwide. In Western countries, the mean -5year relapse-free survival rate of breast cancer patients is approximately 60%, but this value differs significantly across individuals (1-3). Breast cancer is caused due to various potent chemical drugs or epigenetic factors, including regulation of transcription factors, growth factors, etc (4). Various reports denote increased cell proliferation, invasion, suppression of apoptosis and chemoresistance in multiple tumours (4). Several reports indicate that such detrimental effects might be linked with transcription factor NF-kB, which plays a major role in regulating the cell proliferation and chemoresistance of breast cancer (5, 6).

At present, gemcitabine (2'2'-difluorodeoxycytidine), a novel nucleoside analogue of deoxycytidine is employed as a chemotherapeutic drug for the treatment of various cancers which induces NF-kB activity (7, 8). This drug is inactive in the parental form,

Vol. 7 (4) 854-861 October 2013, ISSN 0973-8916 (Print), 2230-7303 (Online)

although it is progressively phosphorylated to its active diphosphate and triphosphate metabolites via kinases in intracellular compartments (9). In addition, its active diphosphate form inhibits ribonucleotide reductase apart from incorporation of its triphosphate into DNA as a fraudulent base in competition with dCTP. Such incorporation into DNA resulted in DNA chain termination during replication and the mimic base is relatively resistant to excision repair. However, gemcitabine treatment might be associated with multiple adverse effects and drug resistance which results in an objective tumour response rate of <10% with a marginal survival advantage (8, 9). Breast cancer cells often develop various mechanisms of drug resistance during tumour progression which is the major reason for the failure of breast cancer therapy. NF-kB is constitutively active in breast cancer cells, which plays a critical role in promoting gemcitabine resistance to breast cancer (8). Hence, certain natural agents that block NF-kB activity are likely to reduce chemoresistance to gemcitabine and are possibly used in combination with gemcitabine as a novel therapeutic regimen for breast cancer patients. Thus, there is a necessity for developing novel strategies with no entity in toxicity that can sensitize breast cancer cells to chemotherapy.

Currently, phytochemicals (naturally occurring chemicals in plants) such as is flavones, gingerol, quercetin, resveratrol and curcumin have been identified to be more advantageous in treating various diseases like cancer, pancreatitis, fibrosis, etc. (10, 11). It is also known that the phytochemical, curcumin (Diferuloylmethane) has a beneficial role in the treatment of various types of cancers of the breast, pancreas, bladder and lungs (12). Curcumin is derived from turmeric (*Curcuma longa*), a pharmacologically safe chemical compound which has been shown to suppress NF-kB activation and its downstream regulation processes such as anti-apoptosis, proliferation, invasion and metastasis (13-15).

Hence, this investigation has focused on evaluating the beneficial role of curcumin in treatment of breast cancer in combination with gemcitabine *in vitro.* Curcumin has shown a positive impact on potentiating the gemcitabine anti-tumor effects as well as minimizing the side effects.

Materials and Methods

The human breast cancer cell lines MCF-7 or MDA MB-231(ER-negative, HER-2-negative) obtained from the American Type Culture Collection (ATCC, Manassas, VA) were grown as a monolayer in DMEM supplemented with 10% fetal bovine serum (FBS, Gibco-BRL, Grand Island, NY). The monolayer cells in the exponential growth phase were used for the experiments conducted in the present study. Gemcitabine and curcumin were obtained from Sigma, Saint Louis, USA.

Cell Proliferation Assay *:* The effect of curcumin and/or gemcitabine on MCF-7 or MDA MB-231 breast cancer cell proliferation were examined by using 3-[4, 5-dimethylthiazol-2-yl]-2, 5-diphenyl-tetrazolium bromide (MTT) dye [16]. Briefly, the monolayer cells in growth phase were trypsinized (0.25% trypsin for 10 min) and 5,000 cells were seeded into 96-well culture plates. The cells were incubated with curcumin (10 or 20 µM) and/or gemcitabine (10 or 100 µM) in DMEM medium in a 96-well culture plates for 48 h at 37 ^{o}C, followed by 2 h incubation with 10 µl of MTT (5 mg/mL in PBS) at 37 ^{o}C. The medium was replaced with 100 µL of 99.8% dimethyl sulphoxide in each well and optical density was measured at 570 nm with reference wave length, 630 nm. All the test samples were analyzed in triplicates.

Live / Dead Assay *:* Live/Dead assay kit was used (Molecular Probes, Carlsbad, CA) to determine the curcumin and/or gemcitabine cell apoptotic effects in breast cancer cells. This method determines intracellular esterase activity and plasma membrane integrity. The assay measures the emitted fluorescence intensity by enzymatic conversion of cell permeable nonfluorescent calcein AM with ubiquitous intracellular esterase present in live cells. In

addition, dead cells were quantitated with ethidium bromide, a red fluorescent homodimer dye which can enter dead cells through damaged membranes and bind to nucleic acids (16). Briefly pre-treated MCF-7 or MDA MB-231 cells (10,000 per well) were incubated in 24-well culture plates either with curcumin (10 or 20 µM; 4 h) or gemcitabine (10 or 100 µM; 24 h). To examine the potentiating effects of curcumin, the pre-treated cultures with curcumin (20 µM; 4 h) were further treated with gemcitabine (100 µM) for 24 h at 37 ºC. After incubation, the cells were stained with Live/Dead assay reagents for 30 min at 37 °C as per the manufacturer's instructions. The number of live and dead cells were observed under a fluorescence microscope (Olympus, Germany), followed by counting live (green at excitation and emission wavelengths of 495 and 515 nm, respectively) and dead (red at excitation and emission wavelengths of 495 and 635 nm, respectively) cells.

Electrophoretic Mobility Shift Assay [EMSA] : The breast cancer MCF-7 or MDA MB-231 cells (2×10^6 cells) were homogenized in buffer A [300 mM sucrose, 60 mM KCl, 15 mM N-2-hydroxyethylpiperazine-N'-2 ethanesulfonic acid (HEPES) pH 7.5 containing 2 mM EDTA, 0.5 mM EGTA, 0.15 mM spermine, 0.5 mM spermidine and 14 mM mercaptoethanol, 10 mM benzamidine, 0.7 mg/ml leupeptin] after incubation with curcumin (10 or 20 µM) and/or gemcitabine in 96-well culture plates (10 or 100 µM) for 2, 4, 6 and 8 h at 37 ºC. All the steps involved in homogenization and extraction process were carried out at 4 ºC and the samples were stored at -80 ºC until the assay was performed (9). The amount of protein in nuclear extracts was determined by Bradford's method according to the manufacturer's instructions (Bio-Rad, Hercules, CA, USA).

Nuclear protein extracts of the breast cancer MCF-7 or MDA MB-231 cells were analyzed using an EMSA to determine NF-kB nuclear translocation (17). The EMSA was conducted by competitive binding with radiolabelled and non-radiolabelled NF-kB probe. 10 µg of nuclear protein was incubated with 0.2 µg of ^{32}P-end-labeled double stranded oligonucleotide containing the NF-kB binding motif (Promega, Madison, WI, USA) and 1 µg of poly (dI-dC) as an inhibitor of non-specific binding in buffer B (20 mM HEPES pH 7.4 containing 60 mM KCl, 5 mM $MgCl_2$, 0.2 mM EDTA, 0.5 mM dithiothreitol, 0.5 mM phenylmehylsulfonyl fluoride, 1% Nonidet P-40 and 8% glycerol) at room temperature for 30 min. The sequence of the double-stranded oligomers used for EMSA was 5'-AGT TGA GGG GAC TTT CCC AGG C-3'. The entire reaction mixtures were run on 5% Tris-glycine EDTA gel electrophoresis, followed by autoradiography for visualizing DNA-protein complexes. The radioactive band intensity was quantitated using the Storm 820 and Image Quant software (Amersham, Piscataway, NJ).

Statistical analysis: All the experiments in the present study were conducted as three independent experiments and thus the obtained values were shown as Mean ± SD. In addition, the data was analyzed by one way ANOVA, followed by Duncan's multiple comparison between control and treatment groups by using Sigma Plot 11.0. The significant differences between two sample means were compared using unpaired Student's *t*-test.*$p \leq 0.05$ is considered as statistically significant.

Results

The aim of the present investigation was to determine the beneficial role of curcumin in potentiating anti-tumor effects of gemcitabine in breast cancer cells. To elucidate the role of curcumin, the present study was conducted on well established breast cancer cell lines, MCF-7 and MDA MB-231. The positive effects of curcumin that came to light in preventing the cancer effects, by suppressing the cell proliferation as well as NF-kB activation were examined.

Curcumin decreased the cell proliferation in breast cancer cells in vitro: In the present study, we have examined the role of curcumin and/or

gemcitabine on the cell viability by using MTT cell proliferation assay. Either curcumin or gemcitabine significantly ($p \leq 0.05$) decreased the MCF-7 and MDA MB-231 cancer cells *in vitro* in dose dependent manner (Fig. 1A). About 70 and 51% MCF-7 cancer cells survived to 48 h exposure of 10 and 20 µM curcumin, respectively in DMEM ($p \leq 0.01$). However, 10 and 100 µM gemcitabine reduced only 11 and 13.4% cells indicating that curcumin has shown major inhibition on cell proliferation ($p \leq 0.001$). In addition, 20 µM curcumin enhanced the gemcitabine anti-proliferation activity to 60.7% at higher dose (100 µM gemcitabine) as used in the present study. Similarly, MDA MB-231 cancer cells also exhibited 45% anti-proliferation activity in presence of 20 µM curcumin in combination with 100 µM gemcitabine ($p \leq 0.01$). Whereas curcumin (20 µM) or gemcitabine (100 µM) alone decreased 30% or 14.7% cell proliferation, respectively ($p \leq 0.05$).

Curcumin enhanced the apoptosis in breast cancer cells in vitro: Further, the potentiating effect of curcumin on gemcitabine induced apoptosis in breast cancer cells was determined by using Live/Dead assay. The assay denoted that curcumin and gemcitabine exposure to both MCF-7 and MDA MB-231 cancer cells enhanced the apoptosis (Fig. 1B). The exposure of 10 and 20 µM of curcumin exhibited 41 and 48% apoptotic cells in MCF-7 cancer cells, respectively ($p \leq 0.05$). Whereas the exposure of 10 and 20 µM of curcumin exhibited 38 and 42% apoptotic cells in MDA MB-231 cancer cells, respectively ($p \leq 0.05$). On the contrary, lesser apoptosis was observed in 10 and 100 µM gemcitabine treated cells (18 and 22% in MCF-7 cells; 14 and 20% in MDA MB-231 cells). However, apoptosis significantly decrease to 61 and 46% in MCF-7 and MDA MB-231 cells, respectively ($p \leq 0.05$) at 100 µM gemcitabine when pre-treated the cells with 20 µM curcumin. These results indicated an increase in the percentage of apoptosis in the presence of chemotherapeutic drug, gemcitabine in combination with phytochemical, curcumin. However, gemcitabine alone had a minimal effect on apoptosis in both the examined breast cancer cell lines.

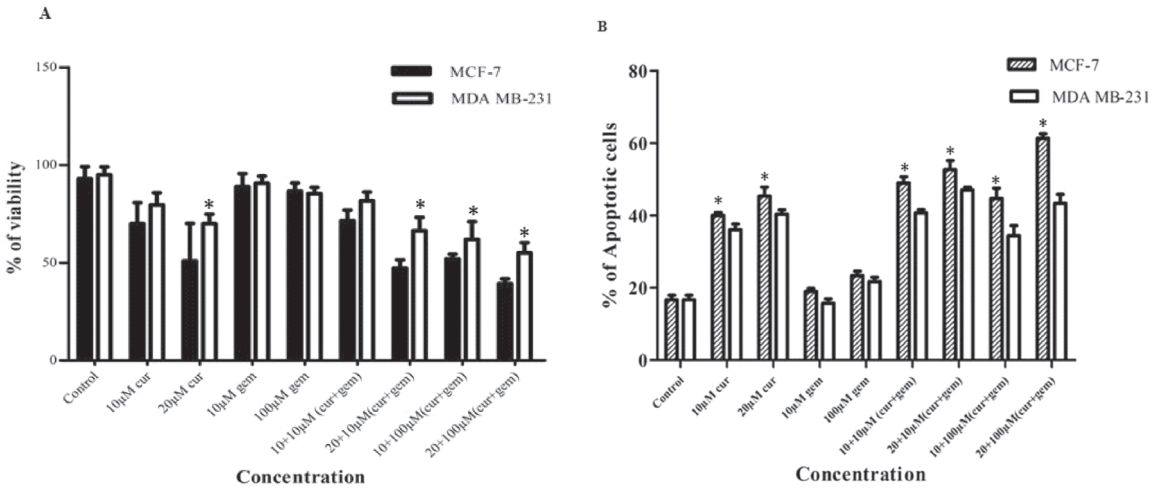

Fig.1. Curcumin inhibits proliferation, potentiates the apoptotic effects of gemcitabine in breast cancer cells in vitro. **A.** MTT assay results showed dose dependent suppression of cell proliferation in all breast cancer cell lines tested. **B.** Live/Dead assay results indicated that curcumin potentiates gemcitabine induced cytotoxicity, percentages, proportions of apoptotic breast cancer cells. Cur: Curcumin, Gem: Gemcitabine

Curcumin inhibited NF-kB activation induced by gemcitabine in breast cancer cell lines : EMSA assay was used to demonstrate whether curcumin suppresses the NF-kB activation induced by gemcitabine in breast cancer cell lines. Breast cancer cell lines were incubated with 100 µM gemcitabine with different time periods to observe maximum NF-kB activation. It has been observed that 100 µM gemcitabine induces NF-kB activation at 6 h and reaches to a maximum level at 8 h in both cell lines (Fig. 2A and Fig. 2B). MCF-7 cells have shown 5 and 5.8 fold increase of NF-kB activation at 6 h and 8 h of incubation respectively, when compared to controls; $p \leq 0.001$. Similarly, MDA-MB-231 cells have shown 5.1 and 6.9 fold increase ($p \leq 0.005$) at 6 h and 8 h of incubation, respectively, while the 20 µM curcumin pre-treated cells exhibited 30% and 20% NF-kB suppression in MCF-7 and MDA MB-231, respectively when compared to their respective controls. Surprisingly, the curcumin in combination with gemcitabine suppressed NF-kB activation in both MCF-7 (Fig. 2C) and MDA MB-231 (Fig. 2D). The dose dependent suppression of gemcitabine induced NF-kB activation by curcumin has been observed in both cell lines. Both the cell lines when pre-treated with 10 µM curcumin for 4 h showed suppression (38%) of gemcitabine (100µM, 8h) induced NF-kB activation ($p \leq 0.005$). In addition, the increase in curcumin concentration to 20 µM suppressed the gemcitabine (100 µM, 8 h) induced NF-kB activation up to 80% in both cell lines ($p \leq 0.005$). The combined results enlightened the potentiating effects of curcumin in apoptosis as well as suppression of gemcitabine induced NF-kB activation.

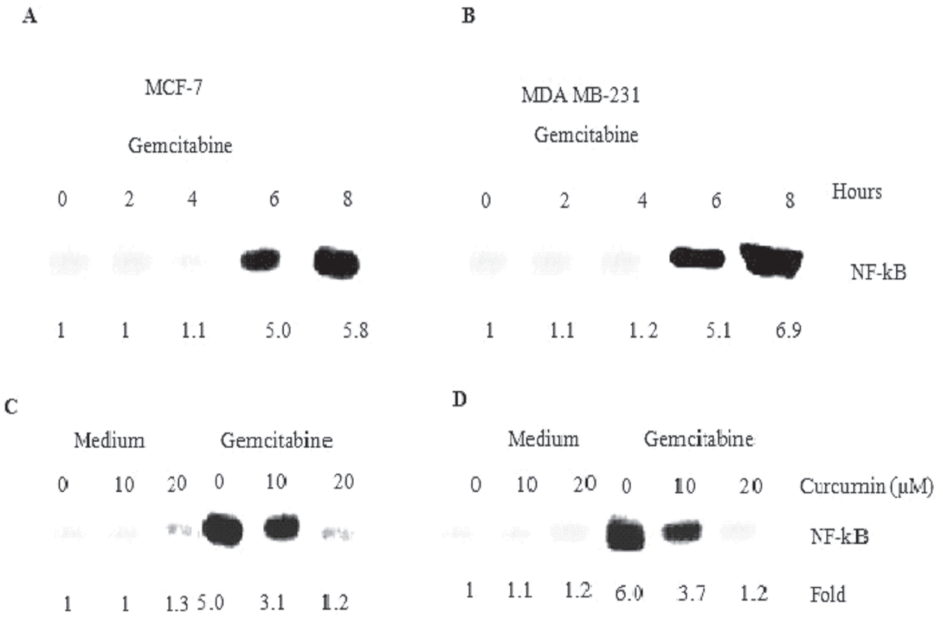

Fig. 2. Curcumin enhances the effect of gemcitabine against expression of NF-kB in breast cancer. A. MCF-7 cells 2×10^6 were treated with 100 µM gemcitabine. B. MDA MB-231 cells 2×10^6 were treated with 10 µM gemcitabine for indicated time intervals. The cells were then analyzed for NF-kB activation using EMSA. C & D. MCF-7 cells and MDA MB-231 cells 2×10^6, were pretreated with 0, 10 and 20 µM curcumin for 4 h. MCF-7 cells were stimulated with 100 µM gemcitabine for 8 h, and MDA MB-231 cells were stimulated with 100µmol /L gemcitabine for same period. The cells were then analyzed for NF-kB activation using EMSA.

Vol. 7 (4) 854-861 October 2013, ISSN 0973-8916 (Print), 2230-7303 (Online)

Discussion

The present study was conducted to elucidate the beneficial role of natural herbal compound, curcumin, to improve the therapeutic effects of gemcitabine in human breast cancer cells *in vitro*. It is well known that curcumin has anti-proliferation activity and it induces a high percentage of apoptosis in human breast cancer cells by regulating the expression of genes associated with programmed cell death (18), a dietary ingredient in many countries, which would be helpful in treatment of cancer (11, 12, 19, 20). In addition, it has shown to suppress NF-kB activation and NF-kB gene products in various models, including rodents and mammals (13, 14, 21). Hence, we have chosen curcumin in combination with gemcitabine that aids in potentiating the apoptosis as well as suppressing the NF-kB activity in human MCF-7 and MDA MB-231 cells. Our results reported here with the gemcitabine alone had minimal effects in anti-proliferation (up to 14%) (Fig. 1A) and apoptosis (up to 14%) (Fig. 1B) in both breast cancer cells. However, in combination with curcumin, the proliferation activity was significantly reduced to 61 and 45% in MCF-7 and MDA MB-231 cells, respectively. In addition, we have reported that the MCF-7 cells have shown more sensitivity than MDA MB-231 cells to both curcumin and gemcitabine. Previous studies have reported the potentiating effects of curcumin in combination with gemcitabine in various cancerous cells such as of human bladder 253JBV (22), KU-7, RT4V6 (14) and pancreas BxPC-3, MIA PaCa-2, Panc-1 and MPanc-96 (18). Even *in vivo* studies in mice revealed the potentiating beneficial role of curcumin in anticancer activity (22). Similarly, human breast cancer cells, MCF-7 and MDA MB-231 showed the significant anti-proliferation activity ($p \leq 0.05$) by combined administration of curcumin and gemcitabine. It is well known that curcumin alone has the ability to suppress apoptosis in human breast cancer cells MCF-7 and MDA MB-231 (23, 24), cholanagioma carcinoma cells, KKU100, KKU-M156, KKU-M213 (25), lung cancer cells, A549 and H1299 (26) and hepatocaricoma cells, HCCJ5 (27). These combined results suggest that curcumin might/does play a role in anti-proliferation activity and reduced apoptosis on breast cancer cell lines. In addition, it is well known that NF-kB has been implicated in cell survival and proliferation (5, 6). Recent reports made on NF-kB and PI3k/akt pathway activation in putative resistance mechanisms for breast cancer. However, NF-kB has been linked with chemoresistance with the therapeutic drugs such as gemcitabine that activates NF-kB in breast cancer lines such as MDA MB-231and MCF-7 as well as in tissue samples of breast carcinoma (23, 24). In the present study, EMSA denoted that the gemcitabine alone enhanced the NF-kB activation significantly ($p \leq 0.05$) in human breast cancer cells, MCF-7 (5.8 fold) and MDA MB-231 (6.9 fold). On the contrary, curcumin reduced the NF-kB activation significantly in MCF 7 and MDA MB-231 cells ($p \leq 0.005$). Some reports suggest that such an activation of NF-kB by human prostate epithelial PZ-HPV-7 cancer cells could be down regulated by curcumin sensitization by blocking phosphorylation of IkBα and its degradation (28), G1/S arrest in mantle cell lymphoma (29). The present investigation reports the dose dependent suppression of gemcitabine induced NF-kB activation by curcumin at 10 (38%) and 20 µM (up to 80%) in both cell lines. Similarly, previous studies using various cancer cell lines showed that curcumin is quite effective in suppressing the proliferation, NF-kB activation and promoting apoptosis, exhibiting more effectiveness when combined with gemcitabine (14,18). Hence, gemcitabine alone does not attain sufficient disease control due to intrinsic or acquired resistance of tumour cells; curcumin may help in adequate management of cancer remedy. The present study suggested that the combinational therapy with herbal compound, curcumin, may perhaps be helpful in the treatment of breast cancer in human population. Further studies of *in vivo* models may help in understanding the beneficial role of curcumin in breast cancer therapy.

References

1. Bieche, I., Tozlu, S., Girault, I. and Lidereau, R. (2004). Identification of a three-gene expression signature of poor and prognosis breast carcinoma. Molecular Cancer, 3, 37. Doi: 10.1186/1476-4598-3-37.
2. Wang, C.Y., Cusack, J.C., Liu, R. and Baldwin, A.S. (1999). Control of inducible chemoresistance: enhanced antitumor therapy through increased apoptosis by inhibition of NF-kB. Nature Medicine, 5,412-417.
3. Chopra, R. (2001). The Indian scene. Journal of Clinical Oncology, 19,106-111.
4. Vo, A.T. and Millis, R.M. (2012). Epigenetics and breast cancers. Obstetrics and Gynecology International, Article ID: 602720. doi:10.1155/2012/602720
5. Aggarwal, B.B. (2004). Nuclear factor-kB: the enemy within. Cancer Cell, 6,203-208.
6. Karin, M. (2006). Nuclear factor-kappa B in cancer development and progression. Nature, 441,431-436.
7. Arlt, A., Gehrz, A., Muerkoster, S., Vorndamm, J., Kruse, M.L., Folsch, U.R. and Schafer, H. (2003). Role of NF-kB and Akt/PI3K in the resistance of pancreatic carcinoma cell lines against gemcitabine-induced cell death. Oncogene, 22,243-251.
8. Burris, H.A., Moore, M.J., Andersen, J., Green, M.R., Rothenberg, M.L., Modiano, M.R., Cripps, M.C., Portenoy, R.K., Storniolo, A.M., Tarassoff, P., Nelson, R., Dorr, F.A., Stephens, C.D. and Von Hoff, D.D. (1997). Improvements in survival and clinical benefit with gemcitabine as first-line therapy for patients with advanced pancreas cancer a randomized trial. Journal of Clinical Oncology, 15, 2403-2413.
9. Kojima, M., Morisaki, T., Sasaki, N., Nakano, K., Mibu, R., Tanaka, M. and Katano, M. (2004). Increased nuclear factor-kB activation in human colorectal carcinoma and its correlation with tumor progression. Anticancer Research, 24, 675-682.
10. Lee, K.W., Bode, A.M. and Dong, Z. (2011). Molecular targets of phytochemicals for cancer prevention. Nature Reviews Cancer, 11, 211-218.
11. Abbruzzese, J.L. and Lippman, S.M. (2004). The convergence of cancer prevention and therapy in early-phase clinical drug development. Cancer Cell, 6,321-326.
12. Aggarwal, B.B., Kumar, A. and Bharti, A.C. (2003). Anticancer potential of curcumin: preclinical and clinical studies. Anticancer Research, 23, 363-398.
13. Singh, S. and Aggarwal, B.B. (1995). Activation of transcription factor NF-kB is suppressed by curcumin [diferuloyl-methane]. The Journal of Biological Chemistry, 270, 24995-25000.
14. Kamat, A.M., Sethi, G. and Aggarwal, B.B. (2007). Curcumin potentiates the apoptotic effects of chemotherapeutic agents and cytokines through down-regulation of nuclear factor-KB and nuclear factor-KB–regulated gene products in IFN-A–sensitive and IFN-A–resistant human bladder cancer cells. Molecular Cancer Therapeutics, 6, 1022-1030.
15. Reed, J.C. (2002). Apoptosis-based therapies. Nature Reviews Drug Discovery, 1, 111-121.
16. Takada, Y., Khuri, F.R. and Aggarwal, B.B. (2004). Protein farnesyltransferase inhibitor [SCH 66336] abolishes NF-kappa B activation induced by various carcinogens and inflammatory stimuli leading to suppression of NF-kappaB-regulated gene expression and up-regulation of apoptosis. The Journal of Biological Chemistry, 279, 26287-99.

17. Chaturvedi, M.M., Mukhopadhyay, A. and Aggarwal, B.B. (2000). Assay for redox-sensitive transcription factor. Methods in Enzymology, 319,585-602.

18. Kunnumakkara, A.B., Guha, S., Krishnan, S., Diagaradjane, P. and Gelovani, J., Aggarwal B.B.(2007). Curcumin potentiates antitumor activity of gemcitabine in an orthotopic model of pancreatic cancer through suppression of proliferation, angiogenesis, and inhibition of nuclear factor- kB-regulated gene products. Cancer Research, 67, 3853-3861.

19. Somasundaram, S., Edmund, N.A., Moore, D.T., Small, G.W., Shi, Y.Y. and Orlowski, R.Z. (2002). Dietary curcumin inhibits chemotherapy-induced apoptosis in models of human breast cancer. Cancer Research, 62, 3868-3875.

20. Jiang, M.C., Yang, Yen, H.F., Yen, J.J. and Lin, J.K. (1996). Curcumin induces apoptosis in immortalized NIH3T3 and malignant cancer cell lines. Nutrition and Cancer, 26,111-120.

21. Wang, W. and Cassidy, J. (2003). Constitutive nuclear factor-kappa B mRNA, protein over expression and enhanced DNA-binding activity in thymidylate synthase inhibitor-resistant tumour cells. British Journal of Cancer, 88, 624-629.

22. Tharakan, S.T., Inamoto, T., Sung, B., Aggarwal, B.B. and Kamat, A.M. (2010). Curcumin potentiates the antitumor effects of gemcitabine in an orthotopic model of human bladder cancer through suppression of proliferative and angiogenic biomarkers. Biochemical Pharmacology, 79, 218-228.

23. Ramachandran, C., Rodriguez, S., Ramachandran, R., Raveendran, Nair, P.K., Fonseca, H., Khatib, Z., Escalon, E. and Melnick, S.J. (2005). Expression profiles of apoptotic genes induced by curcumin in human breast cancer and mammary epithelial cell lines. Anticancer Research, 25, 3293-3302.

24. Ramachandran, C. and You, W. (1999). Differential sensitivity of human mammary epithelial and breast carcinoma cell lines to curcumin. Breast Cancer Research and Treatment, 54, 269-278.

25. Prakobwong, S., Gupta, S.C., Kim, J.H., Sung, B., Pinlaor, P., Hiraku, Y., Wongkham, S., Sripa, B., Pinlaor, S. and Aggarwal, B.B. (2011). Curcumin suppresses proliferation and induces apoptosis in human biliary cancer cells through modulation of multiple cell signaling pathways. Carcinogenesis, 32, 1372-1380.

26. Radhakrishna Pillai, G., Srivastava, A.S., Hassanein, T.I., Chauhan, D.P. and Carrier, E. (2004). Induction of apoptosis in human lung cancer cells by curcumin. Cancer Letters, 208,163-170.

27. Wang, W.H., Chiang, I.T., Ding, K., Chung, J.G., Lin, W.J., Lin, S.S. and Hwang, J.J. (2012). Curcumin-induced apoptosis in human hepatocellular carcinoma J5 Cells: critical role of Ca^{+2}-dependent pathway. Evidence Based Complementary and Alternative Medicine, 5129077. doi:10.1155 /2012/512907

28. Deeb, D., Jiang, H., Gao, X., Hafner, M.S., Wong, H., Divine, G., Chapman, R.A., Dulchavsky, S.A. and Gautam, S.C. (2004). Curcumin sensitizes prostate cancer cells to tumour necrosis factor–related apoptosis-inducing ligand/Apo2L by inhibiting nuclear factor-KB through suppression of IKBA phosphory-lation. Molecular Cancer Therapeutics.7, 803-812.

29. Shishodia, S., Hesham, M., Raymond Lai, Aggarwal, B.B. (2005). Curcumin [diferuloyl-methane] inhibits constitutive NF-kB activation, induces G1/S arrest, suppresses proliferation, and induces apoptosis in mantle cell lymphoma. Biochemical Pharmacology. 70, 700-713.

Current Trends in Biotechnology and Pharmacy
Vol. 7 (4) 861-869 October 2013, ISSN 0973-8916 (Print), 2230-7303 (Online)

Optimization of Protocols for Callus Induction, Regeneration and Acclimatization of Sugarcane (*Saccharum officinarum* L.) Cultivar CO-86032

Srinath Rao* and FTZ Jabeen
Plant Tissue Culture and Genetic Engineering Lab
Department of Post-Graduate Research and Studies in Botany,
Gulbarga University, Gulbarga 585 106, Karnataka, India
*For Correspondence - srinathraomm@gmail.com

Abstract

An efficient protocol for induction of callus and regeneration of a high yielding sugar cane var CO-86032 has been developed and reported here. Callus induction from leaf sheath explants derived from 2-3-month-old plants was achieved on Murashige and Skoog's(MS) medium supplemented with different auxins viz, 2,4-D, 2,4,5-T, NAA, dicamba and picloram (1-3 mgl^{-1}). Among different auxins, 2,4-D at 1mgl^{-1} supplemented with 2% sucrose + 300mgl^{-1} PVP was found favorable in inducing callus and preventing browning. Addition of coconut milk and Kn further enhanced the growth of callus maximum being on MS medium supplemented with 0.5$mg1^{-1}$Kn (1994±0.39mg). Calli were further evaluated for regeneration. MS medium supplemented with 2mg/l Kn+1mg/l BAP was found suitable where 100% calli regenerated with maximum number of multiple shoots per callus mass(168±0.54). Highest number of root emergence (38±0.21) and maximum root length (6.8±0.64cm) was achieved on MS medium supplemented with 5mgl^{-1} NAA. The *in vitro* grown plants were transferred to polycups containing a mixture of sterilized sand and black soil (1:1) for hardening. The hardened plants were transferred to green-house conditions where they survived with 90% frequency.

Key Words: *Saccharum*, callus, leaf explants, organogenesis, sugarcane.

Introduction

Sugarcane (*Saccharum officinarum* L.) is known in India from time immemorial. It belongs to the family Poaceae. It is a tropical grass of high polyploidy (2n= 36-170). Sugarcane accounts for nearly 70% of the worlds' sugar and is an economically important cash crop in tropical and sub-tropical regions (1). Apart from use in sugar production, it is gaining importance for ethanol production. Some other bye-products from sugarcane include molasses, stock feed, alcoholic drinks, bagasses and cane wax (2, 3). Sugarcane is a clonally propagated crop and is especially vulnerable to diseases and propagation from cuttings facilitates the spread of the pathogens and may result in epidemics (4). In India, sugarcane is grown mainly in the states of Maharashtra, Karnataka, Tamil Nadu, Utter Pradesh and Andhra Pradesh. It is an important cash crop of India grown over an area of 4 million hectares. Due to its importance globally, constant efforts are being made world over for its improvement, through tissue culture techniques (5-11). Research in sugarcane tissue culture was started in Hawai in 1964 by Nickel. This was followed by the pioneering works by Heinz and Mee (6), Barba and Nickel (7) who first independently demonstrated that plantlets could be developed from sugarcane callus cultures. From the published results, it is evident that essentially every part of the sugarcane plant is capable of callus production (11). However,

only immature leaf sheath rolls (12) and the inflorescences (11) are capable of producing morphogenic callus to any appreciable level. Callus induction is a very important for inducing genetic modifications in this crop (13). Interest in callus based regeneration will be of significant importance as *in vitro* mutations and somaclonal variants could be induced and subsequently used for sugarcane improvement. Keeping in view of the importance of callus induction and callus mediated regeneration, the present investigations were carried out for optimizing a complete tissue culture protocol (callus induction, regeneration and acclimatization) in a high yielding sugar cane variety Co-86032. Earlier reports on sugarcane have shown that a high genotypic variation exists with regards to source and explants and concentration of 2, 4-D used for callus induction.

Materials and Methods

The plant material was obtained from Aland agricultural farm, Aland, Karnataka State, India. Young leaf sheath of 2-3-months-old plants were used as explants. The explants were thoroughly washed in running tap water to remove particles adhered to the surface and then washed with 1% (v/v) soap solution (Teepol) for 1 minute and further washed with sterilized distilled water till froth was completely removed, then they were surface sterilized for 5minutes in 0.1% (w/v) mercuric chloride, rinsed with sterilized distilled water thrice to remove traces of mercuric chloride. The outer layers of the explants were removed and inner leaves were cut into pieces and placed in 1% sterilized ascorbic acid solution for 5 minute to prevent browning of the explants. Leaf pieces were than inoculated on Murashige and Skoog's (14) medium supplemented with 2% sucrose with or without coconut milk and different types of auxins viz., 2,4-dichlorophenoxyacetic acid (2,4-D), α-naphthaleneacetic acid (NAA),2,4,5-trichlorophenoxyacetic acid (2,4,5-T), picloram and dicamba at various concentrations with or without cytokinins. For solidification of media, 8% agar (w/v) was added. pH of the medium was adjusted to 5.7 prior to autoclaving at a pressure of 121 ºC at 15 psi for 15 minutes, then dispensed into culture tubes (150×15mm) and the cultures were maintained under cool-white florescent light at 60$\mu M^{-2} S^{-1}$ (16 h light/8 h dark) at 26±1 ºC for four weeks. These growth conditions were used for all tissue culture steps in this study. A complete randomized design with 10 explants/callus per culture tube and three replication/treatment were maintained and all the experiments were repeated thrice. Relative growth rate of callus was determined after 4-weeks of culture. For regeneration, approximately 250±10 mg callus were placed on MS medium supplemented with 2% sucrose containing different types of cytokinins alone or in combination.

Results and Discussion

Induction of Callus: Young leaf sheaths of sugarcane were used as starting material to generate callus on medium containing different types of auxins at various concentrations(Table 1).Callus induction was observed within two weeks after inoculation of the explants on the medium. All the growth regulators used viz., 2,4-D 2,4,5-T and NAA used at concentrations between 1-3mg/l induced callus with varying frequencies. Auxin2,4-D induced callus with 100% frequency followed by 2,4,5-T with 70% at 3mg/l and NAA with 50% frequency at 1mg/l.Growth of fresh weight of callus was 685±0.94 mg on 1mgl^{-1}2,4-D, followed by 2,4,5-Twhich was 658±0.49 (Fig. 1a-f) mg/culture and the least was recorded on NAA supplemented medium(237±0.88 mg). With further increase in the concentrations of the auxins, the relative growth rate of callus decreased. Dicamba and picloram were least responsive for callus induction and growth (Table 1). Supplementing coconut water at 5% to 2, 4-D containing medium further increased the growth of callus to 898±0.72mg/culture. Highest growth the callus (1994±0.39 mg) was observed on MS medium supplemented with 1 mg/l 2, 4-D + 0.5 mg/l kinetin (Kn) as shown in Table 2 (Fig. 1g & h).

Leaf as an explants along with auxin 2, 4-D has been reported as the best combination for callus induction in sugarcane (2, 3, 9, 13, 15-

Table 1. Effect of various auxins at different concentrations on frequency of induction and growth of leaf sheath derived callus in sugarcane

Growth % regulators (mg/1)	Frequency of callus induction	Growth of callus after 30 days of culture(mg/culture)	
2,4-D	FW	DW	
1	100	856 ± 0.94[a]	89 ± 0.54[a]
2	100	807 ± 0.51[b]	83 ± 0.51[a]
3	100	735 ± 0.47[c]	79 ± 0.33[b]
2,4,5-T			
1	44.0	324 ± 0.66[f]	68 ± 0.47[c]
2	34.6	457 ± 0.39[e]	79 ±0.72[b]
3	70.6	658 ± 0.49[d]	89 ± 0.40[a]
NAA			
1	50.6	237 ± 0.88[g]	27 ± 0.72[d]
2	20.0	143 ± 0.71[h]	14 ± 0.39[e]
3	18.6	124 ± 0.74[i]	13 ± 0.76[e]
Dicamba			
1	8.0	35 ± 0.04[j]	3.3±0.15[f]
2	8.0	34 ± 0.74[j]	3.2±0.13[f]
3	6.0	29 ± 0.88[k]	2.9±0.01[f]
Picloram			
1	14.6	34 ± 0.02[j]	3.2±0.20[f]
2	8	32 ± 0.84[j]	3.0±0.21[f]
3	8	30 ± 0.33[k]	2.9±0.34[f]

Data represent average of three replicates, and each replicate consists of 25 cultures.
Mean ± Standard error. Mean followed by the different superscript in a column are significantly different from each other according to ANOVA and DMRT P e" 0.05.

Table 2. Effect of coconut water (CW) and kinetin (Kn) on growth of leaf sheath derived callus in sugarcane

2,4-D + CW	Fresh weight(mg)	Dry weight(mg)
1 + 5%	898 ± 0.72[a]	86 ± 0.22[a]
1 + 10%	879± 0.75[b]	86± 0.40[a]
1 + 15%	874± 0.38[b]	85± 0.30[a]
2,4-D + Kn		
1 + 0.5	1994 ± 0.39[b]	98 ±0.12[b]
1 + 1.0	876 ± 0.81[b]	96 ± 0.17[b]
1 +1.5	543 ± 0.84[c]	51 ± 0.34[c]

Data represent average of three replicates, each replicate consists of 25 cultures.
Mean ± Standard error. Mean followed by the different superscript in a column are significantly different from each other according to ANOVA and DMRT P e" 0.05.

22). Other explants like inflorescence (11), shoot tip/meristem (23, 24), seeds (25) have also been reported as source of explants for callus initiation. A survey of literature (21, 24-28) showed that whatever may be the source of explants used for callus initiation, the requirement of 2, 4-D is essential. In the present investigations also, it was noticed that 2, 4-D is an important auxin for callus induction when compared to 2, 4, 5-T and NAA, picloram and dicamba. However, Gallo-Meagher (2) and Khan et al. (29) reported that picloram is better than 2, 4-D for callus initiation and proliferation in the sugarcane cultivars NIA98, NIA204 and BL4. Such contradicting results may be attributed to different genotypes used in these studies. Sugarcane is known to be highly genotype dependent for its response to callus induction (30). Supplementing Kn at 0.5 mg/l or 5% coconut water (CW) resulted in better growth of callus compared to the controls. Such a beneficial effect of coconut milk on the growth of sugarcane callus has been reported by many workers earlier (27, 28, 31).

Organogenesis*:* Callus mediated regeneration has been reported in sugarcane (17, 20, 21, 25, 32). Therefore, callus was evaluated for shoot regeneration on MS medium along with different cytokinins like Kn, 6-benzylaminopurine (BAP), thidiazuron (TDZ, N-phenyl-N'-1,2,3-thiadiazol-5-ylurea) and zeatin at different concentrations either alone, or in combination with other cytokinins. It was noticed that all the concentrations of cytokinins when used alone induced multiple shoots from the callus with varying frequencies depending upon the concentration used. Kn alone induced multiple shoots (152±0.4) with a frequency of 100% at 2mg/l, but further increase in the concentrations decreased the frequency of shoot induction and number of shoots differentiated per explant. In BAP (1 mg/l) supplemented medium,the frequency of multiple shoot induction was 100% with an average of 126±0.27 shoots per callus mass (Fig. 2a). Further increase in its concentration, reduced the number of multiple shoots, butthe frequency of shoot induction was not affected. Behara and Sahoo (24) reported regeneration from meristem derived callus of sugarcane cultivar Nayana, using 2mg/l BAP. However, the number of shoots reported per callus mass was only 4.2. On the contrary Naik et al. (16) reported regeneration from callus at low concentrations of BAP (0.5 mg/l). It appears from these reports that regeneration potential in sugarcane is highly dependent on the concentrations of plant growth regulators besides the genotypes (29, 30, 33).

TDZ and zeatin induced multiple shoots at low concentrations ranging from 0.1 to 0.5 mg/l with a frequency of 40 and 54.6% and 133 and 63 shoots per callus respectively. Further increase in their concentration gradually reduced not only the frequency but alsothe number of shoots formed per callus. Of the four cytokinins, Kn was the most responsive in inducing multiple shoots followed by BAP, TDZ and zeatin. It is noticed that for regeneration of shoots from sugarcane callus, either BAP or Kn are essential. Depending on the verities used it was found that either Kn at low concentration (35) or at high (2mg/l) concentrations (12, 24, 34) or BAP at low (0.2-0.5 mg/l) concentrations (3, 16, 24) is required for shoot induction. It is evidentfrom the study that shoot organogenesis in sugarcane is highly dependent onplant growth regulator concentration. However, organogenesis from sugarcane callus on hormone free media but in the presence of high concentration of sucrose (60g/l) and casein hydrolysate (500 mg/l) has been reported (24).

Effect of the combination of Kn and BAP: Since Kn at 2 mg/l gave better response, it was decided to study its interaction with BAP for the shoot forming ability. It was noticed that supplementing BAP at 0.5-1 mg/l concentrations along with Kn further increased the number of shoots, the maximum being 168 at 1mg/l (Fig. 2b). But, at 1.5 mg/l Kn, shoot formation decreased (Table 3). Supplementing TDZ or zeatin along with Kn was not found beneficial in enhancing the number of shoots differentiated per callus. However, the number of shoot buds

Table 3. Effect of cytokinins on the frequency, average number of shoots and average length of shoots from leaf sheath derived callus in sugarcane

Hormonal concentration (mg/l)	No. of tubes inoculated	% Frequency of shoots formed	Average no. of well developed shoots (~1 cm)	Average length of shoots (cm)
BAP				
1	75	100	128 ± 2.27^{c}	3.81 ± 0.23^{d}
2	75	100	116 ± 2.34^{c}	3.61 ± 0.15^{d}
3	75	100	52 ± 1.24^{f}	3.56 ± 0.12^{d}
Kn				
1	75	100	132 ± 2.49^{c}	4.9 ± 0.10^{c}
2	75	100	152 ± 3.04^{b}	5.2 ± 0.02^{c}
3	75	100	98 ± 2.86^{d}	4.8 ± 0.01^{c}
Zn				
0.1	75	14.0	24 ± 0.08^{h}	1.8 ± 0.10^{f}
0.2	75	24.0	52 ± 0.09^{g}	1.9 ± 0.09^{f}
0.3	75	40.0	63 ± 0.04^{f}	2.1 ± 0.12^{f}
TDZ				
0.1	75	38.6	78 ± 0.15^{e}	2.6 ± 0.14^{e}
0.2	75	44.0	82 ± 0.30^{e}	2.8 ± 0.10^{e}
0.3	75	54.6	94 ± 0.18^{d}	3.0 ± 0.11^{e}
Kn+ BAP				
2 + 1	75	100	168 ± 0.54^{a}	8.8 ± 0.14^{a}
2 + 2	75	100	96 ± 0.62^{d}	8.0 ± 0.05^{b}
2 + 3	75	100	64 ± 0.86^{f}	7.4 ± 0.02^{b}

Data represent average of three replicates, each replicate consist of 25 cultures.
Mean ± Standard error. Mean followed by the different superscript in a column are significantly different from each other according to ANOVA and DMRT P e" 0.05.

Table 4. Effect of auxins on frequency, number of roots and root length per plantlet in sugarcane

Auxins (mg/l)	% Frequency of root differentiation	No. of roots / explant	Root length (cm)
NAA(mg/l)			
1	100	8±0.59 ^{bcd}	3.76±0.11^{a}
2	100	15±0.57^{e}	3.48±0.15 ^{a}
3	100	25±0.74^{g}	5.60±0.54^{cd}
4	100	32±0.44^{b}	5.71±0.67^{cd}
5	100	38±0.21^{i}	6.82±0.64^{d}
IBA(mg/l)			
1	80.6	06±0.36^{b}	4.51±0.25^{b}
2	95.6	10±0.33^{d}	6.87±0.73^{d}
3	100	14±0.15^{e}	6.82±0.48^{d}
4	80.6	8±0.24^{bcd}	3.70±0.34^{a}
5	76.6	4±0.14^{a}	3.10±0.16^{a}

Vol. 7 (4) 861-869 October 2013, ISSN 0973-8916 (Print), 2230-7303 (Online)

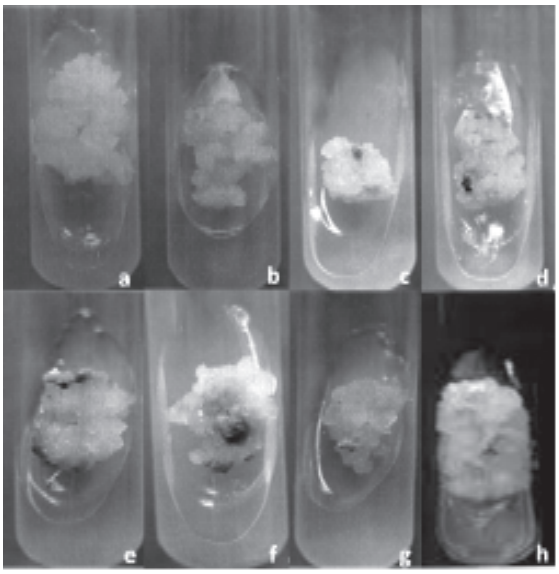

Fig. 1. Callus growth in sugarcane: a, b and c- Callus growing on 1, 2 and 3 mg/l 2,4-D (Note: gradual reduction in callus growth).
d, e and f- Callus growing on 1, 2 and 3 mg/l 2,4,5-T (Note: gradual increase in callus growth but lesser than that of 2,4-D supplemented medium). g) Callus grown on medium containing 1mg/l 2, 4-D and 5% coconut milk. h). Callus grown on medium containing 1 mg/l 2, 4-d + 0.5 mg/l Kn. Note more callus in h than in g.

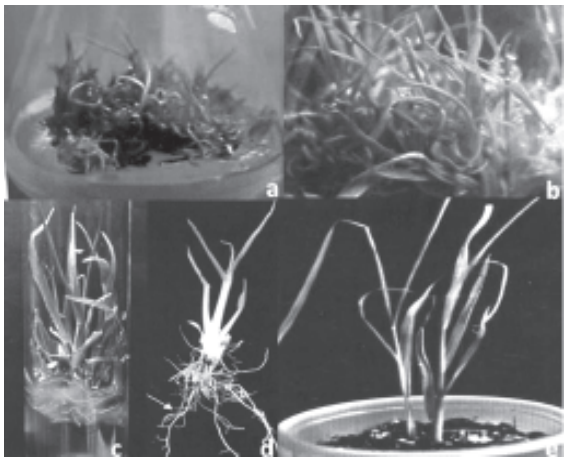

Fig. 2. Organogenesis and rhizogenesis in sugarcane: a) Plantlets growing on MS+2mg/l Kn. b) Plantlets on 2mg/lKn+1mg/l BAP. Note: healthy and increased number of plantlets. c) and d) Rooting of plantlets on MS+5mg/l NAA. e) Plantlets transferred to poly cups.

induced was more when compared with those produced on medium fortified either with TDZ or zeatin alone. Shoot length (3.8 and 8 cm) also decreased in this combination.From these results it can be concluded that TDZ and zeatin do not act synergistically in regulating the process of shoot differentiation in sugarcane.

Rhizogenesis*:* The *in vitro* developed plantlets were transferred to MS medium supplemented with various concentration of NAA or indole-3-butyric acid (IBA) for root induction. Highest frequency (100%) and maximum number of roots per plantlet was obtained on medium containing either 3mgl/l NAA or IBA (Table 4; Fig. 2c & d). Both NAA and IBA (22, 24) are reported to be useful in root induction in sugarcane; however, rooting devoid of any hormones but only at high concentrations of sucrose (6-8%) has been reported (35). Well-rooted plants were later transferred to the poly cups (Fig. 2e) containing soil and sand mixture (1:1). Plantlets were initially covered with plastic bags to maintain high humidity. Hoagland nutrient solution was added to the plantlets on daily basis during this period. After 15-20 days, plastic bags were removed and thus they were acclimatized to the normal temperature with 90% success rate.

Acknowledgement

The authors thank the Chairman of the Department of Botany, Gulbarga University,for the facilities provided during the course of this investigation.

References

1. Chatenet, M., Delage, C. and Ripolles, K. (2001). Detection of sugarcane yellow leaf curl virus in quarantine and production of virus-free sugarcane by apical meristem culture. Plant Disease85: 1177-1180.

2. Gallo-Meagher, M., English, R.G. and Abouzid, A. (2000).Thidiazuron stimulates shoot regeneration of sugarcane embryogenic callus. In Vitro Cell DevBiol-Plant 36: 37-40.

3. Ather, A., Khan, S.I.,Rehman, A. and Nazir, M. (2009). Optimization of the protocols for callus induction, regeneration and acclimatization of sugarcane cv. Thatta-10.PakJ Bot41: 815-820.

4. Schenck, S. and Lehrer, A.T. (2000). Factors affecting the transmission and spread of Sugarcane yellow leaf virus. Plant Disease84: 1085-1088.

5. Nickle, I.G.(1964). Tissue and cell cultures of sugarcane: another research tool.Hawaii Plant Rec.57:223-229.

6. Heinz, D.J. and Mee, G.W. (1969). Plant differentiation from callus tissues of *Saccharum*species. Crop Sci9: 324-348.

7. Barba, R. and Nickel, I.G. (1969). Nutrition and organ differentiation in tissue cultures of sugarcane-a monocotyledon. Planta89: 299-302.

8. Ahloowalia, B.S. and Meretzki, A. (1983). Plant regeneration via somatic embryogenesis in sugarcane. Plant Cell Rep 2: 21-25.

9. Ho, W. and Vasil,I.K. (1983). Somatic embryogenesis in sugarcane (*Saccaharu-mofficinarum* L.): Growth and plant regeneration fromembryogenic cell suspension cultures. Ann Botany 51: 719-726.

10. Irvein, J.E., Benda, G.T.A., Legendre, B.I. and Machado, G.R. (1991). The frequency of marker changes in sugarcane plants regenerated from callus culture. II. Evidence of vegetative and genetic transmission, epigenic effects and chimera disruption. Plant Cell Tiss Organ Cult 26:115-125.

11. Liu, M.C. (1993). Factors affecting induction, somatic embryogenesis and plant regeneration of callus from cultured inflorescences of sugarcane. J Plant Physiol141: 714-720.

12. Irvine, J.E. and Benda, G.T.C. (1987). Transmission of sugarcane disease in plants derived by rapid regeneration from diseased tissue. Sugar Cane6:14-16.

13. Matsuoka, M., Ideta, O., Tanio, M., Hayakawa, A. and Miwa, H. (2001). *Agrobacterium tumefaciens*-mediated transformation of sugarcane using cell suspension culture with a novel method. Inter Soci Sugarcane Tech Proc of the XXIV Congress, Brisbane, Australia, 2: 660-662.

14. Murashige, T. and Skoog, F. (1962). A revised medium for rapid growth and bioassays with tobacco tissue cultures. Physiol Plant15: 473-497.

15. Heinz, D.J., Krishnamurthy, G. and Nickell, G. (1990). Cell tissue and organ culture in sugarcane improvement. In: Applied and fundamental aspects of Plant Cell, Tissue and Organ Cult. (Ed.) Reinert, J., and Bajaj, Y.P.S., Narosa Publishing House, New Delhi, India.pp 13-17.

16. Naik, G.R., HarinathBabu, K. and Lingappa, G.(1990). Studies on *in vitro* selection of Fe-efficient lines in sugarcane. Plant and Soil 129:183-186.

17. Nandlal,P. and Singh, N.N. (1991). Morphogenesis and growth studies on sugarcane callus under different of 2,4-D levels. Indian J Plant Physiol34: 84-88.

18. Taylor, P.W.J., Ko, H.L., Adkins, S.W., Rathus, C. and Birch, R.G. (1992). Establishment of embryogenic callus and high protoplast yielding suspension culture of sugarcane (*Saccharum*spp. hybrids). Plant Cell Tiss Org Cult 28:69-78.

19. Chen, W.H., Davey, M.R., Power, J.B. and Cocking, E.C. (1988). Control and

maintenance of plant regeneration in sugarcane callus. JExpt Bot 39:251-261.

20 Mannan, S.K.A. and Amin, M. (1999). Callus and shoot formation from leaf sheath of sugarcane (*Saccharumofficinarum* L.) *in vitro*.Indian Sugar49: 87-192.

21. Nandlal, P. (2003). High frequency plant regeneration from sugarcane callus. Sugar Tech 5: 89-91.

22. Ramanand, N., Kureen, N., Subhanand, M., Lal, N. and Singh, S.B. (2006). Plantlet regeneration through leaf callus culture in sugarcane. Sugar Tech 8: 85-87.

23. Lee, T.S.G. (1987) Micropropagation of sugarcane (*Saccharum* spp.) Plant Cell TissOrg Cult10:47-55.

24. Behara, K.K. and Sahoo, S. (2009). Rapid *in vitro*micropropagation of sugarcane (*Saccharumofficinarum* L. cv-Nayana) through callus culture. Nature and Science7:1-10.

25. Chengalrayan, K. and Gallo-Meagher, M. (2001). Effect of various growth regulators on shoot regeneration of sugarcane. In Vitro Cell DevBiol – Plant 37:434-439.

26. Patil, S.C., Pawar, S.V., Jambhale, V.M. and Mehetre, S.S. (2003). Callus culture and regeneration studies in sugarcane variety CO-86032. Ad Plant Sci6: 649-561.

27. Alam,R., MafizurRahaman, A.B.M. and Gupta, S. (2003). *In vitro* plant regeneration from leaf sheath callus of sugarcane via organogenesis.Plant Cell Biotech. Mol.Biol.3:131-136.

28. Gopitha, K., Bhavani, L. and Senthil-manickm, J. (2010). Effect of different auxins and cytokinins in callus induction, shoot, root regeneration in sugarcane.Int J Pharma Bio Sci1:1-7.

29. Khan, I.A., Dahot, M.U., Seem, N., Bini, S. and Khatri, A. (2008). Genetic variability in plantlets derived from callus culture in sugarcane. Pak J Bot 40: 547-564.

30. Gandonou, Ch., Errabii, T., Abrini,J., Idaomar, M., Chibi, F. and Skalisenhaji, N.(2005). Effect of genotype on callus induction and plant regeneration from leaf explants of sugarcane (*Saccharum* Sp.). African J Biotech.4:1250-1255.

31. Rahulbaksha, A.K.M., Alam-Ziaulkarim, R., Mannan, S.K.,Mafizur-Rahaman, A.B.M. and Gupta, S. (2003). Anther culture and plant regeneration in sugarcane (*Saccharum officinarum* L.). Plant Cell Biotech. Mol. Biol. 4:179-184.

32. Kale,V.P., Bruno, T.V. and Bhagade, S.V. (2004). Studies on callus initiation and plantlet regeneration in sugarcane (*Saacc-harum*spp).Indian J Genet64:165-166.

33. Maretzki, A. (1987). Tissue culture: Its prospects and problems In: sugarcane improvement through breeding. (Ed.) DJ Heinz. Elsevier Science Publication BV pp. 343-384.

34. Rashid, H., Khan, S.A., Zia, M., Chaudhary, M.F., Hanif, Z.and Chaudary, Z. (2009). Callus induction and regeneration in elite sugarcane cultivar HSF-24. Pak J Bot41: 1645-1649.

35. Meretzaki, A. and Hiraki, P. (1980). Sucrose promotion of root formation on plantlets regenerated from callus of *Saccharum* spp. Phyton38:85-88.

Current Trends in Biotechnology and Pharmacy
Vol. 7 (4) 870-880 October 2013, ISSN 0973-8916 (Print), 2230-7303 (Online)

Effect of Particle size and Alkaline Pretreatment of some Lignocellulosic wastes on Production of Xylanase from Fungal isolates of Raipur

Preeti Singh Parihar* and Vibhuti Rai
Microbiology and Biochemistry Lab, SoS in Life Sciences, Pt. Ravishankar Shukla University, Raipur- 492010, Chhattisgarh, India.
*For Correspondence - preeti.parihar1185@gmail.com

Abstract

In the present study, effect of particle size and alkaline pretreatment of five recorded lignocellulosic wastes on production of xylanase by five fungal isolates was studied. The different raw substrates used were wheat bran, saw dust, maize straw, rice straw, sugarcane baggase. These raw substrates were firstly subjected to different alkali pretreatments (0.5N NaOH, 0.1N NaOH, and 1.0N NaOH) and added to the culture medium for xylanase production. Maximum xylanase production was achieved with 0.5N NaOH pretreated raw substrates as compared to untreated raw substrates in all five fungal isolates. The 0.5N NaOH treated five raw substrates were then passed through 0.2mm, 0.5mm, 0.8mm, 1.4mm and 2.0mm sieves and used for xylanase production . Raw substrates of 0.8mm particle size supported maximum xylanase production in all five fungal isolates. The xylanase activity increased significantly in C*hrysosporium tropicum, Aspergillus fumigatus* and *Aspergillus terrus* from untreated maize straw to 0.5N NaOH and 0.8mm size treated maize straw, the corresponding values increased from 0.204±0.002, 0.118±0.001 and 0.030±0.005 to 0.448±0.004, 0.415±0.002 and 0.441±0.008 µmoles of xylose/min/ml of culture filtrate, respectively. *Malbranchaea sp* and *Emericella nidulans* also exhibited significantly higher xylanase activity with wheat bran, the corresponding values increased from 0.040±0.012 and 0.138±0.003 to 0.513±0.005 and 0.390 ± 0.002 µmoles of xylose/min/ml of culture filtrate, respectively.

Keywords: Xylanases, oat spelt xylan, alkaline pretreatment, wheat bran, maize straw.

Introduction

Xylanases are the microbial enzymes that have aroused great interest recently due to their potential application in many industrial processes viz; production of hydrolysates from agro-industrial wastes (1, 2) nutritional improvement of lignocellulosic feed stuff (3), clarification of juices and wines (4) and biobleaching of craft pulp in paper industry (5).

Xylanases (E.C.2.8.1.8), a group of hemicellulolytic enzymes, are required for the hydrolyisis of β 1, 4-xylans present in lignocellulosic materials (1). Xylan rich cell walls contain significant amounts of lignin which are generally resistant to enzymic hydrolysis and required chemo-mechanical pretreatments like steaming, radiation, acid hydrolysis and alkali digestion (6) before the polysaccharides become accessible to enzymes and can be hydrolysed to monomeric sugars in high yield (7). Compared to acid pretreatments, alkaline processes have less sugar degradation and furan derivative formation is avoided (8).

Vol. 7 (4) 870-880 October 2013, ISSN 0973-8916 (Print), 2230-7303 (Online)

Enzymatic action on the substrate also depends upon the size of the substrate, which is determined by the physical properties of the materials including the crystalline or amorphous nature, accessible and surface area, porosity and mainly particle size (9-11) Thus, structure and size of substrates allow different materials to be available for microbial degradation (12). Hence mechanical separation of any substrate can be useful for specific purposes, such as the cultivation of edible fungi, feed production (13) or more specific production of extracellular enzyme extracts (14)

Lignocellulosic substrates, being cheap and readily available, have recently gained considerable interest because of their possible use in secondary fermentation processes. A number of studies have already been done for production of xylanase on lignocellulosic wastes mainly wheat bran (15-17), sugarcane bagasse (18) and untreated and treated wheat straw (19) using solid substrate fermentation (SSF) or submerged culture fermentation (SmF). This paper presents the potential of some fungal isolates, to produce xylanase on various feed stuffs like wheat bran, maize straw, rice straw, sugarcane baggase and saw dust under submerged fermentation conditions. The purpose of this research was to improve xylanase production by using different particle size and alkaline pretreated lignocellulosic wastes.

Materials and methods

Collection of samples: The soil samples were collected from the various localities in and around Raipur city. The samples were mainly from Govt. Science College Botanical Garden, SOS in Life Science garden, compost; house based waste, stable manure and garbage soil of Raipur.

Isolation of fungi: Isolation of fungi were carried out from the collected soil samples by using two methods, the dilution plate method of (20) and direct plate method of (21).

Identification of fungi: Purified cultures were identified under compound microscope with available literature of (22). Selected isolates were identified from NFCCI, Agharkar Research Institute, Pune.

Screening of xylanolytic fungi: Isolated fungi were screened for xylanolytic activities on xylan agar medium as described by the method of (23). Positive xylanolytic isolates were detected based on the formation of clear zones of hydrolysis on the oat spelt xylan agar plates (24).

Xylanase production medium: To study the effect of different factors i.e alkaline pretreatment and particle size on the production of xylanase, the culture medium i.e. YpSs media of following composition was used. Raw substrate 10g, Soluble starch 5g, Yeast extract 1.0g, $MgSO_4.7H_2O$ 0.5g, KH_2PO_4 1.0g, Distilled water 1000ml pH 7.0. 25ml of medium in 150ml conical flask was inoculated with one fungal mycelial disc from a week old culture and incubated at 45^0C in humidity controlled incubator. At the end of fifth day of incubation, extracellular xylanase activity was assayed in culture filtrates of all five fungal isolates.

Xylanase assay: Xylanase activity was assayed using 1% oat spelt xylan (Sigma chemical) as the substrate. Xylan was dissolved in 50mM Phosphate buffer (pH 6.5). The reaction mixture consisted of 0.5ml oat spelt xylan and 0.5ml crude enzyme, which was incubated in an incubator for 30 min at 50^oC. The enzyme was assayed by estimating the amount of released reducing sugar xylose using 3, 5- dinitrosalicylic acid method (DNS method) (25). One unit of xylanase activity was expressed as 1µmol of reducing sugars (xylose) released in 1 min under the above conditions. Protein content was estimated by method of (26) with BSA (bovine serum albumin, Himedia, India).

Effect of alkaline pretreatment of raw substrate on xylanase production: 1.0 g raw substrate (wheat bran, saw dust, maize straw, rice straw, sugarcane baggase) was added to 10.0ml of 0.5N NaOH, 0.1N NaOH, 1.0N NaOH and autoclaved for 30min in 150ml flasks (27). After 30min washed with running tap water until the pH gets neutralized. The washed substrate

was dried in an oven at 60°C overnight. Alkaline pretreated raw substrates were added to the YPsS medium at 1% concentration and isolates of fungi were grown in this medium. The extracellular xylanase activity was measured in culture filtrates of fungal isolates grown in alkaline pretreated raw substrate to select the suitable treatment of raw substrate for extracellular xylanase production.

Effect of particle size of raw substrate on xylanase production: Raw substrates treated with 0.5N NaOH were grinded using mixer grinder and passed through 2.0mm sieve and substrates which were not sieved again grinded and passed through 1.4mm sieve. Other particle sizes of raw substrates were obtained in similar way in decreasing order of sieve size i.e. 0.8mm, 0.5mm and 0.2mm. Different sizes of raw substrate were added to the culture medium and five isolates were grown in this medium. The extracellular xylanase activity was measured in culture filtrates of all five isolates grown in different size of raw substrates.

Results and Discussion

Isolation and screening of xylanolytic fungi: In the present work, a total of fifty-five fungal isolates were recorded from different soil samples and screened for xylanase activity. After evaluating 55 fungal isolates for xylanase acivity, eighteen isolates showing higher xylanase activity were selected for further study. Out of eighteen, five isolates i.e. *Chrysosporium tropicum* NFCCI 2531*, Malbranchaea sp, Aspergillus fumigatus* NFCCI 2532, *Aspergillus terrus* NFCCI 2533 and *Emericella nidulans* NFCCI 2538 with higher xylanase activity were selected to study effect of different normality alkaline pretreatment and different particle sizes of some lignocellulosic wastes on xylanase production.

Effect of alkaline pretreatment of raw substrate on xylanase production: The effect of alkaline pretreatment on xylanase production was presented in (Table 1a, 1b and Fig. 1a-e). A significant increase in xylanase production was obtained with 0.5N NaOH treated raw substrates as compared to their respective controls and 0.1N NaOH treated raw substrates in all five fungal isolates. However after treatment of all the raw substrates with 1.0N NaOH, the xylanase production decreased significantly with all the five fungal isolates.

It may be due to the decomposition of xylan with severe alkali treatment. Moreover at higher severity of NaOH, more byproducts like furfurals are formed which make the medium somewhat harder to ferment (4). The xylanase activity also increased in *Trichoderma viride* using 0.5N NaOH treated jowar and maize straw (27). *B. subtilis* produced significant level of xylanase activity with

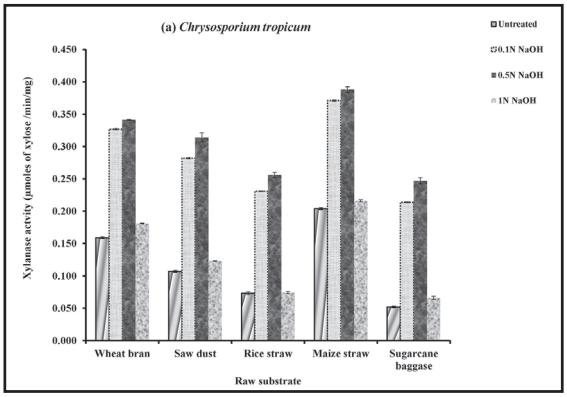

Fig.1 (a): Effect of alkaline pretreatment of raw substrate (0.8mm) on xylanase production.

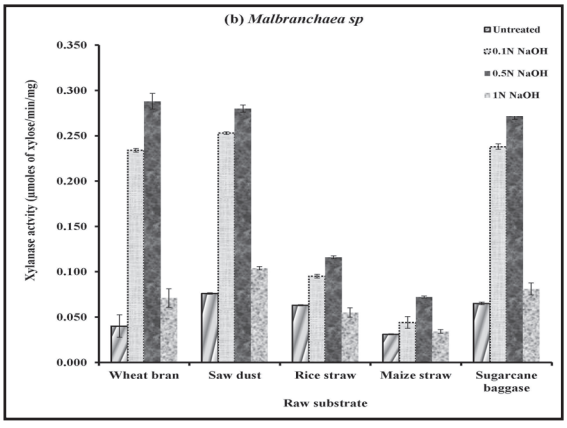

Fig. 1 (b): Effect of alkaline pretreatment of raw substrate (0.8mm) on xylanase production.

Table 1(a). Effect of alkaline pretreatment of raw substrates (0.8mm size) on xylanase production (Mean±SE)

Fungal Isolate	Treatment	Xylanase activity				
		Wheat bran	Saw dust	Rice straw	Maize straw	Sugarcane bagasse
Chrysosporium tropicum	Untreated	0.159 ± 0.002^{d}	0.107 ± 0.002^{d}	0.073 ± 0.002^{c}	0.204 ± 0.002^{d}	0.052 ± 0.001^{d}
	0.1N NaOH	0.327 ± 0.001^{b}	0.282 ± 0.001^{b}	0.231 ± 0.001^{b}	0.371 ± 0.001^{b}	0.214 ± 0.001^{b}
	0.5N NaOH	0.341 ± 0.001^{a}	0.314 ± 0.007^{a}	0.256 ± 0.004^{a}	0.388 ± 0.005^{a}	0.247 ± 0.005^{a}
	1.0N NaOH	0.181 ± 0.001^{c}	0.123 ± 0.001^{c}	0.074 ± 0.002^{c}	0.216 ± 0.002^{c}	0.066 ± 0.003^{c}
Malbranchaea sp	Untreated	0.040 ± 0.012^{d}	0.076 ± 0.001^{d}	0.063 ± 0.001^{c}	0.031 ± 0.001^{c}	0.065 ± 0.002^{d}
	0.1N NaOH	0.234 ± 0.002^{b}	0.253 ± 0.001^{b}	0.095 ± 0.002^{b}	0.044 ± 0.007^{b}	0.238 ± 0.003^{b}
	0.5N NaOH	0.288 ± 0.009^{a}	0.280 ± 0.004^{a}	0.116 ± 0.002^{a}	0.072 ± 0.001^{a}	0.272 ± 0.004^{a}
	1.0N NaOH	0.071 ± 0.010^{c}	0.104 ± 0.002^{c}	0.055 ± 0.005^{c}	0.034 ± 0.002^{c}	0.081 ± 0.007^{c}
Aspergillus fumigatus	Untreated	0.132 ± 0.006^{d}	0.040 ± 0.003^{d}	0.033 ± 0.000^{c}	0.118 ± 0.001^{c}	0.064 ± 0.001^{b}
	0.1N NaOH	0.325 ± 0.002^{b}	0.206 ± 0.002^{b}	0.167 ± 0.001^{b}	0.427 ± 0.001^{b}	0.064 ± 0.001^{b}
	0.5N NaOH	0.346 ± 0.002^{a}	0.237 ± 0.005^{a}	0.194 ± 0.003^{a}	0.450 ± 0.004^{a}	0.098 ± 0.002^{a}
	1.0N NaOH	0.168 ± 0.008^{c}	0.054 ± 0.002^{c}	0.032 ± 0.001^{c}	0.280 ± 0.002^{d}	0.018 ± 0.007^{c}
Aspergilus terrus	Untreated	0.091 ± 0.005^{c}	0.041 ± 0.004^{c}	0.037 ± 0.006^{b}	0.030 ± 0.005^{c}	0.018 ± 0.004^{c}
	0.1N NaOH	0.144 ± 0.009^{b}	0.072 ± 0.008^{b}	0.046 ± 0.003^{b}	0.213 ± 0.001^{b}	0.035 ± 0.011^{b}
	0.5N NaOH	0.202 ± 0.004^{a}	0.092 ± 0.004^{a}	0.069 ± 0.003^{a}	0.261 ± 0.008^{a}	0.056 ± 0.005^{a}
	1.0N NaOH	0.121 ± 0.009^{b}	0.039 ± 0.003^{c}	0.022 ± 0.001^{c}	0.058 ± 0.003^{c}	0.013 ± 0.006^{c}
Emericella nidulans	Untreated	0.138 ± 0.003^{c}	0.130 ± 0.008^{c}	0.110 ± 0 .007^{b}	0.112 ± 0.005^{c}	0.152 ± 0.005^{c}
	0.1N NaOH	0.273 ± 0.009^{b}	0.230 ± 0.006^{b}	0.011 ± 0.001^{d}	0.174 ± 0.003^{b}	0.236 ± 0.009^{b}
	0.5N NaOH	0.336 ± 0.008^{a}	0.258 ± 0.003^{a}	0.165 ± 0.001^{a}	0.204 ± 0.004^{a}	0.292 ± 0.004^{a}
	1.0N NaOH	0.164 ± 0.005^{c}	0.063 ± 0.007^{d}	0.028 ± 0.003^{c}	0.013 ± 0.004^{d}	0.097 ± 0.002^{d}

Activities are expressed as µmoles of xylose released /mg protein/min

Means having similar alphabets as superscripts are not statistically significant from each other at $p<0.05$ (Based on Duncan's Multiple Range Test)

Table 1 (b). One way ANOVA summary for effect of alkaline pretreatment of raw substrates (0.8mm size) on xylanase production.

S.No.	Fungal Isolate	Wheat bran	Saw dust	Rice straw	Maize straw	Sugarcane baggase
1	*Chrysosporium tropicum*	**df** = 3,8 **F** = 7939.544 ***p***<0.001***	**df** = 3,8 **F** = 818.971 ***p***<0.001***	**df** = 3,8 **F** = 1600.712 ***p***<0.001***	**df** = 3,8 **F** = 1215.455 ***p***<0.001***	**df** = 3,8 **F** = 1204.555 ***p***<0.001***
2	*Malbranchaea sp*	**df** = 3,8 **F** = 174.497 ***p***<0.001***	**df** = 3,8 **F** =1700.154 ***p***<0.001***	**df** = 3,8 **F** = 92.025 ***p***<0.001***	**df** = 3,8 **F** = 28.876 ***p***<0.001***	**df** = 3,8 **F** = 578.731 ***p***<0.001***
3	*Aspergillus fumigatus*	**df** = 3,8 **F** = 443.359 ***p***<0.001***	**df** = 3,8 **F** = 988.134 ***p***<0.001***	**df** = 3,8 **F** = 2754.928 ***p***<0.001***	**df** = 3,8 **F** =4888.322 ***p***<0.001***	**df** = 3,8 **F** = 77.373 ***p***<0.001***
4	*Aspergilus terrus*	**df** = 3,8 **F** = 42.994 ***p***<0.001***	**df** = 3,8 **F** = 24.811 ***p***<0.001***	**df** = 3,8 **F** = 24.225 ***p***<0.001***	**df** = 3,8 **F** = 544.746 ***p***<0.001***	**df** = 3,8 **F** = 7.408 ***p***<0.01*
5	*Emericella nidulans*	**df** = 3,8 **F** = 200.511 ***p***<0.001***	**df** = 3,8 **F** =194.650 ***p***<0.001***	**df** = 3,8 **F** = 362.246 ***p***<0.001***	**df** = 3,8 **F** = 406.743 ***p***<0.001***	**df** = 3,8 **F** = 218.054 ***p***<0.001***

Fig.1(c): Effect of alkaline pretreatment of raw substrate (0.8mm) on xylanase production.

Fig.1(d):Effect of alkaline pretreatment of raw substrate (0.8mm) on xylanase production.

Fig.1(e): Effect of alkaline pretreatment of raw substrate (0.8mm) on xylanase production

Table2(a). Effect of particle size of 0.5N NaOH treated raw substrates on xylanase production (Mean±SE).

		Xylanase activity				
Raw substrate	size (mm)	Particle *tropicum*	*Chrysosporium sp*	*Malbranchaea fumigatus*	*Aspergillus terrus*	*Aspergilus Emericella nidulans*
Wheat bran	0.2	0.277 ± 0.003^{c}	0.371 ± 0.011^{c}	0.163 ± 0.002^{c}	0.154 ± 0.007^{d}	0.305 ± 0.003^{d}
	0.5	0.317 ± 0.003^{b}	0.426 ± 0.004^{b}	0.332 ± 0.007^{b}	0.237 ± 0.005^{b}	0.349 ± 0.011^{b}
	0.8	0.347 ± 0.005^{a}	0.513 ± 0.005^{a}	0.411 ± 0.006^{a}	0.279 ± 0.005^{a}	0.390 ± 0.002^{a}
	1.4	0.307 ± 0.004^{b}	0.438 ± 0.007^{b}	0.124 ± 0.002^{d}	0.207 ± 0.005^{c}	0.355 ± 0.003^{b}
	2.0	0.269 ± 0.007^{c}	0.343 ± 0.005^{d}	0.102 ± 0.002^{e}	0.143 ± 0.004^{d}	0.333 ± 0.002^{c}
Saw dust	0.2	0.249 ± 0.004^{b}	0.320 ± 0.009^{d}	0.186 ± 0.004^{c}	0.128 ± 0.006^{d}	0.232 ± 0.005^{c}
	0.5	0.264 ± 0.008^{b}	0.404 ± 0.004^{b}	0.253 ± 0.005^{b}	0.215 ± 0.005^{b}	0.280 ± 0.005^{b}
	0.8	0.324 ± 0.003^{a}	0.441 ± 0.007^{a}	0.318 ± 0.003^{a}	0.252 ± 0.008^{a}	0.366 ± 0.004^{a}
	1.4	0.192 ± 0.005^{c}	0.274 ± 0.006^{e}	0.261 ± 0.005^{b}	0.174 ± 0.005^{c}	0.211 ± 0.006^{c}
	2.0	0.157 ± 0.003^{d}	0.382 ± 0.004^{c}	0.084 ± 0.006^{d}	0.108 ± 0.005^{e}	0.159 ± 0.014^{d}
Rice straw	0.2	0.156 ± 0.003^{b}	0.271 ± 0.011^{c}	0.207 ± 0.002^{c}	0.008 ± 0.003^{c}	0.140 ± 0.001^{c}
	0.5	0.080 ± 0.001^{d}	0.367 ± 0.007^{b}	0.226 ± 0.004^{b}	0.041 ± 0.004^{b}	0.178 ± 0.004^{b}
	0.8	0.199 ± 0.003^{a}	0.432 ± 0.005^{a}	0.287 ± 0.005^{a}	0.069 ± 0.004^{a}	0.297 ± 0.007^{a}
	1.4	0.084 ± 0.007^{d}	0.246 ± 0.008^{d}	0.198 ± 0.002^{c}	0.026 ± 0.007^{b}	0.141 ± 0.002^{c}
	2.0	0.126 ± 0.004^{c}	0.123 ± 0.006^{e}	0.163 ± 0.003^{d}	0.033 ± 0.005^{b}	0.092 ± 0.007^{d}
Maize straw	0.2	0.346 ±0 .005^{c}	0.018 ± 0.006^{c}	0.279 ± 0.000^{d}	0.278 ± 0.004^{c}	0.153 ± 0.002^{c}
	0.5	0.366 ± 0.005^{b}	0.071 ± 0.006^{b}	0.354 ± 0.007^{b}	0.349 ± 0.010^{b}	0.235 ± 0.006^{b}
	0.8	0.448 ± 0.004^{a}	0.216 ± 0.008^{a}	0.415 ± 0.002^{a}	0.441 ± 0.008^{a}	0.307 ± 0.004^{a}
	1.4	0.364 ± 0.012^{b}	0.064 ± 0.006^{b}	0.323 ± 0.004^{c}	0.348 ± 0.007^{b}	0.146 ± 0.003^{c}
	2.0	0.315 ± 0.008^{d}	0.020 ± 0.004^{c}	0.278 ±0.003^{d}	0.237 ± 0.009^{d}	0.131 ± 0.004^{d}
Sugarcane bagasse	0.2	0.083 ± 0.003^{c}	0.327 ± 0.004^{b}	0.134 ± 0.007^{d}	0.026 ± 0.003^{c}	0.058 ± 0.005^{d}
	0.5	0.126 ± 0.001^{b}	0.364 ± 0.008^{b}	0.222 ± 0.007^{b}	0.032 ± 0.005^{b}	0.297 ± 0.007^{b}
	0.8	0.153 ± 0.005^{a}	0.432 ± 0.005^{a}	0.275 ± 0.006^{a}	0.103 ± 0.003^{a}	0.347 ± 0.005^{a}
	1.4	0.127 ± 0.003^{b}	0.052 ± 0.024^{c}	0.177 ± 0.008^{c}	0.044 ± 0.007^{b}	0.160 ± 0.005
	2.0	0.059 ± 0.010^{d}	0.032 ± 0.005^{c}	0.133 ± 0.003^{d}	0.014 ± 0.003^{d}	0.154 ± 0.002^{e}

 # Activities are expressed as µmoles of xylose released /mg protein/min Means having similar alphabets as superscripts are not statistically significant from each other at $p<0.05$ (Based on Duncan's Multiple Range Test).

Table 2 (b). One way ANOVA summary for effect of particle size of 0.5N NaOH treated raw substrates on xylanase production

S.No.	Fungal Isolate	Wheat bran	Saw dust	Rice straw	Maize straw	Sugarcane baggase
1	*Chrysosporium tropicum*	**df** = 4,10 **F** = 44.096 ***p***<0.001***	**df** = 4,10 **F** = 173.739 ***p***<0.001***	**df** = 4,10 **F** = 150.809 ***p***<0.001***	**df** = 4,10 **F** = 45.956 ***p***<0.001***	**df** = 4,10 **F** = 49.834 ***p***<0.001***
2	*Malbranchaea sp*	**df** = 4,10 **F** = 91.330 ***p***<0.001***	**df** =4,10 **F** =115.904 ***p***<0.001***	**df** = 4,10 **F** = 239.556 ***p***<0.001***	**df** = 4,10 **F** = 183.641 ***p***<0.001***	**df** = 4,10 **F** = 245.252 ***p***<0.001***
3	*Aspergillus fumigatus*	**df** = 4,10 **F** = 1059.061 ***p***<0.001***	**df** = 4,10 **F** = 370.523 ***p***<0.001***	**df** = 4,10 **F** = 162.826 ***p***<0.001***	**df** = 4,10 **F** = 208.400 ***p***<0.001***	**df** = 4,10 **F** = 98.699 ***p***<0.001***
4	*Aspergilus terrus*	**df** = 4,10 **F** = 123.504 ***p***<0.001***	**df** = 4,10 **F** =108.930 ***p***<0.001***	**df** = 4,10 **F** = 20.557 ***p***<0.001***	**df** = 4,10 **F** =100.433 ***p***<0.001***	**df** = 4,10 **F** =55.871 ***p***<0.01*
5	*Emericella nidulans*	**df** = 4,10 **F** = 33.575 ***p***<0.001***	**df** = 4,10 **F** = 102.637 ***p***<0.001***	**df** = 4,10 **F** = 252.590 ***p***<0.001***	**df** = 4,10 **F** = 338.575 ***p***<0.001***	**df** = 4,10 **F** = 558.518 ***p***<0.001***

Fig. 2(a): Effect of particle size of 0.5N NaOH treated raw substrates on xylanase production

Fig. 2(b): Effect of particle size of 0.5N NaOH treated raw substrates on xylanase production

Fig. 2(c): Effect of particle size of 0.5N NaOH treated raw substrates on xylanase production

2% NaOH treated raw substrates (rice straw, sugarcane baggase, wheat bran and karaft pulp) (28). Alkali treated wheat straw increased cellulose hydrolysis as compared to untreated wheat straw as reported by (29). Submerged cultures of *Trichoderma reesei* F-522 grown on ethanol-alkali treated wheat straw supported maximum cellulase and xylanase production (30).

Effect of particle size of raw substrate on xylanase production: A significant higher xylanase activity was recorded with 0.8mm particle size raw substrates in all the five isolates with 0.5N alkaline pretreated raw substrates. Any variation in particle size other than 0.8mm affected the enzyme production in the present study (Table 2a, 2b, Fig. 2a-e).

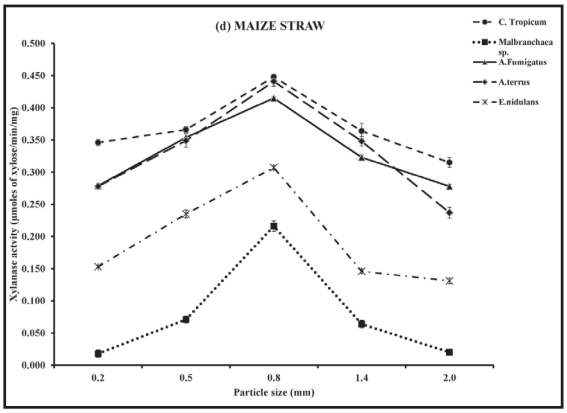

Fig. 2(d): Effect of particle size of 0.5N NaOH treated raw substrates on xylanase production

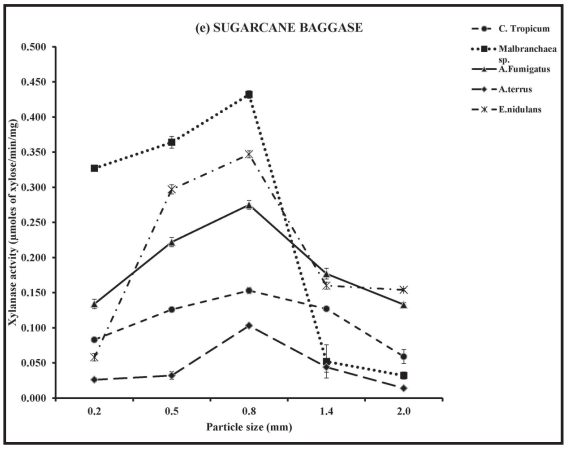

Fig. 2(e): Effect of particle size of 0.5N NaOH treated raw substrates on xylanase production

Higher xylanase production by *Aspergillus* sp.RSP-6 was observed in the medium containing 2.8-1.4mm particle size of palm material (31). *Aspergillus fumigatus* (MTCC 9372) was associated with maximum xylanase production with 1.4-0.71mm particle size of wheat bran (32).Palm kernel cake with the particle size of 500µm and vegetable wastes of 1mm was the most effective in producing higher cellulase activity by *Bacillus sp* (33). Maximum alkaline protease production was reported by *Bacillus* sp. with 1.4-1.0mm particle size of green gram husk (34). Xylanase production by *Aspergillus fumigatus* AR1 in alkaline medium containing low cost substrates i.e. corn cob, baggase, rice straw, wheat straw and wheat bran was studied. Maximum xylanase was produced from rice straw (30U/ml). While wheat bran and baggase recorded low level (17U/ml) of xylanase production(35). Similarly, *Aspergillus terrus* also produced xylanase on various lignocellulosic substrates i.e. wheat bran, sugarcane baggase, soybean hull and rice straw. Maximum xylanase activity was observed with wheat bran (21.2 IU/ml) and minimum with sugarcane baggase (3.5 IU/ml). Soybean hull and rice straw showed 6.2 IU/ml and 10.5 IU/ml (36). Thermotolerant *Emericella nidulans* NK-62, isolated from bird nesting material exhibited maximum production of xylanase (362 IU/ml) with wheat bran and minimum with meal of groundnut shells (37). Highest xylanase production i.e (70 IU/mL) was recorded with corn cob as agricultural residues by *Aspergillus terreus* NRRL 1960 (38). 141.7, 38.0 and 31.2 units/ml xylanase activity was recorded by *Malbranchaea sp., Aspergillus terrus* and *Emericella nidulans var.lata* using 2% corn cob (39).

Conclusions

The results obtained from the present study indicates that the production of xylanase can be increased and made cost effective by using 0.5N

NaOH pretreated and 0.8mm particle size of raw substrates in *Chrysosporium tropicum, Malbranchaea sp, Aspergillus fumigatus, Aspergillus terrus* and *Emericella nidulans*. The xylanase produced by these fungal isolates may be further assessed for industrial exploitation.

Acknowledgements

The authors are thankful to SOS in Life Sciences, Pt. Ravishankar Shukla University, Raipur (C.G) and university grants commission for providing me UGC-BSR fellowship as a financial support to complete my work. Authors are also thankful to Dr. A.K.Pati, professor and and Dr. A.K.Gupta, Head of Department for their encouragement and support.

References

1. Kheng, P.P. and Omar, I.C. (2005). Xylanase production by a local fungal isolate, Aspergillus niger USM AI 1 via solid state fermentation using palm kernel cake (PKC) as substrate. Songklanakarin J. Sci. Technol., 27: 325-336.
2. Gessesse, A. and Gashe, B.A. (1997). Production of alkaline xylanase by an alkaliphilic Bacillus sp. isolated from an alkaline soda lake. J. Appl. Microbiol., 83: 402-406.
3. Wallace, R.J., Wallace, N.M., Nsereko, V.L. and Hartnell, G.F. (2001). Influence of supplementary fibrolytic enzymes on the fermentation of corn and grass silage by mixed ruminal microorganisms in vitro. J. Anim. Sci., 79: 1905-1916.
4. Gable, M. and Zacchi, G. (2002). A review of the production of ethanol from softwood. Appl. Biochem. Biotechnol., 59: 618-628.
5. Yinbo, Q., Peizi, G., Dong, W., Xin, Z. and Xiao, R. (1996). Production, charaterisation and application of the cellulase free xylanase from Aspergillus niger. Appl. Biochem. Biotechnol., 57: 375-381.
6. Sutcliffe, R. and Saddler, J.N. (1986). The role of lignin in adsorption of cellulases during enzymic treatment of lignocellulosic matererial. Biotechnol. Bioeng. Symp., 17: 749-762.
7. Fan, L.T., Lee, Y.H. and Gharpuray, M.M. (1982). The nature of lignocellulosics and their pretreatments for enzymic hydrolysis. Adv. Biochem. Eng., 23: 157-178.
8. Gonzalez, G., Lopez –Santin, J., Caminal, G. and Sola, C. (1986). Dilute acid hydrolysis of wheat straw hemicelluloses at moderate temperature: a simplified kinetic model. Biotechnol. Bioeng., 28: 288-293.
9. Knapp, J.S. and Howell, J.A. (1980). Solidsubstrate fermentation. In: Topics in enzyme and Fermentation Biotechnology. Ellis Horwood Ltd. Chichester. England., (4): 85–143.
10. Viniegra-González, G., Favela-Torres, E., Aguilar, C.N., Romero-Gómez, S., Díaz-Godínez, G. and Augur, C. (2003). Advantages of fungal enzyme production in solid state over liquid fermentation systems. Biotechnol. Eng. J., 13: 157–167.
11. Rodríguez, C.S. and Sanromán, M.A. (2005). Application of solid-state fermentation to ligninolytyc enzyme production. Biochemical. Eng. J., 22: 211–219.
12. Pandey, A. (2003). Solid-state fermentation. Biotechnol. Eng. J., 13: 81–84.
13. Zadrazil, F. and Puniya, A.K. (1995). Studies on the effect of particle size on solid-state fermentation of sugarcane bagasse into animal feed using white-rot fungi. Bioresource. Technol., 54: 85–87.
14. Mazutti, M., Bender, J.P., Treichel, H. and Di Luccio, M. (2006). Optimization of inulinase production by solid-state fermentation using sugar cane bagasse as substrate. Enzyme. Microbial. Technol., 39: 56–59.
15. Gawande, P.V. and Kamat, M.Y. (1999). Production of Aspergillus xylanase by lignocellulosic waste fermentation and its

application. J. Appl. Microbiol., 87: 511-519.

16. Kuhad, R.C., Kapoor, M. and Chaudhary, K. (2006). Production of xylanase from Streptomyces sp. M-83 using cost-effective substrates and its application in improving digestibility of monogastric animal feed. Indian. J. Microbiol., 46: 109-119.

17. Ninawe, S. and Kuhad, R.C. (2005). Use of xylan rich cost effective agro-residues in the production of xylanase by Streptomyce cyaneus SN 32. J. Appl. Microb., 99: 1141-1148.

18. Gutierrez-Correa, M. and Tengerdy, R.P. (1998). Xylanase production by fungal mixed culture solid substrate fermentation on sugar cane bagasse. Biotechnol. Lett., 20: 45-47.

19. Alfani, F., Gallifuoco, A., Saporosi, A., Spera, A. and Cantarella, M. (2000). Comparison of SHF and SSF processes for bioconversion of steam-exploded wheat straw. J. Induct. Microbial. Biotechnol., 25: 192-194.

20. Waksman, S.A. and Fred, E.B. (1922). A tentative outline for the plate method for determining the number of microorganisms in the soil. Soil. Sci., 14: 27-28.

21. Warcup, J.H. (1950). The soil plate method for isolation of fungi from soil. Nature.,166: 117-118.

22. Cooney, D.G. and Emerson, R. (1964). Thermophilic fungi: An account of their biology, activities and classification. WH. Freeman and Co. San Francisco and London., 188.

23. Kar, S., Mandal, A., Mohapatra, P.K., Mondal, K.C. and Pati, B.R. (2006). Production of cellulase-free xylanase by Trichoderma Reesei SAF3. Brazilian. J. Microbiol., 37: 462-464.

24. Muthezhilan, R., Ashok, R. and Jayalakshmi, S. (2007). Production and optimization of thermostable alkaline xylanase by Penicillium oxalicum in solid state fermentation. African. J. Microbiol. Research., 020-028.

25. Miller, G.L. (1959). Use of dinitrosalicylic acid reagent for determination of reducing sugar. Anal. Chem., 31: 426-428.

26. Lowry, O.H., Rosebrough, N.J., Farr, A.L. and Randall, R.J. (1951). Protein measurement with the Folin phenol reagent. J. Biol. Chem., 193: 265–275.

27. Goyal, M., Kalra, K.L., Sareen, V.K. and Soni, G. (2008). Xylanase production with xylan rich lignocellulosic wastes by a local soil isolate of Trichoderma viride. Brazilian. J. Microbiol., 39: 535-541.

28. Saleem, M., Muhammad, S.A. and Jamil, S. (2002). Production of xylanase on natural substrates by Bacillus subtilis. International. J. Agri. Biol., 04: 211-213.

29. Carrillo, F., Lisa, M.J., Colom, X., López-Mesas, M. and Valldeperas, J. (2005). Effect of alkali pretreatment on cellulase hydrolysis of wheat straw. Kinetic study. Process. Biochem., 40: 3360-3364.

30. Szodrak, J. (1988). Production of cellulases and xylanase by Trichoderma reesei F-522 on pretreated wheat straw. Acta. Biotechnol., 8: 509-515.

31. Suvarna Laxmi, G., Satish, T., Subba Rao, Ch., Brahmaiah, P., Hyamavathi, M. and Prakasham, R.S. (2008). Palm fibre as novel substrate for enhanced xylanase production by isolated Aspergillus sp. RSP-6. Current. Trends. Biotechnol. Pharm., 2: 447-455.

32. Beeraka, N., Katikala, P.K., Bobbarala, V., and Tadimalla, P. (2008). Optimization of xylanase production under solid state fermentation by isolated Aspergillus fumigatus (MTCC9372). Ind. J.Multi. Res., 4: 507-516.

33. Norsalwani, T.L and Norulaini, N.A. (2012). Utilization of lignocellulosic wastes as a carbon source for the production of bacterial cellulases under solid state fermentation. Inter. J. Environ. Sci. Develop., 3: 136-140.

34. Prakasham, R.S., Rao, C.H. and Sarma, P.N. (2006). Green gram husk-an inexpensive substrate for alkaline protease production by Bacillus sp. in solid state fermentation. Bioresource. Technol., 97: 1449-1454.

35. Anthony, T., Raj Chandra, K., Rajendran, K. and Gunasekaran, P. (2003). High molecular weight cellulase- free xylanase from alkali tolerant Aspergillus fumigatus AR1. Enzyme. Microb. Technol., 32: 647-654.

36. Gawande, P.V.and Kamat, M.Y. (1999). Production of Aspergillus xylanase by lignocellulosic waste fermentation and its application. J. Appl. Microbiol., 87: 511-519.

37. Kango, N., Agrawal, S.C. and Jain, P.C. (2003). Production of xylanase by Emericella nidulans NK-62 on low value lignocellulosic substrates. World. J. Microbiol. Biotechnol., 19: 691-694.

38. Kocabas, A., Ogel, Z.B. and Bakir, U. (2013). Annals. Microbiol. Xylanase and itaconic acid production by Aspergillus terreus NRRL 1960 within a biorefinery concept. Annals. Microbiol.,

39. Ghatora, S.K., Chadha, B.S., Badhan,A.K., Saini, H.S. and Bhat, M.K. (2006). Identification and characterization of diverse xylanases from thermophilic and thermotolerant fungi. Bioresources. 1: 18-33.

Current Trends in Biotechnology and Pharmacy
Vol. 7 (4) 881-889 October 2013, ISSN 0973-8916 (Print), 2230-7303 (Online)

The Prevalence of β-haemolytic Streptococcal infection among School children in Tripura, North East India

Nilratan Majumdar, Nupur Moitra*, Tapan Majumdar, Subrata Baidya, Anamika Nath
Agartala Govt. Medical College, Agartala, Tripura - 799006, India
*For Correspondence - dr.nupur@ymail.com

Abstract

The genus Streptococcus is comprised of a wide variety of both commensal and pathogenic gram-positive bacteria which are found to exhibit a wide range of hosts, including humans, horses, pigs and cows. Streptococcal infections can cause a wide range of diseases from mild infections to sever. Repeated infection results in the non-suppurative sequelae, acute rheumatic fever, and acute glomerulonephritis. Streptococcus remains sensitive to the antibiotic penicillin which can be administered as a means to treat infection or as prophylaxis. Rheumatic fever and rheumatic heart disease continue to ravage millions of people around the world. Children and adolescents of the developing countries are especially susceptible to this disease. The aim of this study is to assess the effect of invasive Streptococcal infection with an objective to determine the prevalence of streptococcal infection in school children of 5-15 years of age in Tripura, North Eastern part of India**.** From September 2012 - February 2013, a study was conducted on prospective population-based laboratory surveillance of Tripura school children with isolation of Streptococci from throat swab examination of both pharyngitis and non – pharyngitis cases. Throat swabs were collected from 1165 school children, randomly selected from 3 districts of Tripura. These swabs were cultured on blood agar and Mac Conkey plates. Out of 1165 swabs, 43 were alpha haemolytic, 4 were Grp. G (Streptococcus dysgalactiae subsp. equisimilis) and 1063 were of different types than streptococcus. The study present the results of the first prospective surveillance study of Streptococcal infections in north eastern part of India.

Keywords: Acute rheumatic fever, Rheumatic heart disease, Impetigo; Pharyngitis, Post-streptococcal Glomerulonephritis

Introduction

A large genus of spherical or ovoid bacteria that are characteristically arranged in pairs or in chains resembling strings of beads. Many of the streptococci that constitute part of the normal flora of the mouth, throat, intestine, and skin are harmless commensal forms; other streptococci are highly pathogenic. The cells are gram-positive and can grow either anaerobically or aerobically, as they do not require oxygen for metabolic reactions.

The group of β-hemolytic streptococci cause a wide spectrum of clinical diseases. Pharyngitis and associated complications are the most common clinical presentations for group A streptococci (GAS). Invasive GAS infections have increased world-wide during the past decade despite the organism remaining sensitive to penicillin and other commonly used Beta lactam antibiotics (1,2) Group B streptococci (GBS) are a leading cause of infection in neonates and pregnant women and have also been recognised as a cause of invasive diseases

in children and non-pregnant females (2, 3). Group C (GCS) and group G (GGS) streptococci are commensals of the pharynx, skin, gastrointestinal tract and female genital tract; the 'large colony'-forming strains resemble GAS in terms of their virulence (2).

Streptococcal (strep) infections are communicable diseases that develop when bacteria normally found on the skin or in the intestines, mouth, nose, reproductive tract, or urinary tract invade other parts of the body and contaminate blood or tissue. In the last decade, there has been an increase in reports of serious streptococcal infections worldwide (4).Strep infections are an occupational disease of school children between the ages of 5 and 15.

Streptococcal infections with an estimated death rate of over 500,000 individuals/year place GAS among major human pathogens, exceeded by HIV, *Mycobacterium tuberculosis, Plasmodium falciparum* and *S. Pneumonia*e and probably comparable to rotavirus, measles, *Haemophilus influenzae type b (Hib),* and Hepatitis B (5, 6).

Autoimmune response to infection with group A streptococcus is actually resulted into Rheumatic fever. Although the acute illness causes considerable morbidity, and some mortality, the major clinical and public health effects derive from long-term damage to the heart valves, i.e., rheumatic heart disease (RHD). Over the past century, as living conditions have become more hygienic and less crowded, and nutrition and access to medical care have improved, acute rheumatic fever (ARF) and RHD have become rare in developed countries. But, rheumatic fever/ rheumatic heart disease is the commonest cardiac disease in children and young adults and remains a major public health problem in developing countries (7).

GAS infection causes a substantial number of illnesses and deaths, especially in the developing world, withH" 500,000 deaths worldwide annually, attributable mostly to ARF and its sequelae, rheumatic heart disease, and invasive infection (8). The epidemiology of rheumatic fever (RF) is linked with that of Group A beta-haemolytic streptococcal pharyngitis; both have a maximum incidence in the age group of 5 – 15 years (9).

Recently worldwide population based data has been reviewed to estimate the burden of GAS diseases and highlighted deficiencies in the available data (10). According to WHO, at least 15.6 million people have RHD. Out of the 5, 00,000 individuals who acquire ARF every year, 3,00,000 go on to develop RHD; and 2,33,000 deaths annually are attributable to ARF or RHD (11). The greatest burden in streptococcal diseases is due to RHD, with a prevalence of at least 15.6 million cases, with 2, 82,000 new cases and 2, 33,000 deaths each year (8). It is estimated that approximately 600,000 children less than 15 years of age are currently suffering from chronic rheumatic heart disease, and that approximately 121,000 children are newly diagnosed with acute rheumatic fever every year.

During the past two decades, ARF/RHD has become uncommon health problems in developed countries. However, in third world countries such as India, the middle-east, sub-Saharan Africa, RF remains the leading cause of heart disease in children and young adults (12). In India, the disease burden of streptococcal infections is considerable (13). Prevalence of rheumatic heart disease and pharyngitis in India, varies from 1 to 5.4/1,000 (14) and 4.2% to 13.7%, (15, 16) school-age children respectively, which is comparable to the rates reported from developed countries (17). *Streptococcus pyogenes* pharyngitis has a high prevalence in North India (18), whereas pyoderma is more frequent in South India (19). In light of invasive infection, this is a completely neglected field in India and the only data available in the literature is one retrospective study of invasive β-hemolytic streptococcal infections (20). There are considerable socio-economic losses due to high cardiovascular mortality and morbidity of Indian population (21). Incidence of streptococcal pharyngitis has been reported to be 8-18

episodes per week per 1000 children in the age group of 5-15 years in India. Clinical scoring card for diagnosis of Group A Streptococcal sore throat was developed (22). For the last 20 years, in India various research programmes have been carried out at different centres mostly by ICMR and a few by WHO (23). Padmavati, in 1995 examined the status of RF & RHD in India with reference to both prevalence and incidence based on the last 10 years data and showed RHD in 1 to 5.4/1000 and RF in 0.3-0.5/1000 children. Recently the burden of group A streptococcal disease in India was addressed and treatment options standardized by the World Health Organization was also discussed (13).

Streptococcal infections are extremely common due to the overall susceptibility of these organisms to antibiotics, especially penicillin. While infections caused by the Lancefield group A streptococcus (GAS or Streptococcus pyogenes) have dominated the streptococcal medical literature, Lancefield groups C and G share many microbiologic and clinical characteristics with GAS (24). Work in the early 20th century described S. pyogenes as an exclusively human pathogen and detailed the frequency of carriers and the most characteristic infections (25). The pioneering work of Rebecca Lancefield led to the identification of a number of groups of streptococci including A, C and G, producing haemolysis on sheep blood agar, exhibiting different biochemical properties and isolated from a variety of animal species (26). Classification methods based upon the Lancefield methodology were established soon thereafter (27).

Among this diverse group, the group C and group G streptococci have assumed more important clinical roles. For a number of reasons, they can be considered together, separate from other members of the genus Streptococcus. Although less extensively studied, groups C and G streptococci are now appreciated to produce infections quite similar to GAS although they more commonly cause opportunistic and nosocomial infections than GAS. No. of recent reports have described their association with streptococcal syndromes generally caused by GAS such as streptococcal toxic shock syndrome (STSS) (28) and acute rheumatic fever (ARF) (29). This assumes significance in countries like India where ARF continues to be a major health problem.

β-hemolytic streptococcus belonging to Group G (*Streptococcus dysgalactiae* subsp. *Equisimilis)* has attracted attention as possible etiological agents of pharyngitis and post-streptococcal sequelae. Normally present on the skin, in the mouth and throat, and in the intestines and genital tract, Group G Streptococcus (GGS) is most likely to lead to infection in alcoholics and in people who have cancer, diabetes mellitus, rheumatoid arthritis and other conditions that suppress immune-system activity.

Till date, no report is available in Tripura about the streptococcal infection in school children; hence the present study was designed to study the prevalence of β-hemolytic Streptococcal infection among School children in Tripura, North Eastern part of India. This study also provides an opportunity to establish the direction of further investigations and to focus interventions in Tripura.

Materials and Methods

Present study was conducted after the clearance of institutional ethical committee (IET) of Agartala Govt. Medical College and G. B. P Hospital, Agartala. Cross sectional prospective study was conducted to find out the GAS isolates in Tripura, north eastern part of India at Agartala Govt. Medical College and G. B. P Hospital, Agartala. The school children of 5-15 years age group in different schools from 3 districts of Tripura were considered for the study. Besides, patients were not included those who have taken antibiotics prior to this programme. In aseptic condition, throat swabs were collected in duplicate using torch light under direct vision and with the aid of a tongue depressor. Swabs were rubbed quickly but thoroughly over both tonsils and tonsillar fossae. Since the sites of collection

were not very far from the microbiology laboratory so within two hours collected samples were transported to the lab at room temperature.

Sample processing - Two types of plates were used for culturing the sample; Blood agar and Mac Conkey. Blood agar plates were kept in candle jar to have microaerophilic condition whereas the Mac Conkey plates were allowed to incubate for 24-48 hours at 37°C.

After 24-48 hours incubation, bacterial colonies grown on blood agar plates showing beta haemolytic colonies were further processed from the mixed colony and incubate at the same atmosphere for 24 hours. Following day Gram staining was prepared from the suspected beta haemolytic colonies and catalase test was also performed for further confirmation. Based on the gram staining reaction and catalase test result, grouping was performed with the help of Streptex kit.

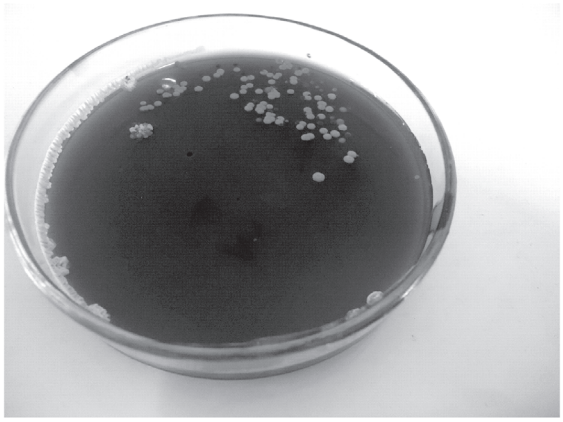

Fig. 1. Mac Conkey Plate

Fig. 2. Plates kept in Candle Jar

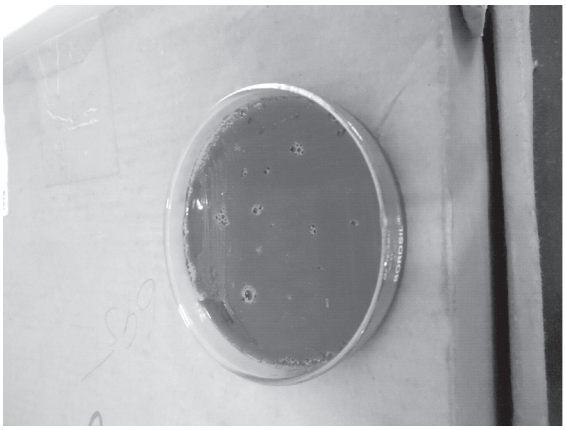

Fig. 3. Streptococcal colonies shown on Blood Agar Plate

Streptococcal Grouping : Streptex agglutination was carried out on colonies from purity plates. The extraction enzyme provided in the Streptex kit was reconstituted by the addition of 11 ml sterile distilled water and was stored at 4°C. With cultures from solid media, colonies were suspended in 4 ml extraction enzyme and incubated at 37°C for 1 hr. The enzyme extract was used for agglutination reactions without any centrifugation. One drop of extract was added to one drop of each of the latex particles coated with group-specific immunoglobulin to groups A, B, C, D, F and G on the clean glass grouping tiles provided. After thorough mixing, the tile was rocked gently for a maximum of one minute and then the agglutination pattern was read. Where agglutination was weak or occurred with more than one latex suspension the test was repeated using the extraction enzyme alone in parallel with the extract (30).

The number of positive throat swabs were then analyzed and represented in tabular form. As a part of external quality control, the methods and materials were supervised by expert of PGI, Chandigarh within our study period.

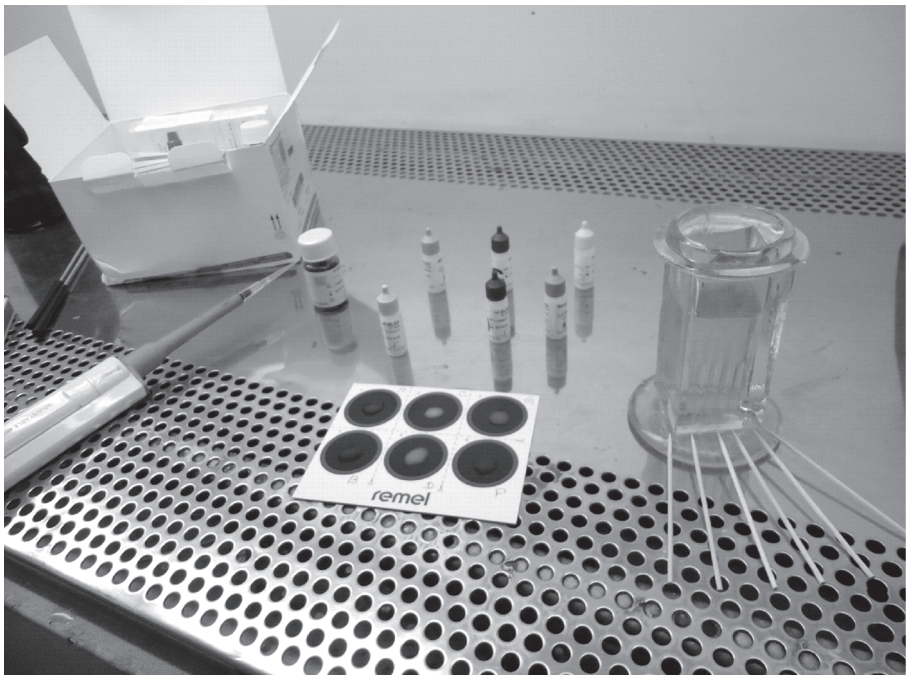

Fig. 4. Grouping of β-haemolytic colonies through Streptex Kit

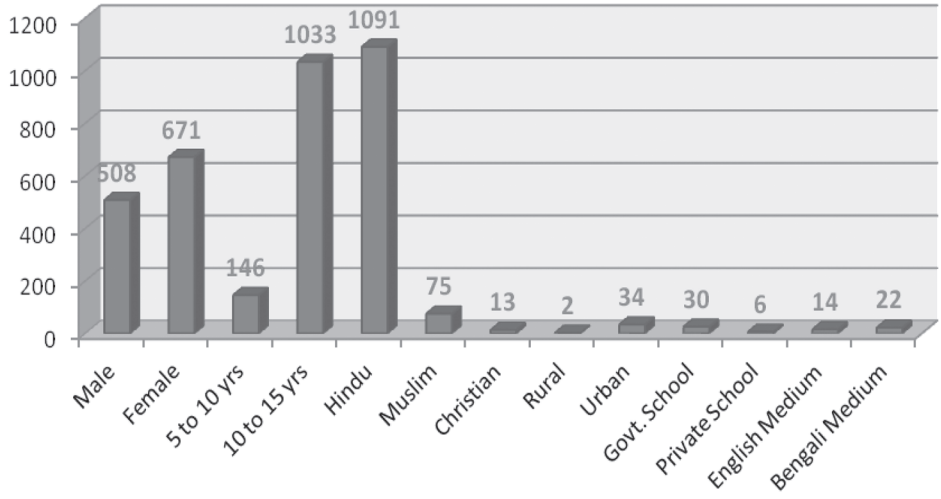

Fig. 5. Distribution of Cases from September, 2012 to February 2013

Results and Discussion

In the present study, 1165 throat swabs were randomly collected from school children of 3 districts of Tripura within a 6 months' time period. Socio demographic profile of the study subjects evaluated on the basis of sex, age and religion which is shown in the figure 5. Out of 1165 throat swabs, female children were more (608) in comparison to male (508). Whereas, 10-15 yrs children were much higher in number (1033) as compared to 5-10 yrs. children (146). So far religion is concerned, number of Hindu children were maximum as compared to Muslim and Christian. In the following figure 5, school children were more from urban area (34) than rural (2). Within same time period, 30 Govt. Schools were visited.

Laboratory investigation reports

Out of 1165 throat swabs cultured, 52 cases were with no growth observed in blood agar. Mixed bacterial colonies were present in Mac Conkey. Out of total cultured samples (1165) 91. 24% cases exhibited different types of bacteria other than Streptococcus. Whereas, 3.94% cases exhibited Alpha haemolytic and 0.34 % exhibited with Beta haemolytic (GGS). The results of throat swab cultures were shown in table 1.

Streptex kit analysis of 4 haemolytic colonies showed only the presence of group G.

Table 1. Result of Throat Swab Examination in blood agar

Month	Beta Hemolytic	Alpha Hemolytic	Bacteria other than *Streptococcus*	No Growth
Sept,2012	0	4	148	10
Oct,2012	0	6	766	34
Nov,2012	0	5	213	8
Dec,2012	0	11	294	0
Jan,2013	0	19	228	0
Feb,2013	4 (Group G)	1	104	0
Total	4	46	1063	52

Out of these 4 cases, 3 were males and one was female.

In our study, carriage rate of Group G Streptococcus (GGS) was higher in males than females. In case of age group, GGS infection was high in the age group of 11 years. Similar studies were conducted in various part of the world with similar findings. In the present study, though GAS was not found but the carriage rate in GGS (Group G Streptococcus) was higher in boys (75 %) than girls (25 %) which were similar to other reports (31,32). Age has been found to be an important factor in the microbiological etiology of pharyngitis, the peak incidence of GAS pharyngitis occurring in children aged 5–10 years (33). In the present study, the Group G Streptococcal infection was higher in 10 – 15 yrs. age group. All the 4 cases of Group G found in this study were of 11 yrs. and of more than 11 yrs. which was similar to other reports (33, 34). In Varanasi (India), the prevalence of beta-haemolytic streptococcal sore throat was 13.6% in a rural area (35). In our study, though GAS could not be isolated but the carriage rate in GGS was predominant in urban area (80 %).

The variations in the carriage rates among different schools in the same village may be explained on the basis of the location which was studied (36). Location wise present study revealed higher rate in govt. school (92 %) than private school (8 %).

Throat cultures have always been considered as the "gold standard" for diagnosing the presence of GAS (37). The healthy carriers of GAS are the sources of a bacterial dissemination and they are able to communicate the disease and even lead to severe epidemics (31). Different studies reported that, GAS is seen more in the pharynges of children as compared to that in adults (31). In the present study, there is a complete absence of Group A Streptococci among the school going children (5-15 yrs.) within the period of 6 months. Early use of antibiotics may be one of the factors for complete disappearance of group A Streptococcus in this

area. The prevalence of beta-haemolytic Streptococcus in healthy individuals in different parts of India has been reported ranging between 11.2-34% (33). Various studies were conducted in different parts of South India like Vellore, South India – 2.3% (1977) (15), Chennai, South India - 5.2 % (2005) and 8.4 % (2006) (38,39), Coimbatore, S.India – 5.09 % (2012) (40) and 4.- B.G. Nagara, Karnataka – 1.9% (2013) (41). In Northern India, the incidences of sore throat and GAS sore throat were-7.05 and 0.95 episodes per child/year (2001) respectively (17).

In Japan, a case of neonatal toxic shock syndrome due to *S. dysgalactiae* subsp. *Equisimilis* was reported (28). Invasive infections caused by this species are also increasingly seen in Japan (42) while one case of necrotizing fascitis and another case of toxic shock syndrome were reported from Norway (43) Due to these reasons, it is believed that GGS strains may be involved in the pathogenesis of post-streptococcal sequelae. Meanwhile, our study was based on a relatively small sample size within only 6 months time period. Hence it is imperative to carry forward to further study in a broader spectrum in different seasons to look for the presence of seasonal variability. We should explore the application of newer technologies to isolate GAS from the study subject. The results of the present study highlighted the importance of regular surveillance programmes to keep the Streptococcus infections and their carriage in check. The children who were found to be carriers could be adequately treated with antibiotics. This would further facilitate the control and the development of non-suppurative sequelae such as acute rheumatic fever and post streptococcal glomerulonephritis, which are debilitating and difficult to treat.

Acknowledgments

The authors are thankful to Indian Council of Medical Research (ICMR) for funding the research project for North East research priority. We also thank the Principal of Agartala Govt. Medical College Agartala for permitting us to conduct this study.

References

1. Schwartz, B., Facklam, R.R. and Breiman, R.F. (1990). Changing epidemiologyof group A streptococcal infection in the USA. Lancet, 336: 1167–1171.
2. Ruoff, K. L. (1998). Streptococcal diseases. In: Collier L, Balows A, Sussman M (eds) Topley & Wilson's microbiology and microbial infections, 9th edn, vol 3: Bacterial infections. London, Arnold., 257–275.
3. Tyrrell, G.J., Senzilet, L.D., Spika, J.S., Kertesz, D. A., Alagaratnam, M., Lovgren, M. and Talbot, J. A. (2000). Invasive disease due to group B streptococcal infection in adults: results from a Canadian population-based, active laboratory surveillance study -1996. J Infect Dis., 182: 168–173.
4. Efstratiou, A. (1990). GroupA Streptococci in the 1990s. J. Antimicrob. Chemother. 2000, 45:3-12.
5. Carapetis, J. R., Steer, A. C., Mulholland, E. K. and Weber, M. (2005). The global 1.burden of group A streptococcal diseases. Lancet Infect Dis. ;5:685–94.
6. World Health Organization. The World Health Report 2004. WHO, Geneva. (http://www.who.int/whr/previous/en/index.html)
7. Mishra, T. K. (2007). Acute Rheumatic Fever and Rheumatic Heart Disease: Current Scenario. JIACM, 8(4): 324-30.
8. World Health Organization. (2005). The current evidence for the burden of group A streptococcal diseases. Geneva: The Organization. page 60.
9. Sainani, G. S. and Sainani, A. R. (2006). Rheumatic fever - how relevant in India today? JAPI, 54: 42-47.
10. Carapetis, J.R,. Steer, A.C., Mulholand, E.K. and Weber, M. (2005). The global burden of group A streptococcal diseases. Lancet Infect. Dis. 5:685.

11. Carapetis, J. R. (2004). The current evidence of the burden of Group A streptococcal diseases. World Health Organisation, 1-57.

12. Veasy, L. G., Wiedmeier, S. E., Orsmond, G. S., Ruttenberg, H. D., Boucek, M. M., Roth, S. J., Tait, V. F., Thompson, J. A., Daly, J. A., Kaplan, E.L. and Harry R. H. (1987). Resurgence of acute rheumatic fever in the intermountain area of the United States. N. Eng. J. Med., 316: 421-427.

13. Shet, A., and Kaplan, E. (2004). Addressing the burden of group A streptococcal disease in India. Indian J. Ped., 71:41-48.

14. Capoor, M. R., Nair, D., Dev, M., Batra, K. and Aggarwal, P. (2006). Resistance to Erythromycin and Rising Penicillin MIC in *Streptococcus Pyogenes* in India. Jpn. J. Infect. Dis., 59: 334-336.

15. Koshi, G. and Benjamin, V. (1977). Surveillance of streptococcal infection in children in a South Indian community: a pilot survey. Ind. J. Medical Research, 66: 379-388.

16. Koshi, G., Jadhar, M. and Myers, R. M. (1970). Streptococcal pharyngitis in children in SouthernIndia. Ind. J. Medical Research, 58: 161–165.

17. Nandi, S. Kumar, R., Ray, P., Vohra, H. and Ganguly, N. K. (2001). Group A streptococcal sore throat in a periurban population of northern India: a one-year prospective study. Bulletin of the World Health Organization, 79: 528–533.

18. Kumar, R., Vohra, H. Chakraborty, A., Sharma, Y.P., Bandhopadhya, S., Dhanda,V., Sagar, V., Sharma, M., Shah, B. and Ganguly, N. K. (2009). Epidemiology of group A streptococcal pharyngitis & impetigo: a cross-sectional & follow up study in a rural community of northern India. Indian J Med Res. 130:765-771.

19. Brahmadathan, K. N. and Koshi, G. (1988). Epidemiology of streptococcal pyoderma in an orphanage community of a tropical country. J. Trop. Med. Hyg., 91:306-314.

20. Mathur, P., Kapil, A., Das, B., Dhawan, B. and Dwivedi, S.N. (2002). Invasive beta-haemolytic streptococcal infections in a tertiary care hospital in northern. India. J Med Microbiol., 51:791-792.

21. Zaman, M. M., Rouf, M. A., Haque, S., Khan, L. R., Chowdhury, N. A., Razzauqe, S. A., Yoshike, N. and Tanaka, H. (1998). Does rheumatic fever occur usually between the ages of 5 and 15 years?. Int J Cardiol., 66: 17-21.

22. Nandi, S., Kumar, R., Ray, P., Vohra H. and Ganguly, N. K. (2002). Clinical score card for diagnosis of group A streptococcal sore throat. Ind. J. Pediatr., 69: 471-5.

23. Padmavati, S. (1987). Rheumatic fever and Rheumatic heart disease in India. Progress in Cardiology 15th ed, (Paul, N. Yu.), Philadelphia, Lea & Febiger.

24. Laura, N. B., Beneden, C.V., Beall, B., Facklam, R., Shewmaker, P.L. and Malpiedi, P. (2009). Population-based study of invasive disease due to beta-hemolytic streptococci of groups other than A and B. Clin Infect Dis., 48:706-12.

25. Rammelkamp, C. H. Jr. (1956). Epidemiology of streptococcal infections. Harvey Lect., 51:113.

26. Lancefield, R. C. (1933). A Serological Differentation of Human And Other Groups of Hemolytic Streptococci. J Exp Med., 57:571.

27. Sherman, J. M. (1937). The Streptococci. Bacteriol. Rev., 1:3.

28. Yamaoka, S., Ogihara, T., Yasui, M., Hasegawa, M., Hira, S., Oue, S., Ubukata, K., Watanabe, H. and Takahashi, T. (2010). Neonatal streptococcal toxic shock syndrome caused by *Streptococcus dysgalactiae* subsp. Equisimilis. Pediatr. Infect. Dis. J., 29:979-981.

29. Haidan, A., Talay, S. R., Rohde, M., Sriprakash, K. S., Currie, B.J. and Chhatwal, G.S. (2000). Pharyngeal carriage of Group C and Group G streptococci and acute rheumatic fever in an Aboriginal population. Lancet, 356:1167-1169.

30. Castled, D., Kessock-Philip, S. and Easmon, C. S. F. (1982). Evaluation of an improved Streptex kit for the grouping of beta-haemolytic streptococci by agglutination. J Clin Pathol., 35:719-722.

31. Nabipour, F. and Tayar, Z. M. (2005). Prevalence of Beta-haemolytic streptococcus carriage state and its sensitivity to different antibiotics among guidance- school children in Kerman-Iran. Am J Infect Dis., 1:128-31.

32. Navneeth, B. V., Nimanda, R., Chawda, S., Selvarani, P., Bhaskar, M. and Sugan-thi, N. (2001). Prevalence of beta -haemolytic *streptococci* carrier rate among school children in Salem. Indian J Paediatr., 68:985-86.

33. Nandi, S., Kumar, R., Ray, P., Vohra, H. and Ganguly, N. K. (2001). Group A Streptococcal sore throat in a periurban population of northern India: a one-year prospective study. World Health Organ., 79 : 528-33.

34. Kaplan, E. L., Bisno, A. L., Gerber, M. A. and Gwaltney, J. M. Jr. (1971). Diagnosis of streptococcal pharyngitis: differentiation of active infection from the carrier state in symptomatic child. Journal of Infectious Diseases, 123: 490–501. 24.

35. Sarkar, S., Biswas, R., Gaur, S. D., Sen, P. C. and Reddy, D. C. (1988). A study on sore throat and beta-hemolytic streptococcal pharyngitis among rural school children in Varanasi with reference to age and season. Indian Journal of Public Health, 32: 191-198.

36. Dumre, S. P., Sapkota, K., Adhikari, N., Acharya, D., Karki, M. and Bista, S. (2009). Asymptomatic throat carriage rate and antimicrobial resistance pat-tern of *streptococcus* pyogenes in Nepalese School children. Kath-mandu University Med J., 7: 392-96.

37. Shet, A. and Kaplan, E. (2004). Addressing the burden of group A streptococcal disease in India. Ind. J. Pediatr., 71 (1):41-48.

38. Anbu, M. and Thangam, M. (2005). Biotyping of the group A Streptococci which were isolated from normal school children in south India. *Indian Journal for the Practising Doctor*. 17-18.

39. Charmaine, A. C. L., Swarna, E. J. and Thangam, M. (2006). Pharyngeal carriage of the group A streptococci in school children in Chennai. Indian J Med Res. 124: 195-98.

40. Muthusamy, D., Boppe, A. and Suresh., S. P. (2012 September). Prevalence of Group A Beta Haemolytic Streptococcal Carriers Among School Children in Coimbatore, South India. Journal of Clinical and Diagnostic Research. 6:1181-1183.

41. Vijaya, D., Sathish, J. V. and Jana Kiram, K. (2013). The Prevalence of Group A Streptococci Carriers AmongAsymptomatic School Children Journal of Clinical and Diagnostic Research, 7: 446-448.

42. Takahashi, T., Ubukata, K. and Watanabe, H. (2011). Invasive infection caused by *Streptococcus dysgalactiae* subsp. *equisimilis*: characteristics of strains and clinical features. J. Infect. Chemother. 17:1-10.

43. Kittang, B. R., Langeland, N., Skrede, S. and Mylvaganam, H. (2010). Two Unusual cases of severe soft tissue infection caused by *Streptococcus dysgalactiae* subsp. *equisimilis*. J. Clin. Microbiol., 48:1484-1487.

Current Trends in Biotechnology and Pharmacy
Vol. 7 (4) 890-903 October 2013, ISSN 0973-8916 (Print), 2230-7303 (Online)

The effect of using two NSAIDs with different solubility on freeze drying technology

Mohamed Aly Abd El Aziz Aly El Degwy[1], Saydia Tayel[2], Mohamed A. El Nabarawi[2] and Randa Tag A. El Rehem[2]

[1]Mepaco Pharmaceutical Company, Egypt
[2]Faculty of Pharmacy-Cairo University, Cairo, Egypt
*For Correspondence - nabrwima@hotmail.com

Abstract

Different non-steroidal anti- inflammatory drugs (NSAIDs) are present in the market with different properties. Two NSAIDs with different solubilities have been selected to study the effect of freeze drying technology on them. Aceclofenac, a water insoluble NSAID, and Diclofenac Potassium, a water soluble NSAID, were taken as candidates for enhancement of *in-vitro* dissolution and *in-vivo* bioavailability; through formulation of orally disintegrating tablet using freeze drying technology. An aqueous dispersion of Aceclofenac (or Diclofenac Potassium), matrix former, filler (sugar alcohol), and an anti-collapse was adopted to prepare freeze dried tablet formulations. The tablets were evaluated compendial (uniformity of weight, uniformity of content, friability, *in-vitro* disintegration time and *in-vitro* dissolution) and non-compendial (wetting time and *in-vivo* disintegration time). The compendial results showed that both freeze dried tablet formulations of Aceclofenac and also Diclofenac Potassium disintegrated within few seconds and showed significantly faster dissolution rate in comparison with both immediate release tablet formulae Aceclofenac tablet (Bristaflam®) and Diclofenac Potassium tablet (Cataflam®). *In-vivo* evaluation for the best chosen Aceclofenac and Diclofenac Potassium ODT formulations (LA#10) and (LD#11), respectively was done for determination of the drug pharmacokinetics in comparison with the immediate release tablet formulations. A randomized crossover design was adopted in the comparative bioavailability study done on four healthy volunteers. Statistical analysis revealed significant difference between the Bristaflam immediate release tablet and Aceclofenac ODT (LA#10) regarding the following pharmacokinetic parameters: C_{max}, T_{max}, $t_{1/2}$, $AUC_{(0-24)}$, $AUC_{(0-\infty)}$ ($p<0.05$); while insignificant difference regarding mean residence time (MRT) ($p>0.05$). The relative bioavailability of the Aceclofenac ODT (LA# 10) was 186.12% relative to the IR tablet (Bristaflam®) taken as reference standard. However, statistical analysis revealed significant difference between the Cataflam immediate release tablet and Diclofenac Potassium ODT (LD#11) regarding the following pharmacokinetic parameters: C_{max} and T_{max} ($p<0.05$); while insignificant difference regarding $t_{1/2}$, $AUC_{(0-12)}$, $AUC_{(0-\infty)}$, and mean residence time (MRT) ($p>0.05$). The relative bioavailability of the Diclofenac Potassium ODT (LD#11) was 101.09% relative to the immediate release tablet (Cataflam®) taken as reference product. Though a significant decrease in the time of onset of action; however no significant increase in the relative bioavailability was observed. Though, both drugs showed increased rate of absorption, however the insoluble NSAID (Aceclofenac) showed higher bioavailability than the soluble NSAID (Diclofenac Potassium). The impact of the relative solubility factor was highly significant on the bioavailability though using the same technology.

Vol. 7 (4) 890-903 October 2013, ISSN 0973-8916 (Print), 2230-7303 (Online)

Keywords: ODT, Lyophilization, Diclofenac potassium, Aceclofenac, Bioavailability

Introduction

Recently, different orally disintegrating tablets technologies have had an increasing interest in the field of pharmaceutical applications. ODTs offer an advantage for populations having dysphagia (difficulty in swallowing). Dysphagia is common among all age especially with pediatric, geriatric, institutionalized patients and patients with nausea, vomiting, and motion sickness complications (1 and 2). ODTs, with good taste and flavor, increase the compliance of bitter drugs and overcome difficulty in swallowing by pediatric and geriatric patients (3). Although the increase of average human life span; however geriatrics develop a higher risk of chronic diseases accompanied by different pains. The use of fast acting dosage forms with high bioavailability of drugs especially as Non steroidal anti-inflammatory drug (NSAIDs) for pain relieving would be highly favored. The most effective technology for preparation of ODTs was freeze drying (lyophilization). Two model NSAIDs, derivatives of the same molecular group, with different aqueous solubility were chosen to study the effect of the difference of drug solubility on lyophilization efficacy. Aceclofenac is poorly water-soluble NSAID having poor bioavailability. Aceclofenac shows high anti-inflammatory, antipyretic and analgesic activity with moderate incidence of gastric side effects and a high therapeutic index (4). Aceclofenac is largely eliminated via first pass effect; therefore, Aceclofenac ODT that is absorbed through the oral cavity directly to the systemic circulation may result in an increase in drug bioavailability together with rapid onset of action (5). Similarly, Diclofenac Potassium, water soluble NSAID, that is highly subjected to first pass metabolism made it a candidate to increase onset of action and enhance its bioavailability with lower adverse effects through pre-gastric absorption from the mouth, pharynx and oesophagus (6). This would result in a rapid onset of action via a more comfortable and convenient delivery route than the intravenous route.

Materials and Methods

Material: Aceclofenac and Diclofenac Potassium were supplied by Sinochem, China. Mannitol was supplied by SPI Pharma Inc, USA. Lactose was supplied by Meggle GmbH, Germany. Maltodextrin was supplied by Grain Processing Corp., USA. Gelatin, glycine, sodium chloride and potassium chloride were received from Adwic, El-Nasr Pharmaceutical Chemicals Co., Egypt. The water used was distilled deionized water. All other chemicals were reagent grade and used as received. Bristaflam® 100 mg tablet (Bristol Myers Squibb, Egypt) and Cataflam® 50 mg tablet (Novartis, Egypt) were used as a reference tablet in in-vivo studies.

Preparation of ODTs: Both Aceclofenac and Diclofenac Potassium ODTs were prepared using three different types of matrix formers (gelatin, hydroxypropylcellulose or xanthan gum) at three different concentrations (1%, 3% and 5% w/v), three different fillers (lactose monohydrate, mannitol or maltodextrin) (at a concentration of 2% w/v); together with 2% w/v glycine as an anti-collapse as shown in Table (1). Different trials were performed to choose the optimum percentage of fillers and anti-collapse that had attained sufficiently strong tablet that could be handled. The matrix former was dissolved in distilled water at 40°C; followed by dissolving the filler and glycine. An accurately weighed amount of Aceclofenac or Diclofenac Potassium powder was dispersed in the prepared aqueous solution using a magnetic stirrer to result in a dose of 100 mg & 50 mg per ml for Aceclofenac and Diclofenac Potassium; respectively. One milliliter of the suspension was then poured in each pocket of a PVC blister pack with a diameter of 13 mm and a depth of 3 mm. The tablet blister packs were kept in a freezer at -22°C for 24 hours. The frozen tablets were freeze dried for 24 hours using a Novalyphe-NL500 Freeze Dryer with a condenser temperature of -45°C and a pressure of 7×10^{-2} mbar. The formulations were evaluated compendial and non-compendial. The

prepared ODTs were kept in tightly closed containers in desiccators over calcium chloride (0% relative humidity) at room temperature until further use.

Characterization of ODTs

Uniformity of Weight: Twenty tablets from each formula were weighed individually and the mean tablet weight was calculated. Results are presented as mean value ± (SD) (7).

Uniformity of content: Ten tablets from each formula were assayed individually for drug content uniformity. The drug in ODTs was assayed by dissolving each tablet in 250 ml simulated saliva fluid (pH = 6.8). The solution was then filtered, properly diluted, and the absorbance was spectrophotometrically measured at λ_{max} = 276 nm and 282 nm for Aceclofenac and Diclofenac Potassium; respectively. Each individual tablet contents must be between 85-115% of the average content and the tablet formula fails to comply with the test if more than one individual tablet content is outside these limits or if one individual content is outside the limits of 75-125% of the average content.

Tablet friability: Twenty tablets from each formula were weighed accurately and placed in the drum of friabilator (Erweka type, GmbH, Germany). The tablets were rotated at 25 rpm for a period of 4 min and then removed, de-dusted and accurately re-weighed. The percentage loss in weight was calculated and taken as a measure of friability (8).

In-vitro Disintegration Time: The disintegration times of six tablets placed in distilled water kept at 37 ± 0.5ºC using a ZT3-3 disintegration tester (Erweka, Germany) were determined. A digital stopwatch was used to measure the disintegration time to the nearest second. Only one ODT was analyzed at a time in order to ensure accuracy. All results are presented as mean value ± SD (n=6) (9).

In-vivo Disintegration Time: The *in-vivo* disintegration time of each formulation was evaluated in four human volunteers after giving written consent. The volunteers had no history of hypersensitivity to NSAIDs. Prior to the test, all volunteers were asked to rinse their mouth with distilled water. Each of the four subjects was given a coded tablet. Tablets were placed on the tongue and the time was recorded immediately. They were allowed to move the tablet against the upper palate of the mouth with their tongue and to cause a gentle tumbling action on the tablet without biting it. After the last noticeable mass had disintegrated, the time was recorded. The subjects were asked to spit out the content of the oral cavity after tablet disintegration and rinse their mouth with distilled water. The swallowing of saliva was prohibited during the test, and also saliva was rinsed from the mouth after each measurement. The test results are presented as mean value ± SD (10).

Wetting Time: Ten milliliters of distilled water containing eosin, a water-soluble dye was placed in a Petri dish of 10 cm diameter. Tablets were carefully placed in the centre of the Petri dish and the time required for water to reach the upper surface of the tablet was noted as the wetting time. The test results are presented as mean value of three determinations ± SD (11).

In-vitro Dissolution Studies: The dissolution profiles of Aceclofenac (or Diclofenac Potassium) ODTs were determined in a dissolution tester (Erweka DT-700 Dissolution Tester, Germany) following the USP paddle method. All tests were conducted in 900 ml simulated saliva fluid without enzymes (SSF) at pH = 6.8. The dissolution medium was maintained at a temperature of 37 ± 0.5°C with a paddle rotation speed at 50 rpm. The amount of drug used was equivalent to 100 mg. At specified time intervals (1, 2, 5, 7, 10, 15 and 30 min), 3 ml of dissolution medium was withdrawn and replaced with an equal volume of fresh medium to maintain a constant total volume. Samples were filtered through 0.45 μm Millipore filter and assayed for drug content spectrophotometrically at 276 nm and 282 nm for Aceclofenac and Diclofenac Potassium; respectively, after appropriate dilution. Cumulative amount of drug dissolved in the

Vol. 7 (4) 890-903 October 2013, ISSN 0973-8916 (Print), 2230-7303 (Online)

preparations was calculated using calibration equation. Dissolution tests were performed in six vessels per formulation (n = 6).

In-vivo Absorption Studies

Subject Population: Four healthy male volunteers (ages between 25 - 35 years; mean age, 27 ± 1.7 years) participated in the study. All were within 10% of their ideal body weights (weights, 72 - 95 kg; mean weight 89 ± 14.1 kg and heights, 165 - 179 cm, mean height, 172 ± 6.8 cm). Health status of the volunteers was confirmed by complete medical history, physical examination and laboratory analysis for complete hematological and biochemical examination. The volunteers did not take any drugs for one week before and during the course of the study. No smoking was allowed 12 hours before and 24 hours after drug intake. On each test day, coffee, tea, and cola beverages were withheld from subjects 12 hours before the administration and till the blood sampling was completed. Each subject read, understood, and signed an informed written consent. All subjects were informed about the risks and objectives of the study.

Study Design: The study was performed to compare the pharmacokinetics of Aceclofenac 100 mg ODT formula (LA#10) and the reference, Bristaflam® 100 mg tablet and Diclofenac Potassium 50 mg ODT formula (LD#11) and the reference, Cataflam® 50 mg tablet using non-blind, two treatments, two periods, randomized cross over design. Under this design half of the subjects were given the immediate release treatment first and the ODT treatment second and the other half were given the treatments in the opposite order. The study was approved by the Research Ethics Committee at Faculty of Pharmacy, Cairo University. After an overnight fast, the subjects were present in the facility at 7 am of the day of study and remained under controlled dietary and liquid intake until the end of the study day. No food was allowed for four hours after dosing. The washout period was one week. The subjects were under medical supervision during the study and were observed for any adverse events. The ODT was administered orally without water, and each subject was asked to keep the ODT in the mouth for few minutes until completely dissolved in the saliva, then water was allowed after 30 minutes (Treatment A). The immediate release tablet, Bristaflam® 100 mg tablet or Cataflam® 50 mg tablet was ingested with 200 ml of water (Treatment B); for Aceclofenac and Diclofenac Potassium; respectively.

Collection of blood samples

Aceclofenac sampling: Venous blood samples were collected in heparinized glass tubes at 0, 15, 30 minutes, 1, 1.5, 2, 2.5, 3, 4, 6, 8, 12 and 24 hours after administration of the Aceclofenac ODT and Bristaflam tablet.

Diclofenac Potassium sampling: Venous blood samples were collected in heparinized glass tubes at 0, 5, 10, 15, 30, 45 minutes, 1, 1.5, 2, 2.5, 3, 4, 6, 8, 10 and 12 hours after administration of the Diclofenac Potassium ODT and Cataflam tablet. All the samples were collected; then the plasma was immediately separated from the blood cells by centrifugation at 6000 rpm for 10 minutes and stored at -20°C until analysis.

Analytical procedure for determination of drug in plasma

Aceclofenac *Assay Method Description and Chromato-graphic conditions:* A simple, rapid, and specific HPLC method for Aceclofenac in human plasma has been developed. The analysis was done on Shimadzu LC Prominence 20 connected with PDA detector; using column ODS 3, Prodigy, (250 x 4.6 mm, 5 µm). The mobile phase was isocratic consisted of acetonitrile: methanol: 50 mM potassium dihydrogen phosphate buffer, in ratio of (30:30:40 v/v) and was delivered to the system at a flow rate of 1.5 ml/min, with an injection volume of 20 µl and the detection wavelength (p_{max}) was 275 nm. Oxazepam was used as internal standard. All assays were performed at ambient conditions.

Preparation of stock and working standard solution: Stock solution of Oxazepam (internal standard) solution was prepared by dissolving 50 mg of Oxazepam in 100 ml acetonitrile; then sonication for 5 minutes (500 µg/ml). The working internal standard was prepared on each day of analysis by diluting the stock solution to contain (5 µg/ml). Stock solution of Aceclofenac was prepared by dissolving 50 mg Aceclofenac in 100 ml acetonitrile; then sonication for 5 minutes (500 µg/ml). The working solution was prepared on each day of analysis by diluting the stock solution with a mixture of (Acetonitrile : Water [1:1]) to give serial dilutions containing 0.5, 1, 2, 3, 4, 5 and 7 µg/ml of Aceclofenac; which were shaken well and filtered over 0.45 µm syringe filter and injected onto HPLC.

Plasma sample preparation for determination of Aceclofenac: The extraction procedure was applied in the preparation of plasma samples and standards, where 1 ml of each human plasma was transferred into 15 ml tube fitted with polyethylene cap. 1 ml of internal standard working solution and 1 ml acetonitrile were added. The mixture was vortexed for 2 minutes and centrifuged at 6000 rpm for 30 minutes. The upper layer was transferred to another tube and filtered through 0.45 µm syringe filter. A 20 µl volume of the supernatant was injected onto the HPLC column. Concentrations of Aceclofenac in unknown samples were calculated with reference to the prepared calibration curve. Retention time of Aceclofenac was 5.8 minutes.

Preparation of in-vivo standard calibration curve: For calibration curve, plasma standards were prepared by spiking 1 ml of blank plasma with 1 ml of the internal standard working solution and appropriate volumes of Aceclofenac working solution to produce concentrations ranging from (0.25, 0.5, 2, 4, 6, 8, 10µg/ml). The spiked plasma standards were processes as described above. The calibration curve was obtained by plotting chromatographic peak area ratios (Aceclofenac/ Oxazepam) against the corresponding nominal Aceclofenac concentration added. Samples were prepared and injected on the same day.

Diclofenac Potassium

Assay Method Description and Chromatographic conditions: A simple, rapid, and specific HPLC method for Diclofenac Potassium in human plasma has been developed. The analysis was performed on Shimadzu LC Prominence 20 connected with PDA detector; using mixed column ODS/Cyano; ACE, (100 x 4.6 mm, 5 µm). The mobile phase was isocratic consisted of Methanol: 50 mM potassium dihydrogen phosphate buffer, in ratio of (50 : 50 v/v) and was delivered to the system at a flow rate of 1.5 ml/min, with an injection volume of 20 µl and the detection wavelength was 280 nm. Diazepam was used as internal standard. All assays were performed at ambient conditions.

Preparation of stock and working standard solution: Stock solution of Diazepam (internal standard) solution was prepared by dissolving 50 mg of Diazepam in 100 ml methanol; then sonication for 5 minutes (500 µg/ml). The working internal standard was prepared on each day of analysis by diluting the stock solution to contain (1.5 µg/ml). Stock solution of Diclofenac Potassium was prepared by dissolving 50 mg Diclofenac Potassium in 100 ml methanol; then sonication for 5 minutes (500 µg/ml). The working solution was prepared on each day of analysis by diluting the stock solution with methanol to give serial dilutions containing 0.25, 0.5, 1, 1.5, 2, 2.5, and 3 µg/ml of Diclofenac Potassium; which were shaken well and filtered over 0.45 µm syringe filter and injected onto HPLC.

Plasma sample preparation for determination of Diclofenac Potassium: The extraction procedure was applied in the preparation of plasma samples and standards; where 1 ml of each human plasma was transferred into 15 ml tube fitted with polyethylene cap. 1 ml of internal standard working solution and 1 ml methanol were added. The mixture was vortexed for 2 minutes and centrifuged at 6000 rpm for 30 minutes. The upper layer was transferred to another tube and filtered through 0.45 µm syringe filter. A 20 µl volume of the supernatant was injected onto the HPLC column. Concentrations

of Diclofenac Potassium in unknown samples were calculated, with reference to the prepared calibration curve. Retention time of Diclofenac Potassium was 6.6 minutes.

Preparation of in-vivo standard calibration curve : For calibration curve, plasma standards were prepared by spiking 1 ml of blank plasma with 1 ml of the internal standard working solution and appropriate volumes of Diclofenac Potassium working solution to produce concentrations ranging from (0.25, 0.5, 1, 2, 3, 4, and 5 µg/ml). The spiked plasma standards were processes as described above. The calibration curve was obtained by plotting chromatographic peak area ratios (Diclofenac Potassium/Diazepam) against the corresponding nominal Diclofenac Potassium concentration added. Samples were prepared and injected on the same day.

Sample calculation: The unknown sample concentration was calculated from the following formula: C = [(R + Y) /S] Where C is drug concentration (Aceclofenac or Diclofenac Potassium), R is the peak area ratio (drug/internal standard), S is the slope of the calibration curve and Y is the Y-intercept.

Pharmacokinetics Calculations: Pharmacokinetic parameters from plasma data following administration of the two treatments were estimated for each subject by using a computer program, WinNonlin® software (version 1.5, Scientific consulting, Inc., NC). The plasma concentration – time data were evaluated, and the following pharmacokinetic parameters were calculated:

C_{max} (µg/ml): it was determined as the highest observed Aceclofenac (or Diclofenac Potassium) concentration during the 24 hours study.

T_{max} (hours); it was taken as the time at which C_{max} occurred.

K_a (hours-^{1}), it is the reciprocal of T_{max}

AUC_{0-t} (ìg.hr/ml)*;* was determined as the area under the plasma concentration-time curve up to the last measured time point calculated by the trapezoidal rule.

$AUC_{0-\infty}$ (ìg.hr/ml): it was determined as the area under the plasma concentration – time curve up to the last measured time point calculated by the trapezoidal rule plus the residual area calculated as the concentration of the last measured time point divided by the elimination rate constant. Where $AUC_{0-\infty} = AUC_{0-t} + C_t/k$; and C_t is the last measured concentration at the time t, and k is the terminal elimination rate constant estimated by log-linear regression analysis on data visually assessed to be a terminal log-linear phase.

$t_{1/2}$ is apparent terminal half life and was calculated as $t_{1/2} = 0.693/k$ plasma half life.

MRT is the mean residence time and was calculated AUMC/AUC

f_{rel} is the relative bioavailability and was calculated as (AUC_{ODT} / AUC_{IR}) X 100.

Statistical analysis of the pharmacokinetic parameters : Statistical evaluation of C_{max}, t_{max}, $t_{1/2}$, AUC_{0-t}, and $AUC_{0-\infty}$ data by one way ANOVA statistical test using SPSS® 11 software (SPSS Inc., Chicago).

Results and Discussion

Characterization of ODT Formulations - ***Aceclofenac ODTs:*** All the tablet formulations were within the acceptable weight variation and content. All formulations containing 3% and 5% matrix former showed acceptable percentage weight loss (less than 1%) except (LA#11) containing 3% hydroxypropylcellulose and lactose. On the contrary, all the formulations containing 3% xanthan gum and 1% matrix former were friable. The decreased mechanical properties of ODTs formulated with 1% matrix former could be attributed to the fewer number of crosslinks formed between the matrix former strands as the concentration decreases. It was reported that increasing the matrix former concentration results in a more strong network after freeze-drying due to increase in the number of matrix fibers forming crosslinks resulting in an

increase in the tablets hardness (12). Tablets containing mannitol showed lower weight losses compared to tablets formulated with lactose and maltodextrin. This may be due to that mannitol as filler produces a stiff mass that increase the hardness of the freeze dried tablets (13). In-vitro disintegration studies showed that ODTs containing lactose and maltodextrin showed longer disintegration times compared to ODTs containing mannitol. This may be due to the matrix forming effect of maltodextrin that synergies the binding property of the matrix former, so hindering the rate of disintegration (14 – 16). Although both mannitol and lactose have same solubility in water; however lactose dissolves at a slower rate than mannitol. The more rapid disintegration rates of formulae containing mannitol can be directly attributed to its better solubility than lactose (17 & 18). ODTs containing 5% matrix former showed longer disintegration times compared to ODTs containing 1% and 3% matrix former. These results indicate that increasing the matrix former concentration in the tablets results in the formation of more cohesive and stable gels that are less likely to break down or dissolve easily. These results were confirmed by wetting time results; where shorter wetting time is indicative of the highly porous nature of the tablet matrix. Also, in-vitro disintegration results correlated with friability results. Results showed that in-vivo disintegration times were shorter when compared to corresponding in vitro disintegration times for all formulations; which may be due to the gentle movement of the tablet in the mouth and hence gentle mechanical stress on the tablet. This is in accordance with the results obtained by Ciper and Bodmeier (19).

Diclofenac Potassium ODTs : All the Diclofenac Potassium formulations showed acceptable weight variation and content uniformity. Friability studies showed that tablets formulated with 3% and 5% matrix former showed acceptable percentage weight loss except all the formulations containing 3% hydroxypropyl cellulose and (LD#22) (containing mannitol and 5% hydroxypropylcellulose). On the other hand, all tablets formulated with 1% matrix former were friable except those containing 1% gelatin. It was also observed that the formulations with mannitol showed lower weight losses compared to tablets formulated with lactose and maltodextrin. In-vitro disintegration studies showed that ODTs containing maltodextrin showed longer disintegration times compared to ODTs containing mannitol and lactose. This may be attributed to the matrix forming effect of maltodextrin that synergies the binding property of the matrix former, so hindering the rate of disintegration (14 - 16). ODTs prepared using 5% matrix former showed statistically significantly longer disintegration times compared to ODTs prepared using 1% and 3% matrix former. These results are further confirmed by wetting time experiments in which tablets containing higher matrix former concentration shows significantly higher wetting times compared to tablets containing of lower matrix former concentration. Short wetting time is indicative of the highly porous nature of the tablet matrix. In-vitro disintegration results are also in accordance with friability results in which harder tablets showed longer disintegration times. Results show that in-vivo disintegration times were shorter when compared to corresponding in-vitro disintegration times for all formulations.

In-vitro dissolution - Aceclofenac ODTs : From the dissolution results as shown in table (4), it was found that the Aceclofenac formulations containing mannitol showed faster drug release than the corresponding formulations containing lactose; which in turn showed faster drug release than the formulations containing maltodextrin. Although both mannitol and lactose have same solubility in water; however lactose dissolves at a slower rate than mannitol. The more rapid disintegration rates of formulations containing mannitol can be directly attributed to its better solubility than lactose (17 and 18). The percentage of Aceclofenac dissolved in the first five minutes was higher in case of presence of gelatin than in case of presence of

hydroxypropylcellulose; which in turn was higher than in presence of xanthan gum at all concentrations. Similar results were obtained by Kimura et al (20), Imai et al (21) and Chono et al (22), where gelatin enhanced the disintegration and dissolution of the drugs. Increasing the concentration of different matrix former decreased the drug release. However, increasing of the percentage of gelatin from 1% to 3% didn't affect the release profile, when used with mannitol as filler, but decreased slightly with lactose. Also, it decreased greatly when using maltodextrin as filler, which may be due to the matrix forming properties of maltodextrin. Therefore, the best formulation from the dissolution profile and compendial evaluation was found to be (LA#10), containing mannitol and 3% gelatin.

Diclofenac Potassium ODTs : As for Diclofenac Potassium formulations as shown in table (5), it was found that the ODTs containing lactose showed faster drug release than the corresponding formulations containing mannitol; which in turn showed faster drug release than the formulations containing maltodextrin. The decrease in disintegration time may be attributed to the increase of the drug wettability, which may be due to conversion of the drug to amorphous form and its solubilization due to hydrophilic carrier (23). This may be attributed to a solid dispersion of maltodextrin or lactose with the soluble Diclofenac Potassium co-precipitated, with a possible Milliard interaction that may have occurred upon lyophilization to give a strong matrix of low friability and high solubility. However, in the presence of maltodextrin as a filler; a major decrease in the drug release occurred which may be due to its matrix former properties. The percentage of Diclofenac Potassium dissolved in the first five minutes was higher in case of presence of gelatin than in case of presence of hydroxypropylcellulose; which in turn was higher than in presence of xanthan gum at all concentrations (20 - 22). Increasing the percentage of different matrix former decreased the drug release significantly. In case of increasing of the concentration of gelatin as matrix former from 1% to 3% didn't affect the release profile significantly; when used with lactose and mannitol as fillers, however it decreased greatly when using maltodextrin as filler; this may be due to the matrix forming properties of maltodextrin. Therefore, the best formula from the dissolution profile and compendial evaluation was found to be (LD#11), containing lactose and 3% gelatin. The percentage of Aceclofenac dissolved in all the formulae was lower than the percentage of Diclofenac Potassium dissolved in the corresponding formulae containing the same excipients; and this may be attributed to the difference in solubility of Aceclofenac (insoluble) from Diclofenac Potassium (soluble).

Assessment of Pharmacokinetic Parameters : The study was completed by the four volunteers who were included in the pharmacokinetic analysis. The volunteers tolerated very well the two treatments and did

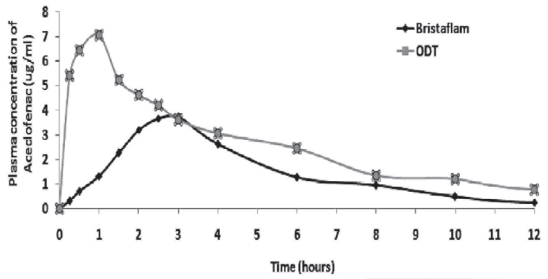

Fig. 1. Relative Bioavailability of Aceclofenac ODT versus Bristaflam Immediate Release Tablet

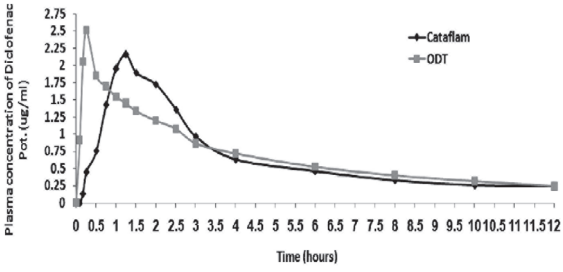

Fig. 2. Relative Bioavailability of Diclofenac Potassium ODT versus Cataflam Immediate release tablet.

Table 1. Composition of Aceclofenac and Diclofenac Potassium freeze dried formulae

Aceclofenac		LA# 1	LA# 2	LA# 3	LA# 4	LA# 5	LA# 6	LA# 7	LA# 8	LA# 9	LA# 10	LA# 11	LA# 12	LA# 13	LA# 14
Diclofenac Pot		LD# 1	LD# 2	LD# 3	LD# 4	LD# 5	LD# 6	LD# 7	LD# 8	LD# 9	LD# 10	LD# 11	LD# 12	LD# 13	LD# 14
% (w/v)															
Filler	Mannitol	2	----	----	2	----	----	2	----	----	2	----	----	2	----
	Lactose	----	2	----	----	2	----	----	2	----	----	2	----	----	2
	Maltodextrin	----	----	2	----	----	2	----	----	2	----	----	2	----	----
Matrix former	Gelatin	1	1	1	----	----	----	----	----	----	3	3	3	----	----
	HPC	----	----	----	1	1	1	----	----	----	----	----	----	3	3
	Xanthan gum	----	----	----	----	----	----	1	1	1	----	----	----	----	----
Anti-collapse	Glycine	2													

Aceclofenac		LA# 15	LA# 16	LA# 17	LA# 18	LA# 19	LA# 20	LA# 21	LA# 22	LA# 23	LA# 24	LA# 25	LA# 26	LA# 27
Diclofenac Pot		LD# 15	LD# 16	LD# 17	LD# 18	LD# 19	LD# 20	LD# 21	LD# 22	LD# 23	LD# 24	LD# 25	LD# 26	LD# 27
% (w/v)														
Filler	Mannitol	----	2	----	----	2	----	----	2	----	----	2	----	----
	Lactose	----	----	2	----	----	2	----	----	2	----	----	2	----
	Maltodextrin	2	----	----	2	----	----	2	----	----	2	----	----	2
Matrix former	Gelatin	----	----	----	----	5	5	5	----	----	----	----	----	----
	HPC	3	----	----	----	----	----	----	5	5	5	----	----	----
	Xanthan gum	----	3	3	3	----	----	----	----	----	----	5	5	5
Anti-collapse	Glycine	2												

not complain of any adverse effects during the course of the study. No signs of GI disturbances or allergic reactions were observed from any of the volunteers during the study.

Aceclofenac : Significant difference was shown between peak plasma concentration (C_{max}, T_{max}, $t_{1/2}$, K_a, AUC_{0-24} and AUC_{0-}) of Aceclofenac following the administration of the ODT and Bristaflam® tablets (ñ < 0.05); while insignificant difference between their mean residence time ($p = 0.366$). According to the mean plasma levels of 4 subjects completing the study the relative bioavailability (f_{rel}) of the test formula was found to be 186.12% based on the mean (AUC_{0-})

Table 2. Characterization of Aceclofenac freeze dried formulae

Formulae	Friability (%)	Wetting time (Seconds) *	In vitro-Disintegration time (Sec) *	In vivo-Disintegration time (Sec) *	Drug content (%) **
LA #1	4.78%	15 ± 1.34	10 ± 0.68	5 ± 0.64	92.8% ± 1.76
LA #2	10.825	23 ± 0.24	18 ± 0.74	12 ± 0.62	94.5% ± 1.46
LA #3	3.61%	28 ± 0.78	23 ± 1.24	16 ± 0.61	95.9% ± 1.43
LA #4	2.76%	100 ± 0.47	90 ± 0.68	80 ± 0.6	98.17% ± 1.64
LA #5	2.51%	112 ± 0.68	100 ± 0.67	92 ± 0.68	97.02% ± 1.27
LA #6	0.82%	28 ± 0.41	22 ± 1.34	17 ± 0.41	100.4% ± 1.98
LA #7	100%	30 ± 0.73	25 ± 0.24	20 ± 0.73	97.96% ± 3.17
LA #8	100%	37 ± 1.28	32 ± 0.78	27 ± 1.28	98.42% ± 2.35
LA #9	10.83%	46 ± 0.27	41 ± 0.47	36 ± 0.27	95.74% ± 1.40
LA #10	0.7%	112 ± 1.34	100 ± 0.00	88 ± 0.39	92.82% ± 1.46
LA #11	2.61%	200 ± 0.24	180 ± 0.00	160 ± 0.64	94.88% ± 2.68
LA #12	Zero	420 ± 0.78	409 ± 0.00	340 ± 0.62	103.6% ± 1.43
LA #13	0.9%	162 ± 0.47	145 ± 0.68	123 ± 0.61	93.37% ± 2.64
LA #14	0.91%	170 ± 0.41	152 ± 0.72	140 ± 0.6	97.82% ± 1.27
LA #15	0.71%	52 ± 0.73	44 ± 0.64	30 ± 0.68	100.2% ± 1.98
LA #16	23.65%	90 ± 1.28	80 ± 0.62	67 ± 0.41	104.99% ± 3.1
LA #17	20.21%	112 ± 0.27	100 ± 0.61	87 ± 0.73	92.49% ± 2.35
LA #18	5.23%	115 ± 0.39	100 ± 0.6	90 ± 1.28	100.74% ± 1.4
LA #19	Zero	165 ± 0.41	154 ± 0.68	130 ± 0.27	104.8% ± 1.76
LA #20	Zero	184 ± 0.73	175 ± 0.41	152 ± 0.39	92.54% ± 1.46
LA #21	Zero	522 ± 1.28	510 ± 0.73	495 ± 0.64	93.94% ± 1.94
LA #22	Zero	223 ± 0.27	210 ± 1.28	190 ± 0.62	97.76% ± 1.68
LA #23	Zero	234 ± 0.39	225 ± 0.27	210 ± 0.61	92.8% ± 1.75
LA #24	Zero	619 ± 0.41	600 ± 0.39	580 ± 0.6	103.1% ± 1.98
LA #25	Zero	764 ± 9.67	745 ± 8.91	730 ± 7.16	92.11% ± 2.98
LA #26	Zero	893 ± 7.23	755 ± 7.98	742 ± 9.67	94.38% ± 2.98
LA #27	Zero	932 ± 10.3	900 ± 9.79	880 ± 11.88	107.44% ± 2.9

* Data are mean values (n = 6) ± S.D
** Data are mean values (n = 10) ± S.D.

compared to that of the reference standard product.

Diclofenac Potassium : Significant difference was shown between peak plasma concentration (C_{max}, T_{max} *and* K_a) of Diclofenac Potassium following the administration of the ODT and Cataflam® tablets (ñ<0.05); while insignificant difference between their $t_{1/2}$, AUC_{0-12}, AUC_{0-} and mean residence time (p>0.05). According to the mean plasma levels of 4 subjects completing the study the relative bioavailability (f_{rel}) of the test formula was found to be 101.09% based on the mean (AUC_{0-}) compared to that of the reference standard reference.

Conclusion

Based on these results, it can be concluded that the greater bioavailability obtained from Aceclofenac ODT (LA# 10) may be attributed to

Table 3. Characterization of the Diclofenac Potassium freeze dried formulae

Formulae	Friability (%)	Wetting time (Seconds) *	In vitro-Disintegration time (Sec) *	In vivo-Disintegration time (Sec) *	Drug content (%) **
LD #1	0.9%	20 ± 1.34	15 ± 0.71	10 ± 0.68	103.82% ± 2.16
LD #2	1.21%	13 ± 0.24	10 ± 0.68	7 ± 0.81	93.55% ± 1.23
LD #3	0.72%	10 ± 0.78	5 ± 0.34	5 ± 0.73	92.76% ± 1.56
LD #4	100%	15 ± 0.47	10 ± 0.89	6 ± 1.28	94.67% ± 1.64
LD #5	100%	11 ± 1.23	7 ± 0.63	5 ± 1.27	91.28% ± 1.72
LD #6	100%	8 ± 1.34	5 ± 0.69	5 ± 1.39	106.1% ± 1.83
LD #7	10.51%	44 ± 0.24	40 ± 0.74	35 ± 0.64	93.99% ± 2.17
LD #8	10.23%	38 ± 0.78	35 ± 1.44	30 ± 0.62	95.49% ± 2.35
LD #9	7.23%	37 ± 0.47	30 ± 0.92	24 ± 0.68	97.92% ± 1.43
LD #10	Zero	37 ± 1.28	30 ± 0.67	23 ± 0.41	98.82% ± 1.59
LD #11	Zero	28 ± 1.27	23 ± 0.94	18 ± 0.73	93.98% ± 2.38
LD #12	Zero	21 ± 1.39	14 ± 0.52	10 ± 1.28	100.15% ± 2.23
LD #13	100%	19 ± 0.64	15 ± 0.49	10 ± 0.27	92.57% ± 2.24
LD #14	100%	14 ± 0.62	10 ± 0.68	7 ± 0.39	93.19% ± 1.31
LD #15	100%	11 ± 0.68	7 ± 0.63	5 ± 0.64	101.31% ± 1.38
LD #16	Zero	420 ± 0.41	400 ± 0.69	390 ± 0.62	102.67% ± 2.12
LD #17	Zero	410 ± 1.28	390 ± 1.73	374 ± 0.61	92.67% ± 2.12
LD #18	Zero	383 ± 1.27	375 ± 0.68	360 ± 0.68	106.21% ± 1.38
LD #19	Zero	114 ± 1.39	103 ± 0.93	93 ± 0.41	102.04% ± 1.82
LD #20	Zero	93 ± 0.64	82 ± 0.68	74 ± 0.73	93.54% ± 1.83
LD #21	Zero	88 ± 0.62	80 ± 0.49	71 ± 1.28	94.97% ± 1.51
LD #22	1.43%	324 ± 0.68	300 ± 0.63	288 ± 0.27	91.98% ± 1.68
LD #23	Zero	293 ± 0.41	270 ± 0.68	253 ± 0.39	93.98% ± 1.75
LD #24	Zero	276 ± 1.28	260 ± 0.67	244 ± 0.64	101.13% ± 1.34
LD #25	Zero	721 ± 7.76	700 ± 8.91	769 ± 7.16	92.56% ± 2.98
LD #26	Zero	745 ± 8.33	705 ± 7.98	700 ± 9.67	94.88% ± 2.98
LD #27	Zero	749 ± 9.34	710 ± 9.79	694 ± 11.8	102.44% ± 2.98

* Data are mean values (n = 6) ± S.D.
** Data are mean values (n = 10) ± S.D

rapid and efficient absorption of Aceclofenac from buccal mucosa resulting in a decreased pre-systemic transformation due to first pass hepatic extraction or metabolism in the epithelium and/or lumen of GI tract or by combination of these processes. Diclofenac Potassium was detected in plasma in the 5 minutes blood sample after administration of the ODT (LD#11); while it did not appear in plasma until the 15 minutes sampling time after administration of the immediate release tablet. However, based on these previous results, it can be concluded that the high rate of absorption with the same extent of bioavailability that was observed in case of Diclofenac Potassium ODT, may be attributed to rapid absorption and faster elimination of Diclofenac Potassium from the buccal mucosa. We may conclude that the effect of freeze drying ODT technology would have greater impact in improvement of the rate and extent of absorption

Table 4. In-vitro dissolution profile of Aceclofenac freeze dried ODTs formulae

Time	Percentage Aceclofenac dissolved												
(Min)	LA #1	LA #2	LA #3	LA #4	LA #5	LA #6	LA #7	LA # 8	LA # 9	LA # 10	LA # 11	LA # 12	LA # 13
1	78.1	75.55	70.67	18.64	13.22	10.71	9.21	8.18	7.22	79.71	63.04	12.49	7.26
2	90.2	89.24	89.10	22.11	19.99	16.82	12.54	11.01	11.12	92.18	81.53	74.23	10.11
5	91.5	94.63	96.88	30.26	26.18	22.12	21.21	18.24	18.13	100.8	101.1	101.9	12.44
7	100.1	98.92	101.0	37.99	34.81	30.89	29.24	24.98	25.68	100.5	100.7	100.7	17.29
10	100.3	100.2	101.2	43.24	40.71	35.77	34.98	31.77	31.18	100.5	101.5	100.9	25.11
15	100.	100.2	100.5	53.11	49.82	41.94	41.12	38.23	37.24	100.7	101.9	101.1	32.22
30	100.2	100.2	101.0	81.18	78.92	71.01	68.92	67.11	62.29	100.3	101.7	101.0	71.11

Time	Percentage Aceclofenac dissolved												
(Min)	LA # 14	LA # 15	LA # 16	LA # 17	LA # 18	LA # 19	LA # 20	LA # 21	LA # 22	LA # 23	LA # 24	LA # 25	LA # 26	LA # 27
1	5.24	3.31	2.63	2.12	2.01	15.7	12.2	5.23	5.19	4.91	2.81	0	0	0
2	7.12	5.00	5.23	4.11	3.82	51.8	49.2	42.1	5.68	5.21	4.11	0	0	0
5	9.21	7.97	7.12	5.23	5.12	64.8	62.1	54.3	6.23	6.01	5.21	0	0	0
7	12.1	12.7	7.89	5.98	6.23	71.0	69.1	62.0	8.46	7.11	5.48	1.22	0.91	0.87
10	20.8	17.3	8.91	6.91	7.28	75.2	72.8	70.1	11.7	9.22	7.21	2.15	2.01	1.09
15	31.2	27.0	11.2	7.22	9.11	98.3	95.6	95.2	15.4	12.3	10.5	3.77	3.00	2.13
30	68.4	64.3	13.6	10.4	11.2	101.	100.	100	28.8	24.1	19.1	4.91	4.09	4.12

Table 5. In-vitro dissolution profile of Diclofenac Potassium freeze dried ODTs formulae

Time	Percentage Aceclofenac dissolved												
(Min)	LD #1	LD #2	LD #3	LD #4	LD #5	LD #6	LD #7	LD # 8	LD # 9	LD # 10	LD # 11	LD # 12	LD # 13
1	78.1	75.55	70.67	18.64	13.22	10.71	9.21	8.18	7.22	79.71	63.04	12.49	7.26
1	82.98	100.01	58.78	16.42	22.24	23.45	10.84	12.34	12.22	80.08	100.28	34.95	52.00
2	93.78	100.02	78.22	22.56	33.11	34.27	16.54	18.67	17.94	90.17	100.27	52.04	75.32
5	100.01	100.03	99.96	34.18	42.66	43.06	25.21	27.89	26.21	100.01	100.42	68.36	93.96
7	100.03	100.02	100.00	39.89	49.89	48.00	32.24	34.84	35.43	100.01	100.20	76.68	100.05
10	100.07	100.01	100.00	47.74	52.14	51.49	40.98	44.78	46.98	100.00	100.27	91.18	100.00
15	100.02	100.03	100.02	56.88	67.11	66.91	51.92	56.22	55.75	100.02	100.23	100.40	100.03
30	100.08	100.07	100.00	81.93	87.18	86.78	70.88	74.28	73.23	100.02	100.33	101.29	100.00

Time	Percentage Aceclofenac dissolved													
(Min)	LD# 14	LD # 15	LD # 16	LD # 17	LD # 18	LD # 19	LD # 20	LD # 21	LD # 22	LD # 23	LD # 24	LD # 25	LD# 26	LD# 27
1	54.98	36.19	1.39	2.66	3.02	76.75	80.45	50.11	12.18	18.17	6.75	0	0	0
2	77.32	58.32	2.55	4.04	4.45	91.34	92.22	72.44	14.76	28.13	14.76	0	0	0
5	99.96	96.96	3.11	5.81	5.23	95.63	97.54	95.46	31.13	50.98	48.85	1.12	1.09	0.98
7	100.0	100.9	4.88	6.54	6.33	98.92	100.0	100.0	38.08	58.86	57.00	3.21	2.78	1.70
10	100.0	100.7	6.92	7.58	7.00	100.0	100.0	100.0	49.45	79.45	80.07	5.31	3.01	2.31
15	100.0	101.0	7.71	8.71	8.71	100.0	100.0	100.0	68.86	91.22	100.0	6.22	5.55	3.95
30	100.0	100.5	10.01	12.68	10.12	100.0	100.0	100.0	101.1	101.1	100.0	7.33	6.12	5.80

Table 6. The mean pharmacokinetic parameters of Aceclofenac 100 mg ODT (LA# 10) and Bristaflam tablet to four volunteers

Parameter	ODT (LA# 10)	Bristaflam tablet	Statistical test
C_{max} (µg/ml)	7.064 ± 0.178	3.76 ± 0.473	$p = 0.00$
T_{max} (h)	1 ± 0.00	2.875 ± 0.25	$p = 0.00$
$AUC_{(0-24)}$ (µg*h/ml)	38.98 ± 0.53	20.5 ± 0.384	$p = 0.00$
$AUC_{(0-\infty)}$ (µg*h/ml)	39.85 ± 1.18	21.41 ± 0.59	$p = 0.00$
$T_{1/2}$ (h)	6.64 ± 1.11	4.36 ± 0.214	$p = 0.007$
MRT (h)	5.88 ± 0.03	5.76 ± 0.242	$p = 0.366$
K_a (h^{-1})	1	0.345	$p = 0.00$
***Relative Bioavailability (f_{rel})* = 186.12%**			

Data are mean value ± S.D

Table 7. The mean pharmacokinetic parameters of Diclofenac Potassium 50 mg ODT (LD#11) and Cataflam tablet to four volunteers

Parameter	ODT (LD# 11)	Cataflam tablet	Statistical test
C_{max} (µg/ml)	2.5 ± 0.11	2.15 ± 0.044	$p = 0.001$
T_{max} (h)	0.25 ± 0.00	1.25 ± 0.00	$p = 0.00$
$AUC_{(0-12)}$ (µg*h/ml)	8.344 ± 0.352	7.88 ± 0.4	$p = 0.777$
$AUC_{(0-\infty)}$ (µg*h/ml)	9.061 ± 0.61	8.963 ± 0.265	$p = 0.777$
$T_{1/2}$ (h)	4.811 ± 0.57	5.32 ± 1.83	$p = 0.612$
MRT (h)	3.92 ± 0.12	3.86 ± 0.153	$p = 0.581$
K_a (h^{-1})	4	0.8	$p = 0.00$
Relative bioavailability (f_{rel}) = 101.09%			

Data are mean value ± S.D

of the water insoluble drugs than that of the water soluble drugs. Though, freeze drying improved both rates of absorption; however it did not increase the bioavailability of the water soluble drug.

References

1. Lindgren, S. and Janzon, L. (1993). Dysphagia: Prevalence of swallowing complaints and clinical finding. Med Clin North Am., 77: 3-5.
2. Sastry, S.V., Nyshadham, J.R. and Fix, J.A. (2000). Recent technological advances in oral drug delivery: A review. Pharm Sci Technol Today, 3: 138-45.
3. Danckwerts, M.P. (2003). Intraoral Drug Delivery: A Comparative Review. American Journal of Drug Delivery; 1(3): 171-186.
4. Dooley, M., Spencer C.M. and Dunn C.J (2001). Aceclofenac: a reappraisal of its use in the management of pain and rheumatic disease. Drugs, 61: 1351 - 78.
5. Chaudhari P., Chaudhari S. and Kolhe S. (2005). Formulation and evaluation of fast dissolving tablets of famotidine. *Indian Drug*, 42: 641 - 649.

6. Hinz B., Chevts J., Renner B., Wuttke H., Rau T., Schmidt A., Szelenyi I., Brune K. and Werner U. (2005). Bioavailability of Diclofenac potassium at low doses. Br. J. Clin. Pharmacol., 59: 80 - 84.

7. British Pharmacopoeia (2013). Appendix XII G; Uniformity of Weight; Ph. Eur. method (2.9.5).

8. British Pharmacopoeia (2013). Appendix XVII G; Friability of Uncoated Tablets; Ph. Eur. method (2.9.7).

9. British Pharmacopoeia (2013). Appendix XII A; Disintegration Test for Tablets and Capsules; Ph. Eur. method (2.9.1).

10. FDA, Guidance of Industry, Food-effect Bioavailability and Bioequivalence Studies, (2002).

11. Sherimeier, S. and Schmidt, P.C. (2002). Fast dispersible ibuprofen tablets, Eur. J. Pharm. Sci., 15: 295 - 305.

12. Djagny, K.B., Wang, Z. and Xu, S. (2001). Gelatin: a valuable protein for food and pharmaceutical industries, Crit. Rev. Food Sci. Nutr., 41: 481–492.

13. Stella, V.J., Umprayn, K. and Waugh, W.N. (1988). Development of parentral formulations of experimental cytotoxic agents I: Rhizoxin (NSC – 332598). *Int. J. Pharm.,* 43: 191–199.

14. Corveleyn, S. and Remon, J.P. (1996). Maltodextrins as lyoprotectants in the lyophilization of a model protein, LDH. Pharm. Res., 13: 146–150.

15. Muyldermans, G. and Vanhoegaerden, R. (1991). Gelatin maltodextrin interactions and synergies application in 25% low fat spreads. Gums and stabilizers for the food industry, 429–439.

16. Corveleyn, S. and Remon, J.P. (1997). International Journal of Pharmaceutics, 152: 215–225.

17. Windholz, M., Budhavari, S., Stroumtsos, L.Y. and Fertig, M.N. (1976). The Merck Index An Encyclopedia of Chemicals and Drugs, Ninth Edition. Rahway: Merck and Co., Inc.

18. Patel, R., Pillay, V. and Danckwerts, M.P. (2005). Mechanistic Profiling of Novel Wafer Technology Developed for Rate-Modulated Oramucosal Drug Delivery.

19. Ciper, M. and Bodmeier, R. (2005). Preparation and characterization of novel fast disintegrating capsules (Fastcaps) for administration in the oral cavity. *Int. J. Pharm.,* 303: 62–71.

20. Kimura, S., Imai, T. and Otagiri, M. (1991). Evaluation of low molecular weight gelatin as a pharmaceutical additive for rapidly absorbed oral dosage formulations. Chem. Pharm. Bull., 39: 1328–1329.

21. Imai, T., Nishiyama, T., Ueno, M. and Otagiri, M. (1989). Enhancement of the dissolution rates of poorly water-soluble drugs by water soluble gelatin. Chem. Pharm. Bull., 37: 8, 2251–2252.

22. Chono, S., Takeda, E., Seki, T. and Morimoto, K. (2008). Enhancement of the dissolution rate and gastrointestinal absorption of pranlukast as a model poorly water soluble drug by grinding with gelatin. Int. J. Pharm., 347: 71–78.

23. Allen, L.V., Levinson, R.S. and Martono, D.D. (1978). Dissolution rates of hydrocortisone and prednisone utilizing sugar solid dispersion systems in tablet form, J. Pharm. Sci., 67: 979-981.

Current Trends in Biotechnology and Pharmacy
Vol. 7 (4) 904-913 October 2013, ISSN 0973-8916 (Print), 2230-7303 (Online)

Enhancement of Japanese Encephalitis Virus DNA vaccine efficacy by using *Mycobacterium avium paratuberculosis* heat shock protein 65

Pallichera Vijayan Shahana[1, 2], Dipankar Das[1], Abhinay Gontu[1], Munish Kumar Durshetty[1], Sudhakar Podha[2] and Lingala Rajendra[1*]

[1]Indian Immunologicals Limited, Rakshapuram, Gachibowli, Hyderabad, Andhra Pradesh, India.5000032.

[2]Department of Biotechnology, Acharya Nagarjuna University, Nagarjunanagar, Guntur, Andhra Pradesh, India. 522510

*For Correspondence - rlingala2005@gmail.com

Abstract

Japanese Encephalitis (JE) is a mosquito borne arboviral infection caused by Japanese Encephalitis Virus (JEV). It is the major cause of viral encephalitis in Asia and a leading cause of pediatric epidemic in India. In the present study we have developed a DNA vaccine with JEV Envelope protein (E) in cytomegalovirus (CMV) promoter based vector. The efficacy of the DNA vaccine is evaluated by the use of heat shock protein 65 (HSP65) of *Mycobacterium avium paratuberculosis* (MAP), which is a potential molecular adjuvant. The efficacy of the vaccine in combination with the HSP65 is evaluated by plaque reduction neutralization test (PRNT). The adjuvant effect of HSP65 was analyzed both as a protein and a DNA when coimmunized in mice with JEV E DNA vaccine. The present study demonstrated that the efficacy of the JEV E DNA vaccine is enhanced in combination with HSP65 protein.

Keywords: Japanese Encephalitis Virus, DNA vaccine, Adjuvant, *Mycobacterium avium paratuberculosis*, heat shock protein 65

Introduction

Japanese Encephalitis (JE) is a mosquito borne arboviral infection caused by Japanese Encephalitis Virus (JEV) (1). It is the leading cause of viral encephalitis in Asia, causing approximately 50,000 deaths annually in JEV epidemic countries like Japan, China, Korea and Taiwan (2). In India the first clinically recorded case of JE was in 1955 at Vellore, Tamil Nadu (3) and has been followed by several reports of outbreaks including the outbreak in 2005 that killed 1700 people mostly children and left thousands more disabled (4). There is no specific treatment for JE and the available treatment is only supportive (5). Vaccines till date remain the best option in preventing the disease. The mouse brain derived inactivated purified vaccine, which was in use for many years is replaced by cell cultured vaccines. Recombinant, sub-unit vaccines provide new options for endemic countries like India because of their improved safety.

JEV is a spherical virion approximately 50 nm in diameter encapsidating a non segmented positive sense RNA genome (6). The RNA comprises of a single open reading frame capped by a 5'UTR 95 bp long and a 3'UTR 580 bp long (7). The viral RNA encodes a single polyprotein cleaved by viral and cellular proteases to produce three structural (capsid, C; membrane, M; and envelope, E), and seven nonstructural (NS1, NS2A, NS2B, NS3, NS4A, NS4B, and NS5) proteins. The E protein is associated with the

induction of protective neutralizing antibody response in hosts and hence, is the principal target for neutralization *in vitro* and *in vivo* by specific antibodies (8).

In the present study, we have attempted to develop a DNA vaccine for JE as DNA vaccinations are safer and cheaper to produce (9). DNA immunizations trigger the *de novo* synthesis of the antigens in the host cells and are able to elicit protective immune response in various animal models (10). The plasmid DNAs are internalized by antigen presenting cells and can induce antigen presentation via MHC class I or class II (11). Structural proteins like E (12), prM and E (13) and non-structural proteins like NS1 (14), NS3 (15) and NS5 (15) have been evaluated as potent DNA vaccines for their ability to induce neutralizing antibody response and for their ability to protect the animals in challenge experiments. Literature reports suggest that E protein alone is not sufficient to generate the neutralizing antibodies in mice (12). Hence we tried to use a heat shock protein (HSP) which might act as an adjuvant and elicit good immune response. The administration of the adjuvant can be either as an immunostimulatory gene or as protein as shown in many *Mycobacterium tuberculosis* genes (16). Here, we used the *Mycobacterium avium paratuberculosis* (*MAP*) HSP65 and evaluated its potential as a molecular adjuvant. The efficacy of the JEV E DNA vaccine was evaluated individually and in combination with HSP65 both as a protein as well as DNA.

Materials and Methods

RNAeasy extraction kit, one-step RT PCR kit, PCR purification kit, gel extraction kit, plasmid isolation kits (Mini and Maxi) and Ni-NTA agarose resin were all procured from Qiagen, Germany. The six well tissue culture plates and 96 well maxisorp plates were procured form Nunc, USA. The restriction enzymes and T4 DNA ligases were from NEB, UK. The lipofectamine reagent is from Invitrogen, USA. The XL Gold competent cells were purchased from Strategene and BL21 pLysS competent cells were purchased from Novogen, USA. HRP-conjugate, TMB substrate and His-Tag antibody were purchased from Sigma, USA. MEM, FBS and penicillin-streptomycin-glutamine mix were purchased from GIBCO-Life Technologies, USA. Luria Bertani media, agar, agarose, tryptone, yeast extract were purchased from Himedia. Urea, sodium chloride, sodium di hydrogen phosphate and disodium hydrogen phosphate were purchased from Merck. Tris, EDTA and imidazole were from Sigma, USA. Skim milk powder was from Difco BD lifesciences, Tween-20 from Calbiochem and Triton X -100 from Fluka.

Virus: Beijing – 1 strain of JEV (CDC, Taiwan) was used in the present study. Vero cells (African green monkey kidney epithelial cells) from ATCC were used to grow the virus. Cells were grown in MEM, supplemented with 10% fetal bovine serum (FBS). The culture supernatant from JEV infected cells was collected after 48 hrs infection when the cytopathic effect (CPE) was visible. These supernatants were stored in aliquots at -70°C. This was used as the source of virus for cDNA synthesis and ELISA experiments. Virus titration was done by plaque assay (17).

Construction of the plasmid : Two DNA vaccine vectors were generated with JEV Env (E) gene and the other with *MAP* hsp 65 in a CMV promoter based vector (18). JEV E gene was PCR amplified from the virus Beijing-1 strain (Acc. No. L489611) using gene specific primers (Table 1: FP MB 308, RP MB 309). PCR amplified cDNA was cloned into a eukaryotic expression vector and named as pCMVE. It has a cytomegalovirus immediate early promoter/ enhancer sequence, multiple cloning sites, bovine growth hormone termination signal, colE1 replication signal and a kanamycin resistance gene. The MAP hsp 65 gene is a mammalian codon optimized synthetic gene from Geneart (Germany). The synthetic gene was PCR amplified with specific restriction site with gene specific primers (Table 1: FP MB 419, RP MB 420) and cloned in the same eukaryotic expression vector and named as pCMVhsp65. Alternatively, JEV E gene was also synthesized

as a synthetic gene optimized for expression in bacteria from Geneart and was cloned into pRSETA vector and named as pRSETAEnv. The MAP hsp 65 gene was also synthesized synthetically and optimized for expression in bacterial expression systems. It was also cloned into pRSETA vector and named as pRSETAhsp65.

Expression of pCMVE and pCMVhsp65 in Vero cells: Vero cells were seeded in 6 well plates ($4x10^5$ cells/well) and once the plates reached ~90% confluencey, they were transfected with both pCMVE and pCMVhsp65 plasmids using lipofectamine reagent as per the manufacturer's instructions. The transfected cells were harvested 48 hrs post-transfection and lysed in lysis buffer 1 (50 mM Tris, 150 mM NaCl, 2 mM EDTA, 1% Triton X-100, pH 7.5). The lysates were centrifuged at 10,000xg for 10 min to clarify and supernatant was inactivated at 56°C in water bath for 1 hr. Samples were then analyzed on a SDS-PAGE using 12% gel and western blotting was performed using known JEV-positive serum .

Expression and purification of Env and HSP65 proteins in E. coli: The recombinant pRSETAEnv and pRSETAhsp65 plasmids were transformed in BL21 pLysS competent cells by heat shock method. The expression of the clones were optimized with TB medium with 1mM IPTG and 4 hrs induction periods at 30°C and analyzed on 12% SDS-PAGE. The expression of the protein was confirmed by western blot probed with the His_6 tag antibody (data not shown). The clones were grown in a 2 liter culture in terrific broth (TB) media and induced with IPTG as mentioned above. The bacterial pellets were analyzed for the localization of the protein and both Env and HSP65 were found to be in the inclusion bodies. The recombinant proteins were purified from inclusion bodies using Ni-NTA agarose column under denaturing condition. The bacterial pellets were resuspended in lysis buffer 2 (50 mM sodium phosphate buffer, 100 mM NaCl, 5 mM EDTA, 1% Triton X 100 at pH 7.5). The resuspended cell pellet was subjected to sonication (Sonics Vibracell, USA) 40% amplitude with 5.5/5.5 pulse rate. The lysed samples were centrifuged at 10,000xg for 30 minutes and the supernatant was discarded. The pellet was resuspended in equilibration buffer (50 mM sodium phosphate buffer and 8M urea, pH 7.5). This sample was passed onto a pre equilibrated Ni-NTA column. Then the column was washed with wash buffer (50 mM sodium phosphate buffer, 8M urea, 30 mM imidazole, pH 7.5) and eluted with elution buffer (50 mM sodium phosphate buffer, 8M urea, 300 mM imidazole, pH 7.5). The eluants were analyzed on SDS-PAGE to check its purity and confirmed by western blot developed with His_6 tag antibody. The pooled eluants were subjected to dialysis (50 mM sodium phosphate buffer, pH 7.5) to remove urea and imidazole. These dialyzed proteins (Figure 2) were used in ELISA for evaluation of humoral response in mice immunized with DNA vaccines. (Table 2 for buffers used in the study)

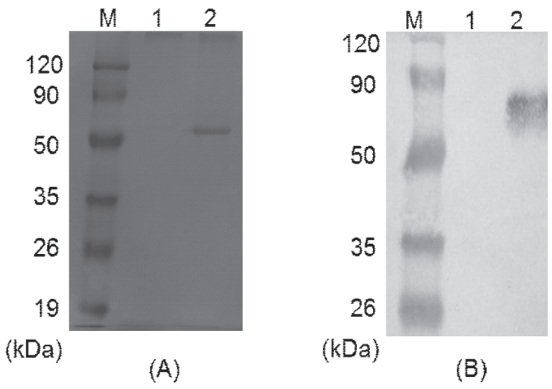

Fig. 1. Western blots on 12% SDS-PAGE showing transient expression of pCMVE and pCMVhsp65 in Vero cells. **(A)** Lane M: standard protein molecular weight marker, Lane 1: vero cell lysate, Lane 2: pCMVE transfected vero cell lysate. Western blot probed with known JEV polyclonal serum. **(B)** Lane M: standard protein molecular weight marker. Lane 1: vero cell lysate, Lane 2: pCMVhsp65 transfected cell lysate. Western blot probed with polyclonal sera raised against HSP65 antigen.

Vol. 7 (4) 904-913 October 2013, ISSN 0973-8916 (Print), 2230-7303 (Online)

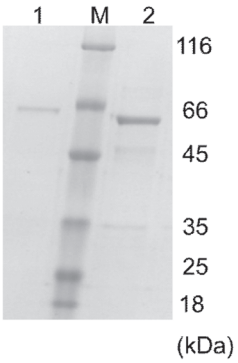

Fig. 2. 12% SDS-PAGE of the purified Env and HSP65 proteins from *E. coli.* Lane 1: HSP65 protein, Lane 2: Env protein. Lane M: standard protein molecular weight markers.

***Mice immunizations**:* All immunizations were carried out in 2-3 week old BALB/c mice divided into 9 groups with 10 mice in each group (Table 3). Three groups received DNA vaccines pCMVE, pCMVhsp65 and a negative control group pCMV vector. Twenty µg of each plasmid in 10 mM Tris-Cl was injected intramuscularly into the right quadriceps muscle of the mice. Groups 4 and 5 received the purified Env and HSP65 proteins injected intramuscularly at 20 µg per mice. Group 6 mice were injected with both DNA vaccine plasmids (pCMVE and pCMVhsp65) simultaneously and group 7 with pCMVE and HSP65 protein. Commercially available JEEV vaccine ® (Biological E) was administered with 1/10th of the recommended adult dose as positive control and unvaccinated mice were treated as the negative control. After the primary immunization a booster dose was given at an interval of 3 weeks. One week after the booster the mice were bled thoroughly and sacrificed. The serum from these samples was used for ELISA and PRNT study.

***ELISAs**:* The ELISA was done to evaluate the presence of the specific antibodies in the serum sample for which the first two ELISAs were performed by coating the plate with purified Env protein and HSP65 protein. The third ELISA was performed to evaluate the specificity of the vaccine candidates. All the mice serum samples were inactivated at 56°C for 30 minutes and then used for ELISA experiments.

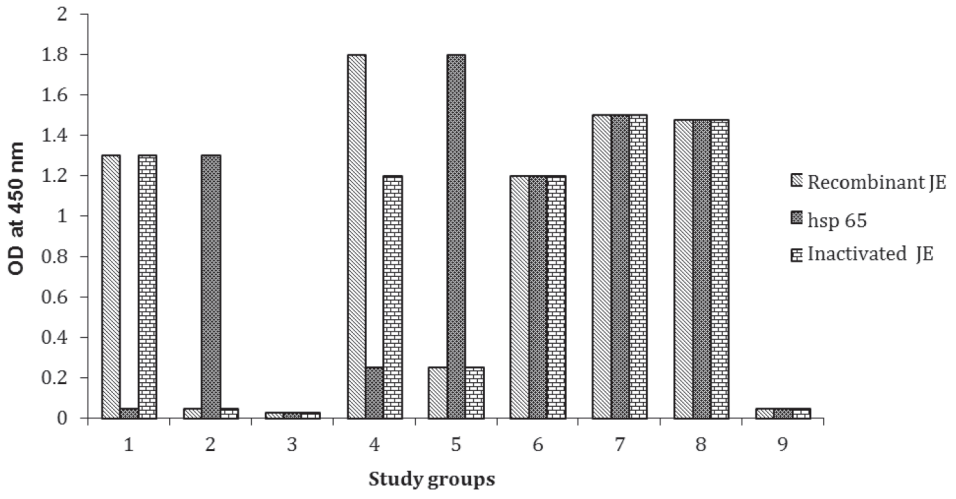

Fig. 3. Reactivity of the serum samples from different study groups vaccinated with different regimens of JE DNA vaccine and HSP65 tested by indirect ELISA. The study groups were vaccinated with: (1) JEV DNA vaccine – pCMVE, (2) HSP65 DNA vaccine - pCMVhsp65, (3) DNA vaccine vector – pCMV, (4) Purified JEV Envelope protein – Env, (5) Purified HSP65 protein - HSP65 antigen, (6) JE DNA vaccine with HSP65 DNA vaccine - pCMVE+pCMVhsp65, (7) JE DNA vaccine with purified HSP65 protein - pCMVE + HSP65, (8) Commercial vaccine – JEEV, (9) Unvaccinated mice - control group.

Table 1. List of primers used

Primer No.	Primer sequence	Purpose
MB 308	ATCGAGATCTTTCAACTGTCTGGGA	Forward primer for JEV DNA vaccine
MB 309	ATCGAGATCTAGCATGCACATTGGTTAA	Reverse primer for JEV DNA vaccine
MB 419	ACGCAGATCTATGGCGAAAACCATT	Forward primer for hsp65 DNA vaccine
MB 420	ACGCAGATCTTTATTAAAAATCCAT	Reverse primer for hsp65 DNA vaccine

Table 2. List of buffers used

S.No.	Buffer name	Buffer composition
1.	Lysis buffer 1	50 mM Tris, 150 mM NaCl, 2 mM EDTA, 1% Triton X-100, pH 7.5
2.	Lysis buffer 2	50 mM sodium phosphate, 100 mM NaCl, 5 mM EDTA, 1% Triton X 100 at pH 7.5
3.	Equilibration buffer	50 mM sodium phosphate and 8M urea, pH 7.5
4.	Wash buffer	50 mM sodium phosphate , 8M urea, 30 mM imidazole, pH 7.5
5.	Elution buffer	50 mM sodium phosphate, 8M urea, 300 mM imidazole, pH 7.5
6.	Dialysis buffer	50 mM sodium phosphate , pH 7.5

To check for JEV Env antibodies: An indirect ELISA format was applied to check for the presence of antibodies against JEV Env protein in the mice sera. The microtiter plate wells were coated (Maxisorp) with 100 µl (500 ng) of the Env antigen in carbonate bicarbonate buffer pH 9.6 per well and incubated overnight at 4°C. Plates were washed thrice with washing buffer (0.1% PBST i.e. PBS +0.1% Tween 20). Then the plates were blocked with 200 µl of blocking buffer 3% (w/v) skim milk in PBST for 1 hr. Plates were washed thrice with washing buffer. The pCMVE, pCMVhsp65, pCMV, Env, HSP65, pCMVE+pCMVhsp65, pCMVE+HSP65 , JEEV and unvaccinated mice serum were diluted in 0.1% PBST at 1: 500 ratio and 100 µl of serum was added to respective wells. The plate was incubated at 37°C for 1 hr followed by three washes with 0.1% PBST. Horseradish peroxidase (HRP)-conjugated goat anti-mouse IgG was diluted 1:5000 in PBS and 100 µl of this secondary antibody was added to wells and incubated for another 1 hr. Following three washes with 0.1% PBST, 100 µl of TMB substrate (1 mg tablet in 10 ml of citrate buffer pH 5.4 and 10 µl H_2O_2) was added to each well and incubated in dark for 10 minutes. The peroxidase reaction was stopped by adding 100 µl of 1 M H_2SO_4 and absorbance values at 450 nm were determined using a plate reader (Spectra Max 190, Molecular Devices, and USA).

To check for MAP HSP65 antibodies: An indirect ELISA format was applied to check for the presence of MAP HSP65 antibodies in the mice sera. The microtiter plate wells were coated (Maxisorp, NUNC) with 100 µl (500 ng) of the HSP65 antigen in carbonate bicarbonate buffer pH 9.6 per well overnight at 4°C. The remaining procedure is same as the first ELISA format.

To check for JEV specificity: An indirect ELISA format was applied to check for the presence of JEV antibodies in the mice sera. The microtiter plate wells were coated (Maxisorp) with 100 µl (500 ng) of the inactivated JEV virus in carbonate bicarbonate buffer pH 9.6 per well overnight at

4°C. The remaining procedure is same as the first ELISA format.

Plaque Reduction Neutralization Test (PRNT): The mice serum samples obtained by the above mentioned immunization schedule were heat inactivated at 56°C for 30 minutes. Vero cells were seeded onto required number of 6 well plates a day before the test (5 X 10^5 cells/well). Virus (suckling mouse passaged Beijing -1 challenge virus strain) was diluted in the virus maintenance media (HMEM with 2 % serum and 1 % penicillin-streptomycin-glutamine) in order to get 50 plaque forming unit (pfu) per well. The heat inactivated sera samples were 2 fold diluted in the virus maintenance media. The virus and serum samples were mixed in equal volumes and incubated for 90 minutes at 37°C with intermediate shaking. The spent media was then discarded from the confluent vero cells and the antigen antibody mix (200 µl) was added to the corresponding wells. After 90 minutes 2 ml of 1% methyl cellulose was overlaid. The plates were incubated for 96 hrs at 37°C in a CO_2 incubator. The methyl cellulose overlay was carefully discarded and the plates are stained with crystal violet. Plaque reduction (50%) when compared to the virus inoculated wells was counted. $PRNT_{50}$ has been calculated as per the standard protocol (19). The neutralizing antibody titer was expressed as the reciprocal of the highest initial serum dilution that inhibited 50% or greater of the plaque formation compared with the virus control titration.

Results

Constructions of recombinant plasmids: The Env and HSP65 genes were cloned into pCMV vector downstream of the immediate early promoter enhancer sequences of cytomegalovirus. The PCR amplified JEV E cloned into pCMV vector showed a release of 1550 bps when digested with BglII. Similarly, the pCMVhsp65 showed a release of 1640 bps when digested with BglII on agarose gel. The restriction digestion analysis of pRSETAEnv and pRSETAhsp65 with BamHI and HindIII showed a release of Env 1550 bps and HSP65 1640 bps respectively (data not shown). Both the clones were analyzed by DNA sequence analysis.

Expression of DNA vaccines in vero cells : Vero cells were transfected with DNA vaccine plasmids pCMVE and pCMVhsp65. After 24 hrs of transfection, same number of cells (control and transfected cells) was analyzed for transient expression**.** Western blot probed with JEV Env and MAP HSP65 polyclonal serum showing a band size of 58 kDa and 60 kDa, respectively on the blot (Figure 1A, B). No visible band was observed in the lane of control (non transfected) cell lysate indicating the absence of Env and HSP65 protein in the sample.

Purification of the E.coli expressed proteins: The Ni-NTA agarose column purified proteins were analyzed on SDS-PAGE for their purity and western blot probed with His_6-Tag antibody for their specificity. The purified eluants were pooled and dialyzed. The dialyzed protein analyzed on SDS-PAGE and showed the correct sized band at 58 kDa and 60 kDa respectively for Env and HSP65 proteins (Figure 2). The purified proteins concentration was estimated using standard protocol by BCA (Bicinchoninic acid) method. The final protein preparation was ~80% pure which were used for animal experiment, PRNT and ELISA.

ELISA: The first ELISA was carried out to verify for the presence of JE specific antibodies in different groups of mice. High titers were observed in group of mice immunized with JEV Env antigen. Antibody titers were also shown by the pCMVE, pCMVE+pCMVhsp65 and pCMVE+HSP65 groups which validates the efficacy of DNA vaccine to generate antibodies against Env protein. The pCMVhsp65, HSP65 and unvaccinated mice groups did not show titers specific to Env. These results indicate that the pCMVE DNA vaccine antibody titer was elicited with pCMVhsp65 and HSP65 and the adjuvant effect of MAP HSP65 is evident with the high titers in pCMVE+pCMVhsp65 and pCMVE+ HSP65 groups.

The second ELISA was carried out to verify the presence of MAP HSP65 antibodies in different groups of mice. High titers were observed in HSP65 and pCMVhsp65 group mice. Where the antigen was used in combination as a protein or DNA respectively. i.e. the pCMVE+HSP65 and pCMVE+pCMVhsp65 groups showed next level titers and the rest of the groups did not show any significant titers as expected.

The third ELISA was carried out to verify the specificity of the inactivated virus in binding to serum of various groups. The pCMVE, Env, pCMVE+pCMVhsp65 and pCMVE+HSP65 groups showed good titers and the rest groups did not show any significant titers. Of these the JEEV vaccinated group served as the positive control group and the unvaccinated group served as the negative control group. pCMVE+HSP65 followed by pCMVE+pCMVhsp65 showed the next high titers followed by the pCMVE group. These results suggest that pCMVE+HSP65 group is able to elicit immune response on par with the commercial JEEV vaccine. The adjuvant effect of the MAP HSP65 was clearly demonstrated in this study. These findings clearly indicate that the DNA vaccine may be a potential vaccine candidate for JEV and its immune response is increased with the use of MAP HSP65 (Figure 3).

PRNT: Serum samples collected on day 35 after the primary and booster immunizations were evaluated for the ability to neutralize JEV in $PRNT_{50}$. A titer above 10 in $PRNT_{50}$ is indicated as a positive result (19). As shown in Table 3 the pCMVE group which is the DNA vaccine group without the adjuvant showed a titer of 20 which is a positive titer and pCMVhsp65 and the pCMV vector group which are the negative control groups showed titers less than 10. The Env group showed a titer of 10 and HSP65 group showed a titre of <10. The group 6 mice which were immunized with pCMVE and pCMVhsp65 simultaneously showed a titer of 35 and the group 7 mice which were immunized with pCMVE and HSP65 simultaneously showed a titer of 40. These results confirm the adjuvant role of MAP *HSP65* supplemented either in the form of protein or DNA. These titers are on par with the commercial JEEV group mice which also showed a titer of 40. Neutralizing antibodies generated by the unvaccinated control group mice is negligible. (Table 3).

Table 3. Animal groups and PRNT titers

Group No	Group Name	PRNT titer
1	pCMVE	20
2	pCMVhsp65	<10
3	pCMV	<10
4	Env	10
5	HSP65	<10
6	pCMVE+pCMVhsp65	35
7	pCMVE+HSP65	40
8	JEEV	40
9	Unvaccinated	<10

Discussion

JEV is the etiological agent for Japanese encephalitis, a disease with high mortality and high disability rate in children. Currently, vaccination remains the only strategy for protection. The first generation JE vaccines i.e. live attenuated mouse brain derived vaccine and the latest cell culture inactivated vaccines have been widely used with significant success in many Asian countries (20). The mouse brain derived JE vaccines are being completely replaced by the cell culture inactivated vaccines due to the adverse side effects of the former vaccine. But the cell cultured vaccines too have a lot of disadvantages like high production costs, poor long-term immunity, and the possible induction of allergic reactions to the vaccines (21). In this scenario a second generation subunit vaccine which could generate strong immune response will be a good alternative.

Alternative vaccine platforms such as peptide vaccine, VLP and DNA vaccines have been successfully developed, aided by the rapid growth in the field of molecular biology and immunology (22, 23). In the DNA vaccine approach instead of delivering a protein or peptide to the host, an expression vector

encoding the protein or its fragment is administered. This vector produces the protein *in vivo* subsequently. DNA vaccines have few advantages over the others in terms of safety (24), ease of design, chemical synthesis, and suitability for large scale production and are cost effective. Key to the immunogenicity of DNA vaccines is the presentation of expressed antigen to antigen presenting cells (APCs). DNA vaccines in general require an effective adjuvant to improve its expression *in vivo* (25) and for the presentation of the antigens to APCs. Developing an effective molecular adjuvant with deeper understanding of apoptosis, APC function and immune cell activation is of high importance (26). The licensure of the first DNA vaccine for Equine West Nile Virus by US Department of Agriculture in 2006 (27) has given a tremendous boost in the development of DNA vaccines for many infectious diseases.

In the present study we attempted to develop a DNA vaccine for JE. Both structural proteins like E (12) prM and E (28) and non-structural proteins like NS1 (29), NS3 (15) and NS5 (15) have been evaluated as potent DNA vaccines for their ability to induce neutralizing antibody response and for their ability to protect the animals in challenge experiments. Studies suggest that Env protein alone is not sufficient to generate the neutralizing antibodies in mice (12). The role of *Mycobacterium tuberculosis* (MTB) specific HSPs in vaccine development has been well characterized (30). We tried to use a HSP of *Mycobacterium avium paratuberculosis* (*MAP*) which might act as an adjuvant and improve the immune response. Various heat shock proteins, chaperones and synthetic peptides have been reported to cross prime with antigenic peptides (31, 32) and the role of HSPs in the regulation of immune response especially in the vaccines is well characterized (33). Here we used the *Mycobacterium avium paratuberculosis* HSP65 and evaluated its potential as a molecular adjuvant.

The role of MAP HSP65 as a potent adjuvant both as a protein as well as a DNA vaccine has been evaluated in the present study. The MAP hsp65 gene was cloned into pCMV vector to obtain pCMVhsp65 and used it in combination with pCMVE. The purified MAP HSP65 protein expressed bacterially i.e. HSP65 antigen was also co-immunized with pCMVE construct. The expression of pCMVE and pCMVhsp65 was initially confirmed by their transient expression in vero cell line on western blot. The mice were immunized with two doses of the vaccine with an interval of three weeks and the blood samples were collected 1 week after the booster. The serum samples were evaluated using ELISAs to check for the presence of specific antibodies and PRNT to check for the generation of the neutralizing antibodies.

The ELISA experiments were carried out to confirm the presence of the JEV Env specific and MAP HSP65 specific antibodies in the different groups of mice serum. The pCMVE, pCMVE+pCMVhsp65 and pCMVE+HSP65 mice serum generated the JE specific antibodies. The JEEV serum also exhibited good antibody titers. The HSP65, pCMVhsp65, pCMVE+pCMVhsp65 and pCMVE+HSP65 mice serum generated MAP HSP65 specific antibodies. In the next evaluation with the inactivated JEV, JEEV sera displayed highest titers followed by pCMVE+HSP65, pCMVE+pCMVhsp65 and pCMVE sera. These results demonstrated that MAP HSP65 acted as a good adjuvant.

The $PRNT_{50}$ titers also corroborate the above observations. The JEEV sera generated a titer of 40 which is similar to that of pCMVE+HSP65 group and pCMVE+pCM Vhsp65 group which showed a titer of 35. pCMVE alone showed a titer of 20 which was increased with the MAP HSP65 to 35 and 40 respectively in pCMVE+pCMVhsp65 and pCMVE+HSP65 groups. These results showed that the efficiency of JE vaccine may be improved with the use adjuvants like MAP HSP65 protein. This is the first report where MAP HSP65 has been used as an adjuvant for a JEV DNA vaccine. These results need to be validated with challenge

experiments to confirm its further efficacy. Nevertheless, the results are encouraging to use MAP HSP65 as an adjuvant with JEV DNA vaccine.

Acknowledgement

We would like to thank Dr P. N. Rangarajan, (IISc, Bangalore) for gifting us with the pCMV vector which is used in the present study to generate DNA vaccine constructs. .

References

1. Halstead, S.B. and Jacobson, J. (2003). Japanese encephalitis. Adv Virus Res. 61, 103-138.
2. Tsai, T. F. (2000). New initiatives for the control of Japanese encephalitis by vaccination: minutes of a W. H. O. /CVI meeting, Bangkok, Thailand, Vaccine. 18 (Suppl. 2), 1-25.
3. Namachivayam, V. and Umayal, K. (1982). Proceedings of National Conference on Japanese Encephalitis. Indian Council of Medical Research, New Delhi. 30-33.
4. Saxena, S.K., Mishra, N., Saxena, R., Singh, M., and Mathur, A. (2009). Trend of Japanese encephalitis in North India: evidence from thirty-eight acute encephalitis cases and appraisal of niceties. J Infect Dev Countries. 3 (Suppl. 7), 517-530.
5. Solomon, T., Ni, H., Beasley, D. W. C. Ekkelenkamp, M., Cardosa, M. J. and Barrett, A. D. T. (2003). Origin and evolution of Japanese encephalitis virus in Southeast Asia. Journal of Virology. 77, 3091-3098.
6. Lindenbach, B., Thiel, H. and Rice, C. (2007). Flavivirus: the virus and their replication. In: Fields Virology, 1101-52, Lippincott Williams & Wilkins, Philadelphia, USA.
7. Harisankar, H.S., Baldev, R., Gulati, B.R., Prabhat, P.K., Birendra, K., Singh, B.K., Virmani, N.N. and Raj, K.S. (2013). Complete genome sequence analysis of Japanese encephalitis virus isolated from a horse in India. Arch Virol. 158(Suppl. 1), 113-122.
8. Verma, S.K., Gupta, N., Pattnaik, P., Babu, J.P., Rao, P.V. and Kumar, S. (2009). Antibodies against refolded recombinant envelope protein (domain III) of Japanese encephalitis virus inhibit the JEV infection to Porcine Stable Kidney cells. Protein Pept Lett. 16(Suppl. 11), 1334-1341.
9. Liu, M.A. (2003). DNA vaccines: a review. J Intern Med. 253 (Suppl. 4), 402–410.
10. Wayne, C.L. and Michael,B. (1998). DNA Vaccine. Crit Rev Immunol. 18, 449-484.
11. Alekseeva, E., Sominskaya, I., Skrastina, D., Egorova, I., Starodubova, I., Kushners, E., Mihailova, M., Petrakova, N., Bruvere, R., Kozlovskaya, T., Isaguliants, M. and Pumpens. P. (2009). Enhancement of the expression of HCV core gene does not enhance core-specific immune response in DNA immunization: advantages of the heterologous DNA prime, protein boost immunization regiment. Genetic Vaccines and Therapy. 7,7.
12. Ashok, M.S. and Rangarajan, P.N. (1999). Immunization with plasmid DNA encoding the envelope glycoprotein of Japanese Encephalitis virus confers significant protection against intra-cerebral viral challenge without inducing detectable antiviral antibodies. Vaccine. 18(1-2), 68-75.
13. Kaur, R., Sachdeva, G. and Vrati, S. (2002). Plasmid DNA immunization against Japanese encephalitis virus: immunogenicity of membrane-anchored and secretory envelope protein. J Infect Dis. 185(Suppl 1),1–12.
14. Lin, Y.L., Chen, L.K., Liao, C.L., Yeh, C.T., Ma, S.H. and Chen, J.L. (1998). DNA immunization with Japanese encephalitis virus nonstructural protein NS1 elicits protective immunity in mice. J Virol. 72(Suppl 1), 191–200.

15. Chen, H.W., Pan, C.H., Liau, M.Y., Jou, R., Tsai, C.J., Wu, H.J., Lin, Y.L. and Tao M.H. (1999). Screening of protective antigens of Japanese encephalitis virus by DNA immunization: a comparative study with conventional viral vaccines. J Virol. 73 (Suppl 12, 10137-10145.

16. Hsu, K.F., Hung, C.F., Cheng, W.F., He, L., Slater, L.A., Ling, M. and Wu, T.C. (2001). Enhancement of suicidal DNA vaccine potency by linking Mycobacterium tuberculosis heat shock protein 70 to an antigen. Gene Ther. 8, 376-83.

17. Mullbacher, A., Lobigs, M. and Lee, E. (2003). Immunobiology of mosquito-borne encephalitic flaviviruses. Adv Virus Res. 60, 87–120.

18. Biswas, S., Ashok, M.S., Reddy, G.S., Srinivasan, V.A. and Rangarajan. P.N. (1999). Evaluation of the protective efficacy of a rabies DNA vaccine in mice using an intracerebral challenge model. Current Science. 76, 1012-1016

19. Hombach, J., Barrett, A. D. T., Cardosa, M. J., Deubel, V., Guzman, M., Kurane, I., Roehrig, J. T., Sabchareon, A. and Kieny, M. P. (2005). Review on flavivirus vaccine development. Vaccine. 23, 2689–2695.

20. Asha, M. and Vrati, S. (2000). Mov34 protein from the mouse brain interacts with the noncoding region of Japanese encephalitis virus. J Virol. 74, 5108–5115.

21. Tsai, T.F., Chang, G.F. and Yu, Y.X., (1999). Japanese encephalitis vaccines. In: Stanley, A.P.,Oreustein, W.A. (Eds.), Vaccines. 672-710.

22. Lacasse, P., Denis, J., Lapointe, R., Leclerc, D. and Lamarre, A. (2008). Novel Plant Virus-Based Vaccine Induces Protective Cytotoxic T-ymphocyte-Mediated Antiviral Immunity through Dendritic Cell Maturation. J Virol 82,785–794.

23. Beard, C.W. and Mason P.W. (1998). Out on the farm with DNA vaccines. Nat. Biotechnol. 16 (13), 1325–1328.

24. Petrovsky, N. and Aguilar, J.C. (2004). Vaccine adjuvants: current state and future trends. Immunol. Cell Biol. 82, 488–496.

25. Moss, R.B. (2009). Prospects for control of emerging infectious diseases with plasmid DNA Vaccines. Journal of Immune Based Therapies and Vaccines. 7, 3.

26. Leitner, W.W. and Restifo, N. P. (2003) DNA vaccines and apoptosis: to kill or not to kill? J. Clin. Invest. 112, 22–24.

27. Petersen, L.R. and Roehrig, J. T. (2007). Flavivirus DNA Vaccines—Good Science, Uncertain Future. The Journal of Infectious Diseases. 196, 1721–1723.

28. Kaur, R., Sachdeva, G. and Vrati, S. (2002). Plasmid DNA immunization against Japanese encephalitis virus: immunogenicity of membrane-anchored and secretory envelope protein. J Infect Dis. 185(1),1–12.

29. Lin, Y.L., Chen, L.K., Liao, C.L., Yeh, C.T., Ma S.H. and Chen, J.L. (1998). DNA immunization with Japanese encephalitis virus nonstructural protein NS1 elicits protective immunity in mice. J Virol. 72(1), 191–200.

30. Robert, J. (2003). Evolution of heat shock protein and immunity. Dev. Comp. Immunol. 27, 449–464.

31. Qazi K.R., Wikman, M., Vasconcelos, N.M., Berzins, K., Stahl, S. and Fernandez, C. (2005). Enhancement of DNA vaccine potency by linkage of Plasmodium falciparum malarial antigen gene fused with a fragment of HSP70 gene. Vaccine 23, 1114-1125.

32. Quintana. F. J. and Cohen, I.R. (2005). DNA vaccines coding for heat-shock proteins (HSPs): tools for the activation of HSP-specific regulatory T cells Vaccines & Antibodies. Review Expert Opinion. 5(4), 545-554.

33. Pockley, A.G. (2003). Heat shock proteins as regulators of the immune response. Lancet. 362(9382), 469-76.

Current Trends in Biotechnology and Pharmacy
Vol. 7 (4) 914-931 October 2013, ISSN 0973-8916 (Print), 2230-7303 (Online)

Surface modified Polymeric Nanoparticles for Brain Targeted drug Delivery

Sunita Lahkar and Malay K Das*
Department of Pharmaceutical Sciences, Dibrugarh University, Dibrugarh - 786004, India
*For Correspondence - du_mkd@yahoo.co.in

Abstract

The aim of any drug delivery system is not only to deliver a drug to specific site of action but also to maintain its therapeutic concentration at the targeted site. Most of the drugs used in CNS disorders cannot cross the blood brain barrier (BBB) due to their large molecular size, less lipid solubility and p-glycoprotein (p-gp) efflux mechanism resulting in low drug concentration in brain. Among the current strategies for brain targeting drug delivery, biodegradable polymeric nanoparticles are significant in delimiting the blood brain barrier, increasing the loading efficiency in brain and also reducing the peripheral toxicity. The present review emphasizes on the surface modified polymeric nanoparticles in enhancing drug delivery across the blood brain barrier.

Keywords: Blood brain barrier, polymeric nanoparticles, drug delivery, brain targeting, coated nanotechnology, ligand nanotechnology

Introduction

Despite tremendous research, the death rate of patients suffering from brain disorders like brain tumors, HIV encephalopathy, epilepsy, cerebrovascular disease, neurodegenerative disorders, are more than that dying of systemic cancer or heart disease. The failure is due to an inefficient drug delivery as drug accessibility to the Central Nervous System (CNS) is limited by the Blood Brain Barrier (BBB) and efflux transport system (1). Essential nutrients and oxygen are supplied to the brain by blood capillaries. The walls of the blood capillaries form the so called Blood Brain Barrier (BBB). A solid connection is present between the blood vessels of BBB, and is formed by special protein complexes of endothelial cells called tight junction. The abluminal side of these endothelial cells contains pericytes, a part of BBB. The pericytes are encapsulated by the basal membrane of the endothelial cells, and are responsible for the synthesis as well as release of different components of the basal membrane and the extracellular matrix such as collagen and glycosaminoglycan. Pericytes maintains the stability of the blood vessel and also the functioning of BBB. Another type of endothelial cell is the astrocyte responsible for the hoemeostatis and the ion regulation in the brain (2). Their endfeets attach to the pericytes and the endothelial cells, covering partially the blood vessels but are not connected to other cells by tight junction (3). Astrocytes allow polar molecules entry into the nerve fluid; while pericytes eradicate the entry of polar molecules through the BBB.

Several mechanisms like passive transport, active transport, receptor mediated transport, endocytosis or transcytosis are followed by several substances to cross the BBB. These are called influx transport system, allowing the entry of essential substances from the blood into the BBB (4). The influx transport system across the BBB describes as passive transport and active transport. Passive transport allows the influx of substances having good lipophillicity, less protein

binding and low molecular weight. The active transport includes transporter mediated transcytosis and receptor mediated endocytosis (5). Transporter mediated transcytosis is responsible for transport of small hydrophilic molecules such as amino acid, glucose and other molecules through the transporters present at the luminal and abluminal side of the endothelial cells. Receptor mediated endocytosis is responsible for transport of large or hydrophilic essential molecules such as hormones, transferrin or iron, insulin and lipoproteins by acting on receptors located on the luminal side of the endothelial cells.

On the contrary is the efflux transport system of P-glycoprotein (Pgp), multidrug resistance protein (MRP) forcing the inverse movement of many substances from the cerebral parenchyma to the blood (6). Thus the tight junction in BBB, efflux transport system restricts entry of most of drugs making many drug based therapy inefficient such as antibiotics, antiviral drugs, antiretroviral drugs etc. The lack of essential characteristics in most drugs like lipid solubility, low molecular size prevents their ability to cross BBB. Some of the large sized molecules like oligonucleotides, antibodies, peptides, proteins are out of reaching BBB (7). Several strategies are followed to overcome these barriers in order to have an efficient brain delivery of drugs. Among the several strategies, nanoparticles are considered as the best to carry drugs across the Blood brain barrier (BBB).

Nanoparticles satisfies many of the characteristics of the magic bullet concept as carrier and also when coated with ligands. Nanoparticles are colloidal matrix of natural/ synthetic polymers ranging in size between 10 and 1000 nm (8). The drugs may be adsorbed to the surface of nanoparticles or entrapped within the matrix. Among the several varieties of nanoparticles polymeric nanoparticles are significant in brain targeted drug delivery due to advantages as they are inert, biocompatible and biodegradable. The smaller size of polymeric nanoparticles (< 100 nm) enables it to cross the BBB. Both hydrophilic and hydrophobic drugs can be delivered across the BBB. They are easily processed, nontoxic, and nonantigenic and also are easily delivered through blood capillaries. They protect the drugs against degradation. They are target specific drug delivery with sustained release behavior (7, 9). Both synthetic and natural polymers can be used for preparing polymeric nanoparticles. Polymers for preparing nanoparticles (10) can be classified as shown in table 2.

Biodistribution of nanoparticles in body

After intravenous administration, polymeric nanoparticles come in contact with plasma/serum proteins before reaching the target cells. The interaction of polymeric nanoparticles with phagocytes is regulated by the balance between two serum components – opsonin which promotes phagocytosis and dysopsonin which suppress the process. The opsonin gets adsorbed to the surface of polymeric nanoparticles and makes it recognisable to the reticuloendothelial cells (RES) (11, 12). Following intravenous administration, polymeric nanoparticles are taken rapidly by RES present in liver, spleen, bone marrow and distributed rapidly into the liver (60-90) % and spleen (2-10) % and to a minor degree into the bone marrow (13). A low concentration

Table 2. Polymers for polymeric nanoparticles

No.	Classification of polymers	Examples
1	Natural biodegradable polymers	Alginates, Chitosan, Gelatin, Pellula, Gliadin
2	Synthetic biodegradable polymers	PLA, PGA, PLGA,Polyanhydride, Polycaprolactone, Polyalkylcyanoacrylate
3	Nonbiodegradable polymers	Polymethylmethacryalte(PMMA),Polymethylacrylate (PMA)

of nanoparticles can enter brain due to their uptake by RES following intravenous administration. Several technologies based on surface modification of nanoparticles are worked out to overcome the problems in connection with phagocytosis so as to enhance the concentration of drug in the brain.

Approaches for surface modification of nanoparticles

Coated nanotechnology: Coated nanotechnology is based on specialized coating of nanoparticles using polymers or surfactants which allow mimicking the molecules that would be normally transported into the brain (5).The coating of nanoparticles is done by Incubation method. In this method, the coating solution is added to the preformed nanoparticle formulation and is kept for stirring or overnight incubation is done. The coating materials for polymeric nanoparticles are discussed below.

Polysorbate 80: Several drugs are being reported to be successfully delivered to brain using polysorbate 80 as coating material. The coating of nanoparticles by polysorbate 80 is done by adding polysorbate 80 (1% v/v) to the already prepared drug loaded polymeric nanoparticles and kept under stirring for 30 minutes (14). It is also reported that after the addition of polysorbate 80 (1% v/v) to a model drug loaded polymeric nanoparticles, it was stored for 24 hrs (15). Dalargin adsorbed on polybutylcyanoacrylate (PBCA) nanoparticles coated with polysorbate 80 was the first compound delivered to the brain, showed positive analgesic effect in rats (16). In a study, polysorbate 80 coated Gemcitabine loaded PBCA nanoparticles; efficiently carried the drug to brain as its antitumour activity was observed on C6 glioma cells of a brain tumour model (17). An attempt was also made for the delivery of Nerve growth factor (NGF) using polysorbate 80 coated PBCA naoparticles as carrier. NGF is needed in age related neurodegenerative diseases such as Amnesia, Parkinsonism; but entry to brain is restricted by the blood brain barrier. NGF loaded PBCA nanoparticles coated with polysorbate 80 could efficiently carry NGF to the brain as evidenced by pharmacokinetic models (18). Polysorbate 80 coated chitosan nanoparticles successfully delivered Gallic acid to brain for antidepressant activity (19). Polysorbate 80 coated nanotechnologies could also efficiently deliver Doxorubicin (20), Rivastigmine (21), Met Enkephalin Kytorphin (22) to brain.

But the mechanism behind the nanoparticles mediated transport across the BBB is yet to be fully understood. Several mechanisms were suggested – an increased retention time of the nanoparticles in the brain capillaries could enhance transport of drug across the BBB, polysorbate 80 increases the drug permeability by fluidization of brain endothelial cell membrane, opening of the brain endothelial cells tight junction by nanoparticles, endocytosis of nanoparticles by the brain endothelial cells deliver the drug into the brain, transcytosis could be possible for drug loaded nanoparticles, polysorbate 80 could inhibit the P-glycoprotein (P-gp) efflux (23). Among the several mechanisms, the most probable mechanism is endocytosis (24). PBCA nanoparticles coated with polysorbate 80 may covalently couple with apolipoprotein E, A-I or B-100 in the bloodstream. Apolipoprotein bound to the surface of PBCA nanoparticles mimics low density lipoprotein (LDL). It acts on the LDL present in the brain endothelial cells and undergoes receptor mediated endocytosis (24). Finally, the drug can be delivered by passive diffusion into the brain. However, the reported most probable mechanism suffers from several disagreements as apolipoprotein E adsorption is not only specific to polysorbate 80 coated nanoparticles surfaces but also get adsorbed onto PEGylated polylactic acid nanoparticles. Polysorbate 80 is not reported to be a good coating material for polymethylmethacryalate (PMMA) nanoparticles and polystyrene nanoparticles because polysorbate 80 coated PMMA nanoparticles are not distributed to brain after intravenous administration and also polysorbate 80 coated polystyrene nanoparticles are not able to deliver Dalargin to brain (25). It is

also reported that a desirable therapeutic concentration of drug in brain cannot be attained due to the fact that polysorbate 80 competes with proteins in blood plasma causing rapid degradation of nanoparticles in serum/plasma inducing desorption of drug adsorb onto polybutylcyanoacrylate (PBCA) nanoparticles. Thus the desorption evidence that the pharmacokinetic profile of drug in brain remains similar to drug solution administered intravenously (26). It is also reported that polysorbate 80 causes an increase in brain permeability due to BBB disturbances (27); polysorbate 80 coated nanoparticles causes BBB toxicity evidenced on the basis of sucrose permeability test (20 mg/kg in rats). Polysorbate 80 coated PBCA nanoparticles decreased locomotor activity in mice when investigated (28) and also reported that its short duration of pharmacological action needs regular intravenous administration which makes it unsuitable for chronic brain disorders. PBCA is also reported as a synergistic factor for enhancing brain permeability. In comparison to PBCA, Polylactide (PLA) or Poly (lactide-co-glycolide) (PLGA) microspheres are reported to be of good CNS biocompatibility (25).

Glutathione: Glutathione is considered better than Polysorbate 80 as a coating material. Unlike polysorbate 80, glutathione is an endogenous peptide and not toxic to body. Using glutathione as a coating material, an attempt has been made for the delivery of Paclitaxel across the BBB. Glutathione coated Polylactide-co-glycolide (PLGA) nanoparticles reported to be a good carrier for Paclitaxel to brain as investigated by PgpATpase assay. Glutathione is reported to act by inhibiting the Pgp efflux transport system (29).

Doxorubicin lacks permeability to brain due to its low lipophillicity, high molecular weight and efflux by Pgp. Glutathione coated on Doxorubicin adsorbed to PLGA PEG nanoparticles act against Pgp efflux transport system making Doxorubicin accessible to brain (29).

Mannan: Mannan coated Gelatin nanoparticles were reported as a successful carrier for Didanosine to brain. Gelatin is a biocompatible, biodegradable polymer (30). Various surface receptors like mannosyl, lectin and galactosyl present in macrophages of brain help in recognisation and endocytosis of nanoparticulate carriers. Due to this fact, nanoparticles containing ligands such as mannosyl, immunoglobulin, fibronectin and galactosyl are better phagocytosed by macrophages than carriers without such ligands. The mannan, coated on the surface of gelatin nanoparticles are recognised by mannosyl receptors present predominantly on the macrophages of brain (31) and phagocytosed by the macrophages leading to an effective delivery to brain. Mannan coating of nanoparticle suspension was done by incubation method (32) where mannan solution (1% m/v) was prepared in hot water and mixed with 1.0ml of preformed nanoparticle suspension; kept overnight stirring at room temperature (31).

Albumin: Albumin can be safely used as a coating material for nanoparticles as albumin coated nanoparticles in mice reported to have no mortality with upto a 2000 mg/kg (25).

Poloxamer: Poloxamer is considered to play a significant role in drug delivery to brain. Probable mechanism of poloxamer coated nanoparticles includes inhibition of Pgp efflux transport system and multi drug resistance protein efflux transport mechanism (33). It is also reported that apolipoproteins adsorbed on the surface of poloxamer coated nanoparticles; ligands and monoclonal antibodies conjugated to the poloxamer coated nanoparticles could cross the BBB via specific endogenous transporters localised within the brain capillary endothelium (34). Poloxamer 188 coated PBCA nanoparticles is reported to be a good carrier for Doxorubicin against an intracranial glioblastoma in rat (35).Poloxamer coating on drug loaded polymeric nanopartcles is also done by Incubation method. As an example, the coating of poloxamer on Acyclovir loaded PLGA nanoparticles was done by mixing poloxamer (1 % w/v) solution with uncoated Acyclovir loaded PLGA nanoparticles followed by overnight incubation (36)

Polyethylene glycol (PEG): Polyethylene glycol (PEG) coating enhances half-life of nanoparticles by several magnitudes. PEG coating provides a hydrophilic protective layer around the nanoparticles which repel the adsorption of opsonin proteins via steric repulsion forces, thereby blocking and delaying the first step in the opsonisation process (37). PEGylated PLGA naoparticles contains a hydrophilic coating of PEG and hydrophobic core of PLGA. An attempt was made to carry both Dalargin (hydrophilic drug) and Loperamide (hydrophobic drug) using PEGylated PLGA nanoparticles. Dalargin got adsorbed on the hydrophilic coat of PEG while Loperamide was entrapped in the hydrophobic core of PLGA. In vitro evaluation showed quick release of Dalargin as free drug while Loperamide HCl showed almost sustained release profile (38). Dalargin loaded PLGA nanoparticles was double coated with polysorbate 80 and polyethylene glycol (PEG). Polysorbate 80 coating provides protection against phagocytosis and PEG provides long circulating characteristics. The Dalargin-loaded polybutylcyano acrylate (PBCA)-nanoparticles were coated by adding up to 2% of Tween 80 and PEG 20000 stepwise to the nanoparticle suspension and kept under continuous magnetic stirring at 9000 rpm for 45 min (39).

PEGylated PLGA nanoparticles reported to carry Cytarabine to brain (40). Confocal microscopy evidenced the fluorescent PEGylated Cytarabine loaded PLGA nanoparticles in brain and spinal cord. It is reported that PEGlyted polyhexadecylcyanoacrylate (PHDCA) nanospheres are good carrier for brain tumour targeting. Probable mechanisms include reduction of blood plasma clearance due to diffusion of nanoparticles across the brain, translocation due to the adsorption of PEGylated nanospheres to the brain endothelial cells (40). A PEGylated polymeric nanoparticle penetrates brain better than polysorbate 80 coated nanoparticles due to the fact that the covalent attachment of polyethylene glycol (PEG) to the polymer prevents desorption of PEG from PEGylated polymeric nanoparticles (41) unlike polysorbate 80 which is adsorbed to the polymer. Till now several drugs are successfully brain targeted by using coated nanotechnology as shown in Table 3.

Ligand nanotechnology : This approach is based on the covalent linkage of ligands to the polymers or the nanoparticles in order to promote receptor mediated endocytosis or transporter mediated transcytosis (49). The ligands can be transferrin, lipoprotein, insulin and thiamine but also synthetic or natural peptides can be used (50). The ligands are attached to the nanoparticles or polymer surface by two techniques

Covalent Chemical conjugation (51, 52 and 53): This is the most commonly established method of chemical conjugation where intially thiolation of ligand is done that is subsequently reacted with maleimide-functionalized drug or nanoparticle to form a stable thioether bond. Thiolated drug or vector can also be reacted with a free cysteine or reduced disulfide bond to yield a disulfide-bonded drug-nanoparticles conjugate. To further ensure functionality of the vector and protein, a chemical spacer $(CH_2)_5NHCO$ $(CH_2)_5NHCO$ or polyethylene glycol (PEG) moiety can be incorporated into the linkage to reduce steric hindrance.

Noncovalent Streptavidin/ Biotin linkages (51, 54, 55 and 56): The therapeutics can be monobiotinylated at lysine residues using N-hydroxysuccinimide (NHS) analogs of biotin, or alternatively, biotin can be attached using biotin hydrazide. The streptavidin can be coupled to the targeting vector via a thioether linkage. A BBB-targeted therapeutic can then be created simply by mixing the biotinylated therapeutic with the streptavidin-functionalized targeting vector. A PEG linkage can be also used.

Transferrin: Transferrin and insulin are reported to be used for the first time in ligand based nanotechnology. Transferrin undergoes receptor mediated endocytosis via transferrin receptors highly expressed on the brain capillary endothelial cells. Transferrin conjugated Polylactide – co-

glycolide (PLGA) nanoparticles could successfully target Nevirapine to brain (52). But Transferrin use in ligand based nanotechnology is limited because blood plasma is almost saturated with endogenous Transferrin. The drug targeting Transferrin competes with the endogenous transferrin for the same transferrin receptor localised in brain endothelial cell, in turn it reduces the efficacy of transferrin conjugated nanoparticles as a carrier to deliver the desired therapeutic concentration of drug to brain. Hence antibodies are used in place of transferrin to overcome its limitation (53). One such antibody is ox26 which is reported to bind an extracellular epitope of transferrin distinct from transferrin binding site, and prevents competition between the drug targeting ligand and the natural endogenous ligand present in blood plasma.The ox26 is attached to the formulation by covalent chemical linkages, where thiolated ox26 antibody is conjugated to the malemide-grafted liposomes according to a sulfhydrylmalemide coupling method (54). One of the relavant work reported is the delivery of Tempol across BBB. Ox26 antibody covalently attached to malemide grafted PLGA nanoparticles using NHSPEG 3500 maleimide crosslinker was a successful carrier for Tempol into brain (55). Attempts were made on the preparation of PEGylated immunonanoparticles (15). One such example is ox26 antibody conjugated PEGylated polylactic acid nanoparticles. Moreover polymers other than polylactic acid are also applied such as Chitosan. Chitosan- PEG nanospheres conjugated with ox26 were prepared by Avidin- Biotin complex. In this technique, Biotin was covelently coupled to PEG followed by covalent coupling of Chitosan to lead to a Chitosan- PEG Biotin copolymer. In

Table 3. Drugs delivered to brain by coated nanotechnology

Drugs	Categories	Techniques of coated nanotechnology	References
Tacrine	Antialzheimer drug	Tacrine loaded polybutylcyanoacrylate nanoparticles coated with polysorbate 80.	(19)
Dalargin	Peptide	Polysorbate 80 coated Dalargin loaded PBCA nanoparticles	(42)
Donepezil	Antidementia drug	Donepezil loaded polybutylcyanoacrylate (PBCA) nanoparticles coated with polysorbate 80	(43)
Resperidone	Antipshycotic Drug	Poloxamer coated Resperidone loaded poly (epsilon-caprolactone) nanoparticles.	(44)
Amphotericin B	Antifungal drug	Amphotericin B loaded poly (lactic acid) – b- poly (ethyleneglycol) nanoparticles coated with polysorbate 80.	(45)
Resperidone	Antipshychotic Drug	Poloxamer 407 coated Resperidone loaded PLGA nanoparticles.	(46)
Estradiol	Hormones	Estradiol loaded polylactide–co-glycolide (PLGA) nanoparticles coated with polysorbate 80.	(47)
Methotrexate	Antifungal Drug	Polysorbate 80 coated Methotrexate loaded chitosan and glycolchitosan nanoparticles.	(48)

parallel, Streptavidin/ox26 conjugate is prepared and incubated with chitosan-PEG Biotin nanoparticles (prepared by ionotropic gelation technique using pentasodium triphosphate as crosslinking agent) to obtain immunonanoparticles(56). PEGylated immunonanoparticles carried caspase inhibitor (peptide z DEWD-FMK) across BBB and reduced the death of neuronal cells after an ischaemic attack. It is also reported that transferrin conjugated PEGylated albumin immunonanoparticles could carry Azidothymidine significantly to brain as observed in rat (57).

Insulin: Insulin is not a suitable ligand based nanotechnology because of rapid degradation in blood stream (serum half-life 10 minutes) and hypoglycaemia due to possible interference with natural insulin balance (58). So, antibody recognising insulin receptors are used as brain targeting ligands. Researches using 83-14 mouse monoclonal antibodies (mAb) against insulin receptor for receptor mediated endocytosis were performed in primates (Rhesus monkey) (59). Attempts were also made to cure mucopolysaccharodosis type VII due to lysosomal deficiency. â glucoridinase, an essential enzyme for lysosomal deficiency, was administered as radiolabelled phosphorylated glucoridinase (131I-P-GUS). Glucoridinase was found to act on mannose-6- phosphate receptor (Insulin like growth factor II) expressed on the endothelial cells of brain and gets delivered via receptor mediated endocytosis (59). Mannose -6-phosphate receptors in brain could be beneficial for ligand nanotechnology in order to treat many neurodegenerative disorders.

Thiamine: Thiamine (a water soluble vitamin B1), a micronutrient essential for normal cell growth and development is reported to cross the BBB by carrier mediated transport system (60). Thiamine as a surface ligand on the nanoparticles specifically targets them to the brain via the BBB thiamine transporter .Thiamine coated solid lipid nanoparticles comprising of emulsifying wax and Brij 78, were reported to act on thiamine transporter in brain as tested in situ by rat perfusion technique (61).

Peptide derived nanoparticles: Several peptide transport mechanisms (receptor mediated, adsorptive mediated, carrier mediated, nonspecific passive diffusion) as well as nontransport processes (endocytosis without transcytosis, absorption and metabolism) are reported. Several strategies are followed to manipulate peptide transport across the BBB so as to deliver drug to brain such as lipidization, chemical modifications of the N-terminal in peptides, coupling of transport with post BBB metabolism and formation of potent neuroactive peptides, upregulation of putative peptide transporters, use of chimeric peptides in which nontransportable peptide is chemically linked to a transportable peptide, use of monoclonal antibodies against peptide receptors and binding of circulating peptides to apolipoproteins (62). Researchers' focuss on manipulating these strategies to target compounds/drugs to brain. One such reported successful work is on 12-32 (g21) of leptin conjugated PLGA nanoparticles which was successfully brain targeted as the confocal microscopy evidenced labelled tetramethylrhodamine g21 conjugated PLGA nanoparticles presence in rat brain (61). Another work is also reported on nanoliposomes containing phosphatidic acid or cardiolipin, which were decorated with two apolipoproetins (ApoE) derived peptides (the fragment 141-150 or its tandem dimers) for brain targeting. Confocal microscopy revealed enhanced brain uptake of nanoliposomes containing phosphatidic acid decorated with fragment 141-150 than its tandem dimers (63). It is reported that 29 amino acid peptide derived from rabies virus glycoprotein (RVG29) peptide conjugated to albumin nanoparticles using noncovalent streptavidin/ biotin linkage significantly facilitate the intracellular delivery of nanoparticles as studied in vitro (64). One relevant work is reported, on viral fusion peptide (gH625) derived from the glycoprotein gH of Herpes Simplex virus type 1 covalently bound to the surface of flouroscent aminated polystyrene nanoparticles, which is found to be an efficient carrier for targeting therapeutics to brain. The gH625 covalently bound to polystyrene

Table 4. Drugs brain targeted through conjugated nanotechnology

Drugs	Categories	Techniques of coated nanotechnology	References
Ritonavir	Antiretroviraldrugs	TAT conjugated Ritonavir loaded Polylactide(PLA) nanoparticles	(68)
Human serum albumin(HSA)	Protein	HSA nanoparticles covalently bound with apolipoprotein.	(69)
Nevirapine	Anti retroviraldrugs	Nevirapine loaded PLGA nanoparticles conjugated with transferrin.	(70)
Loperamide	Antinociceptive drug	Loperamide loaded HSA nanoprticles covalently coupled with insulin or antiinsulin receptor monoclonal antibody (29B4)	(71)
Coumarin 6	Anticoagulant	Coumarin 6 loaded PLGA nanoparticles conjugated with solanum tuberosum lectin.	(72)
Zidovudine	Antiretroviral drug	CRM 197 grafted Zidovudine loaded polybutyl cyanoacrylate (PBCA) nanoparticles.	(73)

Table 5. Drugs brain targeted through modification of polymers

Drugs	Categories	Techniques of coated nanotechnology	References
Didanosine	Antiviral drug	Didanosine loaded chitosan crosslinked with tripolyphosphonate anions nanoparticles.	(79)
Estradiol	Hormone	Estradiol loaded chitosan crosslinked with tripolyphosphonate anion nanoparticles	(80)
Lamivudine	Antiretroviral drug	Lamivudine loaded chitosan crosslinked with glutaraldehyde nanoparticles	(81)

nanoparticles could be easily uptaken by brain as shown by endothelial cells BBB models. It is found that gH625 has high cell translocation potency; the peptide is free of toxicity, and also decreases nanoparticles intracellular accumulation (65). A significant work is reported on Chitosan conjugated pluronic based nanocarrier with a specific target peptide (rabies virus glycoprotein, RVG29) as a successful carrier for the delivery of protein (â galactosidase) to brain significantly (66). Cyclophillin B (Cyclosporin A binding protein) is reported to undergo receptor mediated transcytosis as observed in in vitro model of BBB. Cyclophillin B enables promoting regeneration of damaged peripheral nerves in addition to immunosuppressive activity (67). As cyclophillin B can cross BBB, so it may be utilised in peptide derived nanoparticles for treating brain related disorders. Several drugs efficiently delivered into brain using ligand nanotechnology are given in table 4.

Nanotechnology based on modification of polymer : Both synthetic and natural polymers can be used in nanotechnology for brain targeted drug delivery. One such interesting natural

Table 6. The comparison of PK/PD parameters in presence/absence of surface modification of nanoparticles

Sr. No.	Drugs	Technique of surface modification of nanoparticles	Blood brain barrier crossing ability of		References
			Surface modified nanoparticles	Nanoparticles without any surface modifications	
1	Dextran	PLA nanoparticles coated with Tween 80.	It could cross the Blood brain barrier as observed under flourescence microscope.	It could not cross the Blood brain barrier.	14
2	Tacrine	Tween 80 coated polybutylcyanoacrylate (PBCA) nanoparticles loaded with Tacrine.	A modified nanoparticle has higher concentration of Tacrine in brain upon intravenous administration to rats.	A higher concentration of drug tacrine was observed in liver, spleen and lungs with the unmodified nanoparticles	19
3	Dalargin	Polycyanoacrylate (PBCA) nanoparticles double coated with Tween 80 and poly-ethylene glycol (PEG) 20000.	A central antinociceptive effect of Dalargin by tail flick test in mice is reported.	Absence of central antinociceptive effect of Dalargin by tail flick test in mice is reported	82
4	Amphotericin	Tween 80 coated polylactic acid-b-polyethylene glycol (PLA-b-PEG) nanoparticles.	The colony growth of cryptoccocus neoformans in brain of mice is reduced as observe in vivo.	It couldnot reduce the growth of cryptoccocus neoformans in mice brain as observe in vivo.	31
5	Didanosine	Mannan coated Didanosine loaded Gelatin nanoparticles.	12.4 times higher uptake of Didanosine was found in brain than Didanosine administered in phosphate buffer solution intravenously.	It is not able to cross the Blood brain barrier as reported by flourescence study.	83
6	Ritonavir	Tat-conjugated ritonavir-loaded nanoparticles	The HIV infection of monocyte derived macrophages (MDM) cultures could be reduced.	The HIV infection of monocyte derived macrophages (MDM) could not be reduced.	84
7	Didanosine	Chitosan nanoparticles crosslinked with tripolyphosphonate anions.	A significantly higher concentration ($p< 0.5$) of Didanosine is reported in brain after intranasal administration than that of intravenous administration.	Chitosan is fragile in nature. So, there is a chance of breakage of polymer if it is prepared without crosslinking.	85
8	Resperidone	Poloxamer coated poly (lactide co glycolide) nanoparticles.	A prolonged antipsyhotic effect of Resperidone for 72 hrs was obtained upon subcutaneously administered to mice with lesser extrapyramidal side effects.	No antipshychotic effect is reported as uncoated nanoparticles couldnot cross blood brain barrier.	44,46

9	Methotrexate	Tween 80 coated chitosan or glycol chitosan nanoparticles.	Tween 80 coated flourescent chitosan nanoparticles transport Methotrexate across MDCKII-MDR1 cells	Uncoated nanoparticles could not transport Methotrexate across MDCKII-MDR1 cells	48
10	Human serum albumin (HSA)	Tween 80 coated or covalently bound apolipoprotein E (Apo E) HSA nanoparticles	HSA is reported to be transferred across brain capillary endothelial cells and neurons when injected injected intravenously into SV 129 mice under transmission electron microscopy	Unmodified surface of nanoparticles unable to cross the brain capillary endothelial cells and neurons when injected injected intravenously into SV 129 mice under transmission electron microscopy	69
11	Nevirapine	Transferrin-grafted poly (lactide-co-glycolide) nanoparticles loaded with Nevirapine.	Dioctadecyldimethylam monium bromide (DODAB)-stabilized Nevirapine loaded poly (lactide co glycolide) nano-particles grafted with Transferrin enhances the transport of Nevirapine (NVP) across human brain microvascular endothelial cells (HBMECs)	Unmodifed surface of Nevirapine loaded poly (lactide co glycolide) nanoparticles is not reported to cross human brain microvascular endothelial cells (HBMECs)	70
12	Loperamide	Insulin or an anti-insulin receptor monoclonal antibody (29B4) covalently coupled Loperamide loaded Human serum albumin(HSA)	Induction of antinociceptive effects in the tail-flick test in ICR (CD-1) mice after intravenous injection	Noninduction of antinociceptive effects in the tail-flick test in ICR (CD-1) mice after intravenous injection	71
12	Coumarin 6	Coumarin 6 loaded Solanum tuberosum lectin (STL) conjugated poly (DL-lactic-co-glycolic acid) (PLGA) nanoparticle (STL-NP).	Solanum tuberosum lectin (STL) conjugated poly (DL-lactic-co-glycolic acid) (PLGA) nanoparticle (STL-NP) demonstrated 1.89-2.45 times ($p < 0.01$) higher brain targeting efficiency than unmodified NP of Calu-3 cells. Enhanced accumulation of STL-NP in the brain is reported by near infrared fluorescence probe image following intranasal administration	Unmodified nanoparticles lesser brain targeting efficiency than modified nanoparticles.	72
13	Zidovudine	CRM197-grafted polybutylcyanoacrylate (PBCA) nanoparticles loaded with Zidovudine.	Modified nanoparticles could transverse monolayer of human brain-microvascular endothelial cells (HBMECs)	Unmodified nanoparticles could not transverse monolayer of human brain microvascular endothelial cells (HBMECs)	73

Table 7. Patents for nanoparticle based CNS targeted drug delivery systems

S.No.	Application	Summary of invention	Refrence
1	Receptor targeted drug delivery systems	Chemical conjugate of polymeric nanoparticles for brain targeted delivery	86
2	Drug targeting system, method for preparing same and its use	Dalargin loaded nanoparticles coated with polysorbate 80	87
3	Transport of liposomes across the blood-brain barrier	Monoclonal antibodies (mAb) conjugated liposomes for brain targeted delivery.	88
4	Drug targeting system, method of its preparation and its use	Dextran 12.000 or polysorbate 85 stabilized nanoparticles for brain targeted delivery of Dalargin.	89
5	Use of drug loaded nanoparticles for the treatment of cancers	Coated nanoparticles for the delivery of anticancerous drug (Doxorubicin) to brain.	90
6	Non-invasive gene targeting to the brain	Ox26 monoclonal antibodies conjugated polyethylene glycol (PEG) immunoliposomes for brain targeted delivery.	91
7	Nanoparticles made of protein with coupled apolipoprotein E for penetration of the blood-brain	barrier and methods for the production thereof Avidin-modified Human serum albumin (HSA) nanoparticles with biotinylated apoE for brain targeted delivery.	92
8	Non-invasive gene targeting to the brain	OX26 MAb conjugated PEGylated liposome for gene delivery	93
9	Support system in the form of protein-based nanoparticles for the cell-specific enrichment of pharmaceutically active substances	Preparation of nanoparticles by miniemulsion; surface modification by coating with polysorbate 80 for brain targeting.	94
10	Rapid Diffusion of Large Polymeric Nanoparticles in the Mammalian Brain	Polyethylene glycol (PEG) coated polymeric nanoparticles loaded with drug and gene for brain targeted delivery.	95
11	Drug delivery in neurodegen erativedisorders	Nanoparticles loaded with epidermal growthfactor	96
12	Nanoparticles for protein drug delivery	Nanoparticles composed of chitosan and polyglutamic acids for the brain targeted delivery of protein or bioactive agents.	97

13	Encapsulation of biologically active agents	Encapsulation of biologically active agents such as proteins in particulate carriers such as nano-particles using Hydrophobic ion pairing (Hip) agents	98
14	Polylactide nanoparticles	Pluronic 188 coated drug loaded poly (lactide co glycolide) nanoparticles for brain targeting.	99
15	Nanoparticles made of protein with coupled apolipoprotein e for penetration of the blood-brain barrier and methods for the production thereof	Human serum albumin (HSA) avidin nanoparticles conjugated with ApoE for brain targeted delivey of Dalargin.	100
16	Conjugates for targeted drug delivery across the blood-brain barrier	Conjugates of Distearoylphosphatidy lethanolamine-polyethylene glycol-maleimid e (DSPE-PEG-MAL) with reduced glutathione was prepared for brain targeted delivery.	101
17	Rapid Diffusion of Large Polymeric Nanoparticles in the Mammalian Brain	Polyethylene glycol (PEG) coated polymeric nanoparticles loaded with drug and gene for brain targeted delivery.	101
18	Targeting of drugs and diagnostic agents	Conventional nanoparticles coated withsurfactants to cross blood brain barrier	102
19	Site specific drug delivery across Blood brain barrier	Nanogels prepared from cross-linked polyion polymer fragment and one nonionicwater soluble polymer fragment	102
20	Protein and peptide delivery to brain	Nanoparticles prepared from chitosan and polyglutamic acid	102
21	Inhibition of reperfusion injury to brain	Nanoparticles prepared from inert plasticizers loaded with anti-oxidants	102

Table 8. FDA approved CNS targeted drug delivery systems using nanoparticles (102)

Sr. No	API/ nanoparticle components	Route of administration	FDA approved indication	Product	Company
1	Propofol	Intravenous	Anesthetic	Diprivan	Zenechpharma
2	Colloidal gold nanopar-ticles coupled to TNF and PEG-Thiol (~27 nm)	Intravenous	Solid tumors	Aurimmune (CYT-6091)	CytImmune Sciences
3	Cyclodextrin containing siRNADelivery nanopar-ticles (~50 nm) based on Calando's RONDEL technology	Intravenous	Cancer	CALAA-01	Calando Pharmaceutical
4	Gold-coated silica nanoparticles (~150 nm)	Intravenous	Solid tumors	AuroShell	Nanospectra Biosciences

polymer extensively used in the nanotechnology field due to its nanoparticles forming ability is Chitosan. Chitosan has several characteristics favouring its use in preparing brain targeted nanoparticles such as it is natural, biodegradable, biocompatible, bioadhesive, low molecular weight (LMW) (74). Inspite of these advantages, chitosan nanoparticles suffer from fragile structure, making it unsuitable to use without modification as carrier for drug molecules. Several techniques of modifications are suggested, but the simpler technique (called Ionotropic Gelation) is through chitosan salt formation where some anions may cause crosslinking via ionic interactions (75). In this connections, tripolyphosphonate, sodium citrate, amino acids, sodium sulphate can be used as crosslinkers (76-78, 74). The drugs delivered across the BBB using this technology are given in Table 5.

Conclusion

The Blood brain barrier (BBB) is the most limiting condition for the efficient drug delivery to CNS. Nanoparticles have good prospect in treating brain disorders. It has major contribution in the delivery of inaccessible drug to the brain and thus also helps in treating brain cancer or other neurodegenerative disorder. The pharmocokinetics, patented technology and FDA approved CNS targeted nanoparticles with different drugs are shown in Table 6-8, respectively. In near future nanoparticulate drug delivery systems can be used for exploiting many biological drugs which have poor aqueous solubility, permeability and less bioavailability. Nanoparticles provide ingenious treatment of CNS disorders by enabling targeted delivery and controlled release. Thus nanoparticles can be considered to be significant in brain targeting drug delivery. Nanoparticulate drug delivery technology should be developed further which can be achieved by prompt participation of more research oriented programmes from the governmental as well as corporate sectors.

References

1. Rasheed, A., Theja, I., Silparani, G., Lavanya, Y. and Kumar, C.K.A. (2010). CNS Targeted Drug Delivery. J. Innov. Trends Pharm. Sci., 1 (1): 9 -18.
2. Ballabh, P., Braun, A. and Nedergaard, M. (2004). The Blood Brain Barrier: an overview .structure, regulation and clinical implications. Neurobiol. Dis., 16: 1-13.
3. Gabathuler, R. (2010). Approaches to transport therapeutic drugs across the blood brain barrier. Neurobiol. Dis., 37(1): 48 - 57.
4. Tosi, G., Costantino, L., Ruozi, B., Forni, F. and Vandelli, M.A. (2008). Polymeric nanoparticles for the drug delivery to the central nervous system. Expert Opin. Drug Deliv., 5 (2): 155-174.
5. Karanth, H. and Murthy, R.S.R. (2008). Nanotechnology in brain targeting. Int. J. Pharm. Sci. Nanotech. 1(1): 9-24.
6. Lee, G., Dallas, S. and Hong, M. (2001). Drug transporter in the central nervous system: brain barriers and brain parenchyma considerations. Pharmacol. Rev., 53: 569 – 596.
7. Ringe, K., Walz, C.M. and Sabel, B.A. (2004). Nanoparticle drug delivery to brain. In: Nalwa H.S. (Eds.), Encyclopedia of nanoscience and nanotechnology (4th edition), American Scientific Publishers, California, USA, 7, pp. 91 – 104.
8. Malodia, K., Singh, S.K., Mishra, D.N. and Shrivastava, B. (2012). Nanoparticles: An advance technique for drug delivery. Res. J. Pharm.Bio. Chem. Sci., 3(3): 1186.
9. Mahapatro, A. and Singh, D.K. (2011).Biodegradable nanoparticles are excellent vehicle for site directed invivo delivery of drugs and vaccines. J.Nanobiotech., 9 (55): 1-11.
10. Chakravarti, S.S., Robinson, D.H. and De, S. (2007). Nanoparticles prepared from Natural and Synthetic polymers In: Pathak Y., (Eds.), Nanoparticulate drug delivery system. Informa Healthcare, New York, USA, 166:51-60.
11. Absolom, D.R. (1986).Opsonins and Dysopsonins: An overview. Methods Enzymol., 132: 281-318.

12. Moghimi, S.M. and Patel, H.M. (1998). Serum mediated recognisation of liposomes by phagocytic cells of the reticuloendothelial system – The concept of tissue specificity. Adv. Drug Deliv. Rev., 32: 45–60.

13. Kreuter, J. (2005). Body distribution of polysorbate 80 and Doxorubicin loaded [14c] poly (butylcyanoacrylate) nanoparticles after i.v. administration in rats. J. Drug Target., 13(10): 535 – 542.

14. Suna, W.B., Xiea, C.B., Huafang Wang, H.C. and Hu,Y. (2004). Specific role of polysorbate 80 coating on the targeting of nanoparticles to the brain, Biomater., 25: 3065–3071.

15. Kreuter, J. Shamenkovb, D. Petrovb ,V. Ramge, P. Cychutekc , K. Koch-brandtd, C. and Alautdin,R.(2002). Apolipoprotein-mediated Transport of Nanoparticle-bound Drugs Across the Blood–Brain Barrier. J. Drug Target., 10 (4):317–325.

16. Ramge, P., Kreuter, J. and Lemmer, B. (1999). Circadian phase dependent anti-nociceptive reaction in mice after i.v. injection of Dalargin loaded nanoparticles determined by the hot plate test and the tail flick test. Chronobiol. Int., 17: 767 – 777.

17. Huang, L.S., Huo, L.B., Jiang, L.,Yan, Z.T.,Wang,Y.L. and Chen, Z.L. (2009). Antitumour activity of polysorbate 80 coated polybutylcyanoacrylate nanoparticles in vitro and its pharmacodynamics invivo on C6 glioma cells of a brain tumour model. Brain Res., 1261: 91-99.

18. Kurakhmaeva, K.B., Djindjikhashvili, I.A., Petrov, V.E., Balabanyan, V.U., Voronina, T.A., Trofimov, S.S., Kreuter, J., Gelperina, S., Begley, D. and Alyautdin, R.N. (2009). Brain targeting of NGF using polybutyl(cyanoacrylate) nanoparticles. J. Drug Target., 17(8): 564-574.

19. Nagpal, K., Singh, S.K. and Mishra, D.N. (2012).Nanoparticles mediated brain targeted delivery of Gallic acid in vivo behavioural and biochemical studies for improved antioxidant and antidepressant activity. Drug Deliv., 19 (8): 378-391.

20. Tahara, K., Kato, Y., Yamamoto, H., Kreuter, J. and Kawashima, Y. (2011). Intracellular drug delivery using polysorbate 80-modified poly (D, L-lactide-co-glycolide) nanospheres to glioblastoma cells.J. Microencap., 28 (1): 29-36.

21. Wilson, B., Samanta, M.K., Santhi, K., Kumar, K.P., Paramakrishnan, N. and Suresh, B. (2008).Targeted delivery of tacrine into the brain with polysorbate 80 coated poly (n-butylcyanoacrylate) nanoparticles. Eur. J. Pharm. Biopharm., 70(1): 75- 84.

22. Schroeder, U., Sommerfield, P. and Ulrichs, S. (1998). Nanoparticle technology for delivery of drugs across the blood brain barrier. J. Pharm. Sci., 87 (11): 1305-1307.

23. Kreuter, J. and Gelperina, S. (2008). Use of nanoparticles for cerebral cancer.Tumori, 94: 271-277.

24. Michaelis, K., Hoffmann, M.M., Dreis, S., Herbert,E., Alyautdin, R.N., Michaelis, M., Kreuter, J and Langer, K. (2006). Covalent linkage of apolipoprotein E to albumin nanoparticles strongly enhances drug transport into the brain. J. Pharmacol. Exp. Therap., 317: 1246-1253.

25. Olivier, C.J. (2005). Drug transport to brain with targeted nanoparticles. NeuroRx, 2(1): 108 – 119.

26. Sun, W.,Xie, C.,Wang, H. and Hu, Y. (2004). Specific role of polysorbate 80 coating on the targeting of nanoparticles to the brain.Biomater., 25: 3065-3071.

27. Garcia, E.G., Gil, S., Andrieux, K., Desmaele, D., Nicolas, V., Taran, F., Georgin, D., Andreux, J.P., Roux, F. and Couvereur, P. (2005). A relevant invitro rat model for the evaluation of blood brain barrier translocation of nanoparticles. Cell. Mol. Life Sci., 62(12): 1400-1408.

28. Olivier, C.J., Fenart, L.,Chauvet, R., Pariat, C., Cecchelli, R. and Couet, W. (1999). Indirect evidence that drug brain targeting using polysorbate 80 coated polybutyl-cyanoacryalte nanoparticles is related to toxicity.Pharm. Res., 16(12): 1836-1842.
29. Geldenhuys, W., Mbimba, T., Bui, T.,Harrison, K. and Sutariya, V. (2011). Brain targeted delivery of Doxorubicin using Glutathione coated nanoparticles for brain cancer. J. Drug Target, 19(9): 837-845.
30. Joshi, J.R. and Patel, R.P. (2012). Role of biodegradable polymers in drug delivery.Int.J.Cur. Pharm. Res., 4(4): 74-81.
31. Kaur, A., Jain, S. and Tiwary, A.K. (2008). Mannan coated gelatin nanoparticles for sustained and targeted delivery of Didanosine: in vitro and in vivo evaluation.Acta Pharm., 58 (1): 61-74.
32. Cui,Z., Hsu, C.H. and Mumper, R.J. (2003). Physical characterization and macrophage cell uptake of mannan-coated nanoparticles. Drug Dev. Ind. Pharm., 29: 689–700.
33. Kabanov, A.V. and Batrakova, E.V. (2004). New technology for drug delivery across the blood brain barrier.Cur. Pharm. Des., 10(12): 1355-1363.
34. Zhang W. and Fang X.L. (2008). Significant role of poloxamer in drug transport across Blood brain barrier. YaoXueXueBao, 43 (9): 890-897.
35. Petri, B., Bootz, A., Khalansky, A., Hekmatara, T., Müller, R., Uhl, R., Kreuter, J. and Gelperina, S . (2007). Chemotherapy of brain tumour using Doxorubicin bound to PBCA nanoparticles: revising the role of surfactants.J. Control. Rel., 117 (1): 51-58
36. Kamel, A.O., Awad, G.A.S., Geneidi, A.S. and Mortada, N.D. (2009). Preparation of Intravenous Stealthy Acyclovir Nanoparticles with Increased Mean Residence Time. AAPS PharmSciTech., 10(4): 1427–1436.
37. Donald, E., Owens, III and Peppas, N.A. (2006). Opsonisation, biodistribution and pharmacokinetics of polymeric nanoparticles. Int. J.Pharm., 307 (1): 93-102.
38. Dawaldi, G. and Sunderland, B. (2009). An ion pairing approaches to increase the loading of hydrophilic and lipophillic drugs into PEGylated PLGA nanoparticles. Eur. J. Pharm. Biopharm., 71 (2): 231-242.
39. Das, D. and Lin, S. (2005). Double coated poly (butylcyanoacrylate) nanoparticles drug delivery systems for brain targeting of Dalargin via oral administration. J. Pharm. Sci., 94(6): 134 –1353.
40. Brigger, I. (2002). Polyethylene glycol coated hexadecyanoacrylate nanospheres display a combined effect for brain tumour targeting.J. Pharmacol. Exp. Ther., 303 (3): 928-936.
41. Tosi, G., Costantino, L., Ruozi, B., Forni, F. and Vandelli, M.A. (2008). Polymeric nanoparticles for the drug delivery to the central nervous system. Exp. Opin. Drug Deliv., 5(2): 155-174.
42. Aliautdin, R.N., Petrov, V.E., Ivanov,A.A., Kreuter,J. and Kharkevich, D.A. (1996). Transport of the hexapeptide Dalargin across the hematoencephalic barrier into the brain using polymeric nanoparticles. Eksp Klin Farmakol, 59(3): 57-60.
43. Ali, J., Baboota, S., Ali, M., Sharma, V. and Bhavna. (2007). Preparation and characterisation of Chitosan nanoparticles for nose to brain delivery of a cholinesterase inhibitor. Ind.J.Pharm. Sci., 69:712-719.
44. Muthu, M.S. and Singh, S. (2008). Studies on biodegradable polymeric nanoparticles of Resperidone: Invitro and invivo evaluation. Nanomedicine (lond.), 3(3): 305-319.
45. Ren, T., Xu, N., Cao, C., Yuan, W., Yu, X., Chen, J. and Ren J. (2009). Preparation and therapeutic efficacy of polysorbate 80 coated Amphotericin B/PLA-b-PEG nanoparticles. J. Biomater. Sci., Polym. Ed., 20(10):1369-1380.
46. Muthu, M.S., Rawat, M.K., Mishra, A. and Singh, S. (2009). PLGA nanoparticle formulations of risperidone: preparation and neuropharmacological evaluation. Nanomedicine, 5(3): 323-333.

47. Mittal, G., Carswell, H., Brett, R., Currie, S. and Kumar, M.N.V.R. (2011). Development and evaluation of polymer nanoparticles for oral delivery of estradiol to rat brain in a model of alzheimer's physiology. J. Control. Rel., 150(2): 220 – 228.
48. Trapani, A., Denora, N., Iacobellis , G., Sitterberg, J., Bakowsky, U. and Kissel, T. (2011). Methotrexate loaded chitosan and glycolchitosan based nanoparticles: A promising strategy for the administration of the anticancer drugs to brain tumors. Am. Ass. Pharm.Sci. PharmSciTech., 12 (4): 1302-1311.
49. Herve, F., Ghinea, N. and Scherrmann, J.M. (2008). CNS delivery via absorptive transcytosis.Am. Ass. Pharm. Sci. J., 10(3): 455-472.
50. Mahapatro, A. and Singh, D.K. (2011). Biodegradable nanoparticles are excellent vehicle for site directed invivo delivery of drugs and vaccines. J. Nanobiotech., 9 (55): 1-11.
51. Jones, A.R. and Shusta, E.V. (2007). Blood-Brain Barrier Transport of Therapeutics via Receptor Mediation. Pharm Res., 24(9): 1759–1771
52. Kuo, Y.C., Lin, P.I. and Wang, C.C. (2011). Targeting nevirapine delivery across human brain microvascular endothelial cells using transferrin grafted poly (lactide–co–glycolide) nanoparticles. Nanomedicine (Lond.), 6(6): 1011-1026.
53. Gosk, S., Vermehren, C., Storm,G. and Moos, T. (2004). Targeting antitransferrin receptors antibody (ox26) and ox26 conjugated liposomes to brain capillary endothelial cells using insitu perfusion. J. cereb. Blood Flow Met., 24(11): 1193-1204.
54. Nafee, N., Bhardwaj, V. and Schneider, M. (2010). Transport Across Biological Barriers, In Nanotherapeutics: Drug Delivery Concepts in Nanoscience, edited by Alf Lamprecht, Pan Stanford publishing, Singapore 038988, pp 39-56
55. Carroll, R.T., Bhatia, D., Geldenhuys, W., Bhatia, R., Miladore, N., Bishayee, A. and Sutariya, V. (2010). Brain targeted delivery of Tempol loaded nanoparticles for neurological disorders. J. Drug Target, 18 (9): 665-674.
56. Aktas, Y., Yemisci, M., Andrieux, K., Gursoy, R.N., Alonso, M.J., Megia, E.F., Carballal, R.N.,Quinoa, E., Riguera, R., Sargon, M.F., Celik, H.M., Demir, A.S., Hincal, A.A., Dalkara, T., Capan, Y. and Couvreur, P. (2005). Development and brain delivery of chitosan PEG nanoparticles functionalised with the monoclonal antibody ox26. Biocon. Chem., 16(6): 1503-1511.
57. Mishra, V. (2006). Targeted brain delivery of Azitothymidine via transferrin anchored PEGylated albumin nanoparticles. J. Drug Target, 14 (1): 45-53.
58. Tosi, G., Ruozi, B., Badiali, L., Bondioli, L., Belletti, D., Forni,F. and Vandelli, M.A. (2012). Immunonanosystems to CNS pathologies: State of the Art. In: Sahoo, S.K., (Eds.) Nanotechnology in Health Care, Pan Stanford Publishing Pte. Ltd., 8 Tamasek Boulevard, Singapore, pp 107-168.
59. Jones, A.R. and Shusta, E.V. (2007). Blood Brain Barrier transport of therapeutics via receptor metabolism. Pharm. Res., 24 (9): 1759-1771.
60. Greenwood, J., Love, E.R. and Pratt, O.E. (1982). Kinetics of Thiamine transport across the Blood Brain Barrier in the rat. J. Physiol., 327: 95-103.
61. Lockmann, P.R., Oyewumi, M.O., Koziara, J.M., Roder, K.E., Mumper, R.J. and Allen, D.D., (2003). Brain uptake of thiamine coated nanoparticles. J. Control. Rel. 93 (3): 271-282.
62. Zlokovic, B.V. (1995). Cerebrovascular permeability to peptides: manipulation of transport system at the Blood Brain Barrier. Pharm. Res., 12(10): 1395-1406.
63. Re, F., Cambianica, I., Sesana, S., Salvati, E., Cagnotto, A., Salmona, M., Couraud, P.O.,

Moghimi, S.M., Masserini, M. and Sancini, G. (2010). Functionalization with ApoE derived peptides enhances the interaction with brain capillary endothelial cells of nanoliposomes binding amyloid beta peptide.J. Biotech., 156(4): 341-346.

64. Chen, W. (2011). Targeted brain delivery of Itraconazole via RVG29 anchored nanoparticles. J. Drug Target, 19 (3): 228-234.
65. Guarnieri, D., Falanga, A., Muscetti, O., Tarallo, R., Fusco, S., Galdiero, M., Galdiero, S. and Netti, P.A. (2012). Shuttle mediated nanoparticles delivery to brain. Small, 18 (43): 13678-13685.
66. Kim, J.Y., Choi, W.I., Kim, Y.H. and Tae, G. (2013). Brain targeted delivery of protein using chitosan and RVG peptide peptide conjugated, pluronic basenanocarriers. Biomater., 34 (4): 1170-1178.
67. Cerpentier, M. (1999). Receptor mediated transcytosis of Cyclophillin B through blood brain barrier. J. Neurochem., 73 (1): 260-270.
68. Rao, K.S., Reddy, M.K., Morning, J.L. and Labhasetwar, V. (2008). Tat conjugated nanoparticles for the CNS delivery of anti HIV drugs. Biomater., 29(33): 4429-4438.
69. Zensi, A., Begley, D., Pontikis, C., Legros, C., Mihoreannu, L. and Wagner, S. (2009). Albumin nanoparticles targeted with ApoE enter the CNS by transcytosis and are delivered to neurons. J. Control. Rel., 137 (1):78-86.
70. Kuo, Y.C., Lin, P.I. and Wang, C.C. (2011). Targeting nevirapine delivery across human brain microvascular endothelial cells using transferrin grafted poly (lactide–co–glycolide) nanoparticles. Nanomedicine (Lond.), 6(6): 1011- 1026.
71. Ulbrich, K., Knobloch, T. and Kreuter, J. (2011). Targeting the insulin receptors: nanoparticles for drug delivery across the blood brain barrier (BBB). J. Drug Target, 19 (2): 125- 132.
72. Chen, J., Zhang, C., Liu, Q., Shao, X., Feng, C., Shen, Y., Zhang, Q. and Jiang, X. (2012). Solanum tuberosum lectin conjugated PLGA nanoparticles for nose to brain delivery: *in vivo* and in vitro evaluation. J. Drug Target, 20(2): 174 -184.
73. Kuo, Y.C. and Chung, C.Y. (2012). Transcytosis of CRM197–grafted polybutylcyanoacrylate nanoparticles for delivery of Zidovudine across human microvascular endothelial cells. Colloids Sur. B: Bioint., 1(91): 242- 249.
74. Verma, A., Bansal, A.K., Ghosh, A. and Pandit, J.K. (2012). Low molecular mass chitosan as carrier for a hydrodynamically balanced system for sustained delivery of ciprofloxacin hydrochloride. Acta Pharm., 62: 237-250.
75. Remawi, M.M.A. (2012). Properties of chitosan nanoparticles formed using sulphate anions as crosslinking bridges. Am. J. Appl. Sci., 9 (7):1091-1100.
76. Rana, V., Babita, K., Goyal, D. and Tiwary, A.K. (2005). Sodium citrate crosslinked chitosan films: optimisation as substitute for human/rat/rabbit epidermal sheets. J. Pharm. Pharmaceut. Sci., 8(1):10-17.
77. Bhumkar, D.R. and Pokharkar, V.B. (2006). Studies on effect of pH on crosslinking of Chitosan with sodium tripolyphosphonate: A technical note. Am. Ass. Pharm. Sci. Pharm. Sci. Tech, 7(2): 138-148.
78. Tsai, S.P., Hseih, C.Y., Wang, D.H., Huang, L.L.H., Lai, J.Y. and Hseih, H.J. (2007). Preparation and cell compatibility evaluation of chitosan/ collagen composites scaffolds using amino acid as crosslinking bridges. J. Appl. Polym. Sci., 105: 1774-1785.
79. Ghananeem, A.L.A.M., Saeed, H., Florence, R., Yokel, R.A. and Malkawi, A.H. (2010). Intranasal drug delivery of Didanosine loaded Chitosan nanoparticles for brain targeting; an attractive route against infection caused by AIDS virus. J. Drug Target, 18 (5): 381-388.
80. Wang, Z.H., Wang, Z.Y., Sun, C.S., Wang, C.Y., Jiang, T.Y. and Wang, S.L. (2010). Trimethylated chitosan conjugated PLGA

nanoparticles for the delivery of drugs to the brain. Biomater., 31(5): 908-915.

81. Dhanya, K.P., Santhi, K., Dhanaraj, S.A. and Sajeeth, C.I. (2011). Formulation and evaluation of chitosan nanospheres as a carrier for the targeted delivery of Lamivudine to the brain. Pharmacie Globale. Int. J. Comprehen. Pharm., 2(5): 1-5.
82. Das, D. and Senshang L, S. (2005). Double-coated poly (butylcynanoacrylate) nanoparticulate delivery systems for brain targeting of dalargin via oral administration. J. Pharm. Sci., 94 (6).
83. Ren, T.A., Xu,N. B., Cao, C.A., Yuan, W.A., Yu, X.A.,Chen,J. B. and Ren, J. (2009). Preparation and Therapeutic Efficacy of Polysorbate-80-Coated Amphotericin B/PLA-b-PEG Nanoparticles, J. Biomater. Sci., 20 : 1369–1380.
84. Borgmann, K., Rao, K.S., Labhasetwar, V. and Ghorpade, A. (2011). Efficacy of Tat-conjugated ritonavir-loaded nanoparticles in reducing HIV-1 replication in monocyte-derived macrophages and cytocompatibility with macrophages and human neurons, AIDS Res Hum Retroviruses, 27(8):853-62.
85. Ghananeem, A.A.M., Saeed, H., Florence, R., Yokel, R.A. and Malkawi, A.H. (2010). Intranasal drug delivery of didanosine-loaded chitosan nanoparticles for brain targeting; an attractive route against infections caused by AIDS viruses. J Drug Target., 18(5):381-388.
86. Nye, J.S. and Snyder, S.H. (1987). Receptor-targeted drug delivery systems, WO 1987007150 A1.
87. Alyautdin, R.N., Karkevich, D.A., Kreuter, J. and Sabel, B. (1996). Drug targeting system, method for preparing same and its use, EP0740548 A1.
88. Huwyler, J. and Pardridge, W.M. (1998). Transport of liposomes across the blood-brain barrier, WO1998022092 A1.
89. Sabel, B.A. and Schroeder, U. (1998). Drug targeting system, method of its preparation and its use, WO1998056361 A1.
90. Gelperina, S., Kreuter, J., Sabel, B.A. and Schroeder, U. (2000). Use of drug-loaded nanoparticles for the treatment of cancers, WO2000074658 A1.
91. Pardrige,W.M. (2001). Non-invasive gene targeting to the brain, WO2001082900 A1.
92. Alyautdin, R.N., Kreuter, J., Langer, K. and Weber, C. (2002). Nanoparticles made of protein with coupled apolipoprotein e for penetration of the blood-brain barrier and methods for the production thereof, WO 2002089776 A1.
93. Pardrige, W.M. (2003). Non-invasive gene targeting to the brain, EP1282403 A1.
94. Balthasar, S. (2006). Support system in the form of protein-based nanoparticles for the cell-specific enrichment of pharmaceutically active substances, EP1722816 A2.
95. Cheifetz, P.M. (2006). Drug delivery formulations for targeted delivery WO2006125074 A1
96. Sung, M.H. (2010). Adjuvant composition comprising (poly-gamma-glutamate)-chitosan nanoparticles, WO2006125074 A1.
97. Liang, H,F., Sung, H.W. and Tu, H. (2011). Nano-particles for protein drug delivery, US 7863257 B2.
98. Papanicolaou, I. (2011). Encapsulation of biologically active agents, EP2273986 A2.
99. Gelperina, S., Khalanskiy, A., Kreuter, J. and Maksimenko, O. (2011). Polylactide nanoparticles, US8003128 B2.
100. Alyautdin, R.N., Kreuter, J., Langer, K. and Weber, C. (2011).Nanoparticles made of protein with coupled apolipoprotein Efor penetration of the blood-brain barrier and methods for the production thereof, EP1392255 B1.
101. Gaillard, P. J. (2013). Conjugates for targeted drug delivery across the blood-brain barrier, EP2308514 B1.
102. Dikpati, A., Madgulkar, A.R., Kshirsagar, S.J., Bhalekar, M.R. and Chahal, A.S. (2012). Targeted Drug Delivery to CNS using Nanoparticles, J.Adv.Pharm. Sci., 2(1):171-191.

Current Trends in Biotechnology and Pharmacy
Vol. 7 (4) 932-946 October 2013, ISSN 0973-8916 (Print), 2230-7303 (Online)

Current trends on the role of Copper on Conformational Polymorphism of DNA: Relevance to Human Health

M. Govindaraja[1,2] U.J.S. Prasada Rao[3], K.R.S. Sambasiva Rao[1] and KS Rao[4]*
[1]Department of Biotechnology, Acharya Nagarjuna University, Nagarjunanagar - 522 510, Guntur, A.P., India
[2]Indian Institute of Science, Bangalore – 560 080, India
[3]Department of Biochemistry and Nutrition, CSIR-Central Food Technological Research Institute, Mysore, India
[4]INDICASAT, City of Knowledge, Clayton, Republic of Panama
*For Correspondence – kjr5n2009@gmail.com

Abstract

Copper is one of the most prevalent biological transition metals, and plays a fundamental role in the biochemistry of the human nervous system. Without its catalytic presence, in trace or ultra trace amounts, many biochemical reactions would not take place. Copper becomes potentially toxic to cells when its concentration surpasses normal levels, because at higher concentrations, it generates free radicals (ROS). ROS damages DNA by breaking the DNA strands or modifying the bases and/or deoxyribose sugars, leading to conformational changes and stability of DNA. These conformational changes in DNA may lead to DNA stability in neurodegenerative disorders such as Alzheimer's disease and Parkinson's disease. In this review, we have focused on copper induced conformational change in DNA and DNA damage, and its implications on Alzheimer's disease.

Keywords: Trace metals, Alzheimer's disease, DNA polymorphism, oxidative stress, DNA damage, Parkinson's disease

Introduction

Metals play an important role in the biological processes of living systems and also in most of the chemical reactions in the body. They play a critical role in many of the enzymatic and metabolic reactions. Small deviations from normal levels of metals are recognized as symptoms of malfunctions or diseases (1). Several metals such as Na, K, Mg, Ca, and P present fairly at large concentrations and are known as macro-elements in organisms and are essential to serve as structural components of tissues of the body, and essential for the development and function of the brain (2,3). A second set of metals that are present in relatively small quantities are known as trace elements or trace metals; they control essential biological processes of living cells and without their catalytic presence many biological reactions would not take place. Their presence in optimum levels is very important in health point of view. Some of the examples for the trace metals are Fe, Cu, Mn, Zn, Co, Mo, Cr and I. Trace elements are grouped into three main categories: 1) Essential metals like Fe, Cu, Zn and Mn, which participate in the control of various metabolic and signaling pathways. 2) Beneficial, but not essential elements like F, V, Br and Li. 3) Pb, Cd, Hg, Ag and Al, which are not essential but associated with toxic effects (4-6).

Trace metals are very essential to help in a variety of important cellular events, such as catalysts for chemical reactions or electron transport during energy production. However, their rich coordination chemistry and redox properties are such that they are capable of escaping out of the control mechanisms such as homeostasis. A growing amount of results provide evidence that these metals interact with nuclear proteins and

DNA, and cause oxidative deterioration of these biological macromolecules (7). Due to their redox properties and importance, cells have evolved complex machinery for strict control of metal-ion homeostasis for the survival of living organisms (8). Metal ion transporters participate in maintaining the required levels of various metal ions in the cellular compartments (9). However, disruption of these mechanisms, or absorption of detrimental metals, alters the ionic balance and their chemical reactivity, and become harmful to the body. Oxidative damage to DNA and proteins can result in a disease state, including several neurodegenerative disorders such as Alzheimer's disease (10-12). Understanding the interactions of metal ions with various intracellular and extracellular components of the central nervous system is essential. The importance of copper for brain function and its role in human health is one of the most important current research areas. Hence, in the present review, the current trends on the role of copper on conformational and polymorphism of DNA with relevance to human health is discussed.

Copper Metabolism : Copper is the third most abundant transition metal in the body and the brain and second most important metal that may participate in oxygen-dependent physiological functions that serve to maintain normal cellular process (13). Copper exists physiologically in two oxidation states, as a divalent cupric [Cu(II)] extracellular circulating copper and as a monovalent cuprous [Cu(I)] intracellular. Changes in oxidation state make copper a paradoxical trace element. As a matter of fact, Cu(I) ↔ Cu(II), reversible transition can interchange between these forms by accepting or donating an electron. This allows the copper to participate in biochemical reactions as a reducing or oxidizing agent and can bind readily to many enzymes in both the oxidation states (14,15). Because of this dual role, copper can be essential or toxic depending on the oxidation states (16). Intracellular copper is not free but it is bound/ chelated to either transport proteins such as ceruloplasmin and copper-albumin, storage proteins (metallothioneins), or copper containing enzymes (17,18). Some of the copper dependent enzymes for the normal function of the cells and tissues are cytochrome c oxidase, Cu/Zn superoxide dismutase (SOD1), ceruloplasmin (Cp), and dopamine β-hydroxylase (Table 1). Either a deficiency or an excess of Cu can result in serious consequences to the organism. When the Cu concentration is insufficient, cells do not have enough copper for production of active enzymes, since Cu is important functional catalytic center for some enzymes. The decreased production of active enzymes leads to a decline of metabolic activity. For example, cytochrome c oxidase, involved in energy metabolism, is negatively affected by unusually low Cu concentrations since it does not produce active enzyme under these conditions. Therefore, the cell is unable to carry out its essential metabolic activity (19). In addition to the enzymes involved in energy metabolism, other enzymes are responsible for the removal of cellular free radicals is greatly affected when the available Cu is decreased. The clearest case for this is that of superoxide dismutase (SOD), which has Cu and zinc at its catalytic center (20). On the other hand, an excess of Cu is associated with oxidative stress and can be toxic at both the cellular and tissue level. Cu is generally found in its bivalent state (Cu^{2+}), but, in its monovalent form (Cu^{+}), it is able to transfer one electron and generate reactive oxygen species (ROS) such as hydroxyl radicals (21,22). These radicals are responsible for cellular damage due to protein oxidation, lipid peroxidation in membranes and DNA damage (Fig. 1).

In biology, copper is vital for cells because it participates directly in the biological processes, but can become toxic on overexposure. The toxicity of this metal makes them dangerous for the body at certain levels of micromolar concentration. Hence, controlled metal homeostasis is essential. Public health point of view, importance of its deficiency or excess in the human body is the subject of current research. It is estimated that an healthy adult human body

(70 kg) contains 110 mg of copper of which, 10 mg in the liver, 8.8 mg in the brain, 6 mg in the blood, 46 mg in the skeleton and bone marrow and 26 mg in the skeletal muscle (23). WHO recommended daily intake for adult body is around 1-1.6 mg which meets body needs. There is a continual turnover of copper with most of it being recycled. About 15% of the copper absorbed from the diet and the remaining 85% is excreted as bile; liver plays a central role in copper homeostasis. Copper is absorbed via the intestinal epithelium in to the blood circulation, where it is bound/chelated to the albumin, transcuprin or histidine and forms an exchangeable pool of Cu(II). Liver is a central organ in copper metabolism as it receives all dietary copper and regulates the whole body copper content by excretion in the bile. The balance between intracellular and extracellular content of copper is driven by cellular compartmentalization (24). The balance between copper necessity and toxicity is achieved both at the cellular and the tissue and organ levels. Cells regulate the traffic of copper ions and maintain the amount necessary

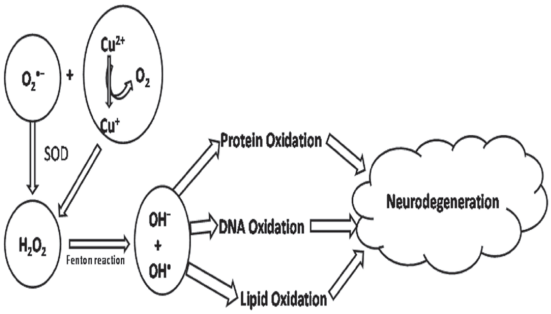

Fig. 1. Generation of free radicals and its machanism of induced Neurodegeneration,

Table 1. Some enzymes in humans that use copper a cofactor

Cu containing enzymes	Functions	Consequences of loss or deficiency
Tyrosinase	Synthesis of dopamine, epinephrine, norepinephrine which are the important neurotransmitters. It also assists the synthesis of melanin.	Loss of pigmentation : albinism
Dopamine β-hydroxylase	Norepinephrine synthesis	Hypoglycemia, hypotension
Ceruloplasmin	A carrier protein required for normal Fe metabolism and antioxidant production	Anemia, Neurodegeneration, Diabetes.
Cytochrome c oxidase	Energy production through electron transport chain in the mitochondria. Reduces oxygen to water in muscle and other tissues.	Respiratory deficiency, Encephalopathy, Cardiac failure
Cu/Zn Superoxide dismutase	anti-oxidant property/ Antioxidant defense	Oxidative stress, Neurodegeneration, Hepatocellular carcinoma
Lysyl oxidase	Covalent cross-linking of collagen and elastin	Arterial aneurysms, Cardiovascular dysfunction

for biological functions avoiding excess levels. Increase or decrease in the copper level in the cells due to failure of copper homeostasis may lead to many diseases including neurodegenerative disorders such as Alzheimer's disease. Copper levels in normal and AD brain are shown in table-2.

Copper and oxidative stress

Copper is a redox-active metal that participates in diverse metabolic processes in living organisms. Copper is known to have a definite role in the nucleus. It is an essential component of chromatin and is involved in chromatin scaffold proteins. Physiologically, it exists both as oxidized Cu (II) and as reduced Cu (I), and can bind readily to many enzymes in both oxidation states, preferentially via thiol groups (25). The cupric ion [Cu(II)] in the presence of superoxide anion radical can be reduced to cuprous ion [Cu(I)] and it is the most toxic ion, which can induce the production of more reactive ROS such as highly reactive hydroxyl radicals through the decomposition of hydrogen peroxide via the Fenton or Harber–Weiss reactions (26). Biomolecular damage may occur from the reaction of $O_2^{-\bullet}$ with copper (II) as follows.

$$Cu(II) + O_2^{\bullet-} \rightarrow Cu(I) + O_2$$

$$Cu(I) + H_2O_2 \rightarrow Cu(II) + OH^{\bullet} + OH^{-}$$

The hydroxyl radical is highly reactive with a half-life in aqueous solution of less than 1 nanosecond (27), hence, it instantaneously reacts with DNA, proteins, membrane lipids, resulting in extensive impairment of cellular functions. Interaction of $^{\bullet}OH$ with DNA causes severe damage to DNA, which ultimately leads

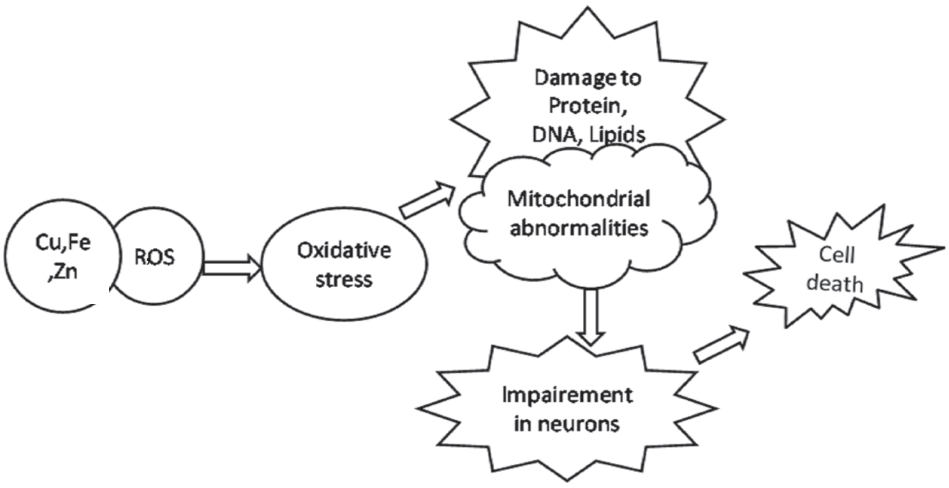

Fig. 2. Machanism of oxidative stress induced cell death

Table 2. Evidence for the metal Dyshomeostasis in Alzheimer's Disease (AD)

	Copper	Iron	Zinc
Control neuropil	4 μg/g	19 μg/g	23 μg/g
Total amyloid plaque	25 μg/g	53 μg/g	69 μg/g
AD neuropil	19 μg/g	39 μg/g	51 g/g

Source: Lovell, M. A., Robertson, J. D., Teesdale, W. J., Campbell, J. L. and Markesbery, W. R. (1998). Copper, Iron and Zinc in Alzheime's disease senile plaques. J. Neurol Sci., 158:47-52.

to mutations, such as strand breaks and oxidation of bases (28). It has been proposed that the extent of DNA strand breaking by $^{\bullet}OH$ is governed by the accessible surface areas of the hydrogen atoms of the DNA backbone. In intact cells, the damage to DNA may come from endogenous copper ions exposed to oxidants (Fig-2), which will affect adversely the biological processes, such as signal transduction and transcription.

Brain is vulnerable to oxidative stress, since it utilizes about 7.3% of total body copper, which is comparable to that of the liver (about 9%) (29,30). The brain comprises 2% of the total body mass, but it exhibits the highest rate of oxidative metabolism, consuming about 20% of total body oxygen inspired and carries out the ATP turnover at a high rate (31). Since approximately 5% of the oxygen consumed by cells is estimated to be reduced to ROS, relatively higher amounts of ROS may be generated in the brain as compared to other tissues that use less oxygen. Moreover, the brain is rich in poly-unsaturated fatty acids, amino acids and neurotransmitters, which are particularly susceptible to ROS damage (32-34). Paradoxically, the brain is endowed with disproportionately low levels of antioxidant activity, which makes it particularly susceptible to oxidative stress (35). Over exposure to oxidative radicals can adversely affect gene expression and basic metabolic processes (36). Increasing evidence suggests that oxidative stress is associated with normal aging, and neurodegenerative diseases such as AD, PD, Huntington's disease (HD) and ALS (37-40). Several studies suggest that mutations acquired during ageing by nuclear and mtDNA can contribute to physiological decline occurring with age and age-related neurodegeneration (41-42). Various studies report the action of copper-containing compounds in the induction of DNA damage. Becker *et al* (43) reported that the DNA strand breaks in PM2 phage DNA were induced by aliphatic and aromatic aldehydes in combination with $CuCl_2$. Therefore, the increased oxidative DNA damage may lead to DNA instability in neuronal cells. The decrease in anti-oxidant defenses and a reduction in base excision repair may contribute to reduced gene expression in the human brain. DNA damage may contribute to reduced gene expression (44), which may influence the rate of subsequent functional decline and the vulnerability of the brain to age-related neurodegenerative diseases.

Copper and Apoptosis : Copper is a redox active metal. Exposure of excessive copper to cells and tissues can result in acute damage to the cell membranes. This leads to loss of cell integrity and thereby cell death. Chronic excessive copper accumulation in brain and other organs lead to the production of reactive oxygen species (ROS). ROS are products of normal cellular metabolism and plays a dual role as both deleterious and beneficial species (45). Beneficial effects of ROS occur at moderate concentrations and involve physiological roles in cellular responses to noxia, in defense against infectious agents and in the function of a number of cellular signaling systems (46). The harmful effects of free radicals include oxidative stress and this occurs in biological systems when there is an overproduction of ROS on one side and a deficiency of enzymatic and non-enzymatic antioxidants on the other (47-49). Disturbances in the normal redox-state of cells can cause toxic effects through the production of highly reactive free radicals that damage to biological molecules inhibiting their normal function, which may be implicated in a number of human diseases as well as in the ageing process (50-52). Further, some reactive oxidative species act as cellular messengers in redox signaling. Thus, oxidative stress can cause disruptions in normal mechanisms of cellular signaling.

Over accumulation of copper in brain and other organs will increase in the rate of radical formation leading to several undesirable effects of proteins, lipids and DNA damage leading to cell death. This oxidative damage/stress is believed to be involved not only in the toxicity in the brain but also in the impairment in neuronal and endocrine function, which can lead to cell death (53). It is reported that the DNA damage in

AD brain occurs due to oxidative stress (54). Literature data and our un published data suggests that copper at the micromolar concentrations may lead to structural alterations in DNA that may cause the DNA damage and impairment in neurons, and ultimately neuronal cell death (apoptosis).

Copper induced DNA damage : ROS formed due to excess amount of copper in cells can damage cellular macromolecules, such as nucleic acids, lipids, and proteins (55). Hydroxyl radical is known to react with all components of DNA molecule in nucleus and mitochondria. It slots in to DNA double bonds of DNA bases as well as deoxyribose backbone, interacts with purine and pyramidine bases and also with the deoxyribose backbone, and causes permanent damage to DNA (56). Exposure of DNA to copper ions has been reported to result in single strand and double-strand breaks, affecting DNA-DNA and DNA-protein interaction and DNA base modification that could lead to alterations in transcription, incorporation of replication errors, genomic instability (57-59) and induction of signal transduction pathways (60). Several reports indicate that guanine is the most vulnerable to oxidative damage (61- 62). It is well established that $OH^{\bullet}$ radicals adds to position 8 in the ring structure of guanine in DNA, and forms an initial product called 8-hydroxy-2-deoxyguanosine radical (8OHdG) (63), which is a good biomarker of oxidative stress of an organism and a potential biomarker in the pathogenesis in Alzheimer's disease (64, 65). Oxidative genomic DNA modifications, oxidative damage and the induction of mutation in DNA may participate at multiple stages of neurological disorders. Because of the critical role of DNA in cellular function, oxidative damage to DNA may be one of the important factors in neuron degeneration in AD as reported by Nunomura *et al* (66). Copper ion induces significantly more DNA base damage, showing a propensity for guanine-containing regions (67). Copper is an important structural metal ion in chromatin, being present at about one copper ion per kilo base (68,69). For these reasons, there is increased interest in the ability of copper ion to participate in DNA damaging reactions *in vivo.* Mutation or disrupted expression of genes that increase DNA damage often result in premature aging. Oxidative DNA damage has effects on cells and is intermediate biomarkers of a disease, which plays a role in the etiology of neurological disorders.

Copper-induced conformational changes in DNA : DNA is a supercoiled negatively charged polymer of nucleotide units and found in cells usually as right handed double helix, B-DNA. The two strands have complementary sequences of nucleic acid bases, with the sugar-phosphate groups on the outside and the base pairs linked with the hydrogen bonding in the interior is inter twined in a helix. The positively charged copper ions interact directly or indirectly with the sites of negatively charged residues of DNA and it will result in conformational changes of the DNA structure. The binding sites on DNA could be the negatively charged phosphates of the backbone of both the strands and the electron donor atoms of the bases arranged in the helix. The predominant mode of copper binding takes place at the N7 and O6 of guanine and N1 of adenine bases and the N3 of cytosine bases, but copper will not bind to thymine. Binding of copper (II) ions to A-T base pairs is much less effective than binding to G-C base pairs. Copper is a redox trace metal essential for many biochemical processes. Because of the partially filled d-orbitals, they readily lose their water molecule and give inner sphere coordinated complexes (70). Reports of many authors show that copper binds directly to the bases and indirectly to the phosphate groups. Copper reacts chemically with the N_7 of guanine and N_3 of cytosine (71) and perturbs the double helix, which leads to the change of conformation and damage to the DNA. This change in conformation leads increased vulnerability to oxidation induced by ROS. It also damages the DNA through radical generation. It was theoretically postulated that the guanine base present in DNA would be more susceptible to $^{\bullet}OH$ radical induced conformational variations due to

overexposure to copper (72). When copper binds to stacked G-C base pairs, the DNA backbone conformation distorted and therefore, a change in conformation of B-DNA to an altered B-conformation takes place due to unwinding of the helix, which affects the DNA-protein interaction. The conformations of DNA and associated proteins are critical to the replication and transcription.

The conformational changes induced in native DNA by binding with copper (II) ions were of special interest, because it has been suggested that copper ions are able to regulate local DNA secondary structures. The B-form DNA are characterized by a positive long wavelength band at about 260–280 nm and a negative band around 245 nm. However, the position and amplitude of the CD bands show marked differences in terms of sequence diversity (73). Pertz *et al* (74) reported changes in DNA conformation in the presence of copper. Woisard *et al* (75) reported right handed B-DNA to Z-DNA (left handed helix) conformation conversions induced by copper and copper complexes. Poly d(GC).d(GC) oligonucleotide with alternating G-C sequence can exist in a left handed as well as a right handed conformation (76). Our study (77) and other studies (78,79) show that Al-maltolate induces the left handed Z-form of DNA with a characteristic negative band at 290 nm and a positive band at 270 nm and extremely deep negative band at 205 nm. Z-DNA has characteristic zig-zag phosphate backbone and the uniform alternating Watson-Crick base pairing is achieved by purines adopting syn conformation and C3'-endo sugar-pucker. Z-DNA forms excellent crystals. These features of major DNA conformations are summarized in Table-3 and CD spectral data is summarized in Table-4. CD changes of Z-DNA were also noticed in $(CCG)_{12}$ sequence (80) and scDNA (81). These findings may be applicable to DNA in the presence of copper. Thus, the interactions of Al and Cu with DNA at different sites can lead to a variety of changes in DNA structure.

The stability of the DNA double helix is very important for DNA structure; slight variations in the DNA sequence can have profound implications on the stability of the DNA. In addition to hydrogen bonding, base stacking, interaction with copper(II) ions with DNA plays an important role in DNA duplex stability (82). At higher concentrations of Cu(II) ions and increased temperatures, an increase in T_m was observed due to DNA damage, which was resulted due to perturbation of DNA base stacking (83)

Supercoiling is an important aspect of DNA physiology in both prokaryotes and eukaryotic cells. Supercoiling-induced alterations in DNA structure and dynamics could affect the interaction with Copper. Copper preferentially binds to N_7 atom of guanine and at least is capable of forming chelation complexes with the O_6 in the same guanine and with other nearby bases resulting the 8-oxoG and strand breaks. Copper bind to G-C bases and breaks the hydrogen bonds between bases, thus tilts the bases leading to conformational change from B-DNA to C-DNA (84). The binding of copper to DNA leads to DNA damage through radical generation from oxidation by H_2O_2 (85). Double strand breaks, cross-linking and mispairing of DNA as a result of oxidative DNA damage have shown the positive role of aberrant copper. These changes in DNA conformational effects have important implications for genetic information transfer and activity of RNA polymerase. Conformation of the DNA is important for the normal activities of the cellular processes (86). Any change caused by Cu or Al in the conformation of DNA, alters the ability of the DNA to act as a template for RNA synthesis that also affects the function of neurons and the neurotoxic effects (87).

Dopamine is one of the neurotransmitters and plays an important role in neuronal function. In PD, dopaminergic neuronal cell loss is observed, which alters the levels of dopamine contributing to movement disorders. Even though it is an essential neurotransmitter required for the neuronal function, at high concentrations it

Vol. 7 (4) 932-946 October 2013, ISSN 0973-8916 (Print), 2230-7303 (Online)

becomes cytotoxic in the presence of copper and induces oxidative stress leading to DNA damage (88, 89). Several groups showed a possible link between copper-mediated oxidative DNA damage and dopaminergic neuronal cell death (90, 91). It is reported that dopamine content in CSF is 30± 6 pg/ml in AD, compare to that of the normal 10± 6 pg/ml. Dopamine induced DNA damage in the presence of Cu(II) ions normally takes place in the brain leading to dopaminergic neuronal cell death (92). Copper induced conformational changes in DNA are more progressive in the presence of dopamine, and can significantly disturb neurotransmission in a more systematic manner in the brain of AD patients and thus play an important role in neuropathology of AD and PD.

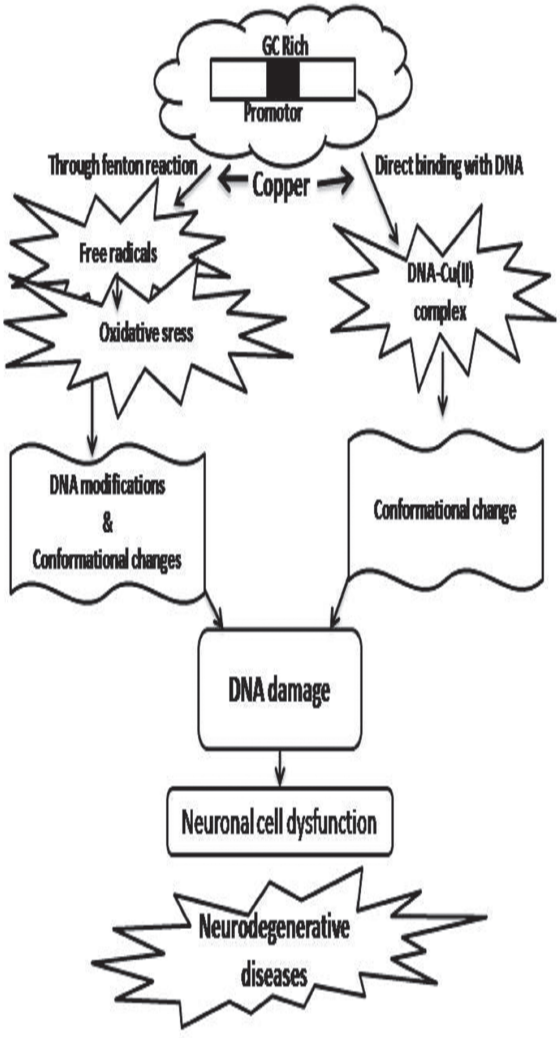

Fig. 3. Copper interaction with scDNA involved in copper mediated genotoxicity as well as oxidative damage via different mechanisms in brain cells

Effect of copper on gene expression and health : DNA conformations play a vital role in gene expression (93). B-DNA a predominant conformation participates in the gene expression. Any conformational change in the region of the gene is likely to have a profound effect on the transcription (94). Among the altered conformations, altered B-DNA and Z-DNA are observed in the promoter region of specific genes and correlated to their expression patterns (95). Copper dependent transcription factors regulate transcription of specific genes (96, 97). Genes regulated by copper-dependent transcription factors include genes for copper/Zinc superoxide dismutase (Cu/Zn SOD), catalase and proteins related to the cellular storage of copper. In yeast, copper promotes expression of enzymes protecting against oxidative stress, while it suppresses expression of genes that transport copper in to cells (Ctr1 and Ctr3) as well as reductases. Cleavage of the DNA strand by copper induced oxidative damage has the ability to cause the conformational change and become toxic to cells (98, 99). DNA damage in the brain has been implicated in a number of neurodegenerative diseases, such as Alzheimer's disease (AD).

SOD-1 has a major role in the defense against oxidative stress by catalyzing the dismutation of $O_2^{\cdot-}$ to molecular oxygen (O_2) and H_2O_2 using copper as cofactor, which can be converted by catalase and glutathione peroxidase (GPX) to water. Imbalance in the ratio of the reaction, results in the accumulation of H_2O_2. A recent observation reveals that SOD-1 forms proteinaceous aggregates that are related with senile plaques in AD brain and these are implicated the involvement of oxidative damage to SOD-1 in the AD pathogenesis (100). Enhanced antioxidant enzyme activity may affect

the gene expression by altering the binding and/or availability of transcription factors such as nuclear factor kappaB (NFκB) (101) and the activator protein AP-1 (102) to DNA.

In humans, two Cu(I)-ATPases, ATP7A and ATP7B are expressed in all the tissues, particularly in the brain and the heart. ATP7B is predominant in liver and expressed in small amounts in brain and in both the genes mutations were discovered. The importance of ATP7A and ATP7B in copper homeostasis is illustrated by two genetic diseases, arising from these mutations, which promote the dysfunction of the ATPases and are sources of severe diseases, the Menks syndrome for ATP7A and the Wilson disease for ATP7B (103,104). Menkes disease occurs due to copper accumulation in intestinal cells and copper deficiency in blood. As a result, essential cuproenzymes lack their cofactor and death occurs during early childhood (105). The Wilson disease results in copper overload in the liver and brain with risk of cirrhosis and neurological problems, and this disease is fatal in the absence of treatment. Both deficiency and overload of copper in human body has a consequence on health. B-DNA is a highly variable structural form of the DNA double-helix, and the sequence dependent structural variations play a critical role in protein recognition and binding. Changes in DNA conformation (altered B-DNA, A-DNA, CDNA and Z-DNA) can potentially affect various

Table 3. Structural parameters of DNA helices

Structural parameters	A-DNA	B-DNA	Z-DNA
Direction of helix rotation	Right handed	Right handed	Left handed
Residue per helical turn	11	10.5	12
Axial rise per residue	2.55A°	3.4A°	3.7A°
Pitch (length) of the helix	2.82A°	3 4A°	44.4A°
Base pair tilt	20°	-6°	7°
Rotation per residue	32.7°	34.3°	-30°
Diameter of helix	32A°	20A°	18A°
Back bone	Altered smooth path	Smooth path	Zigzag path
Configuration	Anti	Anti	Anti
Glycosidic bond	Anti	Anti	Syn
Sugar puckering	C3' endo	C2' endo	C2' endo

Source: Sinden, R.R (1994). DNA structure and Function. Academic press Inc , London p.27

Table 4. Copper-induced conformational changes in DNA

Conformation	CD at Wavelength		
	~240-250 nm	~260-270 nm	~280-290 nm
A-DNA	Weakly negative	Strongly positive	Strongly positive
B-DNA	Negative	Zero	Positive
C-DNA	Negative	Positive	Positive
Z-DNA	Positive	Positive	Negative
Ø-DNA	———-	Negative	Negative

DNA reactions, including replication, transcription and epigenetic modifications (106), which may cause diseases in humans.

Conclusions

Copper exists in the cell nucleus at a relatively high concentration and closely associated with chromosomes and bases. Copper ions bind to the DNA, leads to DNA damage in two mechanisms. The "direct" damage may involve conformational changes of DNA. On the other hand, "indirect" damage is a consequence of copper induced formation of reactive oxygen species involving superoxide is shown in Fig. 3. B-DNA conformation is essential for the normal activities of the cell. Any variations in the conformation leads to changes in DNA conformation (altered B-DNA, A-DNA, C-DNA and Z-DNA), which can potentially affect various DNA reactions, including replication, transcription and epigenetic modifications. These conformational variations will have a biological importance in relevance to the brain disorders. Copper and its impact on the conformations of nucleic acids and production of ROS emphasizes the role of copper in the brain disorders, including Alzheimer's disease and Parkinson's disease. The histone and non-histone proteins present in chromatin protect the bases in DNA from oxidative DNA damage.

References

1. Shier, D., Buttler, J. and Lewis, R. (1996), Hole's Human Anatomy & Physiology, 10th ed., McGraw-Hill, Boston,
2. Mertz, W. (1981), The essential trace elements. Science, 213: 1332-1338.
3. Bray, A., Lews, J. and Walter, R.R. (1998), Essential Cell Biology. An Introduction to the Molecular Biology of the Cell, Garland Publishing, Inc, New York,
4. Whitefield, J.B, Dy, V., Mcquilty, R, Gu, Z., Health, A.C, Montgomery, G.W. and Martin, N.G. (2010), Genetic effects on toxic and essential elements in humans: Ar, Cd,Cu,Pb,Hg,Se,and Zn in erythrocytes. Environ. Health Perspect., 118:776-782.
5. Xiu, Y.M. (1996). Trace elements in health and diseases. Biomed. Environ. Sci., 203:130-136.
6. O'Corner, (2001), Trace elements and DNA damage. Biochem. Soc. Trans., 29:354-357.
7. Leonord, S.S., Harris, G.K. and Shi, X. (2004), Metal induced oxidative stress and signal transduction. Free. Radic. Biol. Med., 37:1921-42.
8. Bertini, G., Cavallaro, G. (2008), Metals in the "omics" world: copper homeostasis and cytochrome c oxidase assembly in a new light, J. Biol. Inorg. Chem., 13: 3–14.
9. Rolfs, A. and Hediger, M.A. (1999), Metal ion transporters in mammals: structure, function and pathological implications, J. Physiol., 518:1-12
10. Halliwell, B. and Gutteridge,J.M.C. (1990), Role of free radicals and catalytic metal-ions in human disease-an overview, Methods Enzymol., 186: 1–85.
11. Zacca, L., Youdim, M.B., Riederer, P., Connor J.R. and Crichton, R.R. (2004), Iron, Brain aging and neurodegenerative disorders, Nat. Rev. Neurosci., 5: 863-873.
12. Bayani, U., Singh, A V., Zamboni P., and Mahajan, R.T. (2009), Oxidative stress and neurodegenerative diseases: A review of upstream and downstream antioxidant therapeutic options. Curr. Neuropharmacol., 7 :65-74.
13. Frausto da Silva, J.J.R. and Williams, R.J.P. (2001), The Biological Chemistry of the Elements, Ed 2. Oxford University Press, New York.
14. Alberts, B., Bray, D., Lewis, J, Raff, M., Roberts, K. and Watson, J. D. (1994), Molecular Biology of the cell, 3rd edn. Garland Publishing Inc, New York & London.
15. Bonda, D.J,, Lee, H.G., Blair, J.A., Zhu, X., Perry, G. and Smith, M.A. (2011), Role of metal dyshomeostasis in Alzheimer's disease. Metallomics, 3:267-270.

16. Cuillel, M. (2009), The duel personality of ionic copper in biology. J. Incl. Phenom. Macrocycl. chem., 65:165-170.

17. Solomons, N.W. (1985), Biochemical, metabolic, and clinical role of copper in human nutrition. J. Am. Coll. Nutr., 4 : 83-105.

18. Ranganathan, P.N., Lu, Y., Jiang, L., Kim, K. and Collins, J.F. (2011), Serum ceruloplasmin protein expression and activity increases in iron-deficient rats and is further enhanced by higher dietary copper intake. Blood, 118:3146-3153.

19. Dimauro, S., Lombes, A., Nakase, H. (1990), Cytochrome c oxidase deficiency. Pediatr. Res., 28:536-541.

20. Rosen, D.R., Siddique, T., Patterson, D., Fiqlewicz, D.A., Sapp, P., Hentati, A., Donaldson, D. and Goto, J. (1993), Mutations in Cu/Zn superoxide dismutase gene are associated with familial amyotrophic lateral sclerosis. Nature, 362:59-62.

21. Pal, A,, Badval, R,K, Vasishta, R,K,, Attri, S.V., Thapa BR, Prasad., R. (2013), Biochemical, histological and memory impairement effects of chronic toxicity: a model for non-wilsonian brain copper toxicosis in wistar rat. Biol. Trace. Elem. Res., 153:257-268.

22. Halliwell, B. and Gutteridge, J.M. (1984), Oxygen toxicity, oxygen radicals, transition metals and disease. Biochem. J., 219:1-14.

23. Linder, M.C., Wooten, L., Cerveza, P., Cotton, S., Shulza, R. and Lomeli, N. (1998), Copper transport. Am. J. Clin. Nutr., 67: 965S-971S.

24. Harris, C.D. (1991), Copper transport: An overview. Proc. Soc. Exp. Biol. Med., 196:130-140.

25. Linder, M.C., Hazegh-Azam, M. (1996), Copper biochemistry and molecular biology. Am. J. Clin. Nutr., 63:797S-811S.

26. Cooke, M S, Evans, M.D., Dizdaroglu, M., and Lunec, J. (2003), Oxidative DNA damage: Mechanisms, mutation and disease. FASEB J., 17: 1195-1214.

27. Pastor, N., Weinstein, H., Jamison, E. and Brenowitz, M. A. (2000), Detailed interpretation of OH radical footprints in a TBP-DNA complex reveals the role of dynamics in the mechanism of sequence specific binding. J. Mol. Biol., 304: 55–68.

28. Halliwell, B. (1994). Free radicals, antioxidants, and human disease: curiosity, cause, or consequence? Lancet, 344 : 721-724.

29. Wang, X. and Michaelis, E.K. (2010), Selective Neuronal Vulnerability to Oxidative Stress in the Brain. Front. Aging Neurosci., 2: 1-13.

30. Gaggelli, E., Kozlowski, H., Valensin, D. and Valensin, G. (2006), Copper Homeostasis and Neurodegenerative Disorders (Alzheimer's, Prion, and Parkinson's Diseases and Amyotrophic Lateral Sclerosis). Chem, Rev., 106:1995–2044.

31. Swaminathan, N. (2008), Why does the brain need so much Power? Sci Am. 298: 78-9.

32. Gilgun-Sherki, Y., Melamed, E., Offen, D. (2001), Oxidative stress induced-neurodegenerative diseases: the need for antioxidants that penetrate the blood brain barrier. Neuropharmacology, 40: 959–975.

33. Perry, G., Nunomura, A. and Hirai, K. (2002), Is oxidative damage the fundamental pathogenic mechanism of Alzheimer's and other neurodegenerative diseases? Free Radic. Biol.Med., 33:1475–1479.

34. Benzi, G. and Moretti, A. (1995), Are ROS involved in AD. Neurobiol. Aging., 16: 661-674.

35. Floyd, R.A. (1999), Antioxidants, Oxidative Stress, and Degenerative Neurological Disorders. Proc. Soc. Exp. Biol Med., 222:236-245.

36. Potashkin, J.A, and Meredith, G.E. (2006), The role of oxidative stress in the

dysregulation of gene expression and protein metabolism in neurodegenerative disease, Antioxid. Redox Signal. 8:144–151.

37. Weissman, L. de Souza-Pinto, N.C. Stevnsner, T. and Bohr, V.A. (2007), DNA repair, mitochondria, and neurodegeneration, Neurosci., 145: 1318–1329.

38. Halliwell, B. (2006), Oxidative stress and neurodegeneration: where are we now? J. Neurochem., 97: 1634–1658.

39. Cui, K., Luo, X., Xu, K., Ven Murthy,M.R. (2004), Role of oxidative stress in neurodegeneration: recent developments in assay methods for oxidative stress and nutraceutical antioxidants. Prog Neuro. psychopharmacol Biol. Psychiatry., 28:771-799.

40. George, P., Sayre, L.M., Atwood, C.S., Castellani, R.J., Cash, A. D., Rottkamp, C.A., Smith, M.A. (2002), The Role of Iron and Copper in the etiology of Neurodegenerative Disorders: Therapeutic Implications. CNS Drugs, 16:339-352.

41. Lin, M. T. and Beal, M. F. (2006), Mitochondrial dysfunction and oxidative stre ss in neurodegenerative diseases, Nature, 443:787–795.

42. Wang, J., Xiong, S., Xie, C.. Markesbery, W. R. and Lovell, M.A. (2005), Increased oxidative damage in nuclear and mitochondrial DNA in Alzheimer's disease, J. Neurochem. 93:953–962.

43. Becker, T. W., Krieger, G. and Witte, I. (1996), DNA Single and Double Strand Breaks Induced by Aliphatic and Aromatic Aldehydes in Combination with Copper(II). Free Radic. Res. 24: 325-332.

44. Myhre, O., Utkilen, H., Duale, N., Brunborg, G. and Hofer, T. (2013), Metal dyshomeostasis and inflammation in Alzheimer's disease and Parkinson's disease: Possible impact of environmental exposures. Oxid. Med. Cell. Longey., 2013: 726954-726972.

45. Valko, M., Rhodes, C. J., Moncol, J., Izakovic, M., and Mazur, M. (2006), Free radicals, metals and antioxidants in oxidative stress-induced cancer. Chem. Biol. Interact., 160:1-40.

46. Alfadda, A.A. and Sallam, R.M. (2012), Reactive Oxygen species in Health and disease. J Biomed & Biotech, 2012: 1-14.

47. Kovacic, P., and Jacintho, J. D. (2001), Mechanisms of carcinogenesis: Focus on oxidative stress and electron transfer. Curr. Med. Chem., 8:773–796.

48. Valko, M., Morris, H., Mazur, M., Rapta, P., and Bilton, R. F. (2001), Oxygen free radical generating mechanisms in the colon: Do the semiquinones of Vitamin K play a role in the aetiology of colon cancer? Biochim. Biophys. Acta., 1527:161–166.

49. Valko, M., Rhodes, C. J., Moncol, J., Izakovic, M., and Mazur,M. (2006), Free radicals, metals and antioxidants in oxidative stress-induced cancer. Chem. Biol. Interact., 160:1-40.

50. Roberts, B.R., Ryan, T.M., Bush, A.I., Masters, C.L. and Duce, J.A. (2012), The role of metallobiology and amyloid-â Peptides in Alzheimer's disease. J. Neuro Chem. 120, (suppl 1):149-166.

51. Gaggelli, E., Kozlowski, H.,Valensin, D. and Valensen, G. (2006). Copper homeostasis and neurodegenerative disorders (Alzheimer's, prion, and Parkinson's diseases and amyotrophic lateral sclerosis). Chem. ReV. 106, 1995-2044.

52. Brewer, G.J., (2010), Risks of copper and iron toxicity during aging in humans. Chem. Res. Toxicol. 23, 319–326.

53. Uttara, B., Singh, A.V., Zamboni, P. and Mahajan, R.T. (2009), Oxidative stress and neurodegenerative diseases: A review of upstream and downstream antioxidant therapeutic options. Curr. Neuropharmacol., 7: 65-74.

54. Butterfield, A., Jennifer, D. D, Pocernich, C., and Castegna, A. (2001), Evidence of oxidative damage in Alzheimer's disease brain: central role for amyloid β-peptide. Trends Mo.l Med,7: 548-554.

55. Valko, M., Rhodes, C. J., Moncol, J., Izakovic, M., and Mazur,M. (2006). Free radicals, metals and antioxidants in oxidative stress-induced cancer. Chem. Biol. Interact., 160:1-40.

56. Dizdaroglu, M., Jaruga, P., Birincioglu., M. Rodriguez., H. (2002), Free radical–induced damage to DNA: mechanisms and measurement. Free Radic. Biol. Med. 32:1102-1115.

57. Halliwell, B., Aruoma, O. I. (1991), DNA damage by oxygen-derived species. FEBS Lett. 281:9-19.

58. Dizdaroglu, M. (1992), Oxidative damage to DNA in mammalian chromatin. Murat. Res. 275:331-342.

59. Sohal, R.S., Weindruch, R. (1996), Oxidative stress, caloric restriction, and aging. Science, 273:59–63.

60. Cooke, M.S., Evans, M.D., Dizdaroglu, M. and Lunec, J. (2003), Oxidative DNA damage: mechanisms, mutation and disease, FASEB J. 17 :1195–1214.

61. Dizdaroglu, M., Jaruga, P., Birincioglu, M., and Rodriguez, H. (2000), Free radical-induced damage to DNA: mechanism and measurement. Free.Radic.Biol.Med., 32:1102-1115.

62. Birincioglu, M., Jaruga, P., Chowdhury, G., Rodriguez, H., Dizdaroglu, M. and Gates, K.S. (2003), DNA base damage by the antitumer agent 3-amino-1, 2, 4-benzotriazine 1, 4-dioxide. J. Am. Chem. Soc, 125:11607-11615.

63. Kasai, H. (2002), Chemistry–based studies on oxidative DNA damage: formation, repair and mutagenesis. Free Radic. Biol. Med., 33:450-456.

64. Mecocci, P., MacGarvey, U., Kaufman, A. E., Koontz, D., Shoffner, J.M., Wallace, D.C. and Beal, M.F. (1993). Oxidative damage to mitochondrial DNA shows marked age-dependent increases in human brain, Ann. Neurol., 34: 609-616.

65. Mecocci, P., MacGarvey, U. and Beal, M. F. (1994), Oxidative damage to mitochondrial DNA is increased in Alzheimer's disease Ann. Neurol. 36:747-751.

66. Nunomura, A., Perry, G., Pappolla, M. A., Wade, R., Hirai, K., Chiba, S. and Smith, M.A. (1999), RNA oxidation is a prominent feature of vulnerable neurons in Alzheimer's disease. J. Neurosci. 19:1959-1964.

67. Kawanishi, S., Hiraku, Y. and Ooikawa, S. (2001), Mechanism of guanine-specific DNA damage by oxidative stress and its role in carcinogenesis and aging. Mutat. Res., 488:65-76.

68. Bryan, S. E., Vizard, D. L., Beary, D.A., Labiche, R.A., Hardy, K.J. (1981) Partitioning of zinc and copper within subnuclear nucleoprotein particles. Nucleic Acids Res. 9:5811-5823

69. Lewis, C.D., Laemmli, U.K. (1982), Higher order metaphase chromosome structure: Evidence for metalloprotein interactions. Cell, 29:171-181.

70. Anastassopoulou, J. (2003), Metal –DNA ineractions, J. Mol. structure, 651-653:19-26.

71. Gao,Y.G., Sriram, M and Wang, A.H, (1993), Crystallographic studies of metal ion-DNA interactions: different binding modes of cobalt(II),copper(II) and barium(II) to N7 of guanines in Z-DNA and a drug-DNA complex. Nucleic Acids Res. 21:4093-4101.

72. Jomova, K., Vondrakova, D., Lawson, M., Valko, M. (2010), Metals, oxidative stress and neurodegenerative disorders. Mol. cell Biochem., 345:91-104.

73. Alexeev, D. G., Lipanov, A. A., Skuratovskii, I. (1987), Poly (dA) ·poly (DT) is a B-type double helix with a distinctively narrow minor groove. Nature, 325: 821–823.

74. Pritz, W. A, Butler, J and Land, E. J. (1990), Interaction of copper (I) with nucleic acids. Int. J. Radiat. Biol. 58:215-234.

75. Woisard, A,. Fazakerley, G. V. and Guschlabauer, W. (1985), Z-DNA is Formed by poly (dC-dG) and poly (dm5C-dG) at micro or nanomolar Concentrations of some zinc (II) and copper (II) complexes. J. Biomol. Struct. Dyn. 2: 1205-1220.

76. Wang, A. H. J., Quigley, G. J., Kolpak, F. J., Vandermarel, G., Vanboom, J. H., Rich, A. (1981), Left-handed double helical DNA-variations in the backbone conformation. Science, 211:171-176.

77. Govindaraju, M., Monica, F. S., Berrocal, R., Sambashiva Rao, K. R. S. and Rao, K. S. (2012), First evidence for Al-maltol driven B to Z-DNA conformational transition in poly d(GC.d(GC): relevance to Alzheimers disease. Current trends in biotechnology and Pharmacy, 6: 204-209.

78. Ivanov, V. I., Minyat, E.E. (1981), The transitions between left- and right-handed forms of poly (dG-dC).Nucleic Acids Res., 9: 4783–4798.

79. Lezius, A.G. and Gottschalk, E.M. (1970), A reversible cooperative conformational change of a synthetic DNA under the influence of high salt concentrations. Hoppe-Seylers Z. Physiol. Chem., 351:413-416.

80. Latha, K.S., Anitha, S., Rao, K.S. and Viswamitra, M.A. (2002), Molecular understanding of Al-induced topological changes in (CCG)12 triplet repeats: relevance to neurological disorders, Biochem. Biophys. Acta., 1588: 56-64.

81. Hegde M L., Anitha, S., Latha, K.S., Mustak, M.S., Stein, R., Ravid, R. and K.S.J. Rao. (2004), First evidence for helical transitions in supercoiled DNA by amyloid-α peptide (1-420 and aluminum. J. Mol. Neurosci. 22: 19-31.

82. Lyras, L., Cairns, N. J., Jenner, P., Halliwell, B. (1997). An assessment of oxidative damage to proteins, lipids and DNA in brain from patients with Alzheime's disease. J. Neurochem, 68: 2061-2069.

83. Trumbore, C N, Ehrlich, R S., and Myers, Y N.,(2001), Changes in DNA Conformation Induced by Gamma Irradiation in the Presence of Copper. Radiation Res. 155:453-465.

84. Ibanez, S., Alberti, F.M., Pablo, J., Miguel, S. and Lippert, B. (2011), Exploring the metal coordination properties of the pyrimidine part of purine nucleobases: Isomerization reactions in heteronuclear Pt(II)/Pd(II) of 9-methyladenine. Inorg. Chem. 50: 10439-10447.

85. Prasal, Z. (1986), Structural organization of copper (II) ions in complexes with DNA,. Acta Biochim. Pol. 33:153-167.

86. Ghosh, A., Bansal, M. A. (2003). Glossary of DNA structures from A to Z. Acta crystallogr D Biol. Crystallogr., 59:620-626.

87. Suram, A., Rao, K.S., Latha, K.S, Viswamitra, M.A. (2002), First evidence to show the topological change of DNA from B-DNA to Z-DNA conformation in the hippocampus of Alzheimer's brain. Neuromolecular Med., 2: 289-297.

88. Hastings, T G., Lewis, D. A. and Zigmond, M J. (1996), Role of oxidation in the neurotoxic effects of intrastriatal dopamine injections. Proc. Natl. Acad. Sci. U.S.A., 93:1956-1961.

89. Sayre, L M., Moreira, P. I., Smith, M.A. and Perry, G. (2005), Metal ions and oxidative protein modification in neurological disease, Ann.1st.Super Sanita, 41:143-164.

90. Oikawa, S., Hiresawa, I., Tada-aoikawa, S., Furukawa, A., Nishiura, K., Kawanishi,S,

(2006). Mechanism for manganese enhancement of dopamine-induced oxidative DNA damage and neuronal cell death. Free Radic. Biol, Med., 41:748-756.

91. Modorikawa, K., Uchida, T., Okamota, Y., Toda, C., Sakai, Y., Ueda, K., Hiraku,Y., Murata, M., Kawanishi, S. and Kojima, N. (2004), Metabolic activation of carcinogenic ethylbenzene leads to oxidative DNA damage. Chem. Biol. Interact., 150:271-281.

92. Li, Y., Cao, Z. (2002). The neuroprotectant ebselen inhibits oxidative DNA damage induced by dopamine in the presence of copper ions. Neurosci. Lett. 330:69–73.

93. Bacolla, A., Wojciechowska. M, Kisminder, B., Larson, J.E. and Wells, R.D. (2006), The involvement of non-DNA structures in gross chromosomal rearrangements. DNA Repair (Amst), 5: 1161-1170.

94. Niu, Y., Ding, L., Rao, P.N., Braun, R., Yang, J.H. (2005), ADAR1 interacts with NF90 through double stranded RNA and regulates NF90-mediated gene expression independently of RNA editing. Mol, Cell. Biol., 25: 6956-6963.

95. Hassette, R., Kosman, D. J. (1995). Evidence for Cu(II) reduction as a component of copper uptake by Saccaharo-myces cervevisae. J. Biochem, 270:128-134.

96. Eide, D.J. (1998), Molecular biology of metal ion transport in Saccaharomyces cervevisae. Annu. Rev.Nutr.18:441-469.

97. Andersen, J.K. (2004), Oxidative stress in neurodegeneration: cause or consequence? Nat Rev. Neurosci., 10:S18-25.

98. Liu, J., Li, Q., Yu, Y. and Fang, X. (2003), Spectroscopic and electroscopic studies of DNA breakage induced by dopamine and copper ion. Anal. Sci., 19:1099-1102.

99. Choi, J., Rees, H.D., Weintraub, S.T., Levey, A.I., Chin, L.S., Li, L. (2005), Oxidative modifications and aggregation of Cu, Zn-superoxide dismutase associated with Alzheimer and Parkinson diseases. J Biol Chem; 280:11648–55.

100. De Haan, J.B., Cristiano, F., Iannello, R.C. and Kola, I. (1995), Cu/Zn-superoxide dismutase and glutathione peroxidase during aging. Biochem. Mol. Biol. Int., 35:1281–97.

101. Abate, C,, Patel, L., Rauscher, III F.J., Curran, T. (1990), Redox regulation of FOS and Jun DNA-binding activity in vitro. Science, 249:1157–61.

102. Mercer, J.F. (2001). The molecular basis of copper transport diseases. Trends Mol. Med, 7 : 64-69.

103. La Fontaine L, S. and Mercer, J.F (2007), Trafficking of copper-ATPases, ATP7A and ATP & B: role in copper homeostasis. Arch. Biochem. Biophys. 463: 149-167.

104. El Meskini, R, Culotta, V.C, Mains R.E., Eipper, B.A. (2003), Supplying copper to the cuproenzyme peptidylglycine alpha-amidating monooxygenase. J. Biol. Chem., 278:12278-12284.

105. Wang, G. and Vasquez, K.M. (2006), Non-BDNA structure-induced genetic instability. Mutat. Res., 598:103-119.

106. Boussouf, A., and Gaillard, S. (2000), Intracellular pH changes during oligodendrocyte differentiation in primary culture. J. Neurosci. Res., 59:731–739.

107. Waggoner, D. J., Bartnikas, T. B., and Gitlin, J. D. (1999), The Role of Copper in Neurodegenerative Disease. Neurobiol. Dis. 6: 221–230.

NEWS ITEM

A Group of Brigham and women's Hospital, and Harvard Stem Cell Institute Researchers, and Collabo-rators At Mit and Massachusetts General Hospital Have Found a way to use Stem Cells as Drug Delivery Vehicles on Oct. 4th, 2013

The researchers inserted modified strands of messenger RNA into connective tissue stem cells -- called mesenchymal stem cells -- which stimulated the cells to produce adhesive surface proteins and secrete interleukin-10, an anti-inflammatory molecule. When injected into the bloodstream of a mouse, these modified human stem cells were able to target and stick to sites of inflammation and release biological agents that successfully reduced the swelling.

"If you think of a cell as a drug factory, what we're doing is targeting cell-based, drug factories to damaged or diseased tissues, where the cells can produce drugs at high enough levels to have a therapeutic effect," said research leader Jeffrey Karp, PhD, a Harvard Stem Cell Institute principal faculty member and Associate Professor at the Brigham and Women's Hospital, Harvard Medical School, and Affiliate faculty at MIT.

Karp's proof of concept study, published in the journal Blood, is drawing early interest from biopharmaceutical companies for its potential to target biological drugs to disease sites. While ranked as the top sellers in the drug industry, biological drugs are still challenging to use, and Karp's approach may improve their clinical application as well as improve the historically mixed, clinical trial results of mesenchymal stem cell-based treatments.

Mesenchymal stem cells have become cell therapy researchers' tool of choice because they can evade the immune system, and thus are safe to use even if they are derived from another person. To modify the cells with messenger RNA, the researchers used the RNA delivery and cell programming technique that was previously developed in the MIT laboratory of Mehmet Fatih Yanik, PhD. This RNA technique to program cells is harmless, as it does not modify the cells' genome, which can be a problem when DNA is used (via viruses) to manipulate gene expression.

"This opens the door to thinking of messenger RNA transfection of cell populations as next generation therapeutics in the clinic, as they get around some of the delivery challenges that have been encountered with biological agents," said Oren Levy, PhD, co-lead author of the study and Instructor of Medicine in Karp's lab. The study was also co-led by Weian Zhao, PhD, at University of California, Irvine who was previously a postdoctoral fellow in Karp's lab.

One such challenge with using mesenchymal stem cells is they have a "hit-and-run" effect, since they are rapidly cleared after entering the bloodstream, typically within a few hours or days. The Harvard/MIT team demonstrated that rapid targeting of the cells to the inflamed tissue produced a therapeutic effect despite the cells being rapidly cleared. The scientists want to extend cell lifespan even further and are experimenting with how to use messenger RNA to make the stem cells produce pro-survival factors.

"We're interested to explore the platform nature of this approach and see what potential limitations it may have or how far we can actually push it," Zhao said. "Potentially, we can simultaneously deliver proteins that have synergistic therapeutic impacts."

Acceptance Speech by the President Of India, Shri Pranab Mukherjee at the Ceremony Conferering Honoris Causa by the University Of Istanbul, Turkey on October 5th 2013

Today, despite challenges, and occasional setbacks, India is no longer defined by her problems but by her achievements and the opportunities it offers. We have become a trillion dollar economy, the largest in Southeast Asia. We also have the largest middle class in the region. The last decade has seen India emerge as one of the fastest growing nations in the world. During this period, our economy grew annually at an average rate of 7.9 per cent. We are self-sufficient in food grains production, the largest exporter of rice and the second largest exporter of wheat. However, achieving equitable economic growth is still a challenge. So also is the complete elimination of poverty, although a declining trend in the poverty rate is clearly visible.

Rapid creation of employment opportunities is an essential aspect of good governance. It is the approximately 350 million middle-class Indian citizens that have put India on the world map over the past two decades or so. In my Address to the Indian nation on the eve of 15th August, which marked the

66thAnniversary of our Independence, I referred to the need to provide our citizens entitlements backed by legal guarantees in terms of right to employment, education, food and information. We also need to ensure that these entitlements lead to real empowerment of the people. It will be essential to develop and sustain robust delivery mechanisms to make these legislations work.

Our trajectory of high level growth will need to be sustained. Our continued success will need to be earned. In spite of our achievements during these transformational decades, there remains much work to be done. Indeed, sustaining India's transformation will require the hard work and diligence of the country's people, and particularly, good governance that its leaders have to steer. We will have to also strengthen the rule of law and good governance practices. We will have to ensure harmonious relations among our diverse ethnic and religious groups which, in a secular polity, is of supreme importance for nation building.

I certainly hope that with all this, in 2047—after one hundred years of independence—my vision of an India fully transformed into a democratically mature, stable and peaceful nation with freedom and opportunity for all will become a reality. It will be an India that is economically prosperous at all levels of society. In 1947, with an India coming into being after two centuries of colonial rule, many would have thought this vision as being far-fetched, but as envisioned by our national leaders, I am proud to say that today, this is a future well within our reach.

I am reminded of the Nobel laureate Indian poet and philosopher, Rabindranath Tagore whose work, Geetanjali, includes these lines which summarize my hopes and dreams for a successful and fully developed India ready to take its rightful place in this world:

Giant Moon-forming impact blew off Earth's atmosphere have been proposed on Oct 6th, 2013 scientists, including one of Indian-origin.

The lunar body came into existence after several planet-size space bodies smashed into the early Earth one after the other, researchers said.

Scientists, until now, believed it was unlikely that the early Earth could lose its atmosphere because of a giant Moon-forming impact.

The study is based on recent research showing that at its infancy Earth had magma oceans and was spinning so rapidly that a day was only two or three hours long. They also looked at elements found in volcanoes that sample the upper mantle, such as mid-ocean ridge basalts at the bottom of the Atlantic, the report said.

They found that elements in the deep mantle that retain a very ancient chemistry, from the times of the Earth's formation, are very different from those in the upper mantle found today.

China's smog polluting Fuji, new study says

"Whenever readings were high, winds were blowing from the continent (China)," Osamu Nagafuchi, the lead scientist on the study, said recently.

Mount Fuji was chosen "because it's a place unaffected by urban pollution," said Nagafuchi, an environmental science professor at the University of Shiga.

Pollution levels on Mount Fuji have been monitored annually since 2007, he said, adding the decision to carry out the study on the 3,776-meter peak had nothing to do with it being designated a UNESCO World Heritage site earlier this year.

The designation, delayed by years of efforts to remove tons of trash from the iconic peak, which figures heavily in Japanese art and literature, preceded this summer's climbing season.

Mercury levels around the top of the mountain were up to double the levels detected in other places free of heavy pollution, according to the survey, conducted in August with nonprofit group Valid Utilization of Mount Fuji Weather Station.

The mercury levels were as high as 2.8 nanograms per cu. meter of air. That exceeds the 1.0 to 1.5 nanograms normally detected in clean locations but is well below the government's 40-nanogram threshold for posing risks to human health. A nanogram is one-billionth of a gram.

The higher-than-expected readings are likely due to Chinese factories burning coal, which releases mercury and other toxic elements such as arsenic, whose levels were also elevated, according to Nagafuchi.

The study comes as fast-industrializing China wrestles with a severe urban smog problem linked to hundreds of thousands of premature deaths. Last month, the Chinese government vowed to reduce levels of atmospheric pollutants in Beijing and other major cities by as much as 25 percent to try to improve their dire air quality.

♦ ♦ ♦

MS in Pharmacy from USA

1st semester at Alliance - JNTUH in India and remaining courses & research in USA at the University of the Pacific, California, USA.

University of the Pacific, USA has entered into collaboration with JNTUH & Alliance Institute, India, for offering Masters (MS) program in Industrial Pharmaceutics. In this program students take courses in the first semester at Alliance-JNTUH and after successful completion of first semester at Alliance and fulfilling admission, TOEFL and visa requirements, students can go to USA to complete remaining courses and research at Thomas J Long School of Pharmacy and Health Sciences, University of the Pacific. Upon successful completion of the requirements, University of the Pacific will award Master's degree.

If students fail to meet University of the Pacific admission/ visa requirements, they have an option to continue their course and research work at Alliance -JNTUH or do research work at the Pacific to fulfill requirements for MS degree in India.

Admissions are based on
GPAT / PGECET / JNTUH Entrance

MS DEGREE AWARDED BY
University of the Pacific, Stockton, CA- USA

ALLIANCE INSTITUTE OF ADVANCED PHARMACEUTICAL AND HEALTH SCIENCES

#604A, Aditya Trade Centre, Ameerpet, Hyderabad – 500 038, India
Phone: 040-66663326 / 23730072, Website: www.allianceinstitute.org

About Alliance: Alliance, located conveniently in the heart of Hyderabad, trains industry-ready graduates by bridging education with industry needs in pharmaceutical sciences. Alliance's visionary management built state of the art facilities and laboratories to provide quality education meeting national and international standards.

Collaboration with JNTUH, India: Alliance is having collaboration with **Jawaharlal Nehru Technological University, Hyderabad (JNTUH)**, which is a premier institution with academic and research–oriented programs, offered through the constituent and affiliated colleges. Alliance's syllabi, academic regulations and course structure are **approved by the JNTUH. JNTUH awards the degrees after fulfilling the degree requirements.**

Collaboration with University of the Pacific, USA: University of the Pacific, ranks in the top 100 among the 3000 national universities in the United States. Alliance has entered into research collaboration with Thomas J Long School of Pharmacy and Health Sciences, University of the Pacific.

Alliance students have an option to do research work at the University of the Pacific to fulfill requirements for MS degree in India. Pacific faculty teaches Alliance students via live online classes. Pacific is also interested to offer admissions to Alliance students based on their performance at Alliance.

Programs offered :

* MS in Industrial Pharmaceutics
* MS in Pharmaceutical Analysis & Quality Control
* MS in Drug Development & Regulatory Affairs

For admissions, application forms and additional information visit online at www.jntuh.ac.in/alliance or www.allianceinstitute.org.

Registered with Registrar of News Papers for India
Regn. No. APENG/2008/28877

Association of Biotechnology and Pharmacy

(Regn. No. 28OF 2007)

Executive Council

Advisory Board

Executive Members

Printed, Published and owned by Association of Bio-Technology and Pharmacy # 6-69-64 : 6/19, Brodipet, Guntur - 522 002, Andhra pradesh, India. **Printed at :** Don Bosco Tech. School Press, Ring Road, Guntur - 522 007. A.P., India **Published at :** Association of Bio-Technology and Pharmacy # 6-69-64 : 6/19, Brodipet, Guntur - 522 002, Andhra pradesh, India.
Editors : Prof. K.R.S. Sambasiva Rao, Prof. Karnam S. Murthy